DISS. ETH NO. 25374

Structural Folding for Architectural Design

A new approach to the design of folded plate structures in architecture

A thesis submitted to attain the degree of

DOCTOR OF SCIENCES of ETH ZURICH

(Dr. sc. ETH Zurich)

presented by

PIERLUIGI D'ACUNTO

Dottore Magistrale in Ingegneria Edile-Architettura, Università di Pisa

born on 17.01.1983

citizen of Italy

accepted on the recommendation of

Prof. Dr. Joseph Schwartz (ETH Zurich)

Prof. Dr. Denis Zastavni (Université Catholique de Louvain)

Prof. Dr. Corentin Fivet (École Polytechnique Fédérale de Lausanne)

2018

Acknowledgements

First of all, I would like to express my gratitude to my advisor Prof. Joseph Schwartz, for his continuous assistance, input, and encouragement during every stage of my research and for granting me the unique opportunity of being part of the Chair of Structural Design at ETH Zurich. I am particularly thankful to him for sharing his immense knowledge and valuable experience as a structural designer with me, throughout countless and always inspiring conversations. His approach to engineering and architecture has been particularly important for the development of my research.

Furthermore, I would like to thank my co-advisors Prof. Denis Zastavni and Prof. Corentin Fivet. I am especially grateful to Prof. Denis Zastavni for his constant availability and always precise and helpful advice on my work. His critical view on architectural and structural design had a significant influence on my dissertation. Prof. Corentin Fivet supported me regularly with his precious suggestions. His constructive feedback and insightful comments have been essential guidance during the development of my thesis.

Over the last few years, personal exchanges with various researchers and practitioners of engineering and architecture have contributed to the enrichment of my dissertation. Particularly relevant was the input of Prof. Juan Carlos Sancho, whose outstanding work, developed together with Sol Madridejos, has always been a fundamental reference for my research. In addition, I am extremely thankful to Prof. Tomohiro Tachi for his valuable feedback on my work.

I am deeply grateful to all my colleagues at the Chair of Structural Design for the pleasant time I spent with them in the past years. It has always been a pleasure to prepare together student exercises, tutorials, and lectures, as well as to collaborate on various research projects. Special thanks go to Juanjo Castellón for his important contribution to my work and his essential support in the development of many teaching activities, above all the course *Experimental Explorations on Space and Structures*. I am particularly thankful to Patrick Ole Ohlbrock for his inestimable generosity and dedication, as well as creativeness and enthusiasm, which I had the pleasure to experience throughout the development of several research projects, including our exploration of 3D graphic statics. I would like to thank Lukas Ingold for his helpful feedback on my work and the enlightening discussions concerning our shared investigation on the structural engineer Sergio Musmeci. I am very grateful to Mario Rinke, Lluis Enrique,

and Vahid Moosavi for helping me on several occasions during the development of my thesis. Moreover, I would like to acknowledge Prof. Toni Kotnik, for his constructive comments on my work, particularly in the first stage of my research.

My sincere appreciation goes to Jean-Philippe Jasienski and Jean-François Rondeaux from the research group LOCI at UC Louvain. Given their constant and precious support and enthusiasm, it has been a pleasure to work with them on various academic collaborations. Furthermore, I am grateful to the RAPLAB at ETH Zurich and particularly to Alessandro Tellini for his generous help and strong commitment in all the research and teaching activities that I developed in collaboration with him.

Finally, I would like to thank all the people that in different ways assisted me during these years. Special thanks go to my family and my closest friends for their endless support and continuous encouragement.

Contents

Design Method   139

Case Studies   165

Conclusions   207

Bibliography   218

Abstract

From an architectural standpoint, folding as a design operation enables the creation of forms that can deal with different requirements in terms of both space and programme. Moreover, from an engineering perspective, folding is an effective strategy to generate efficient structures that withstand the applied loads through their form. Although these two aspects have been explored extensively as independent research questions, so far, only a few attempts have been made to define design methods that can take into account both spatial and structural opportunities of folding at the same time.

This research presents a new approach to the design of folded plate structures in architecture. A design method that takes advantage of the interaction between the spatial and structural features of folding is proposed, which aims at merging architecture and engineering based on a holistic approach to design. The proposed method is intended to assist the creation of folded plate structures since the initial phase of the design development and can be used by both architects and engineers. The method builds on a process that relies on the implementation of geometric operations in three dimensions. In particular, a statically rigid folded plate structure is defined within a kinematically stable reference grid. While generating the structure, an architectural space is produced at the same time. Without compromising the topological properties of the folded plate structure, its form and the distribution of its internal forces can be adjusted by the designer to meet specific architectural and structural requirements. This goal is achieved by controlling the position of the nodes of the reference grid while abiding by a series of designer-defined geometric constraints.

Grounded on 3D graphic statics and the theory of plasticity, a specific strut-and-tie model for folded plate structures is introduced as the structural basis for the design method. In this model, the internal forces are transferred via linear members both along the folded edges and within the folded plates. Based on the strut-and-tie model, in-plane stress fields in the folded plates can be derived. The applicability of the proposed approach is facilitated by the implementation of the design method into a parametric digital toolkit, which can be employed to create folded plate structures at various scales. The potential of the method in real design scenarios is demonstrated through a series of experimental designs as case studies, including full-scale prototypes.

Zusammenfassung

Operationen mit Faltungen ermöglichen aus architektonischer Sicht die Erzeugung von Formen, welche sehr unterschiedlichen räumlichen und programmatischen Anforderungen gerecht werden können. Aus ingenieurwissenschaftlicher Sicht erlaubt das Entwerfen mit Faltungen äusserst effiziente Strukturen zu kreieren, welche rein durch ihre Form verschiedenen Beanspruchungen standzuhalten vermögen. Obwohl diese beiden Aspekte als eigenständige Forschungsfragen ausgiebig erforscht wurden, gibt es bisher nur wenige Versuche, Entwurfsmethoden zu definieren, welche gleichzeitig die räumlichen als auch die strukturellen Potenziale des Faltens berücksichtigen.

Diese Forschung präsentiert einen neuen Ansatz für die Gestaltung von Faltwerken in der Architektur. Die entwickelte Entwurfsmethode zielt darauf, das Wechselspiel zwischen räumlichen und strukturellen Eigenschaften zu nutzen, um auf effektive Weise das architektonische und ingenieurwissenschaftliche Denken in einem ganzheitlichen Entwurfsansatz zu verschränken. Die vorgeschlagene Methode richtet sich sowohl an Architekten als auch an Ingenieure und zielt darauf, die Konzeptionierung von Faltwerken von Beginn weg zu unterstützen. Der Entwurfsprozess basiert ausschliesslich auf dreidimensionalen, geometrischen Operationen. Konkret wird eine statisch starre Faltwerkstruktur innerhalb eines kinematisch bestimmten Referenzgitters erzeugt. Mit der Generierung der Faltwerkstruktur entsteht gleichzeitig ein architektonischer Raum. Ohne die inhärenten topologischen Eigenschaften aufzugeben, kann die Form des Faltwerks und die Verteilung der inneren Kräfte vom Planer an die spezifischen architektonischen und strukturellen Anforderungen angepasst werden. Dies wird durch die Kontrolle der Position der Gitterknoten als auch durch die Einhaltung einer Reihe geometrischer Bedingungen, welche vom Entwerfer definierten werden, erreicht.

Ein spezifisches, räumliches Stabwerkmodell für Faltwerke, welches auf der dreidimensionalen Anwendung der Grafischen Statik und der Plastizitätstheorie basiert, wird als strukturelle Grundlage für die Entwurfsmethode eingeführt. In diesem Modell werden die inneren Kräfte durch lineare Elemente transferiert, sowohl entlang der gefalteten Kanten als auch innerhalb der Platten. Ausgehend vom Stabwerkmodell lassen sich dann ebene Spannungsfelder in den gefalteten Platten herleiten. Die praktische Anwendbarkeit des Verfahrens wird durch die Implementierung der Methode in ein parametrisches, digitales Toolkit

ermöglicht. Mit diesem lassen sich unterschiedlichste Faltwerkentwürfe in verschiedenen Massstäben erzeugen. Das Potenzial der Methode für reale Entwurfsszenarien wird durch eine Serie experimenteller Entwürfe, inklusive 1:1 - Prototypen, demonstriert.

Introduction

1. Folding as Integration of Architecture and Engineering

Architecture and Engineering in the Conceptual Design Phase   Towards the end of the 20th century, thanks to the generalised digitalisation of the design process within the discipline of architecture, the chance to generate and control non-standard geometries opened up the possibility for the creation of new architectural forms (Macdonald 2001). At the beginning of the 1990s, as soon as computer-aided design tools became widely available within the architectural community, architects have been granted the opportunity to generate buildings with unconventional three-dimensional shapes, especially using curvilinear geometries (Lynn 1993b; Carpo 2004; Frichot 2013).

As an immediate consequence of this phenomenon, which has been termed by Carpo as the *Digital Turn* (Carpo 2013), a paradigm in architectural design has been strengthened where the focus was predominantly put on the expressiveness of the architectural form. Such an approach gave limited relevance to the fundamental relationship between the shape of a building and its inherent structural behaviour (Schwartz 2016a). Structural questions were thus addressed by the engineer only in the advanced phase of the design process after the architectural form had been first defined by the architect within the conceptual stage (Vrontissi et al. 2018). That is, the structural engineer was merely asked to verify the stability of the structure and to calculate the size of the load-bearing elements while having limited influence on the design of the actual shape of the building. This design practice resulted in the contribution of the structural engineer being generally dependent on the one of the architect (Oxman and Oxman 2010), hence establishing a hierarchical relationship between the two disciplines (Kotnik and D'Acunto 2013). Such an operative model further enhanced the distinction between the roles of the architect and the engineer within the building sector (Saint 2007); a separation that had its origin in the 18th century (Addis 2007) and had been officially formalised by the creation of the first polytechnic universities during the 19th century (Rinke and Kotnik 2013).

As observed by Macdonald (2001), the lack of structural insight during the conceptual phase of the design process can be regarded as responsible for a series of shortcomings in several projects of contemporary architecture. Issues that are often the cause of delays in design development, and that enforce the

excessive use of material resources in the final built constructions, as already pointed out by Nervi (1965). In fact, the early stage of the design process represents the fundamental moment when the initial ideas are outlined, and it has a relevant influence on all the subsequent design phases. Structural awareness in the conceptual design phase thus becomes a crucial requirement for the success of the entire design process (Nervi 1965; Musmeci 1979b; Schwartz 2016a; Fivet and Meng 2017).

Over the last few years, increased attention has been put on addressing structural questions at the initial stage of the design. Based on this strategy, the structure has become an essential aspect of the design process and in some instances, the primary driver for the overall design advancement. This phenomenon has been evidently revealed by the recently increasing number of interdisciplinary collaborations between architects and structural engineers, who started to cooperate from the outset of the design development (Kara 2010; Nordenson 2010; Kotnik and D'Acunto 2013). Such a paradigmatic shift in the architectural and engineering design production has been referred to by Oxman and Oxman (2010) as the *New Structuralism*.

This new model advocates in favour of crossing the boundaries between the architectural and engineering disciplines. Unlike the common hierarchical and sequential exchange between the architect and the engineer, in this emerging collaborative relationship, the architectural and engineering aspects of the design are addressed together and developed at once during the entire design process (Kotnik and D'Acunto 2013). The expertise and creativeness of the engineer thus encounter the ones of the architect and open dialogue is established between the two professions (Muttoni 2011). As explained by Flury (2012), this new model has generated a condition in which the architect and the engineer are prone to go beyond the boundaries of their own disciplines. Such a relation between the two professions entails an attitude to building design where both architects and engineers take on the entire design process and assume authorship on its outcome (Vrontissi et al. 2018).

In compliance with this new model, the correlation between the architectural form and its inherent structural capacity is regarded as a fundamental notion for design (Schwartz 2016a). Such clear relationship between architecture and engineering can be recognised in the past building production only in those projects developed by architect-engineers such as Dieste, Candela, Torroja, and Nervi, among others (Kotnik and D'Acunto 2013). In fact, for these master builders of the 20th century, one of the most relevant components for the success of the design development was the definition of an explicit static concept already in the first phase of the design process (Nervi 1956). In this regard, as highlighted by Schwartz and Kotnik: "Elegant constructions can therefore only arise if the inner logic of the technical and scientific necessity becomes a unity with the external logic of creative freedom, and if the two mutually condition each other." (Schwartz and Kotnik 2010)

Folding as a Design Operation   The notion of folding has a multiplicity of different meanings, which embrace a considerable number of possible applications. As explained by Lebée (2015), the emergence of the idea of *folded surface* is directly related to the tradition of paper folding. This practice has its origin in the Japanese art of *origami*, which brings together the notions of *oru* (fold) and *kami* (paper) (Lebée 2015).

In this research, folding is regarded as an *abstract design operation* applied to architectural design, which results in the creation of folded geometries. The interest in folding, being this the main object of investigation of the present research, relies on the assumption that such a design operation may represent an effective medium to combine coherently architectural intentions and engineering thinking within a holistic approach to design (D'Acunto and Castellón 2015). In this way, referring to the previously described relationship between architects and engineers, the use of folding in design is here recognised as a way to promote an exchange between the two disciplines, starting from the early conceptual stage of the design process. In fact, as clearly highlighted by Iwamoto (2009), the effects produced by folding allow this design operation to address at the same time various aspects related to both architecture and engineering:

> "Folding turns a flat surface into a three-dimensional one. It is a powerful technique not only for making form but also for creating structure with geometry. When folds are introduced into otherwise planar materials, those materials gain stiffness and rigidity, can span distance, and can often be self-supporting. Folding is materially economical, visually appealing, and effective at multiple scales." (Iwamoto 2009, p. 62)

First, through folding an initially planar geometry is able to enter the third dimension (Fig. 1.1), thus inherently achieving a spatial configuration. In this transformation, particularly relevant is the notion of folding acting as a "unitary gesture" (Sancho 2014a, p. 12), which allows the different constituent parts of the folded geometry to keep continuity. That is, while the folding operation is applied, the various components of an initially flat geometry are not individually transformed, but they follow a coherent global movement, which entails the existence of spatial interdependences between the parts.

Second, the geometry resulting from the application of folding has not only spatial connotations but also intrinsic structural properties. In fact, by transforming an initially flat surface into a three-dimensional folded geometry, the surface implicitly gains static depth. Such a principle is here referred to as *structural folding* (Kotnik and D'Acunto 2013). This principle opens up the possibility of using folding to create efficient structural systems that are able to support the externally applied loads through form. Thanks to this property, folded geometries possess their own structural integrity and are generally self-supporting, hence not requiring the use of auxiliary supporting structures.

Third, the application of folding results in the creation of three-dimensional geometries whose constituent parts are planar. This aspect is particularly relevant in relation to construction since it allows the use of a large variety of

Figure 1.1: Transformation of a flat geometry into a three-dimensional one through folding.

materials and relatively simple manufacturing techniques. Moreover, in terms of visual perception, the planarity of its parts makes a folded geometry clearly intelligible and immediately understandable, no matter its inherent geometric complexity.

Finally, being a design operation, folding is generally scale-independent. This enables the use of folding at different scales and, consequently, to apply it to diverse design scenarios.

The aforementioned effects of folding as a design operation have great importance at the scale of architecture. Considering a building as a folded geometry, thanks to the inherent spatial and structural features of such a geometry, a clear interdependency between the building's architectural form and structural behaviour can be established. Such a correlation is the one that qualifies the "strong structures" (Schnetzer et al. 2012, p. 194). These are load-bearing constructions that do not serve their purpose as frameworks concealed behind building envelopes, but instead translate the structural demands into an occasion for the creation of architectural space (Kotnik and D'Acunto 2013). Hence, through the folded geometry, supporting structure and building envelope are merged into one single element, and the potential of folding to integrate architecture and engineering is directly revealed (Buri 2010).

2. Applications of Folding to Architecture

This research specifically deals with the use of folding at the scale of architecture. In this context, one can identify three main applications: *deployable structures*, *folded developable surfaces*, and *folded plate structures* (D'Acunto and Castellón 2015).

Deployable Structures   A structure is deployable if can be unfolded from a packed configuration to an expanded layout and folded back (Pellegrino 2001). Deployable structures can be used to generate architectural elements, such as retractable roofs or façade components, which can be stored in a compact state and deployed when necessary. Deployable structures that are used at the scale of architecture include, among others, *structural mechanisms* made of rigid bars connected via movable joints (Calatrava 1981; Pellegrino 2001) and *foldable tensegrities*, whose transformation can be controlled by changing the lengths of their constituting elements (Motro et al. 2001).

Folded Developable Surfaces   Folded geometries as developable surfaces can be mapped onto a plane using isometric transformations (Dureisseix 2012) and are usually designed starting from an initial *folding* or *crease* pattern. This pattern is applied to a two-dimensional sheet of material, which is subsequently deployed into space through physical folding. As described by Buri (2010), examples of traditional folding patterns derived from *origami* are the *diamond pattern* or *Yoshimura pattern* (Hunt and Airo 2005), the *herringbone pattern* or *Miura Ori pattern* (Miura 1989), and the *diagonal pattern*. Each folding pattern is characterised by a specific configuration of *valley folds* and *mountain folds*[1] (Fig. 2.1). The definition of more complex folding patterns may be obtained as free-form variations of the classical origami patterns (Tachi 2010b), generally using parametric digital tools (Tachi 2009b). Folded geometries as developable surfaces can also be used to generate deployable structures. In this case, panels

---

[1]The application of folding to a flat sheet of material generates a mechanism in which one part of the sheet can rotate about the other one; the two possible directions of rotation are commonly defined as valley and mountain folds, whether the final folded geometry is concave or convex (Dureisseix 2012).
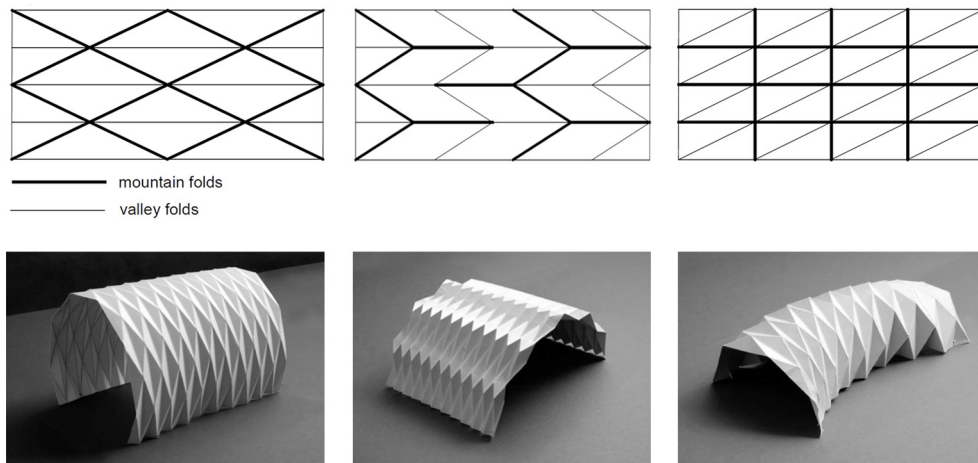
Figure 2.1: Three different types of folding patterns that can be used for the creation of folded developable surfaces. (Left) Diamond pattern. (Centre) Herringbone pattern. (Right) Diagonal pattern. Adapted from (Buri 2010, pp. 42–47).

that can be rigidly folded and unfolded[2] are generally employed. At the scale of architecture, these geometries require the introduction of specific solutions that can accommodate for the thickness of the panels during the folding and unfolding transformations (Tachi 2011).

.

Folded Plate Structures   Folded plate structures consist of plates rigid in their planes that are connected in space to generate folded geometries, globally working as statically rigid structure systems (Fig. 2.2). Folded plate structures are not necessarily developable, and their construction does not generally imply an actual process of physical folding. Because of the lack of geometric constraints imposed by the developability requirement, folded plate structures can be designed in a broader range of geometric configurations in comparison to folded developable surfaces. That is, other than starting from a two-dimensional folding pattern, whose mechanism has to be inevitably fixed to generate a kinematically stable structure (Trautz et al. 2012; Gioia et al. 2012; Lebée 2015), folded plate structures can also be designed directly in three dimensions.

According to Engel (2013), folded plate structures can be regarded as a subcategory of surface-active structure systems. These are assemblies of structural surfaces, which redirect forces in space through their geometry and without the need for extra supports. At the same time, folded plate structures define architectural spaces. Because of their inherent structural and spatial potentials, folded plate structures have been extensively investigated in architectural and structural design (Trautz and Herkrath 2009; Trautz et al. 2014).

---

[2]A folded geometry is rigid-foldable if its parts stay rigid during the folding transformation (Lebée 2015).
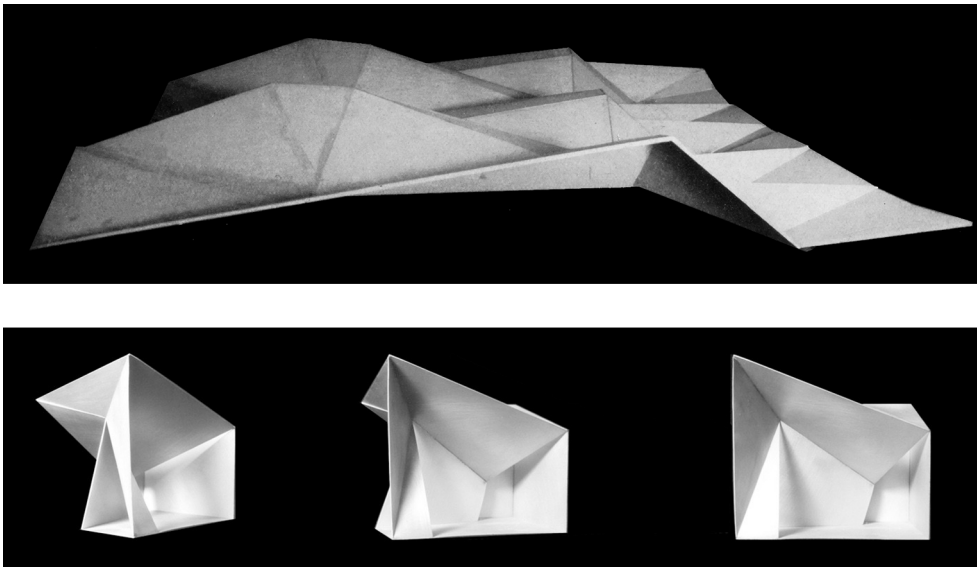
Figure 2.2: Applications of folded plate structures to architecture. (Top) Physical model of the roof of Stabilimento Raffo in Pietrasanta by Musmeci as a *folded surface structure* (Musmeci 1960, p. 711). (Bottom) Physical model of the Chapel in Valleacerón by Sancho and Madridejos as a *folded volumetric structure* (*Chapel in Valleacerón - S.M.A.O.* ArchDaily, 30.04.2009, `https://www.archdaily.com/20945/chapel-in-villeaceron-smao/`, ISSN 0719-8884. Accessed 25.05.2018. Photos: Sancho-Madridejos Architecture Office).

From a geometric standpoint, a distinction is made in this research between a folded plate structure as a *folded surface structure* (Sedlak 1978) and as a *folded volumetric structure*. In the first case, the geometry consists in a discrete open surface, which can be often regarded as an approximation of a double curved smooth surface; folded surface structures are generally used for the design of roofs and façades. In the second case, the geometry is a self-connected, often non-manifold, discrete surface that generates a porous structure; folded volumetric structures can be employed as the architectural envelopes of continuous yet differentiated spaces. On the one hand, a remarkable investigation into the possibilities offered by folded surface structures is due to the structural engineer Musmeci (Musmeci 1979a). In this context, exemplary is the roof of the marble factory *Stabilimento Raffo in Pietrasanta* (1956) (§ 4.2.2), whose geometry is a direct manifestation of the flow of the forces within the structure (Fig. 2.2, top). On the other hand, important examples of folded volumetric structures are epitomised by those projects of the architects Sancho and Madridejos (Sancho 2001), like the *Chapel in Valleacerón* (1997-2000) (§ 5.2.2), where folding is used to modulate diverse spatial conditions (Fig. 2.2, bottom) (D'Acunto and Castellón 2015).

Thanks to their intrinsic ability to resist the externally applied loads by form and their possibility to generate space, this research is primarily focused on *folded plate structures* and their use in architectural design.

3. Research Overview

Various methodological approaches to the use of folding in design have been introduced over the years, particularly in the field of education. In this regard, one of the first implementations of folding as a design operation is due to the artist and educator Albers (Buri 2010; Lebée 2015), who in the 1920s developed a series of exercises based on the use of folding as part of his introductory course on design at the Bauhaus (Albers 1952).

More recent applications of folding to architectural design involve, among others, the use of origami techniques (Jackson 2011) for the creation and transformation of *folded surface structures*, or the morphological exploration of sheet material folding (Vyzoviti 2003) to generate *folded volumetric structures*. Within these design experimentations, however, the fundamental correlation between space and structure in the folded geometries is not always made evident. As a result, the designer often deals with this aspect only on an elementary level, being the structural integrity of the folded geometries generally analysed only after the architectural design has been first defined. In this way, the structural and spatial opportunities of folding cannot always be exploited, especially during the conceptual design phase (D'Acunto and Castellón 2015).

Although the structural and spatial possibilities of folding have been already extensively investigated in the practical and scientific domains as independent research fields, up to now, only a few consistent explorations aimed at integrating these two aspects into the design process have been developed.

Research Focus   While promoting a synthesis between the disciplines of architecture and engineering, the primary aim of this research is to introduce a novel method for the design of folded plate structures in architecture. In this context, folded plate structures are regarded as *strong structures* (Schnetzer et al. 2012, p. 194; Chapter 1) due to the inherent relationship between their load-bearing capacity and their space making potential.

Thanks to the proposed approach, the design of folded plate structures is supported during the entire design development, starting from the initial phase. In particular, while implementing simple geometric operations, the designer is guided throughout the creation process of a folded plate structure that forms the building envelope of an architectural space. The method gives the designer the opportunity to control the dimensions and proportions of the space and

thus its qualities. At the same time, the designer is able to assess the load-bearing behaviour of the structure, with a particular focus on the static rigidity, the equilibrium of the internal forces, and the stress distribution. As a result, by promoting the use of spatial and structural features of folding as essential drivers for the design development, the efficacy of folding as a design operation is brought to the fore (D'Acunto and Castellón 2015).

Thesis Structure   The remainder of this thesis is organised in five main parts: *Research Framework*, *Structural Model*, *Design Method*, *Case Studies*, and *Conclusions*.

The first part (*Research Framework*) gives an account of the theoretical context within which the proposed design method for structural folding in architecture has been formulated. Chapter 4 is an overview of a series of historical examples of folded plate structures, whose design has been especially based on the search for structural efficiency while taking advantage of the principle of resistance through form. Particular attention is drawn to the context of the post-war period in Italy when peculiar applications of structural folding have been developed by the main protagonists of the structural engineering scene of that time. Within this domain, the work of the engineer Musmeci is analysed as a key reference for the development of a strategy to design efficient folded plate structures. Chapter 5 is devoted to applications of folding to architectural design, with a particular focus on the context of the 1990s, when folding becomes a significant research topic for several architectural practices worldwide. In particular, the design experimentation of the architecture office of Sancho and Madridejos is examined as an exemplary case of the use of folding for the creation of architectural space. Chapter 6 is an overview of current strategies for the design of folded plate structures at the scale of architecture. Finally, Chapter 7 defines the scope of the present work and highlights the research process undertaken for the development of the proposed design method for structural folding in architecture.

The second part (*Structural Model*) presents the structural basis that is at the core of the developed design approach. Grounded on considerations of topology and static rigidity, in Chapter 8 a novel strut-and-tie model for folded plate structures is delineated. This model represents a combination of the dual structural archetypes of space, namely the lattice and the plate models, which are introduced and described in details. Thanks to the use of the strut-and-tie network, the global mechanical behaviour of a folded plate structure can be modelled using only linear members, which are placed either along the folded edges or within the folded plates. Chapter 9 then highlights how vector-based 3D graphic statics could be used to assess and control the external and internal

equilibrium of the strut-and-tie network. Eventually, in Chapter 10 an approach to derive in-plane stress fields in the folded plates is described.

The third part (*Design Method*) is focused on the developed method for the design of folded plate structures in architecture, which relies on the strut-and-tie model introduced in the previous part. After a general overview of the main features of the proposed method in Chapter 11, Chapter 12 outlines a series of design operations that can be used for the definition of the topology of a folded plate structure, while addressing both structural and spatial questions at the same time. Chapter 13 presents those design operations included in the proposed method that consent to control the dimensions and proportions of a folded plate structure. Thanks to these operations, both architectural and engineering aspects can be addressed through the mediation of geometry.

The fourth part (*Case Studies*) introduces three case studies that have been regarded as design experiments to test the applicability of the developed design method. Chapter 14 offers an outlook on the general features of the case studies, which comprise folded plate structures at various scales. More specifically, the design experiments include a cantilevering table, a hanging structure, and a small building. The application of the proposed design method to the development of each case study is depicted respectively in Chapter 15, Chapter 16, and Chapter 17.

The fifth part (*Conclusions*) includes a discussion on the overall content of the thesis, with specific reference to the contributions and limitations of the research and a final overview of future developments.

Research Framework

4. Folding and the Search for Structural Efficiency

4.1   Resistance through Form and Structural Folding

Thanks to *structural folding* (Chapter 1) it is possible to confer to an initial flat geometry the ability to resist out-of-plane loads by increasing its structural depth. The application of this principle at the scale of architecture gives rise to the folded plate structure system (Engel 2013, p. 219), where plates rigid in their planes generate kinematically stable folded geometries. The correlation between the form and the internal forces in a folded plate structure delineates an explicit structural logic. This relationship is expressed by the principle of *resistance through form*, as outlined by the architect-engineer Dieste (1917–2000):

> "The resistant virtues of the structures that we make depend on their form. It is through their form that they are stable and not because of an awkward accumulation of materials. There is nothing more noble and elegant from an intellectual point of view than this, resistance through form." (Pedreschi 2000, p. 21)

The application of the principle of resistance through form allows making use of structural elements in their most effective way and consequently to produce efficient structures. From the point of view of the feasibility of construction, the use of folded plates generally enables the production of complex geometries based on the assembly of simple flat elements. If compared to other types of form-active structure system such as double-curved shells, thanks to the planarity of their constituting elements, folded plate structures are relatively easy to fabricate. This aspect is especially true in the case of reinforced concrete, as the construction of folded plate structures does not generally require the use of complex formwork.

Among the first applications of structural folding to architecture are the Hangars at Orly (1921–1923) by the engineer Freyssinet (1879–1962) (Fernandez Ordoñez 1979). Especially because of their inherent structural potentials and relatively convenience of fabrication, folded plate structures have been subsequently employed worldwide, markedly during the 1950s and 1960s (Meyer 2017), when the search for structural and construction efficiency led to the production of numerous examples of innovative buildings (Fig. 4.1).

1955

Assembly Hall at UNESCO
Paris, France (1953–58)
M. Breuer, B. Zehrfuss and
P. L. Nervi
reinforced concrete

Gunma Music Center
Takasaki, Japan (1955-61)
A. Raymond
reinforced concrete

Chiesa San Luca
Roma, Italy (1956)
Studio Passerelli and R. Morandi
reinforced concrete

Stabilimento Raffo
Pietrasanta, Italy (1956)
L. Calini, E. Montuori and
S. Musmeci
reinforced concrete

Basel College of Art
Basel, Switzerland (1956-61)
H. Baur, H. P. Baur,
F. Bräuning and A. Dürig
reinforced concrete

Town Hall
Imabari, Japan (1957-59)
K. Tange
reinforced concrete

Christ Church
Bochum, Germany (1957-59)
D. Oesterlen
reinforced concrete

Chiesa Sacro Cuore
Ivrea, Italy (1958)
M.Oliveri, M. Nizzoli and A. Favini
reinforced concrete

State Farm Center
Champaign, USA (1958-63)
Harrison-Abramovitz
and Ammann & Whitney
reinforced concrete

Trauerhalle Westhausen
Frankfurt, Germany (1958-63)
G. Bock and O. H. Hajek
reinforced concrete

Independent Congregational Church
Florissant, USA (1959-61)
Manske & Dieckmann
timber

1960

Saint John's Abbey Church
Collegeville, USA (1961)
M.Breuer and P. L. Nervi
reinforced concrete

Church Santo Antonio da Polana
Maputo, Mozambique (1962)
N. C. Lopes
reinforced concrete

U.S. Air Force, Cadet Chapel
Colorado Spring, USA (1963)
W. Netsch of S.O.M.
steel

Guardian Angel Cathedral
Las Vegas, USA (1963)
P. R. Williams
reinforced concrete

1965

Cinema in Kongsberg
Norway (1965)
Ø. Ljøterud, E. Odegaard
and S. Jystad
reinforced concrete

Tagore Memorial Hall
Ahmedabad, India (1965)
BV Doshi, Mahendra Raj
reinforced concrete

Saint Paulus Church
Neuss, Germany (1966-68)
F. Schaller and S. Polonyi
reinforced concrete

Teatro Regio
Torino, Italy (1963-73)
C. Mollino, S. Musmeci, and F.
Bertone
reinforced concrete

Sports Centre
(unbuilt)
Jeddah, Saudi Arabia (1967)
J. Utzon and M. Walt
reinforced concrete

Pilgrimage Church
Neviges, Germany (1968-72)
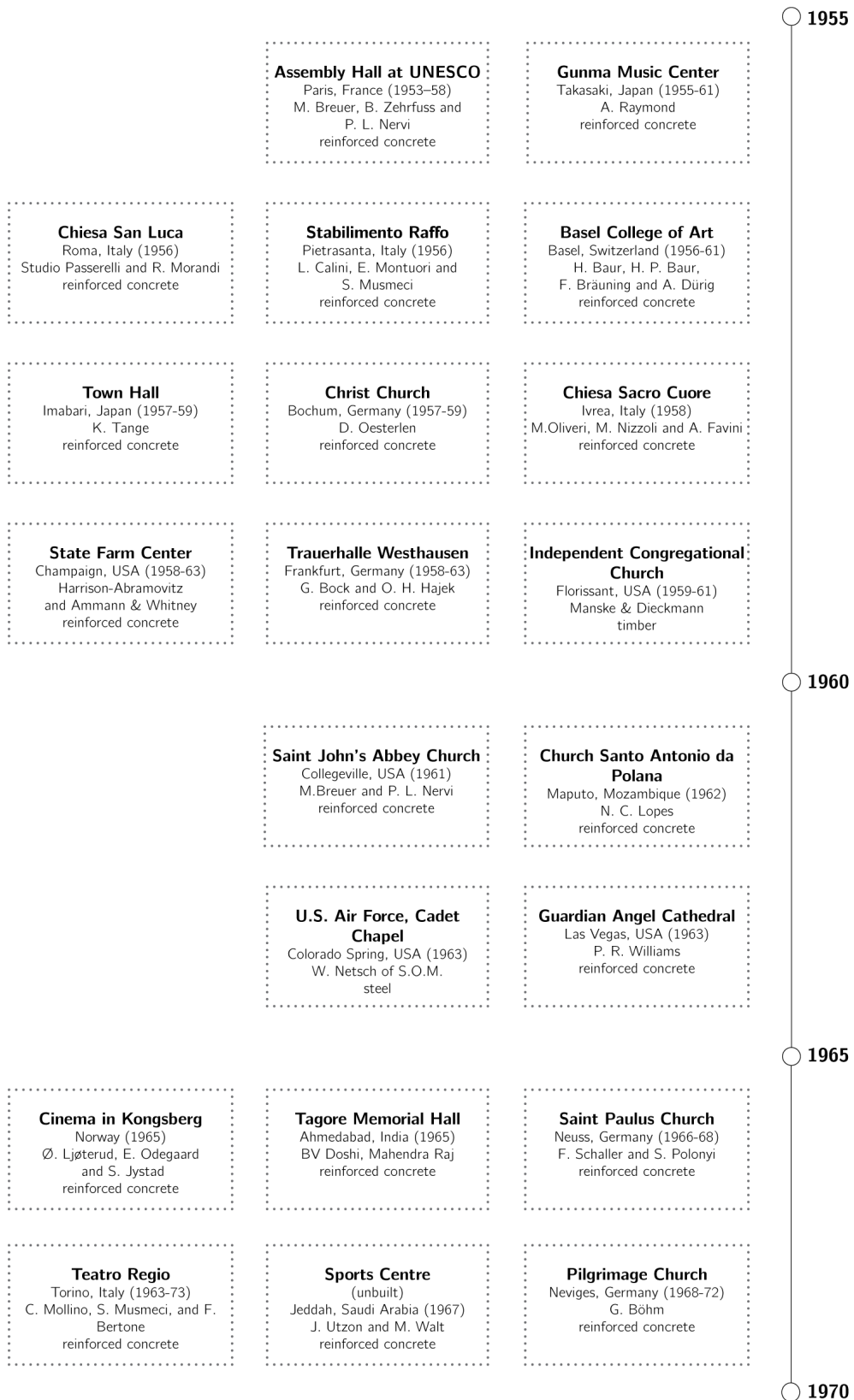G. Böhm
reinforced concrete

1970

Figure 4.1: Overview of some of the most relevant folded plate structures built during the 1950s and 1960s worldwide, including churches, conference halls and sports centres.

4.1.1 Structural Folding in Post-war Italy

The proliferation of folded plate structures is particularly evident in the structural engineering production of Italy in the post-war period. At the end of World War II, Italy experienced an important advancement in both fields of architecture and civil engineering. On the one hand, the rapid economic development of the post-war years supported a dramatic expansion of the building industry, which resulted in the deployment of many new real estate interventions and infrastructural projects (Ingold and D'Acunto 2017). On the other hand, the lack of availability of new manufacturing techniques and materials of the period preceding the war, still impaired the building sector (Poretti 2008). To overcome these limitations, structural engineering was pushed to search for new structural typologies, mainly experimenting on new uses of reinforced concrete (Iori 2011). This exploration was supported by the adoption of new building technologies, such as prestressing and prefabrication, other than the application of the principle of resistance through form (Poretti 2010; D'Acunto and Ingold 2016).

The resort to structural folding in the work of some of the most prominent engineers of post-war Italy, such as Nervi (1891–1979), Morandi (1902–1989), Favini (1916–2012) and Musmeci (1926–1981), bears witness to the search for structural and construction efficiency of that time. The relatively extensive collection of buildings designed using folded plates in Italy during the 1950s and 1960s offers a fundamental occasion to examine the various attitudes to the topic by the most prominent structural engineers of that period. Based on the analysis of specific projects of Nervi, Morandi, Favini, and Musmeci, a rich catalogue of structural solutions emerges, mostly in the form of *folded surface structures* (Chapter 2), in which each engineer proposes his own interpretation of the concept of structural folding.

Structural Corrugation and Prefabrication by Nervi   Nervi's Capannone alla Magliana in Roma (1946) represents one of the first examples of the application of structural corrugation in combination with early prefabrication techniques at the scale of a building. The shed (Fig. 4.2, top) of around 22.0 m by 11.5 m, which is erected by the Nervi & Bartoli construction company as a storehouse, gives the engineer the occasion to test for the first time his *ferrocementitious felt* for the creation of different types of full-scale building components (Gargiani and Bologna 2016). This innovative material system patented by Nervi in 1943 (Greco 2008, pp. 287–288), consists of two layers of steel meshes overlaid with cement mortar through mechanical compression. Hence, the steel meshes work both as reinforcement and as mould, thus allowing for the fabrication of bespoke elements. In the Capannone alla Magliana, this material system is exploited by Nervi to produce 3.0 cm-thick components with corrugated geometries (Fig. 4.2, bottom) that are able to resist locally the externally applied loads through their undulated forms (Nervi 1965). Thanks to the overall modularity of the system, a
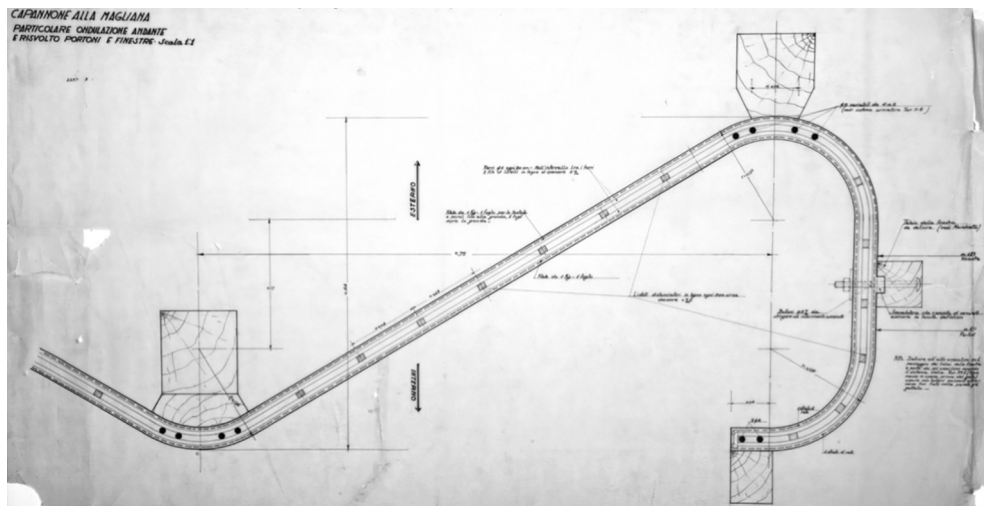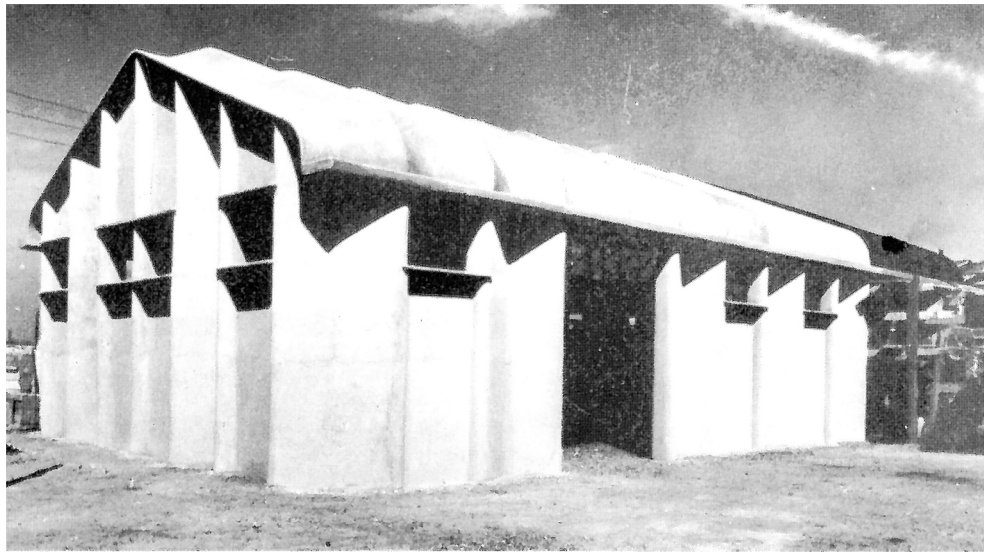
Figure 4.2: Capannone alla Magliana in Roma - Nervi (1946). (Top) Exterior view (Nervi 1965, tav. XIII). (Bottom) Detail of one of the wall components (Gargiani and Bologna 2016, p. 147; Archivio Pier Luigi Nervi - Università degli Studi di Parma, coll. 268/1).

limited amount of different component types is used for the definition of the walls and the roof of the building (Gargiani and Bologna 2016). This strategy gives, in turn, the chance to standardise the manufacturing process of the components. The tests conducted by Nervi in the Capannone alla Magliana pave the way for his later applications of *ferrocement* to larger scale projects.

The Compositional Approach of Morandi   The design of the roof of the Chiesa San Luca in via Gattamelata in Roma (1956, with Studio Passarelli) (Pedio 1959) represents for Morandi an opportunity to put forward his approach to structural folding. In order to keep an average thickness of the reinforced con-
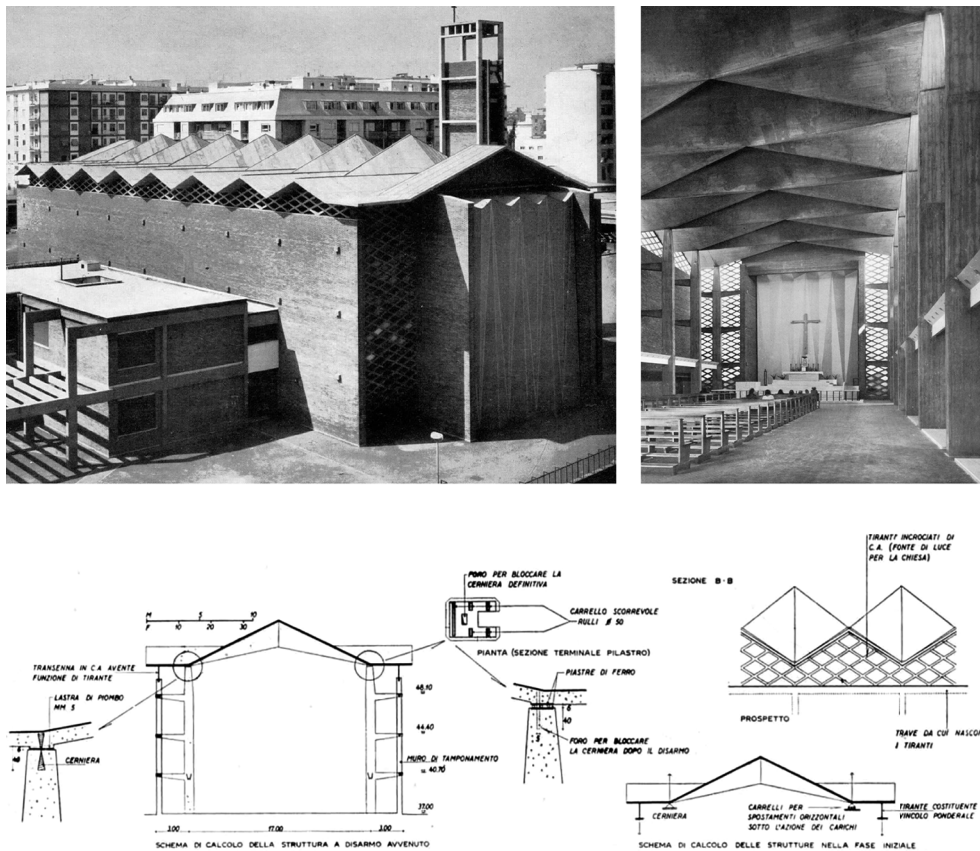
Figure 4.3: Chiesa San Luca in Roma - Studio Passerelli and Morandi (1956). (Top left) Exterior view. (Top right) Interior view. (Bottom) Details (Pedio 1959, pp. 597–599).

crete plates of 12.0 cm, Morandi develops a peculiar structural scheme, where the folded plate roof is punctually supported by intermediate pillars. The roof is then pulled down to the ground on its perimeter by a diffuse reinforced concrete cable net, which is itself anchored to perimeter walls (Fig. 4.3, top). Due to this structural composition, the pulling effect of the cable net consents to counterbalance the self-weight of the roof, thus reducing the deflection of the roof along its mid-axis. As a result, the folded plate roof can span 17.0 m between the pillars and cantilever for 3.0 m on each side (Fig. 4.3, bottom). In comparison to a conventional solution where the roof is supported directly along its perimeter, this configuration gives the chance to enlarge the space covered by the roof. Moreover, the introduction of the cable net on the perimeter of the church generates a fretwork through which the natural light can penetrate inside the church (Pedio 1959).

Prestressed Folded Plate Structures by Favini   The specificity of the approach of Favini to structural folding consists in his use of folded plate structures combined with prestressing technologies. This is particularly evident in the
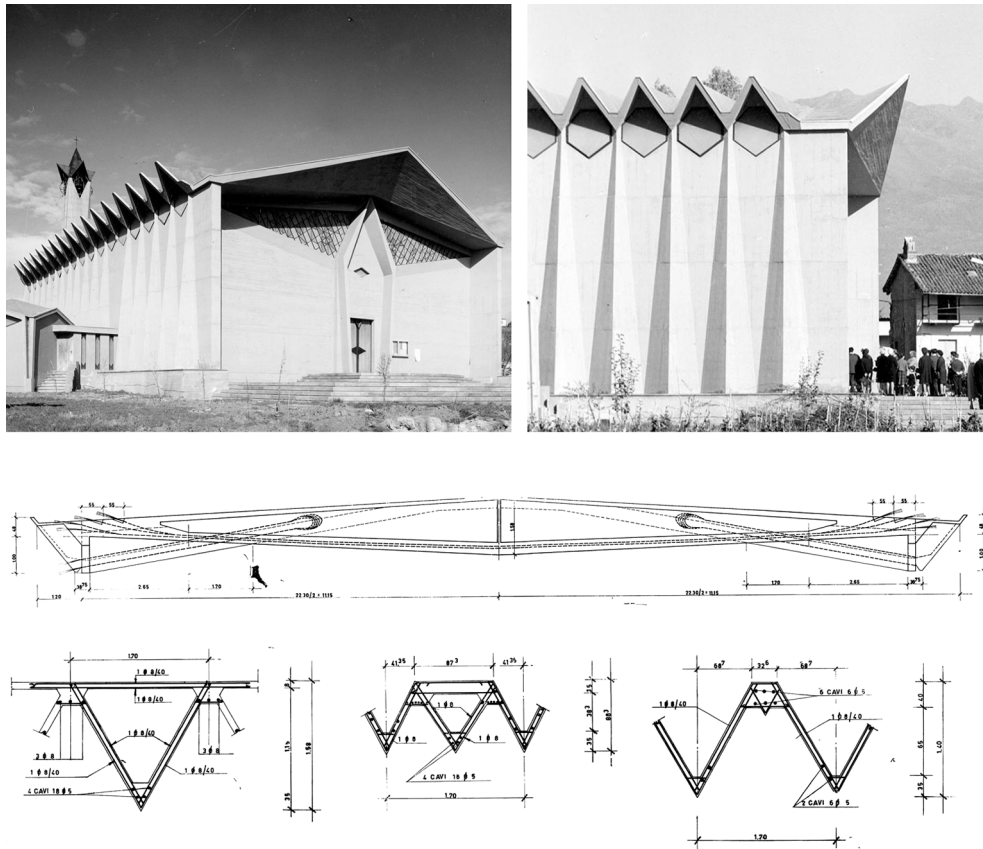
Figure 4.4: Chiesa del Sacro Cuore in Ivrea - Oliveri, Nizzoli and Favini (1958). (Top) Exterior views (Fondazione Aldo Favini e Anna Gatta, `http://www.fondazionefavini.it/opere/chiesa-parrocchiale-canton-vesco/`. Accessed 15.06.2018). (Bottom) Construction details (Favini 1962, p. 315).

project of Chiesa del Sacro Cuore in Ivrea, (1958, with Oliveri and Nizzoli). The church has a rectangular floor plan with overall dimensions of 22.3 m by 28.9 m. The structure of the reinforced concrete roof consists of seventeen identical folded plate modules that are pre-stressed and simply supported on longitudinal corrugated walls (Fig. 4.4, top) (Barazzetta 2004). The folding pattern used is the typical origami reverse fold. Each module of the roof is symmetrical about the mid-span and is made of a folded plate profile with a variable cross-section (Fig. 4.4, bottom). The section has a form of an inverted *V-shape* at the support and morphs gradually into a triangular hollow shape at mid-span, with the structural depth ranging from 140.0 cm to 158.0 cm (Favini 1962). The proprietary prestressing technology used in the roof is created by Favini himself, who patents it in 1951 and employs it in several other projects (Barazzetta 2004). Four prestressing tendons splitting into twelve cables towards the supports are allocated within each plate. Because of the variable cross-section and the use of prestressing, the thickness of the majority of the plates constituting the folded modules can be maintained constant at 8.0 cm (Favini 1962).

4.2   The Approach of Musmeci to Structural Folding[1]

Thanks to the experimental nature of his work, Musmeci holds an exceptional position within the Italian School of Engineering of the post-war period. Musmeci's peculiar view on structural design is supported by the search for novel structural forms, which is initiated by his exploration into structural folding. Contrary to the other protagonists of the Italian School of Engineering, whose remarkable experimentation with structural folding is confined to a few designs (§ 4.1.1), Musmeci explores the topic in an extended series of projects at the beginning of his professional career. These projects are emblematic of Musmeci's desire for experimentation in the field of structural design and give clear evidence of the evolution in the concept of structural folding within the design approach of the engineer. Musmeci's exploration is encompassed within the theory of minimal structures based on his life-long research on structural design involving the optimal use of materials (Musmeci 1967; Musmeci 1968; Musmeci 1971).

In particular, the engineer investigates structural folding in a series of eight roof structures in reinforced concrete. Considering the specific significance of the projects, these can be categorised within three main phases that outline a clear genealogy (Ingold and D'Acunto 2017).

4.2.1   Musmeci and his Research on Structural Folding

The first phase (Fig. 4.5, top) includes the early design experiments by Musmeci on the structural properties of folding. The design of the roof of the gymnastic hall of Scuola di Atletica in Formia (1954, with Vitellozzi) is the first occasion in which the engineer works with a folded plate structure (Vaccaro 1956). To minimise the use of materials and achieve the required static height, the engineer proposes a solution consisting in a typical accordion-like corrugated slab on a regular rectangular plan; the fold lines are parallel and oriented along the short side of the rectangle. One year later, while working on the project of Cinema Araldo in Roma (1955, with Ammannati), Musmeci designs a roof as a network of equally compressed polygonal arches spanning over a non-regular dodecagonal plan (Musmeci 1956). Plates are used here to fill the fields in-between the arches and not as the main elements of the load-bearing system of the roof.

In the second phase (Fig. 4.5, centre), Musmeci introduces a design strategy to relate the form of the folded plate structure to its static behaviour. The roofs of Stabilimento Raffo in Pietrasanta (1956, with Calini and Montuori) (Musmeci 1960) and of Cinema San Pietro in Montecchio Maggiore (1957, with Ortolani) (Morgan 1961) are designed in relation to the distribution of the bending moments within the structures. For the project of Cappella dei Ferrovieri in Vicenza (1957, with Ortolani and Cattaneo), Musmeci proposes a three-dimensional folded plate structure that is equivalent to a three-hinged

---

[1]Contents of this section have been previously published in (D'Acunto and Ingold 2016).
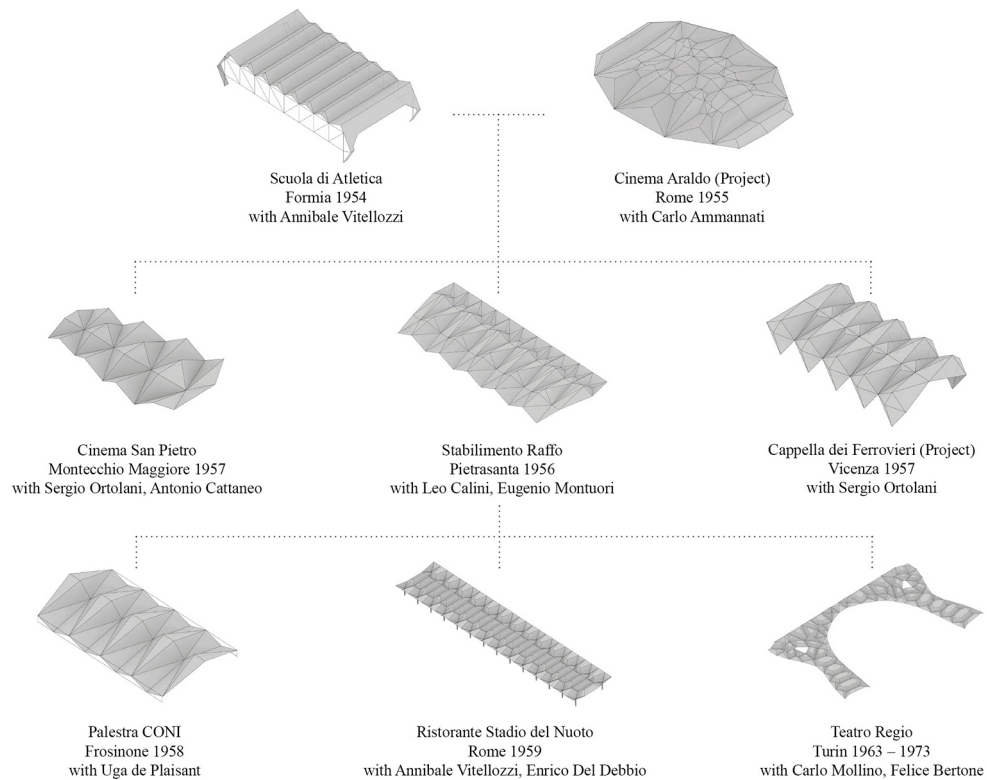
Scuola di Atletica
Formia 1954
with Annibale Vitellozzi

Cinema Araldo (Project)
Rome 1955
with Carlo Ammannati

Cinema San Pietro
Montecchio Maggiore 1957
with Sergio Ortolani, Antonio Cattaneo

Stabilimento Raffo
Pietrasanta 1956
with Leo Calini, Eugenio Montuori

Cappella dei Ferrovieri (Project)
Vicenza 1957
with Sergio Ortolani

Palestra CONI
Frosinone 1958
with Uga de Plaisant

Ristorante Stadio del Nuoto
Rome 1959
with Annibale Vitellozzi, Enrico Del Debbio

Teatro Regio
Turin 1963 – 1973
with Carlo Mollino, Felice Bertone

Figure 4.5: Genealogy of the folded plate structures by Musmeci (Ingold and D'Acunto 2017).

frame. In this case, structural folding is not limited only to the roof, but it is applied to the entire building.

In the third phase (Fig. 4.5, bottom), which is associated to the roof of Palestra CONI in Frosinone (1958, with de Plaisant), the ceiling of Ristorante del Nuoto in Roma (1959, with Vitellozzi and Del Debbio) and the foyer's ceiling of Teatro Regio in Torino (1966, with Mollino and Bertone), Musmeci explores the design of *folded volumetric structures* (Chapter 2). These roofs are different from the previous ones made as *folded surface structures* (Chapter 2) since they are composed of a combination of polyhedral cells. These examples can be considered as hybrids between folded plate structure systems and spatial trusses, and directly relate to the later interest of the engineer on antiprismatic geometries (Musmeci 1979a; Ingold and D'Acunto 2017).

4.2.2   The Design of the Roof of Stabilimento Raffo

Among the various folded plate structures conceived by Musmeci, particularly relevant is the roof of Stabilimento Raffo in Pietrasanta (1956), for the design of which the engineer develops a peculiar design methodology that is subsequently applied to other projects involving structural folding. The roof is a self-supporting slab on a rectangular plan of around 1000 m^2 with a uniform thickness of 10.0 cm

Figure 4.6: Stabilimento Raffo in Pietrasanta (1956). Interior view (Musmeci 1960, pp. 712).

Figure 4.7: Stabilimento Raffo in Pietrasanta (1956). Interior view (Musmeci 1960, pp. 713).

(Fig. 4.6). The slab consists of a *folded plate module* that is repeated five times along the longitudinal axis of the roof. It is supported by two rows of six V-shaped pillars, with a maximum span of 12.4 m (Fig. 4.7).

Musmeci devises the roof of Stabilimento Raffo in line with his belief that in the process of structural design the form and not the internal stresses should be regarded as the unknown (Musmeci 1979b). As pointed out by the engineer himself, it is not because of its dimensions or any construction principle

adopted that the roof stands out from other contemporary examples of folded plate structures. On the contrary, the uniqueness of the design solution relies on the ability of the form to express its static behaviour in an explicit, nearly diagrammatic way:

> "The roof of Stabilimento Raffo had to be built quite quickly and above all with a low budget. It had to comply with nothing else but the static requirements, defined by the free spans that had to be realized. Therefore, it was a good occasion to make a kind of experiment [...]: to see to which extent a thin vault is able to express its statics through its own form."[2]
> (Musmeci 1960, p. 712)

The aim of Musmeci is to reach a true integration between structure and architecture, where the form predominantly argues for its expressiveness through the statics; a form whose load-bearing behaviour is explicitly communicated to the observer (Brodini 2013). In fact, the roof is designed in such a way that the form follows the internal forces directly. In this way, the engineer proposes a specific design interpretation of the common principle of resistance through form and develops an explicit strategy on how to apply it to structural design. Considering the relevance given by Musmeci to this project, which reflects his peculiar attitude to structural design, Stabilimento Raffo in Pietrasanta marks a crucial moment in his research on structural folding.

The Geometry of the Roof in Plan   As highlighted in relation to the development of other projects (Adriaenssens et al. 2015), also in the case of Stabilimento Raffo, Musmeci makes use of diverse tools and models, both analytical and physical. Of particular interest is the topological study of the folded plate pattern of the roof of Stabilimento Raffo in plan, developed by Musmeci as a hand sketch (Fig. 4.8). This drawing shows a series of topological variations that share the same support conditions. By changing the position of the nodes as well as the number and connectivity of the folded edges, the engineer investigates diverse configurations, which imply different structural behaviours for the distribution of the forces within the roof.

One of the main ideas followed by Musmeci for the definition of the global geometry of the folded plate module is to activate in the roof a specific load-bearing mechanism where the principal tensile stresses are confined to the folded edges and the compressive stresses are diffused within the plates:

> "In reinforced concrete, the tensile stresses are channelled into the main reinforcement bars, and considering that these stresses tend to be confined to specific edges, it is natural to try to keep them as straight and continuous as possible. These edges are the ones that should connect geometrically the different parts of the structure, likewise a rigid truss. The intuition that along them tensile stresses run contributes to fix the form of the vault, moving away from any sense of arbitrariness. Compressive stresses have

---

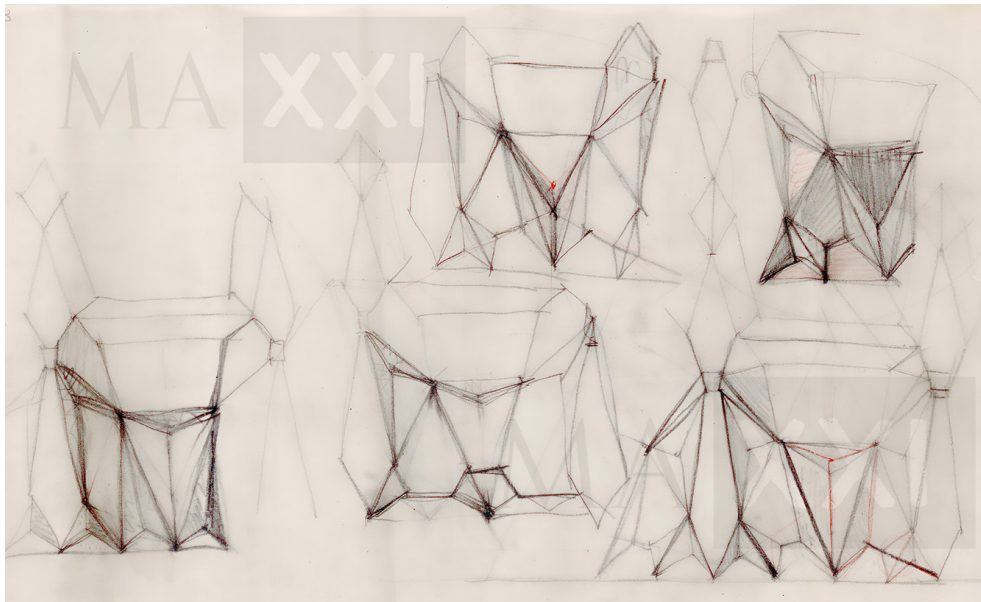[2]Translation of the quotation from Italian to English by the author.

Figure 4.8: Stabilimento Raffo in Pietrasanta (1956). Sketch of design variations of the roof plan by Musmeci (Archivio MAXXI Musmeci e Zanini, 28843 mirrored).

> always been kept in large sections of the slab in order to facilitate their diffusion and, again, with the intention of expressing this characteristic structural behaviour in the form."[3] (Musmeci 1960, p. 713)

Among the various tools used by Musmeci, remarkable is the parametric model developed by the engineer to define the geometry of the folded plate module in plan (Fig. 4.9, top). The use of this parametric model suggests a design strategy different from the conventional one, in which the geometry of a folded plate structure is generated using physical models based on an initial folding pattern (Chapter 2). Musmeci's model is built upon a two-dimensional grid, whose nodes are located at the intersection of three main vertical grid-lines parallel to the transversal axis of the roof, and four horizontal grid-lines parallel to the longitudinal axis. The main vertical grid-lines are located at the transversal axes of the V-shaped pillars, and the distance between them is represented by the constant i. Various offset distances from the main and secondary vertical lines are defined with the variables x, y, z, and t. The main horizontal grid-lines coincide with the two longitudinal axes of the V-shaped pillars and the projections of the two overhanging roof edges. The distance between the axes of the V-shaped pillars is described by the parameter b. The two asymmetric overhang lengths are designated with the variables a and c respectively. An additional variable u is used to set the distance of two secondary horizontal lines offset from one of the pillar's axis; the variable v is used to set the distance of another secondary horizontal line that is offset from the other pillar's axis. Grounded on this set-up, the projection in plan of each edge of the folded plate module is represented by

---

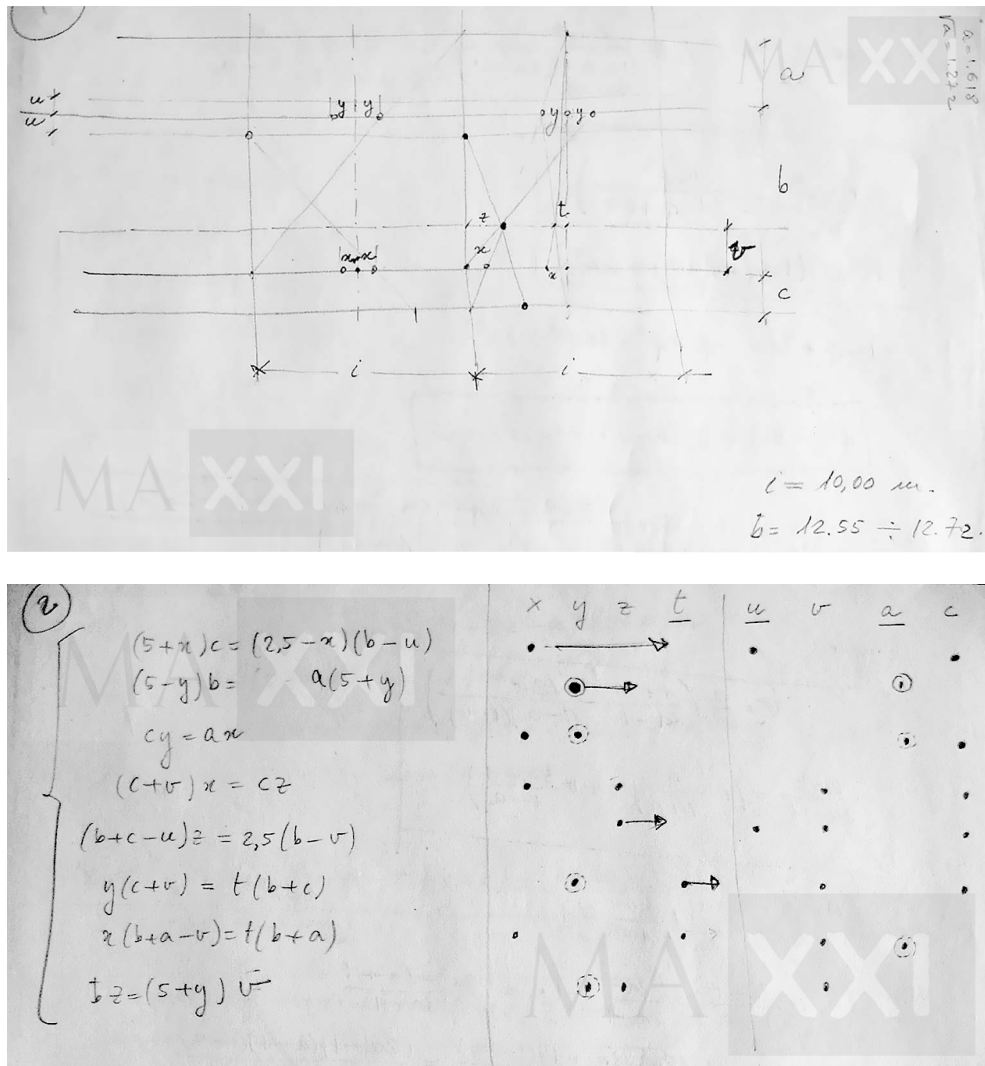[3]Translation of the quotation from Italian to English by the author.

Figure 4.9: Stabilimento Raffo in Pietrasanta (1956). (Top) Parametric model used by Musmeci to describe the geometry of the folded plate module of the roof (Archivio MAXXI Musmeci e Zanini, 023.F12-7). (Bottom) System of equations used by Musmeci to control the parametric model (Archivio MAXXI Musmeci e Zanini, 024.F12-7).

a segment that connects two nodes of the grid. A series of relationships on the slopes of the segments is then established by Musmeci in an analytical form. This leads to the definition of a system of eight independent equations in eight variables and one parameter (Fig. 4.9, bottom). By conveniently reworking the equations, the variables x, y, z, and t can be expressed as functions of u, v, a, b, c, and i; by allowing the parameter b to vary within its domain, the space of the solutions of the system can be explored.

The Geometry of the Roof in Elevation In parallel, the diagram of the distribution of the bending moments on the transversal section of the roof (Fig. 4.10, top) is used as a guideline to arrange the folded edges in elevation (Musmeci
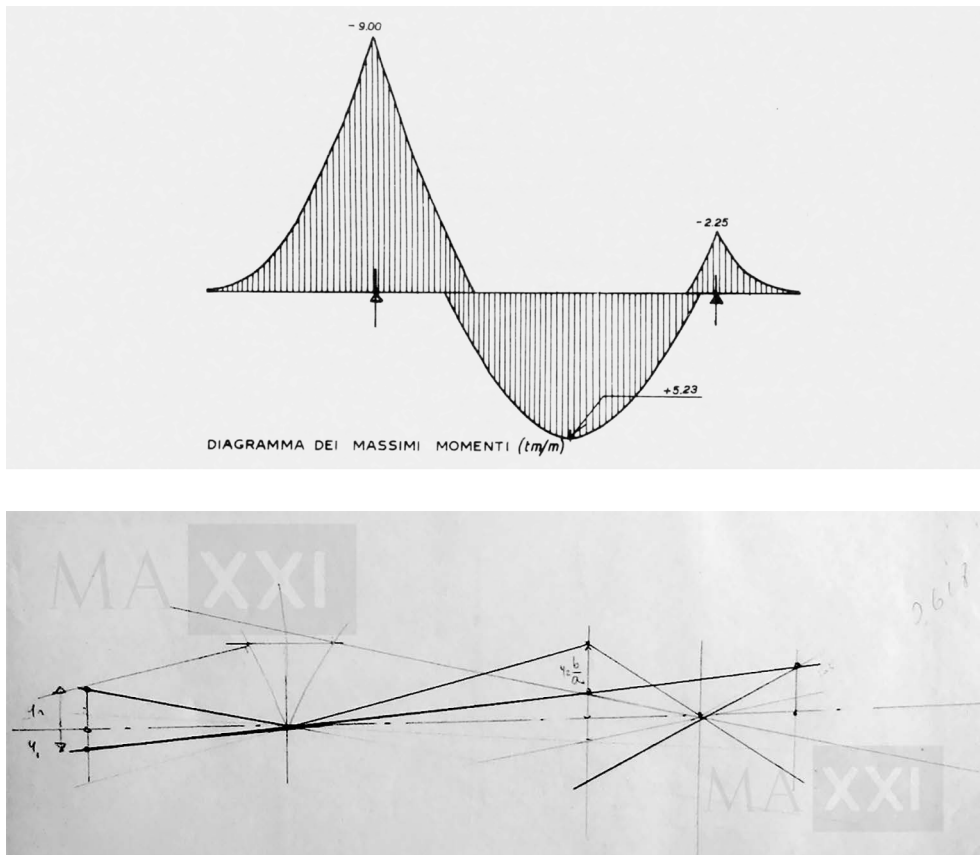
Figure 4.10: Stabilimento Raffo in Pietrasanta (1956). (Top) Diagram of the maximum bending moments on the transversal section of the roof (Musmeci 1960, p. 710). (Bottom) Construction of the transversal section of the roof (Archivio MAXXI Musmeci e Zanini, F12-7).

1960), with the aim to achieve a uniform distribution of the bending stresses within the structure. In the diagram, the transversal section of the roof is outlined as a continuous beam on two pin-jointed supports with asymmetric overhangs. The position of the supports and the length of the overhangs are related to the previously described parametric model of the roof in plan.

The diagram shows the envelope of the bending moments generated by a series of uniformly distributed vertical loads. Giving a design interpretation to the principle of resistance through form, the engineer adjusts the elevation of the nodes of the folded plate module in relation to the variation of the bending moments (Fig. 4.10, bottom). That is, the distance between the portion of the folded plates under tension and the one under compression is adapted by Musmeci to relate to the magnitude of the bending moments along the transversal axis of the roof. As a result, the distribution of bending stresses within the folded plate structure is kept relatively uniform, allowing the engineer to adopt a plate thickness of 10.0 cm all over the roof. In fact, this approach could be regarded as an early example of form-finding based on mathematical models (Ingold and Rinke 2015).
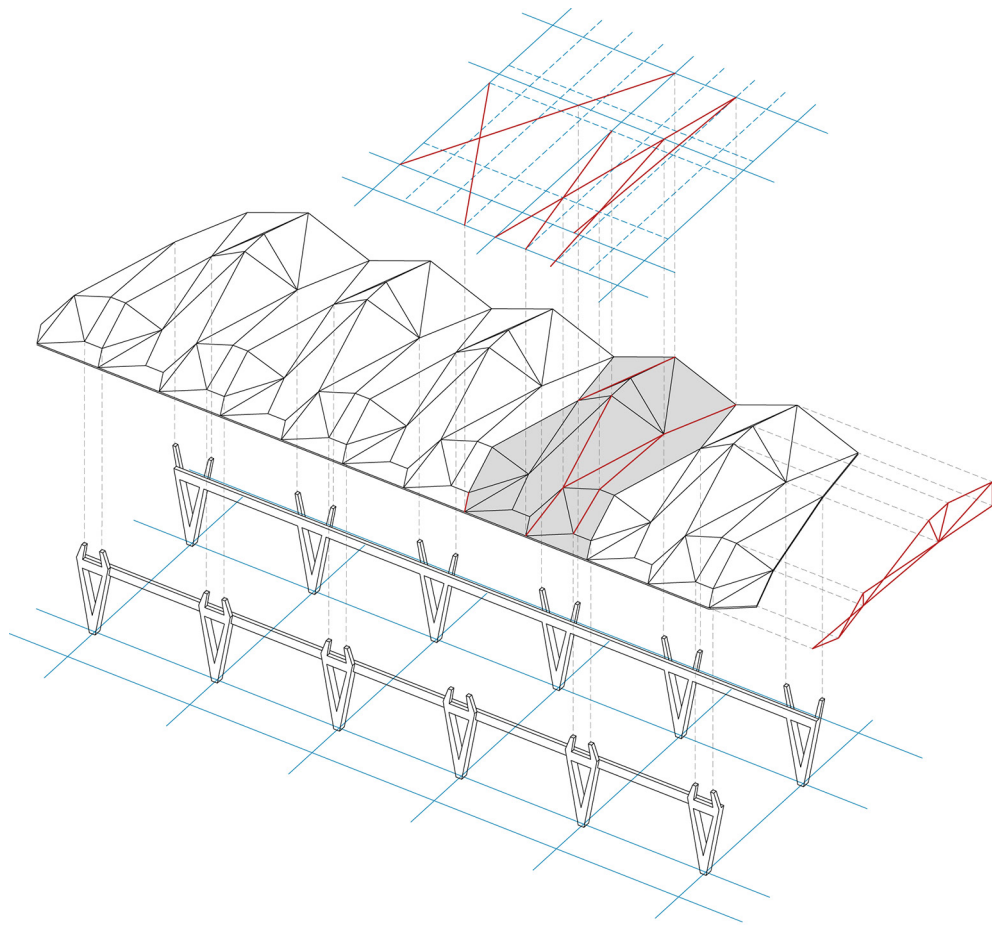
Figure 4.11: Stabilimento Raffo in Pietrasanta (1956). Axonometric diagram of the roof constructed from the projections of the roof in plan and elevation (D'Acunto and Ingold 2016).

The Final Geometry of the Roof   Grounded on the projections of the folded plate module of the roof in plan and in elevation, the geometry of the roof in three-dimensions can be derived through a series of geometric constructions (Fig. 4.11). To visualise the complex geometry of the roof in space, Musmeci eventually makes use of a physical model (Fig. 2.2, top), which is assembled as a non-developable surface conforming to the geometry generated using the previously described parametric model.

As shown in the final plan of the roof depicting the layout of the reinforcement (Fig. 4.12), according to the design intentions of Musmeci, the positioning of the primary reinforcement bars is directly related to the geometry of the roof. That is, the tensile stresses of the structure are confined to specific edges of the folded plate module, while the principal compressive stresses are allowed to spread on wide sections of the slab. In this way, the form of the roof expresses its static behaviour explicitly.
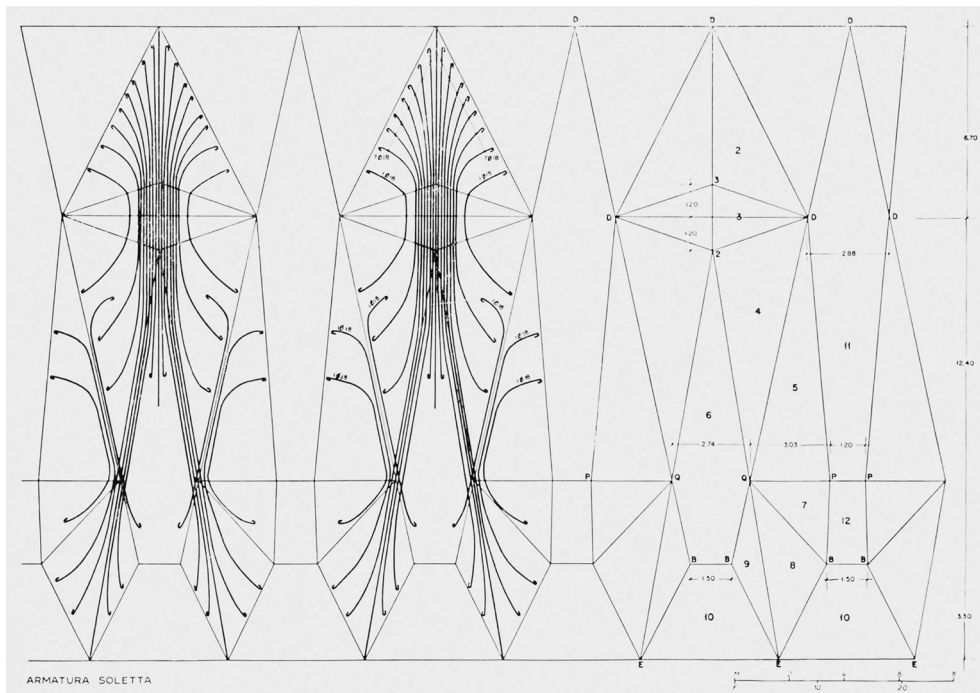
Figure 4.12: Musmeci: Stabilimento Raffo in Pietrasanta (1956). Final plan of the roof with the main reinforcement layout (Musmeci 1960, p. 711)

A Design Methodology for Folded Plate Structures   With the project of Stabilimento Raffo, Musmeci brings forward an approach for the design of folded plate structures based on parametric models. The folded geometry of the roof is designed in three dimensions using projections. This is possible considering that the roof is a modular *folded surface structure* and thus can be easily described in plan and elevation. The approach of Musmeci differs from the more conventional one that relies on the use of physical folding. Thanks to this procedure, unnecessary constraints such as rigid-foldability and developability of the geometry can be neglected entirely as not relevant considering the scope and the scale of the design. Additionally, specific structural and architectural constraints can be implemented directly and controlled in the parametric model in the form of geometric relationships. This design methodology can be directly applied to any folded plate structure whose geometry can be described by means of projections.

Although the design of Stabilimento Raffo achieves an integration between engineering requirements and architectural expression, due to the simplicity of the architectural programme, the project does not completely explore the potentials of folding as a strategy for space making. That is, the systematic repetition of the same folded plate module along the longitudinal axis of the roof ultimately generates one single undifferentiated internal space, as typical of any modular folded surface structure.

5. The Fold and the Exploration of Space Making

5.1 The Architecture of the Fold

The use of folding in architectural design implies a wide range of applications, each of them based on a different understanding and interpretation of the concept of the fold. Folding regarded as a geometric transformation can be used to generate coherent forms that consent to address various spatial and programmatic necessities. That is, folding enables the creation of *continuous* and *differentiated* architectural shapes. It is this understanding of folding that promotes its widespread application to architectural design starting from the 1990s. This renewed interested in folding follows the first explorations on folded plate structures in the 1950s and 1960s, which as opposed were fundamentally driven by the search for structural efficiency (Chapter 4). Although these two lines of investigation are rather dissimilar since they are grounded on entirely different contexts, both of them still define applications of folding at the scale of architecture. Therefore, it is crucial to examine the topic of folding from both points of view in order to comprehend how load-bearing and spatial opportunities of the fold may be combined in architectural design.

The discourse on the role of folding in architecture is initiated in the early 1990s when the architect Eisenman introduces in the architectural domain the notion of the fold as a generator of continuity and differentiation (Eisenman 1992). The interest of Eisenman in the fold and its significance in the field of architecture derives from his reading of *Le Pli: Leibniz et le Baroque* (Deleuze 1988), published in 1988 by the philosopher Deleuze. After the first explorations of Eisenman (Eisenman 1991), folding becomes an important research topic for many architectural practices, as highlighted by the architect Lynn in the seminal publication *Folding in Architecture* (Lynn 1993b).

Le Pli: Leibniz et le Baroque In his monograph *Le Pli: Leibniz et le Baroque*, Deleuze proposes an original and multifaceted interpretation of the work of the philosopher and mathematician Leibniz (1646–1716), who is regarded by the author as the emblematic representative of the Baroque philosophy. As observed by Carpo, the majority of the work of Deleuze can be regarded as a "vast

hermeneutic of continuity" that is carried out on the base of the reading of Leibniz's metaphysics (Carpo 2004, p. 14). The focus is primarily put on the concepts of the *monads*, on Leibniz's mathematical theory of *differential calculus*, and on the various manifestations of the Baroque in the arts (Carpo 2004, p. 14). Central to the discourse of Deleuze is the notion of *variation*, which constitutes one of the pillars of Leibniz's mathematics of continuity:

> "The definition of Baroque mathematics is born with Leibniz. The object of the discipline is a *new affection* of variable sizes, which is variation itself [. . .] where fluctuation of the norm replaces the permanence of a law; where the object assumes a place in a continuum by variation." (Deleuze 1993, pp. 18–20)

According to Deleuze, variation manifests itself in the Baroque in the form of the fold: "The Baroque refers not to an essence but rather to an operative function, to a trait. It endlessly produces folds [. . .] Yet the Baroque trait twists and turns its folds, pushing them to infinity, fold over fold, one upon the other" (Deleuze 1993, p. 3). Deleuze thus regards the fold as an abstract notion rather than an actual physical entity. Its relationship to the Baroque and its application to the sciences and the arts is explicated extensively by the philosopher through a series of examples. References are found in the fields of philosophy, mathematics, architecture, music, and poetry.

Based on Leibniz's supposition that "atoms of matter are contrary to reason" (Leibniz 2001, p. 142), the world is conceived by Deleuze as a continuum constituted by folds (Laerke 2010, p. 26). These folds unfold themselves to infinity as in an endless labyrinth (Deleuze 1993, p. 6). Deleuze's conception of the world directly reflects Leibniz's mathematical assumption that a continuous curve is a succession of *differential relations (dy/dx)*, each defining the way in which the curve *varies* (Laerke 2010, p. 28). In this regard, particularly relevant is the mathematical notion of *point of inflexion*, the point of a curve where a change in the sign of the curvature takes place. This is, according to Deleuze, the "ideal genetic element" of the fold, the so-called "point-fold" (Deleuze 1993, p. 15). As highlighted by Cache (1995), contrary to the stationary points of maximum and minimum, the point of inflexion is independent of any chosen coordinate system, and therefore it is an inherent property of the curve, an "intrinsic singularity" (Cache 1995, p. 17). Consequently, the point of inflexion as point-fold becomes the epitome of variation itself.

This concept, in turn, unfolds the idea of the "objectile" (Deleuze 1993, p. 20; Cache 1995, p. 88), a new conception of the object related to Leibniz's differential calculus. Instead of representing an instance of an object, the objectile expresses all its possible variations, like a function that can yield an infinite number of objects (Carpo 2004, p. 16). Based on these assumptions, the fundamental operation produced by the Deleuzian fold is thus to generate *differentiation* while keeping *continuity* (Bouquiaux 2005, pp. 43–45).

Folding in Architecture   At the time of the discovery of *Le Pli: Leibniz et le Baroque* by the architectural community in the early 1990s, theory and practice in architecture are still largely dominated by the research on Deconstruction (Johnson and Wigley 1988). This architectural paradigm is notably marked by the collaboration between the philosopher Derrida and the architect Eisenman, and it is reflected in the architectural production of various architects of that time, including Gehry and Tschumi among others. In this context, the application of the Deleuzian fold to architecture, with its "fluid logic of connectivity", stands for an appropriate alternative to the "contradiction and conflict" of the Deconstructivist Architecture (Lynn 1993a, p. 10).

As editor of the publication *Folding in Architecture* (Lynn 1993b), Lynn explicitly acknowledges the architecture of the fold as a new pivotal tendency in the architectural domain of the 1990s (Lynn 1993a, p. 8). In his introductory essay to *Folding in Architecture*, Lynn specifically emphasises the possibilities offered by folding in architecture. The main point of his discourse is the ability of the fold to produce differentiation through variation while preserving continuity: "If there is a single effect produced in the architecture of folding, it will be the ability to integrate unrelated elements within a new continuous mixture" (Lynn 1993a, p. 9).

As observed by Lynn in the revised edition of *Folding in Architecture* (Lynn 2004), the extrapolation of the Deleuzian fold into architecture passes through two different phases. The first phase occurs in the early 1990s, and it is reflected in the projects published in the first edition of *Folding in Architecture*. In this phase, if some architects work with metaphors of folding, many others rely on actual physical models made of folded sheet materials in order to give formal architectural expression to the abstract notion of the Deleuzian fold (Lynn 2004, p. 11). That is, many of these first explorations of folding in architectural design stay confined to "literal foldedness" (Frichot 2013, p. 86).

Following the spreading of the work of Deleuze in the architectural community, during the second half of the 1990s, various avant-garde architectural practices start reflecting on the notion of folding as a design operation. In this second phase, numerous built and speculative projects are thus developed in relation to the concept of folding in architecture. As pointed out by Carpo, this second phase coincides with the rise of the digital revolution in architecture, the so-called *Digital Turn* (Carpo 2013). In this context, folding is mostly used as a formal device that allows taking advantage of the new emerging computational tools (Chapter 1). In fact, these tools permit the creation of three-dimensional shapes that transcend the traditional Cartesian geometries and consent to explore new forms of architectural space (Carpo 2004, p. 16). As a result, this phase is mostly characterised by the implementation of folding in the form of digitally generated curvilinear geometries, as a natural and direct adaptation of the mathematical notion of differential calculus to architectural design. "As the design process of 'folding' developed and became more nuanced it seemed inevitable that its aesthetic qualities would continue to rely on smooth, continuous

curvilinearity" (Frichot 2013, p. 87). The architecture of the fold can thus be regarded as the fundamental theoretical basis that establishes the ground, in the field of architectural design, for the abrupt transition from an analogue practice to a digital one (Lynn 2004). As pointed out by Carpo:

> "[. . .] the theory of folding created a cultural demand for digital design, and an environment conducive to it [. . .] If we look at *Folding in Architecture* now, we cannot fail to notice that digital technologies were then the main protagonist *in absentia*. Not surprisingly, they would not remain absent for long [. . .] In the process, folding evolved towards a *seconda maniera* of fully digital, smooth curvilinearity. Folds became blobs." (Carpo 2004, p. 16)

5.2   The Fold in the Work of Sancho and Madridejos

Within the context of folding in architecture, the investigation conducted on the fold by the architects Sancho and Madridejos represents a notable exception, as it is not mere formal experimentation. On the contrary, their work on folding emerges as a rigorous and intellectually driven exploration of the implications of the fold as the generator of architectural space (García-Abril 2003, p. 1). As highlighted by the architects (Sancho and Madridejos 2014, p. 6), this configures itself as actual research in the field of architectural design that eventually leads to the definition of a specific design proposition for folding in architecture.

5.2.1   The Design Approach of Sancho and Madridejos

According to Sancho and Madridejos, the notion of the fold has a specific cultural and artistic connotation and thus a significance that goes beyond the generic operation of physical folding (Sancho 2014a, p. 34). The starting point of their discourse on the use of the fold in architecture is the distinction made by Deleuze between organic and inorganic folds (Sancho 2001, p. 118). According to Deleuze, organic and inorganic matter is defined by two fundamentally different types of folds (Deleuze 1993, pp. 7–10). Hence, two types of forces are accounted for the transformation of organic and inorganic matter. As observed by Sancho, these forces are different in relation to their field of action and origin:

> "[. . .] Deleuze proposes on the one hand what he calls the forces that confront matter, the terse internal universe of matter with its intrinsic natural laws [. . .] These forces give rise to the organic fold, linked to movement, change and transformation. On the other hand, with the inorganic fold which has arisen from the subsequent presence of forces based on aims that are extrinsic to matter [. . .] we arrive at stable events [. . .] They depend on the cultural outlook or the moment in history, that are thus external, variable, changing, diverse, partial but nonetheless richer and simpler in their action." (Sancho 2001, p. 118)

Organic and inorganic folds thus entail two different meanings. The organic fold depicts the effects of an interior movement guided by natural action, such as the motion of a body, and it is not mediated by external factors. On the contrary, the inorganic fold is the result of conscious manipulation of matter to convey an abstract concept or a specific intention (Sancho 2001, p. 118).

The intellectual investigation on the fold serves to Sancho and Madridejos as a theoretical basis for the maturation of their personal understanding of the fold in architecture (Sancho 2001, p. 118). The fold used to create architectural space from a two-dimensional initial condition can be regarded as the primary object of their investigation. Based on these assumptions, Sancho and Madridejos relate their work to the Deleuzian category of the inorganic fold (Sancho 2001, p. 118). In this context, architectural space can be recognised as the result of the application of intentional rules that define how the fold is generated and deployed from two to three dimensions.

In this way, the exploration of the fold carried out by Sancho and Madridejos goes in a different direction in comparison to other theoretically informed investigations, such as the one of Eisenman. In fact, Eisenman regards folding not as a controlled design operation but instead as an incidental transformation that is applied to the architectural space as a process of morphogenesis and which "[...] presents the possibility of an alternative to the gridded space of the Cartesian order" (Eisenman 1992, p. 149).

The Fold as a Unitary Gesture   As acknowledged by the artist Chillida (Madridejos and Sancho 1996, p. 22), in the process of generating space the fold keeps unity among the different geometric elements of which it is composed. That is, the fold acts as a "unitary gesture" (Sancho 2014a, p. 12). In this way, the operation of folding enables to generate simultaneously a continuous yet differentiated space. At the same time, the folded geometry resulting from this space making process has inherent structural properties (Sancho 2014a, p. 34), which allow the geometry to resist the applied loads through its form (§ 4.1). As a result, the fold creates both space and structure.

Types of Folds   Starting from the second half of the 1990s, the fold is explored by Sancho and Madridejos in a series of projects that bear witness to the evolution in the design experimentation of the architects. The investigation of Sancho and Madridejos is characterised by two intertwined lines of research, the first one related to the use of straight folds and the second one focused on curved folds (Sancho 2014a, p. 34). Within these two main categories, five basic types of folds (Sancho and Madridejos 2014, p. 36) can be identified:

- right fold: Chapel in Valleacerón (1997–2000), Church in Pintu (2000–2001), Church in Qingpu (2004–2006);
- pleat fold: 14 Viñas Winery Picón (2005–2009);

- curved fold-cupola: Arts and Technology Centre in Segovia-Artistic Centre (2008–2014), Technology Centre in Zamora (2012), Madrid Business School Auditorium (2012).

- curved fold-void: Arts and Technology Centre in Segovia-Entrepreneur Centre (2008–2014);

- curved fold-dome: Swimming Pool in Cantalares (2006–2014), Chapel in the forest, Madrid (2012).

The *right fold* and *pleat fold* are produced by folding along straight fold lines. The former implies the generation of actual architectural space in the form of a *folded volumetric structure* (Chapter 2); the latter defines a pleated surface as a *folded surface structure* (Chapter 2), that can be deployed, for example, to envelop an architectural space.

The *curved folds -cupola*, *-void*, *-dome* can be regarded as three different implementations of curved folding, which relies on curved creases in place of straight fold lines. In the first case, the fold can be used, for example, as a ceiling that covers an architectural space. In the second case, the fold can be employed to define the boundary of a spatial void within the solid mass of a building. In the third case, the fold can be regarded as a surface structure that encloses an architectural space.

The Design Process of Sancho and Madridejos   The design process suggested by Sancho and Madridejos for the creation of their architectural projects generally relies on the use of physical models made out of initially planar sheets of material. The initial step of the process consists in the definition of the "base-fold", which constitutes for the architects the primary driver for the development of a project (Sancho 2014b, p. 64).

Among the different types of folds, particularly relevant is the *right fold*, being the type of fold that Sancho and Madridejos have employed starting from their initial investigations on folding. It is produced by defining a series of fold lines and straight cuts on a single planar sheet of material. Based on this operation, a series of polygonal faces are created onto the sheet, whose edges are represented by the fold lines and the straight cuts.

The fold enters the third dimension and gains its spatiality through a rigid folding transformation of the initially planar sheet, after the application of external forces (Sancho 2014a, p. 35). During this transformation, the fold lines behave as hinges, around which the initially coplanar polygonal faces of the sheet rotate rigidly, each of them along a well-defined trail. In this process, the pair of edges generated by each straight cut, initially aligned, separate from each other and fold into space to produce the contour of a polygonal opening. As observed by Sancho, this process implies an original approach to design where a two-dimensional operation is used to control a three-dimensional form: "So,

slicing a plane means drawing in space, opening an incision that folds in response to the external stress" (Sancho 2014a, p. 35). As a result, a partially enclosed space is created. The enclosure of the space is then completed by combining the base-fold with additional folds (Sancho and Madridejos 2014, p. 44).

Since the fold is generated out of a rigid transformation, the edges keep their lengths invariant while folding and their vertices are constrained to follow specific path curves in space within a single global movement. As outlined by García-Abril, the result of this folding transformation is a geometry with strong three-dimensional qualities and unexpected formal connotations:

> "The shapes lack intrinsic meaning, though we may subconsciously guess at associations with artistic models and references that stimulate our imagination and confront the values of the creative system used. This creative system is their justification and represents the scientific skeleton of their architecture. The structure's lines can be logically deduced as the trail left by the points as they move through space, releasing the folded planes from their potent geometry and totally destabilising former conceptions of handling space." (García-Abril 2003, p. 2)

The resulting spatial configuration is directly determined by the initial layout defined on the planar sheet. Therefore, the number and connectivity of fold lines and straight cuts can be used as parameters to define the topology of the fold. For a given topology, the lengths of the fold lines and straight cuts and the angles between them can be used as parameters to control the actual geometry of the fold, and the space thereby generated, in terms of proportions and dimensions. In fact, once these parameters are defined, as observed by the architects, a "set of relationships" among the different elements constituting the fold is established, which in turn affects the way in which the fold is deployed into space (Sancho and Madridejos 2014, p. 43).

The creation of an architectural space from a fold is an iterative process (Sancho 2014b, p. 64). At each iteration, the initial planar layout has to be adjusted and its deployment in three dimensions tested. Each design instance is thoroughly evaluated, with regard to the specific spatial qualities produced by the fold, until the sought architectural aims are achieved. In this process, the geometric parameters are continuously varied, and a family of different folded geometries that share the same topology is created.

During the design process, various internal and external variables are taken into account, such as the materiality, the scale, the relationship with the landscape and with the light, all having a crucial influence on the spatial configuration of the fold (Sancho and Madridejos 2014, p. 50). As pointed out by García-Abril: "Sancho-Madridejos' work clearly seeks to be expressive, and this makes it possible for them to create by using a simple set of rules they have established in advance [...]" (García-Abril 2003, p. 1). Nevertheless, as acknowledged by Sancho, this process cannot be formalised in a linear design method and systematically applied to every design project (Sancho and Madridejos 2014, p. 6).

It is rather the result of continuous design exploration, in which some ideas are fully developed into real projects, and other ones are kept in the state of design experiments in progress, like in a "working laboratory" (Sancho and Madridejos 2014, p. 6).

The Role of the Structure in the Design Development   When approaching the design of folded forms using physical folding, the kinematic stability of the generated geometries is obtained by fixing the structural mechanism produced after the folding operation is applied (Chapter 2). The folded forms designed by Sancho and Madridejos using physical models have evident structural integrity since they comply with the principle of resistance through form (§ 4.1). Considering the size and proportions of the individual folds and the loads that they have to withstand, the folds are classified by the architects according to their structural capacity (Sancho and Madridejos 2014, p. 52).

The design process put forward by Sancho and Madridejos does not consider the use of explicit structural variables in the actual definition of the folded geometries, as seen, for example, in the approach suggested by Musmeci (§ 4.2). In that case, structural parameters such as the distribution of the internal forces and their relation to the designed folded forms were part of the initial design concept. The internal stresses within the folded forms created by Sancho and Madridejos are assessed after a first instance of the global geometry has been first set. This analysis is performed using structural simulations based on the finite element method (FEM) (Sancho and Madridejos 2014, p. 52).

5.2.2   The Chapel in Valleacerón

The *right fold* is applied for the first time by Sancho and Madridejos in the design of the Chapel in Valleacerón, Ciudad Real (1997–2000). It is then further explored and developed for the design of the Church in Pintu (2000–2001) and the Church in Qingpu (2004–2006).

The Chapel in Valleacerón represents the most emblematic building where the architects explore the architectural opportunities of folding as an operation for space making (D'Acunto and Castellón 2015). In fact, the chapel effectively exemplifies all the qualities that Sancho and Madridejos recognise in the architecture of the fold, among all its inherent spatiality:

> "The project at Valleacerón, [. . .] embodies a desire to draw us into the architectural space from this constructive sense of the fold, from its spatiality. The chapel unit concentrates this aims in a radical way, almost in the form of a manifesto." (Sancho 2001, p. 120)

The chapel, which is part of a series of four buildings,[1] is an isolated architectural object located at the top of a hill, and it has overall dimensions of

---

[1]Other than the chapel, the project includes a villa, a hunting pavilion and the guard's residence (Sancho and Madridejos 2003, p. 9).
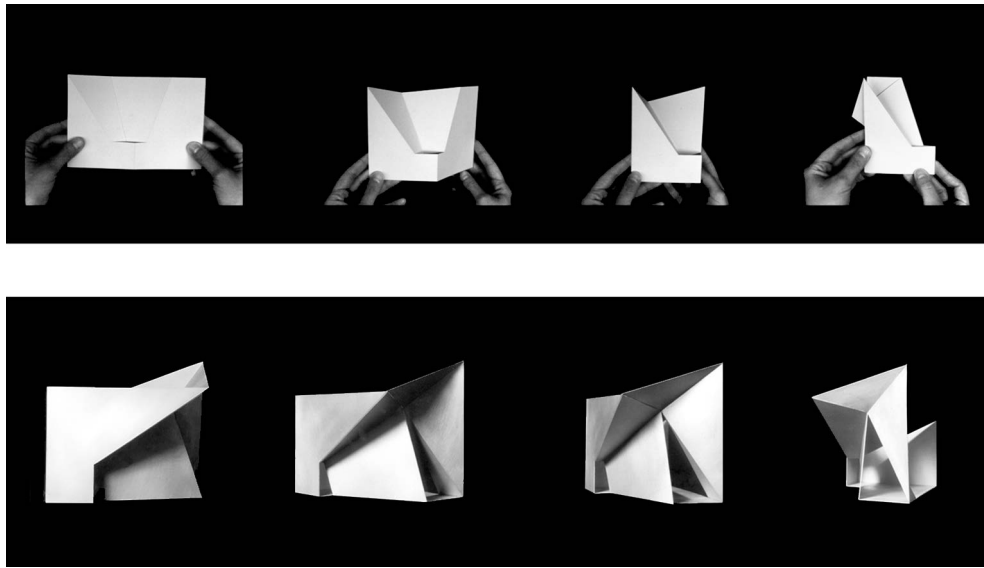
Figure 5.1: Chapel in Valleacerón (1997–2000). (Top) Definition of the base-fold using a paper model. (Bottom) Physical model of the final proposal (*Chapel in Valleacerón - S.M.A.O.* Arch-Daily, 30.04.2009, `https://www.archdaily.com/20945/chapel-in-villeaceron-smao/`, ISSN 0719-8884. Accessed 25.05.2018. Photos: Sancho-Madridejos Architecture Office).

11.2 m by 8.4 m in the floor plan and 10.6 m in elevation. As explained by the architects, the chapel is built around the concept of the "box-fold" (Sancho 2001, p. 121), which consists in a right fold that is inserted within a box. This approach produces a folded geometry that can be regarded as a *folded volumetric structure* (Chapter 2). The connection between the fold and the box establishes a definite duality between an architecture constituted by edges and planes, and an architecture defined by volumes (Sancho 2014a, p. 34).

The creation of the base-fold and its correlation to the box are the result of extensive experimentation developed by Sancho and Madridejos using physical models (Fig. 5.1). After the topology of the fold is determined, various initial layouts of the unfolded sheets are tested until the desired relationship among the different elements constituting the fold is achieved. The physical models are especially used by the architects to control the space generated by the combination of the folded geometry and the box. In parallel, a series of three-dimensional diagrams are employed to define the spatial articulation of the folded geometry within the box and to specify its overall proportions and dimensions (Sancho and Madridejos 2014, p. 100).

The Architectural Expression of the Fold   The design approach used by Sancho and Madridejos eventually leads to the generation of a building that presents fundamentally different formal qualities on its various exterior sides. Based on the point of view from which the building is observed, the chapel appears either as a massive enclosed volume, thus suggesting the idea of a static Cartesian
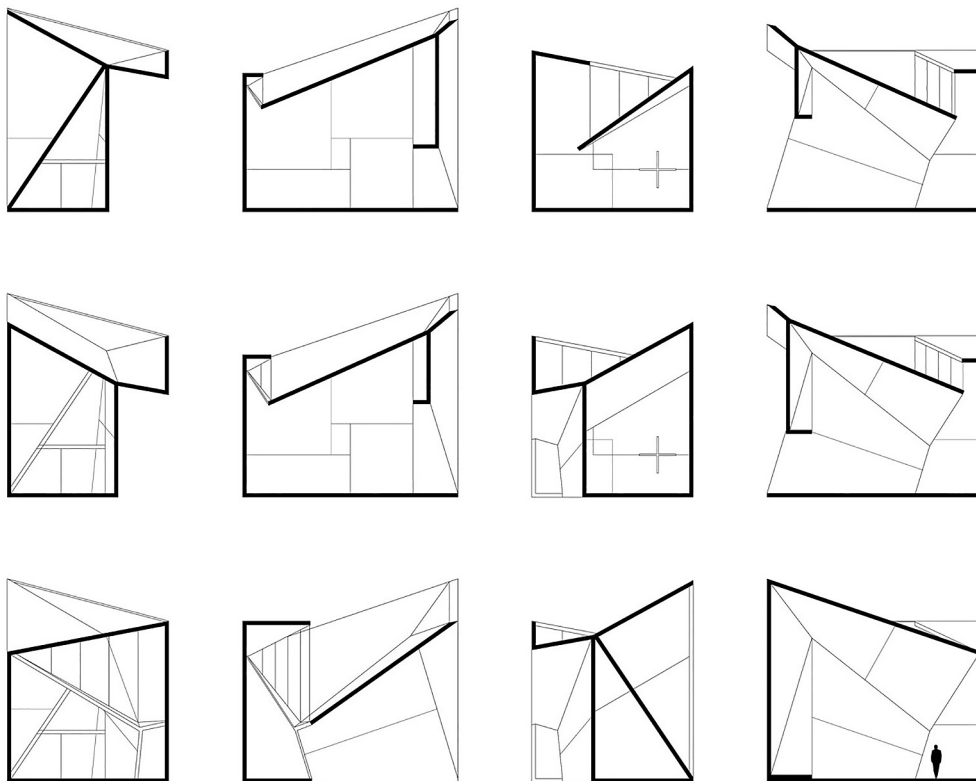
Figure 5.2: Chapel in Valleacerón (1997–2000). Sections of the building expressing its spatial differentiation (*Chapel in Valleacerón - S.M.A.O.* ArchDaily, 30.04.2009, `https://www.archdaily.com/20945/chapel-in-villeaceron-smao/`, ISSN 0719-8884. Accessed 25.05.2018. Diagrams: Sancho-Madridejos Architecture Office).

geometry or as a lightweight open surface articulated in space, which indicates the presence of a dynamic architectural object (García-Abril 2003, p. 2).

This duality is made explicit to the visitor along the path that gives access to the chapel. In fact, the path runs around the building and enables the visitor to experience it from various perspectives (Sancho and Madridejos 2003, p. 11). The formal differentiation between the various sides of the building, however, does not entail the idea of disconnection. The negotiation between the antipodal architectural conditions that are present in the building is due to the unifying effect of the fold, which connects the different parts of the chapel into one single architectural system (García-Abril 2003, p. 2).

The continuous variation of the space is reflected in the sections of the building (Fig. 5.2), which underline highly differentiated spatial conditions due to the presence of the folded geometry (García-Abril 2003, p. 2). In fact, the topological articulation of the space and its proportions change dramatically from one section to another, while preserving the continuity of the building envelope. The perception of the inner space of the chapel varies constantly based on the diverse natural lighting conditions that can be experienced throughout the

day (Sancho and Madridejos 2003, p. 11). The box geometry protects the inner space of the chapel from the direct sunlight coming from the south. In this condition, the diffuse light coming from the opening to the north and the skylight on the ceiling illuminates the individual plates of the folded geometry in a delicate way, thus contributing to the definition of contemplative interior space. This state is wholly overturned when the direct sunlight from the west penetrates the building through its various openings. In this case, the light casts the shadows of the folded geometry and the window frames directly onto the interior walls. As a result, space is perceived as fragmented, and the interior appearance of the chapel is completely transformed (Sancho 2001, p. 121).

Integration of Space and Structure In the Chapel in Valleacerón, architecture and structure are coincident. In fact, from a structural point of view, the building complies with the principle of resistance through form. That is, the folded plates that generate the inner space of the chapel are at the same time the load-bearing elements in the structural system of the building. The structure is thus not in the background as a hidden skeleton but actively participates to the definition of the architectural space. In this regard, the project shows a coherent synthesis between structural and architectural solutions.

6. Current Methodologies of Folding in Architecture

The current investigations on the application of folding at the scale of architecture are generally oriented towards the independent analysis of specific aspects of the topic such as structural efficiency, formal expression, or manufacturing processes. Moreover, most of the existing research is focused on *folded surface structures* (Chapter 2), while the spatial and structural potentials of *folded volumetric structures* (Chapter 2) are not yet entirely explored.

This chapter presents a brief review of current methodologies for the design of folded plate structures in architecture. The review is specifically focused on those approaches where architectural and structural inputs are both used as part of the design process.

Parametric Design of Folded Plate Structures In his doctoral thesis, Buri (2010) explores a strategy for the design of folded plate structures that can be subsequently built with cross-laminated timber panels in the form of *folded surface structures* (Chapter 2). Different geometric configurations inspired by traditional origami folding patterns, including the diamond, herringbone, and diagonal ones (Chapter 2) are first analysed in terms of structural and spatial potentials. These configurations are then reproduced within a three-dimensional digital modelling environment.

Based on the parametrisation of these models, a design tool is put forward, which extends the scope of the method and consents to generate free-form folded plate structures. The tool enables to produce complex folded geometries and adjust in real time various parameters such as the type of folds, the width of the folds, the number of folded edges, and the dihedral angles between the folds (Fig. 6.1, top) among others. The structural behaviour of the folded geometries is then evaluated numerically using the finite element method (FEM). The parametric tool is specifically used by Buri to design various folded plate structures as case studies, which are materialised using cross-laminated timber panels (Fig. 6.1, bottom).

Overall, the research of Buri provides essential findings in the field of folded plate structures, especially in relation to the use of timber plates. On the one hand, the parametric tool allows the designer to take easily advantage of the
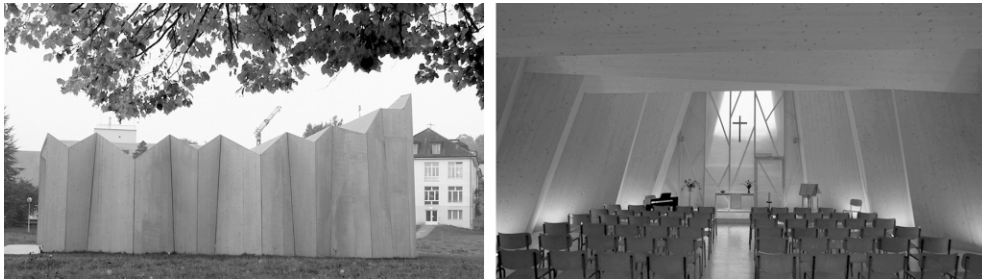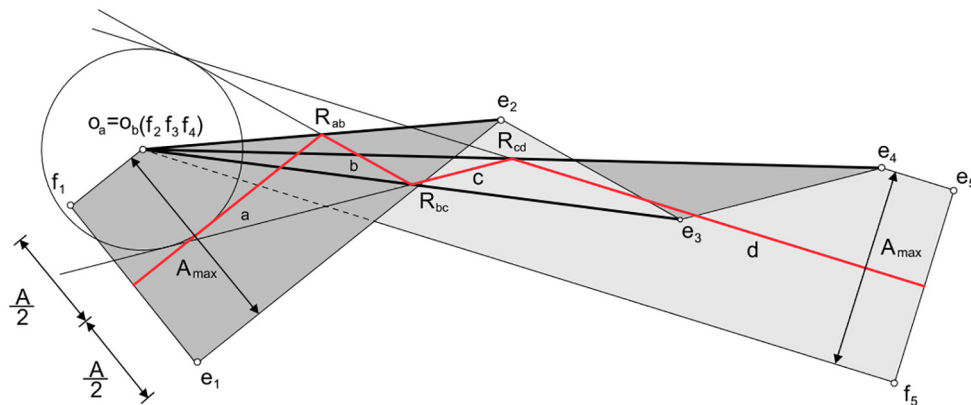
Figure 6.1: (Top) Parametric set-up showing the variables used for the modelling of a folded surface structure based on the herringbone pattern in the design method developed by Buri (Buri 2010, p. 175). (Bottom) Implementation of the method for the design and construction of the Chapel of Saint-Loup at Vaud, Switzerland (Buri 2010, p. 269, photos F. Hatt).

formal potentials of folding. On the other hand, the method proposed relies on a sequential design process in which the folded geometry is first generated and then analysed structurally with FEM simulations. Because of the use of FEM, the correlation between form and internal forces may not always be explicitly revealed.

The work of Samuelsson and Vestlund (2015) aims at exploring the possibilities of structural folding in architecture with the goal of bringing forward a design method for the creation of folded plate structures. Like in the present research, the starting point of the investigation is the assumption that folded plate structures represent an effective way to enclose space and create load-bearing systems at the same time. The work of Samuelsson and Vestlund is focused explicitly on folded surface structures. The structural properties of different folded geometries created from various origami patterns are analysed using physical models. The patterns include the diamond, the herringbone, and the diagonal ones, as seen in the research of Buri.

By referring to the theory of Wester (1984) on the duality of structures in space (Chapter 8), the static rigidity of the physical models is intuitively
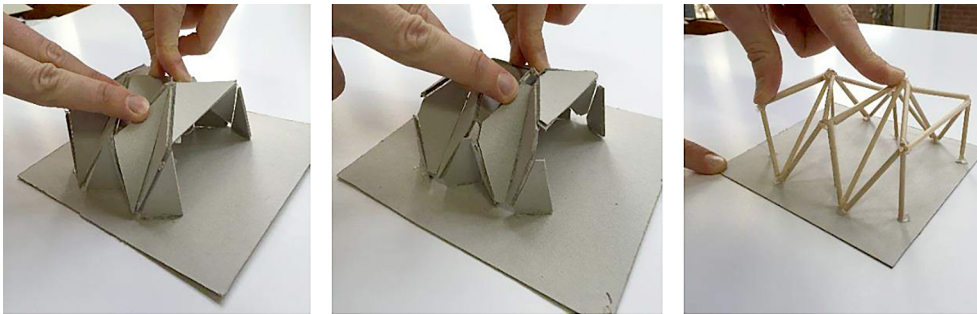
Figure 6.2: Evaluation of the static rigidity of a folded geometry generated from a diagonal pattern with respect to different structure systems. (Left) Combination of lattice and plate structure. (Centre) Plate structure. (Right) Lattice structure (Samuelsson and Vestlund 2015, p. 75).

evaluated by analysing them as lattice, plate, or combination of lattice and plate structures (Fig. 6.2). Detailed structural analysis is subsequently carried out using FEM to define the stress patterns in the folded plates under various loading conditions. The physical models are then translated into digital models and used for the definition of a parametric tool for *folded surface structures*. The tool is eventually used to design a full-scale prototype in the form of a corrugated wall.

The work of Samuelsson and Vestlund suggests an effective way to evaluate the kinematic stability of folded plate structures based on fundamental notions of static rigidity (§ 8.2.1). As in the case of Buri, the use of FEM for structural analysis does not generally provide information on how to adjust the shape of the structure with respect to the internal forces.

Similar to the work of Buri, the research of Meyer (2017) is focused on the definition of a digital toolkit (Fig. 6.3, top) for the design of pleated structural envelopes at the scale of architecture (Fig. 6.3, bottom). Like in the case of Buri, the investigation is specifically focused on the design of folded plate structures made of laminated timber panels as folded surface structures. The numerical model elaborated by Meyer is intended to facilitate the control of the geometry of pleated structures with the aim of integrating engineering requirements and architectural intentions within the design process, while taking into account also specific construction constraints.

The design method includes two main phases. In the first phase, the global geometry of the pleated envelope is set using a reference surface on which a folding pattern is applied. The reference surface and the profile of the pleating are defined directly in the three-dimensional digital model. Given a first instance of the pleated geometry, several evaluations are conducted to test the validity of the proposal according to various criteria, including structural efficiency, thermal performance, and acoustic response. The pleated geometry is iteratively modified until all the criteria are fulfilled. In the second phase, questions related to the materialisation of the geometry are taken into account. These aspects include
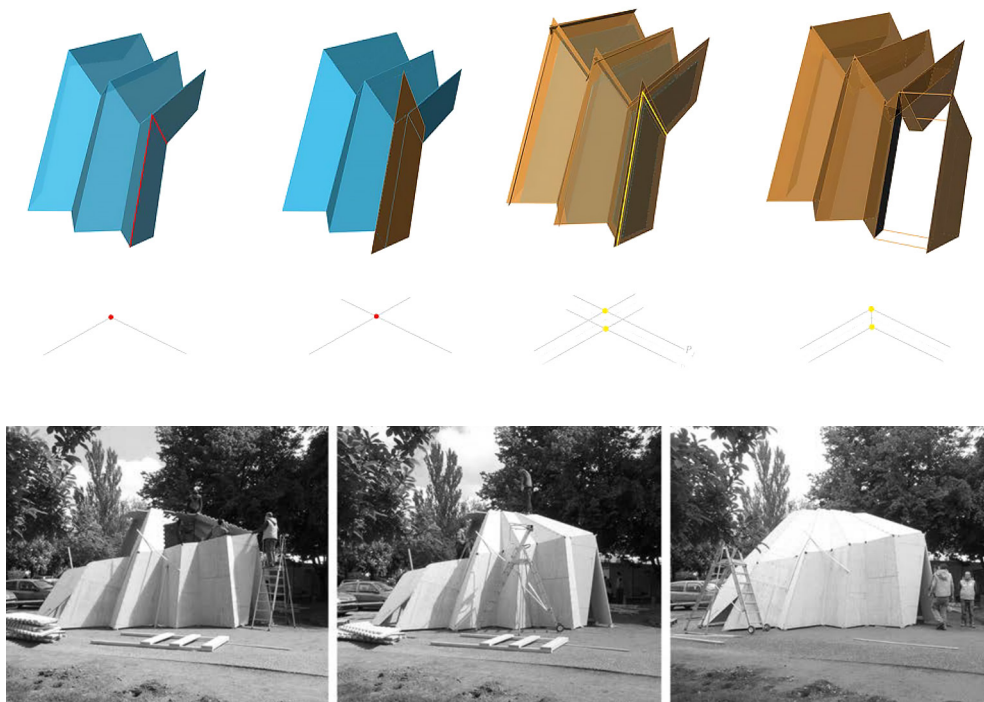
Figure 6.3: (Top) Parametric model used within the method developed by Meyer for the design of pleated structural envelopes. Adapted from Meyer (2017, p. 190). (Bottom) Full-scale prototype of a pavilion (*New-Yourte*) used by Meyer as a proof of concept of the proposed design approach (Meyer 2017, p. 129).

the definition of the thickness of the plates, the creation of the nodes, and the design of the edges of the plates based on the desired type of connection. The resulting detailed geometry is then re-evaluated and, if necessary, further refined. The implementation of the numerical model into a digital toolkit allows testing different design variations.

On the one hand, the toolkit brought forward by Meyer permits to take into account diverse aspects related to the design of pleated envelopes as folded surface structures in an interactive way. On the other hand, architectural and engineering questions are not necessarily addressed simultaneously. The evaluation of the structural effectiveness of the design solution takes place after a first instance of the global geometry of the folded surface structure is defined. In turn, such an approach necessitates a sequential procedure until the desired structural requirements are met.

Constraint-based Design of Folded Architectural Forms   The research of Tachi deals with a broad range of aspects related to origami and its application to engineering and architecture. These include, among others, the generalisation of rigid-foldable origami (Tachi 2009a) and their simulation (Tachi 2009b), the free-form variation of origami (Tachi 2010b), and the design of rigid-foldable
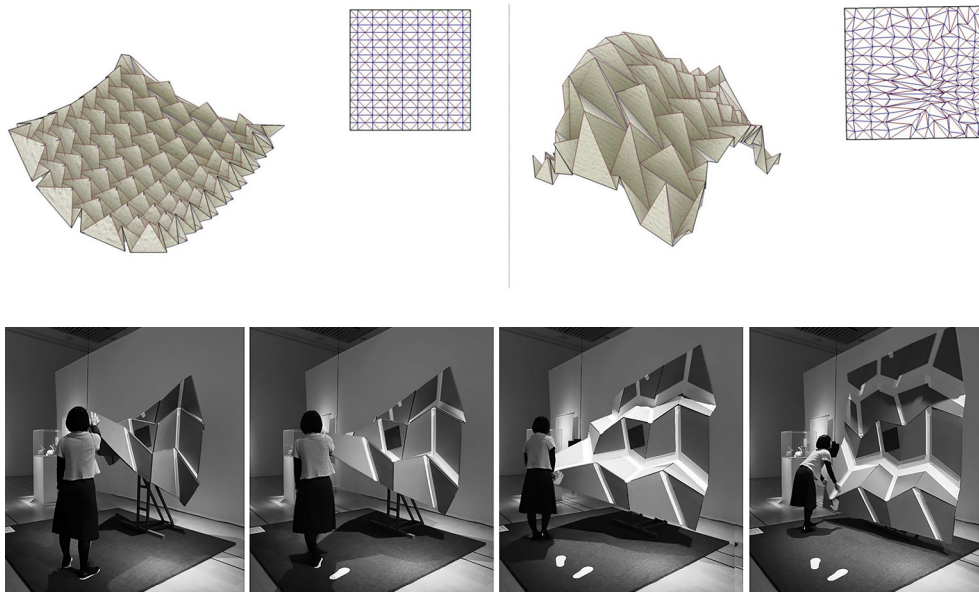
Figure 6.4: (Top) Three-dimensional simulation of free-form origami. (Bottom) Application of the design strategy developed by Tachi to the construction of an adaptable wall. Adapted from Tachi (2010a).

thick origami (Tachi 2011). Particularly relevant is the investigation on the design of architectural forms based on computational origami (Tachi 2010a). In this work, many of the individual contributions of the research of Tachi are combined together for the definition of an origami theory for design. One of the objectives of this work is to enable the design of free-form thick origami models that still comply with the inherent properties of origami, such as developability, flat-foldability, and rigid-foldability (Tachi 2010b). The solution put forward by Tachi consists in a computational tool that relies on an analytical formulation of the kinematics of origami and that incorporates the previously defined properties of origami as constraints. The computational tool can be used for the design of architectural components (Fig. 6.4) or simple architectural spaces that can be regarded as deployable mechanisms in the form of developable surfaces made of rigid panels (Chapter 2). As such, these designs are transformable, but they also perform structurally.

The approach suggested by Tachi represents a fundamental reference in the development of constraint-based computational tools for origami folding. In the current state of the research, the direct control of structural parameters is not yet completely integrated within the proposed method.

Folding as a Morphogenetic Process in Architectural Design   The concept of folding as space generator is the main focus of the design research of Vyzoviti (2003), conducted as an educational activity with architecture students at the Delft University of Technology. Built upon the understanding of folding as a pro-
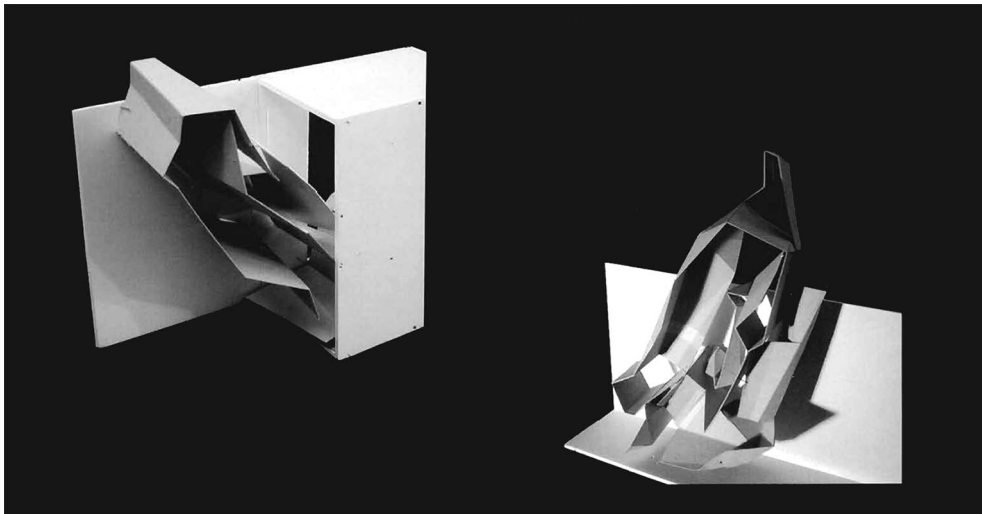
Figure 6.5: Generation of folded geometries within the design experimentation proposed by Vyzovity (Vyzoviti 2003, pp. 92–93, photo S. Vyzoviti, student: J. van Boekhold).

cess of morphogenesis in architectural design, the research investigates the topic through a series of design experiments that rely on a non-linear and bottom-up strategy. The design process consists of four phases: exploration of matter and functions; definition of folding algorithms; introduction of explanatory diagrams; construction of architectural prototypes. In the first phase, the students are asked to experiment with paper folding to get familiar with the materiality and the transformations applicable to the physical models. Multiple design operations, including cutting, are explored in combination with pure folding, leading to the creation of geometrically complex physical models in the form of *folded volumetric structures* (Fig. 6.5). In the second phase, algorithms are defined to describe the sequence of operations used to generate the physical models. In the third phase, the paper constructions are regarded as architectural models, and they are described using spatial, structural, and organisational diagrams. In the last phase, the previous diagrams are translated into architectural prototypes. In this context, folding is regarded as a medium to integrate diverse elements into a continuous but differentiated architectural formal system (§ 5.1).

The goal of the work of Vyzoviti is to formalise an operative approach for folding in which questions related to space and structure are addressed simultaneously. Due to the educational context of the research, these aspects are explored mainly at a conceptual level.

7. Research Scope

7.1 Problem Statement

The versatility of the operation of folding consents to design structures and
spaces at the intersection of the disciplines of architecture and engineering. The
analysis of current strategies for the design of folded plate structures in archi-
tecture (Chapter 4; Chapter 5; Chapter 6) has highlighted the strengths and
limitations of such approaches.

Discussion on Existing Approaches On the one hand, the experimentation
with structural folding carried out during the 1950s and 1960s (Chapter 4) has
proved that the use of folding in design allows producing efficient structures at
the scale of architecture. The examined precedents by Nervi, Morandi, Favini,
and Musmeci (§ 4.1.1) clearly demonstrate how folded plate structures can resist
the externally applied load through their form. In this regard, exemplary is the
project of the roof of Stabilimento Raffo in Pietrasanta by Musmeci (§ 4.2.2), for
the design of which the engineer developed a specific methodology to directly
correlate the form of the structure to its load-bearing behaviour. However,
this roof design and the other projects analysed in the proposed precedents
based on *folded surface structures* do not completely exploit the opportunities of
folding as a strategy for space making. In fact, these designs do not develop full
spatial solutions, where the folded plate structures can modulate and differentiate
various spatial conditions.

On the other hand, the design explorations developed through the 1990s
(Chapter 5) have proved that the use of folding in design consents to generate
architectural forms that can deal with given spatial and programmatic needs.
The analysed design approach of Sancho and Madridejos (§ 5.2.1), in particular,
bears witness to the opportunities of folding to achieve spatial differentiation
within a coherent and continuous architectural formal system. In this context,
the project of the Chapel in Valleacerón (§ 5.2.2) shows explicitly how it is
possible to attain a seamless integration between architectural intention and
structural solution within the same folded geometry. Nonetheless, it has been
observed that in those design processes which are mostly based on the use of
physical models, explicit structural parameters such as the flow of the internal

forces are not generally taken into account and used to inform the design from the initial stage.

As highlighted in relation to the current investigations on the application of folding to architectural and structural design (Chapter 6), only a few attempts have been made aiming at defining design methods for folding that address both structural and architectural issues at the same time starting from the early phase of the design process. Most of the analysed approaches take advantage of contemporary digital tools for the parametric design of the folded geometries, including the possibility to integrate additional constraints within the computational set-up. As demonstrated by the works of Buri, Samuelsson and Vestlund, and Meyer, the typical strategy in this field is to resort to a sequential process in which the folded geometry is first generated and then analysed structurally. This operation is generally executed using computer programmes grounded on the finite element method (FEM) and the theory of elasticity.

Although FEM may prove to be helpful for the analysis and dimensioning of structural elements in already defined building designs, its use during the conceptual stage of the design is somewhat debatable. In fact, the visual representations produced by FEM simulations can give at most insights on the structural performance of the analysed building, but do not explicitly suggest in which way to modify its global geometry to enhance the load-bearing behaviour of the structure (Kotnik and D'Acunto 2013). That is, through FEM analysis, the relationship between the form of a structure and the repartition of its internal forces is not revealed in a clear and diagrammatic way. As a result, FEM-based analysis is generally performed by structural engineers only in the advanced phase of the design process. However, the use of FEM to assess the performance of a structure, after the design of its geometry has been executed based on criteria different from structural considerations, is not particularly suitable to promote a dialogue between the disciplines of architecture and engineering during the first steps of the design development (Kotnik and D'Acunto 2013). In fact, this practice implies a hierarchical organisation of the tasks between architects and structural engineers (Chapter 1).

Research Questions   Building upon the above considerations, the main problem addressed in this research can be stated as follows:

- How can *spatial and structural potentials* of folded plate structures be addressed simultaneously, starting from the *initial phase of the design* process, in a consistent design method that is accessible to *both architects and engineers*?

On the one hand, the solution to this problem necessitates the development of a structural model for folded plate structures that can be easily comprehended by both architects and engineers, and that can stimulate a productive exchange between the two professions. In turn, this aspect poses the following question:

- Which formulation of a *structural model for folded plate structures* conveys a clear description of the load-bearing behaviour while intuitively showing the correlation between *form* and distribution of the *internal forces*?

From the analysis of the precedents, it can be concluded that for the correlation between the form and internal forces to be made explicit, a formulation of a structural model for folded plate structures is required that is not based on FEM and the theory of elasticity. Moreover, to allow the exploration of the spatial potentials of folding, the structural model has to rely on a geometric set-up that can be easily adapted to complex spatial configurations.

On the other hand, a design approach intended for the conceptual phase of the design process has to be flexible enough to permit the exploration of various solutions, in terms of both space and structure, in a quick an intuitive fashion. This aspect suggests the following question:

- How can a design method for folded plate structures in architecture allow testing different *design variations* in an interactive way in the conceptual design stage?

The analysed precedents suggest that a design approach exclusively grounded on the use of physical models may limit the range of design variations that can be obtained in the context of folded plate structures. In fact, physical models generated starting from origami or folding patterns generally impose a series of geometric constraints on the resulting folded geometries (such as developability, flat-foldability, and rigid-foldability) that are often unnecessary when working at the scale of architecture. This observation is valid considering that the scope of the method is the design of folded plate structures, as opposed to deployable structures or folded developable surfaces (Chapter 2).

7.2 Research Objective and Methodology

With the intention to go beyond the limitations of the existing approaches, the primary goal of this research is to define a design method that consistently integrates structural folding in architectural design. The scope of the design method is to promote a non-hierarchical exchange between the disciplines of engineering and architecture in the context of the design of folded plate structures. In this regard, the proposed strategy relies on a series of design operations that can be easily understood by both architects and engineers.

Grounded on the definition of a model for folded plate structures that works as a structural diagram (Kotnik and D'Acunto 2013), the design method is intended to benefit from the interplay of the structural and spatial properties of folding, in order to promote a holistic approach to design where architecture

and engineering are seamlessly combined. Thanks to its level of synthesis and intuitiveness, the proposed approach is intended to sustain the design process starting from the conceptual stage of the design development.

As explained in details in the next parts of this thesis, the formalisation of the design method has involved a research process grounded on three main pillars:

1. Definition of a *structural model* that consents to control the load-bearing behaviour of folded plate structures in a synthetic and intuitive way.

2. Creation of a *set of rules* for the design of folded plate structures that take into account both spatial and structural criteria and that are implemented in the form of a parametric digital toolkit.

3. Design and production of a series of *prototypes* of folded plate structures at various scales as case studies to test the applicability of the method to various design scenarios.

Structural Model: Graphic Statics and Theory of Plasticity A specific formulation of a structural model has been defined that complies with the aims of the proposed design method in terms of clarity. The approach used in the present research relies on a *graphical* representation of the load-bearing behaviour of a folded plate structure. While focusing only on equilibrium solutions, a strategy based on the *theory of plasticity* has been implemented (Chapter 10). Working as a structural diagram (Kotnik and D'Acunto 2013), the proposed structural model can be used as an operative medium starting from the initial phase of the design development.

In particular, a discrete *strut-and-tie model* for folded plate structures (§ 8.3) has been developed, which consists of the combination of the dual lattice and plate structural archetypes (§ 8.1). In compliance with the theory of plasticity, the folded plate structure is modelled as an assembly of linear members representing the lines of action of the stress resultants within the structure. Such a structural model can be easily comprehended by both architects and engineers.

Contrary to a FEM model grounded on the theory of elasticity, such a strut-and-tie model can directly show the correlation between form and flow of forces within the structure. In this context, various *3D graphic statics* procedures (Chapter 9) have been formulated as synthetic vector-based graphical applications to control the three-dimensional force flow within the folded plate structures. Moreover, a strategy to derive *stress fields* from the strut-and-tie model has been introduced to obtain an overview of the distribution of the stresses in the structure (§ 10.2).

Set of Rules: A Design Method for Structural Folding in Architecture A method for the design of folded plate structures in architecture both in the form

of *folded surface structures* and *folded volumetric structures* has been formulated and implemented within a software-based computational toolkit (Chapter 11). A set of rules based on simple geometric operations have been defined to control both spatial and structural questions at the same time. These rules operate at the level of *topology* (Chapter 12) and *Euclidean geometry* (Chapter 13). Hence, using an algorithmic procedure, the systemic interaction between structure and form within the design operation of folding has been explicitly formalised. The set of rules, built around the previously defined strut-and-tie model, allows the designer, either engineer or architect, to take direct advantage of the structural and architectural potentials of folding.

Based on the geometrical definition of the strut-and-tie model and in compliance with the theory of plasticity, the computational toolkit is generally free of scale and material-independent. By taking advantage of graphic statics, the toolkit enables the designer to modify the geometry of the folded plate structure interactively while having real-time control on the distribution of the internal forces in the strut-and-tie model.

Prototypes: Design Experiments at Various Scale   Using the computational toolkit, several design experiments at different scales (Chapter 14) have been carried out in parallel to the theoretical systematisation of the design method. This has led to the production of various prototypes, which in turn have been used to prove the efficacy of the proposed design approach with respect to structural performance and architectural potentials.

Structural Model

8. Static Rigidity of Folded Plate Structures

In this chapter, a structural model for folded plate structures, which is grounded on a *strut-and-tie* modelling approach, is introduced. The proposed model is derived from the *lattice* and the *plate* structural models, which are described in details in the following sections, based on considerations of static rigidity.

8.1 Duality of Lattice and Plate Structures

Structures in space can be generated as assemblies of individual structural elements. These elements vary according to their corresponding geometric dimensions, such as nodes (0D points), straight bars (1D lines), plates (2D planes), and rigid bodies (3D volumes). Among the possible structure systems that can be constructed in space, particularly relevant are the *lattice structures* and the *plate structures* for their relatively common use in the building practice.

The lattice structure model, whose prerequisites have been highlighted by Culmann for the definition of the ideal planar truss (Culmann 1866, p. 359), consists of a combination of straight *bars* that are connected to each other at common endpoints by means of frictionless articulated *nodes* (pin-joints). The bars are statically rigid along their length; that is, no relative motion between the endpoints of the same bar is allowed along the length of the bar. Moreover, because of the articulation of the nodes, each individual bar is, in principle, locally free to rotate around its endpoints. As suggested by Engel (2013), lattice structures can be regarded as vector-active structure systems; that is, structure systems in which the bars constituting the structure can transfer normal forces in the direction of their axes. The redistribution of the internal forces among bars connected to the same node is achieved by a force-vector repartition at the node. This description implies that loads in a lattice structure are applied directly to the nodes or along the direction of its bars. Loading components perpendicular to the bars can also be taken into consideration by assuming the activation of a supplementary mechanism of resistance. This mechanism consists in a *local beam action* on the loaded bar, which redistributes the perpendicular loading components directly to the nodes.

The plate structure model, as described by Wester (1984) and Whiteley (1987), consists of assemblies of *plates*, plane polygonal elements that are joined along common *hinge lines*. The plates are regarded as statically rigid in their planes, in such a way that no relative motion among the vertices of the same plate is permitted on the plane of the plate. Due to the presence of the hinge lines, the plates are, in principle, locally free to rotate around their edges. According to the categorisation of Engel (2013, p. 41), plate structures are comprised within the surface-active structure systems. The main load-bearing mechanism of these structures is the plate action, which is activated when the applied loads are parallel to the plates. Loads that are applied directly to the edges are split into two in-plane components in the two adjacent plates. For loading components perpendicular to the plates, it can be assumed that the plates are able to mobilise a secondary load-bearing mechanism in the form of *local slab action*. As such, the out-of-plane loads are transferred to the edges of the plates through bending and then decomposed into in-plane components (Wester 1993; Almegaard and Hansen 2007; Bagger 2010).

As discovered independently by Wester (1984) and Whiteley (1987), lattice structures (defined by Whiteley as *bar-and-joint frameworks*) and plate structures (defined by Whiteley as *hinged sheetworks*) are geometrically and statically correlated to each other, based on the *principle of duality* (Coxeter 1987, p. 24). As stated by Wester (2011, p. 229), who regards lattice and plate structures as the two *structural archetypes* of space, the properties of one type of structure can be directly inferred by the other one thanks to their duality. This principle is valid both at the level of topology and static rigidity (§ 8.2) and at the level of Euclidean geometry and static equilibrium.
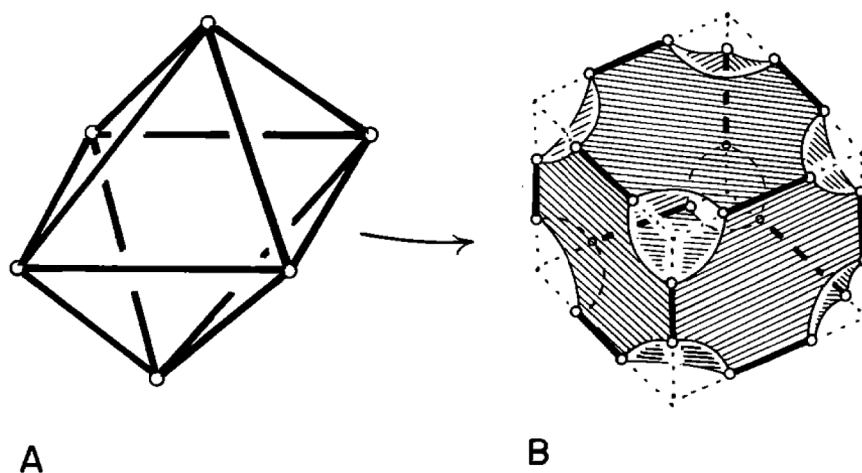

A   **B**

Figure 8.1: Duality between a lattice structure (A), constructed on the geometry of an octahedron and a plate structure (B) as a truncated cube (Whiteley 1987, p. 342).

Combinatorial Duality   From a topological point of view, the correlation between lattice and plate structures is built upon the principle of *point-to-plane duality* (Wester 1996). That is, each node (point) of a lattice structure can be mapped to a plate (section of a plane) of its dual plate structure and vice versa. Each set of bars connected to the same node in a lattice structure has a corresponding set of hinge lines along the boundary of a dual plate in the dual plate structure. The duality between lattice and plate structures is particularly evident when the two structures are topologically equivalent to three-dimensional convex polyhedra (Fig. 8.1). In this case, the nodes, bars, and meshes delimited by bars in a lattice structure correspond respectively to the vertices, edges, and faces of a polyhedron. Likewise, the plates, hinge lines, and points of intersection of hinge lines of a plate structure correspond respectively to the faces, edges, and vertices of a dual polyhedron. In this way, each vertex of a polyhedron corresponds to a face in the dual polyhedron and vice versa, while each edge of one polyhedron has a dual edge in the dual polyhedron. The topological duality of convex polyhedra is directly exhibited by Euler's polyhedral formula (Wester 1996, p. 223):

$$V - E + F = 2 \qquad\qquad\qquad (8.1)$$

where F is the number of faces, V is the number of vertices, E is the number of edges. In fact, in this formula, V and F can be exchanged, without altering E.

Within the context of graph theory, given a convex polyhedron, a *polyhedral graph* can be constructed by projecting the vertices and edges of the polyhedron onto the plane or onto the sphere (Baracs 1975). Based on Steinitz's theorem, a polyhedral graph is 3-vertex-connected and planar (Grünbaum 1967). A graph is 3-vertex-connected if at least three vertices have to be removed to disjoint it (Crapo and Whiteley 1993). A graph is planar if it is possible to embed it in the plane or on the sphere. This condition is attained when its vertices are repositioned so that the edges intersect each other only at their shared vertices. A planar graph that is embedded in the plane or on the sphere is defined *plane graph* (Harary 1969, p. 102). The plane graph of a convex polyhedron corresponds to its *Schlegel diagram*, which is the perspective projection onto the plane of the skeleton of the polyhedron from a point of view just outside the centre of one of its faces (Coxeter 1989, p. 152). The edges of the plane graph of a convex polyhedron bound faces, including an infinite exterior face, which encloses all the other ones. Considering the number of vertices V, edges E, and faces F of this graph, Euler's formula (Eq. 8.1) is still valid (Harary 1969, p. 102). Given the plane graph of a convex polyhedron, its dual graph can be generated by introducing a new vertex in every face of the given graph, including one in the infinite exterior face. A new edge is then introduced to connect any pair of newly inserted vertices, provided their containing faces in the given graph share an edge (Baracs 1975). In this way, the dual of the given plane graph of a convex polyhedron represents the plane graph of the dual polyhedron (Fig. 8.2).
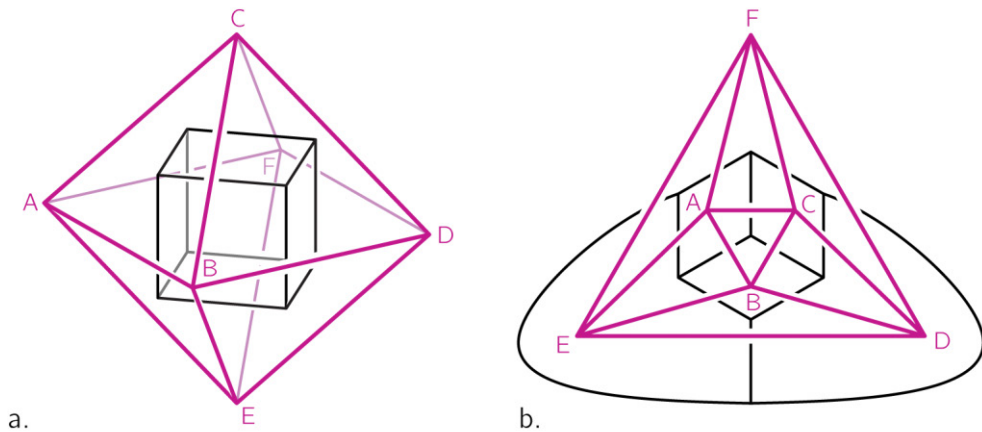
Figure 8.2: (a) Duality between an octahedron and a cube. (b) Duality between the corresponding graphs.

As highlighted by Wester (2011, p. 230), when applied to the Platonic solids (tetrahedron, cube, octahedron, dodecahedron, and icosahedron), this property allows relating each of them to its topological dual, which is another Platonic solid. As a result, the five archetypical Platonic solids can be grouped in dual pairs: the tetrahedron and its dual tetrahedron, the octahedron and its dual cube and the icosahedron and its dual dodecahedron (Fig. 8.3).
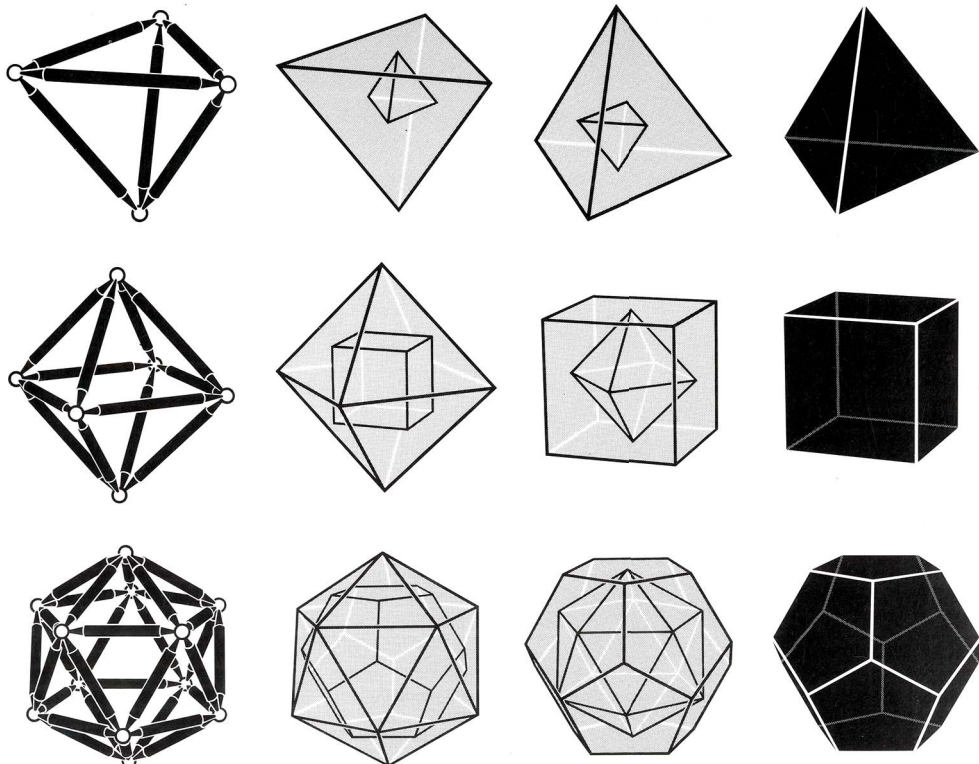
Figure 8.3: Duality between lattice and plate structures regarded as Platonic solids (Wester 1984, p. 11).

Projective Duality   Within the framework of projective geometry[1], regarding lattice and plate structures as polyhedral surfaces, one can be transformed into the other and vice versa through the application of a *polarity* (Konstantatou et al. 2018). This transformation, which is a *correlation* and an *involution* (Coxeter 1987, pp. 60–62), maps a point of the projective space into a plane, a plane into a point and a line into a line. By means of linear algebra and using homogeneous coordinates, a generic point P $(x_P, y_P, z_P, 1)$, the *pole*, is mapped into its *polar plane* π $(\boldsymbol{p}^T \boldsymbol{C} \boldsymbol{x} = 0)$ through the following general polar transformation (Pedoe 1988, p. 370):

$$
\begin{bmatrix} x_P & y_P & z_P & 1 \end{bmatrix}
\begin{bmatrix}
c_{11} & c_{12} & c_{13} & c_{14} \\
c_{21} & c_{22} & c_{23} & c_{24} \\
c_{31} & c_{32} & c_{33} & c_{34} \\
c_{41} & c_{42} & c_{43} & c_{44}
\end{bmatrix}
\begin{bmatrix} x \\ y \\ z \\ 1 \end{bmatrix} = 0
\tag{8.2}
$$

where $\boldsymbol{C}$ is a symmetric or anti-symmetric matrix, whether the polarity is generated with respect to a *quadric surface* or it is a *null polarity* (Pedoe 1988, p. 375).

In particular, in case the matrix $\boldsymbol{C}$ in (8.2) is symmetric (i.e. $c_{ij} = c_{ji}$), $\boldsymbol{C}$ can be associated to the following general quadric equation, in Cartesian coordinates (Smith 1886, p. 46):

$$
c_{11}x^2 + c_{22}y^2 + c_{33}z^2 + c_{44} + 2c_{12}xy + 2c_{13}xz + 2c_{23}yz + 2c_{14}x + 2c_{24}y + 2c_{34}z = 0
\tag{8.3}
$$

The quadric in (8.3) is the locus of all the self-conjugate points with respect to the polarity. These are the points that lie on their own polar planes, which are themselves tangent to the quadric (Coxeter 1998, p. 68). A second matrix $\boldsymbol{D}$ can be then defined by removing the fourth row and fourth column from $\boldsymbol{D}$ (Zwillinger 2002, s. 4.18):

$$
D = \begin{bmatrix}
c_{11} & c_{12} & c_{13} \\
c_{21} & c_{22} & c_{23} \\
c_{31} & c_{32} & c_{33}
\end{bmatrix}
\tag{8.4}
$$

The eigenvalues of $\boldsymbol{D}$ are thus the roots λ of the equation $\det(\boldsymbol{D} - \lambda \boldsymbol{I}) = 0$, where $\boldsymbol{I}$ is the 3x3 identity matrix, that is:

$$
\begin{vmatrix}
c_{11} - \lambda & c_{12} & c_{13} \\
c_{21} & c_{22} - \lambda & c_{23} \\
c_{31} & c_{32} & c_{33} - \lambda
\end{vmatrix} = 0
\tag{8.5}
$$

---

[1]Projective geometry is a branch of geometry that, as opposed to the Euclidean one, does not deal with the notion of measurement (Coxeter 1987, p. v). The objects of investigation of projective geometry are those geometric properties that are preserved under projective transformations. In projective geometry, the Euclidean space is extended by adding an ideal point (*point at infinity*) to every line in space, as well as an ideal line (*line at infinity*) to every plane of space. The set of all ideal lines thus defines an ideal plane (*plane at infinity*), which together with the Euclidean space constitutes the *projective space* (Coxeter 1987, p. 109).

In the specific case in which $det(C) < 0$, $det(D) \neq 0$ and the non-zero eigen-values of D have the same signs, the equation (8.3) represents a real ellipsoid (Zwillinger 2002, s. 4.18; Fortuna et al. 2016, p. 49).

Referring to a Cartesian coordinate system the ellipsoid can be described in its standard form as:

$$\frac{x^2}{a^2} + \frac{y^2}{b^2} + \frac{z^2}{c^2} = 1 \tag{8.6}$$

As a special case, if $a = b = c = r$, the ellipsoid is a sphere with centre in the origin O of the coordinate axes and radius r. Considering its standard form (in Cartesian coordinates):

$$x^2 + y^2 + z^2 = r^2 \tag{8.7}$$

a point P (x_P, y_P, z_P) is mapped into its polar plane π (Smith 1886, p. 70):

$$x_P x + y_P y + z_P z = r^2 \tag{8.8}$$

through the polarity (in homogeneous coordinates):

$$\begin{bmatrix} x_P & y_P & z_P & 1 \end{bmatrix} \begin{bmatrix} 1 & 0 & 0 & 0 \\ 0 & 1 & 0 & 0 \\ 0 & 0 & 1 & 0 \\ 0 & 0 & 0 & -r^2 \end{bmatrix} \begin{bmatrix} x \\ y \\ z \\ 1 \end{bmatrix} = 0 \tag{8.9}$$

Given a lattice structure, by applying the polar transformation (8.9) to all the points corresponding to the nodes of the structure, the planes that contain the dual plates of the dual plate structure can be obtained. The intersections between the planes then define the hinge lines of the plate structure, which are dual to the bars of the lattice structures (Fig. 8.4).
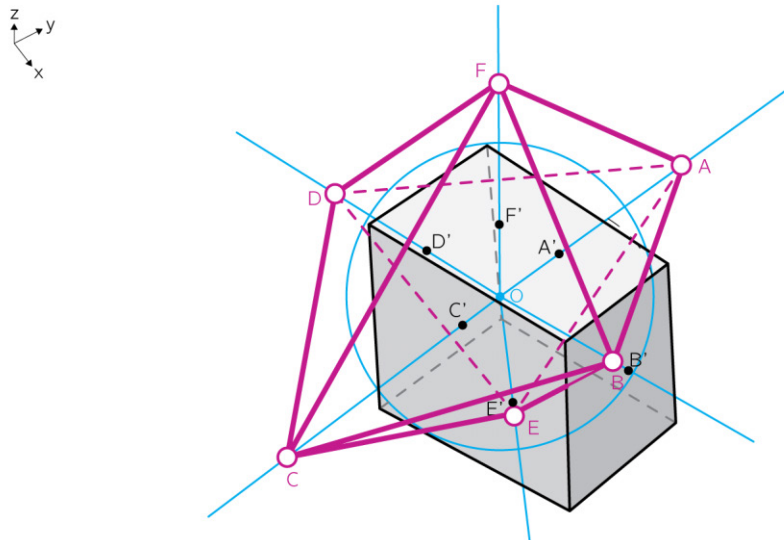
Figure 8.4: Polarity between an octahedron as a lattice structure and a cube as a plate structure.
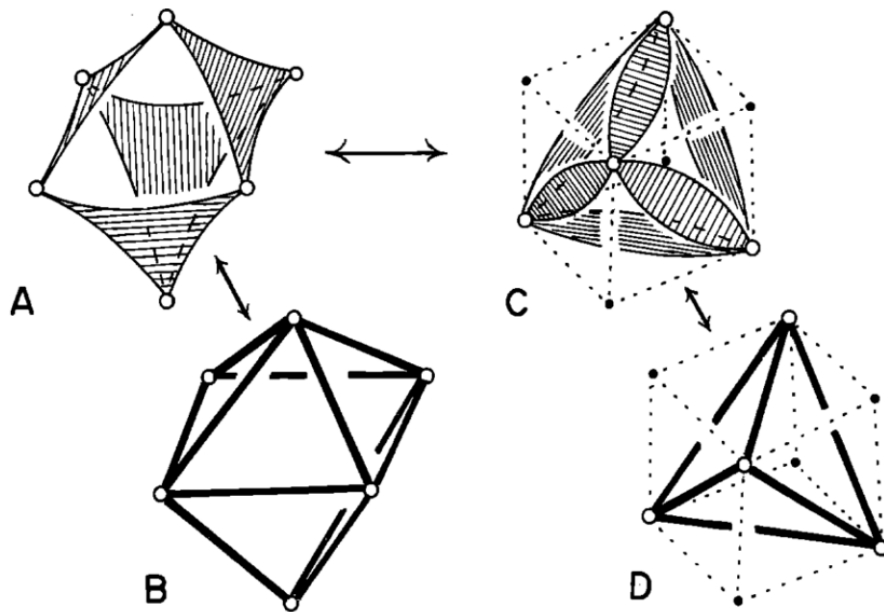
Figure 8.5: (A) Isostatic sheetwork constructed on the opposite faces of a convex octahedron. (B) Model of (A) as an octahedral framework. (C) Isostatic sheetwork, polar to (A), constructed on the opposite vertices of a cube. (D) Model of (C) as a tetrahedral framework (Whiteley 1987, p. 338).

This analytical procedure is equivalent to the geometric construction, firstly introduced by Monge (Rosenfeld 1988, p. 148), to determine the polar plane of a given pole with respect to a quadric (Konstantatou et al. 2018). For a pole outside the quadric, the polar plane is found as the plane containing the intersection (a conic) between the quadric and the cone tangent to the quadric and having its vertex in the pole (Coxeter 1998, p. 69).

As a generalisation of the duality between bar-and-joint frameworks (i.e. lattice structures) and hinged sheetworks (i.e. plate structures), Whiteley introduced a new class of structure, the *jointed sheetwork* (Whiteley 1987, p. 338). This structural system is constituted by sheets statically rigid in their planes (plates) that are connected to each other through frictionless articulated nodes (i.e. pin-joints). Contrary to lattice and plate structures, the jointed sheetworks are self-polar, that is the polar of a given jointed sheetwork is itself a jointed sheetwork (Fig. 8.5, A and C). In fact, through a polarity, a joint in a jointed sheetwork is transformed into a sheet and vice versa. Within this context, as highlighted by Whiteley (1987, p. 350), bar-and-joint frameworks and hinged sheetworks can be regarded as special cases of jointed sheetworks.

A bar-and-joint framework can be converted into a jointed sheetwork by replacing any plane-statically rigid bar-and-joint assembly (such as a bar-and-joint triangle) with a plane-statically rigid sheet (Fig. 8.5, A and B) (Whiteley 1987). In the simplest case, this is achieved by replacing each bar with a plane-statically rigid sheet (Fig. 8.5, C and D).

8.2 Rigidity of Lattice and Plate Structures

A structure is *statically rigid* when any relative finite and infinitesimal internal motion among its constituting elements is prevented; the structure thus behaves as a *rigid body*, and it can only be subjected to rigid motions of the entire space (Crapo 1979)[2]. As a result, a statically rigid structure is able to support any external equilibrium loading.

As pointed out by Baracs (1975), one of the most relevant findings of *rigidity theory* is that the static rigidity of a structure is determined exclusively by the *topological* and *projective* properties of its geometric configuration. In this regard, neither the metrical properties of the structure, including the dimensions of its constituting elements, nor the physical properties of it, including the distribution of the internal forces, are fundamental to its static rigidity. As shown in the following subsections, different rules can be defined for the generation of statically rigid lattice and plate structures (§ 8.1).

8.2.1 Rigidity of Lattice Structures

A statically rigid (i.e. *kinematically stable*) and finite spatial lattice structure not connected to a rigid foundation (i.e. non-supported) fulfils Maxwell's rule (Maxwell 1864; Maxwell 1890; Guest and Hutchinson 2003):

$$E_{LS} \geq 3V_{LS} - 6 \qquad (8.10)$$

where E_{LS} is the number of bars, V_{LS} is the number of nodes, 6 is the number of rigid-body motions of space. In case $E_{LS} = 3V_{LS} - 6$, the structure is *statically determinate*, since any external equilibrium loading on the structure results in a unique distribution of internal forces. Based on the (8.10), the *degree of static indeterminacy n* of a spatial lattice structure connected to a rigid foundation (i.e. supported) can be defined as follows (Marti 2013, p. 143):

$$n = E_{LS} - 3V_{LS} + k \qquad (8.11)$$

where k is the number of independent kinematic restraints at the supports (i.e. support force variables, 6 minimum). In relation to the (8.11), lattice structure are generally classified as *statically determinate* if $n = 0$, *statically indeterminate* if $n > 0$ and *kinematically unstable* (i.e. statically non-rigid) if $n < 0$. A structure is *internally statically indeterminate* if E_{LS} is higher than the minimum required attaining the static determinacy. It is *externally statically indeterminate* if there are redundant kinematic restraints at the supports (Marti 2013, p. 143). It should be noted that the conditions expressed by the (8.10) and (8.11) are

---

[2]A rigid motion of space is an *isometry* that can be represented as the composition between a rotation about an axis and a translation along the same axis (*screw motion*). Any motion of a structure that is not a rigid motion is an internal motion. In case the motion is finite, a *mechanism* evolves (Crapo 1979).

necessary but not sufficient, since they rely on a global counting scheme of the number of edges and nodes of the structure but do not take into account the specific connectivity of these elements (Laman 1970). For example, lattice structures exist for which $n = 0$ but the system is locally statically indeterminate and locally kinematically unstable at the same time. To address this aspect, the (8.11) can be reformulated according to the *extended Maxwell's rule* (Calladine 1978; Pellegrino and Calladine 1986), to define the number s of independent states of self-stress and the number m of independent inextensional mechanisms (i.e. zero-energy deformation modes):

$$s - m = E_{LS} - 3V_{LS} + k \tag{8.12}$$

Accordingly, $s > 0$ for a *statically indeterminate* spatial lattice structure, $m > 0$ for a *kinematically indeterminate* one, $s = 0$ for a *statically not indeterminate* one (i.e. *determinate* or *overdeterminate*), and $m = 0$ for a *kinematically not indeterminate* one (Tarnai 2001). The values of s and m can be found based on the *rank r* of the ($3V_{LS} - k$ by E_{LS}) *equilibrium matrix* $\boldsymbol{A}$ of the structure, respectively of its (E_{LS} by $3V_{LS} - k$) *kinematic matrix* $\boldsymbol{B}$, with $\boldsymbol{B} = \boldsymbol{A}^T$ (Crapo 1979; Pellegrino and Calladine 1986; Pellegrino 1993). In this regard, the following relationships can be defined (Pellegrino and Calladine 1986, p. 415):

$$s = E_{LS} - r \qquad m = 3V_{LS} - k - r \tag{8.13}$$

Hence, the rank r of the equilibrium matrix $\boldsymbol{A}$ of a statically determinate structure is equal to the number of its bars E_{LS}. On the contrary, in a statically indeterminate structure, the rank r of $\boldsymbol{A}$ is lower than E_{LS}. This is due to the linear dependency of the column vectors of the equilibrium matrix $\boldsymbol{A}$ (respectively row vectors of the kinematic matrix $\boldsymbol{B}$), which in turn reflects the presence of linear dependency among the bars of the structure (Crapo 1979).

Construction of Rigid Lattice Structures As explained by Baracs (1975), edges (regarded as bars rigid along their lengths) can be used to create six different types of kinematically stable linkages between the three structural elements of space, namely points, lines, and rigid bodies. In this regard, the least number of edges required to generate rigid connections between these elements can be defined by the following *topological conditions* (Baracs 1975):

1. A point can be linked to another point with a single edge (Fig. 8.6.1).

2. A point can be linked to a line with two edges (Fig. 8.6.2).

3. A point can be linked to a rigid body with three edges (Fig. 8.6.3).

4. A line can be linked to another skew line with four edges. Based on (2), two points on the first line can be linked to the second line each using two edges (Fig. 8.6.4).
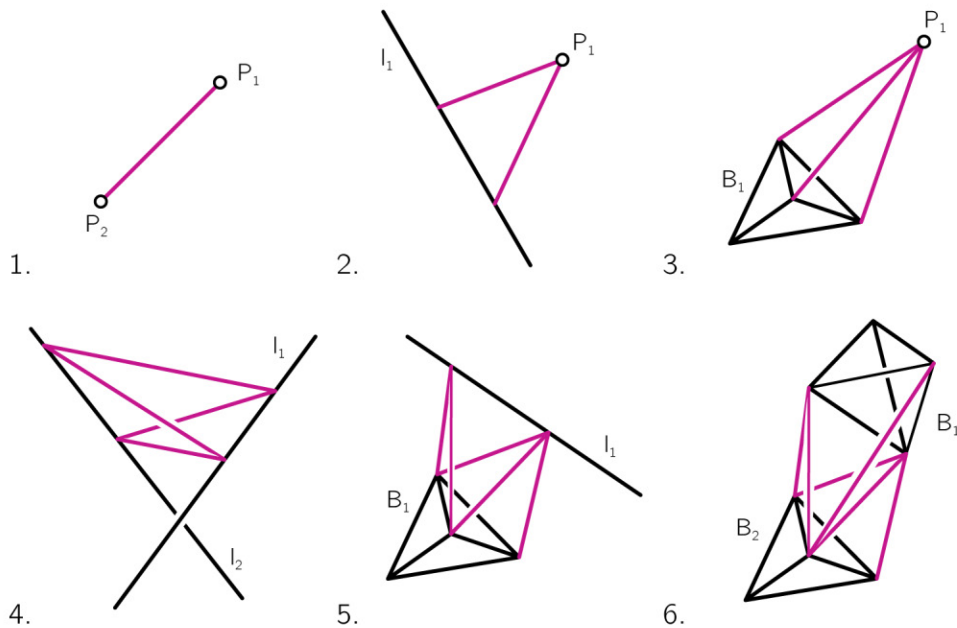
Figure 8.6: Six different types of rigid linkages to connect the three structural elements of space (points, lines, and rigid bodies).

.

5. A line can be linked to a rigid body with five edges. Considering the (3), a first point on the line can be linked to the rigid body with three edges, while the second point on the line can be linked to the rigid body with two additional edges (Fig. 8.6.5).

6. Two rigid bodies can be linked to each other with six edges. Considering that the second rigid body is supported by a line linked to the first rigid body with five edges as explained at (5), one supplementary edge could be used to create an overall rigid connection (Fig. 8.6.6).

The respect of the number of edges in the previously described linkages is a necessary but not sufficient condition to achieve rigid connections. As highlighted by Crapo (1979), a given linkage is statically rigid if and only if the rank of the edges of the linkage is no lower than the least number of edges required by that linkage. This *projective geometric condition* results in the edges of the linkage being linearly independent (Baracs 1975). For example, in relation to the linkage in Fig. 8.6.2, an infinitesimal mechanism evolves if the two edges belong to the same line. In the case of the linkage in Fig. 8.6.3, in order for the rank of the edges to be three, these must not belong to the same plane. Likewise, for the linkage in Fig. 8.6.4, an infinitesimal mechanism is generated if the four edges lie on the same plane. The linkage in Fig. 8.6.5 is not rigid if, for example, its five edges are all incident with the same line on the rigid body. For the linkage

in Fig. 8.6.6, the six edges should not belong to the same *line complex* (Crapo 1979).

Regarding points as nodes, edges and lines as bars and rigid bodies as rigid spatial trusses, the linkages described above can be used to assemble statically and kinematically determinate spatial lattice structures. More specifically, the iterative application of the linkage defined at (3) leads to the generation of *simple structures* (Baracs 1975). That is, starting with a truss in the shape of a tetrahedron, which is a rigid body, a simple structure can be built by adding a new node and three new non-coplanar bars at every iteration. For example, this can be achieved by creating a chain of tetrahedra in which each tetrahedron shares one of its faces with a preceding tetrahedron in the chain (Coates et al. 1987). The employment of the linkages outlined at (4), (5) and (6) results in the creation of *compound structures* (Baracs 1975).

Rigid Lattice Structures as Polyhedra   Rigid spatial lattice structures that are not generated using the aforementioned linkages are denominated *complex structures* (Baracs 1975). Among others, belong to this category those spatial lattice structures that are constructed in the shape of convex polyhedra. As pointed out previously (§ 8.1), in this case, the nodes, bars, and meshes delimited by bars in a lattice structure correspond respectively to the vertices, edges, and faces of the polyhedron.

As outlined by Whiteley (1987), the first consistent study on the rigidity of convex polyhedra is due to Cauchy (1813), who proved that a convex polyhedron is rigid if it is constituted by flat polygonal faces that are rigid in their planes. Cauchy's work has been subsequently further developed by Alexandrov (1958), who demonstrated that a convex polyhedron is rigid if it is triangulated with vertices placed anywhere along its natural edges, but not in the interior of its natural faces. Moreover, as proved by Whiteley (1984), in a spatial lattice structure in the shape of a polyhedron, whose faces are made of plane-rigid bar-and-joint frameworks, substituting a face with another plane-rigid bar-and-joint framework that is built on the same vertices does not affect the rigidity of the structure.

As observed by Wester (1984), a statically rigid non-supported spatial lattice structure in the shape of a convex polyhedron must respect at the same time both the (8.1) and the (8.10) (Wester 1984, p. 14):

$$\begin{cases} V_{LS} - E_{LS} + F_{LS} = 2 \\ E_{LS} \geq 3V_{LS} - 6 \end{cases}$$

These conditions result in (Wester 1984, p. 14):

$$2E_{LS} \leq 3F_{LS} \tag{8.14}$$

where E_{LS} is the number of bars of the lattice structure (i.e. edges of the polyhedron), and F_{LS} is the number of meshes of the lattice structure (i.e. faces
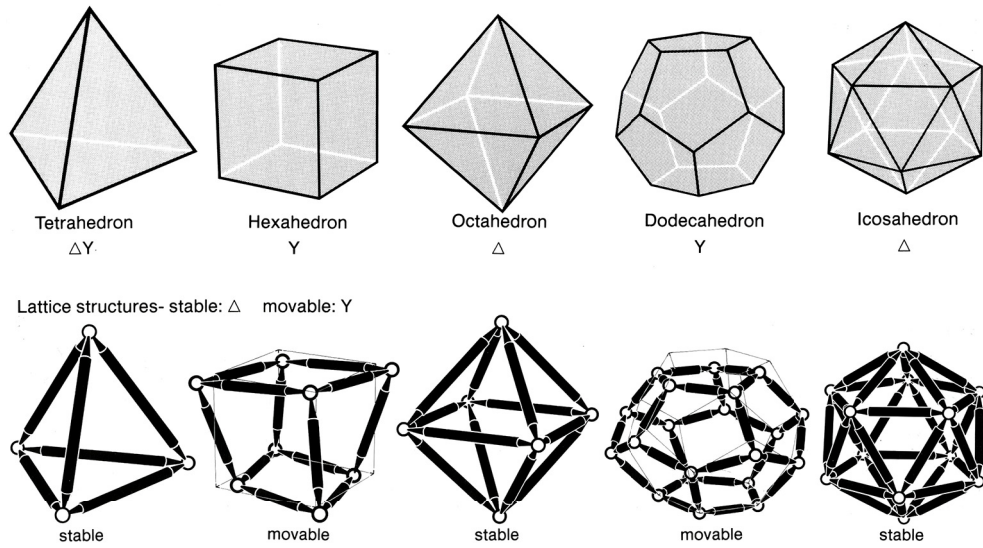
Figure 8.7: (Top) The five Platonic solids. (Bottom) The three Platonic solids with *3-valent faces* that are rigid as spatial lattice structures, and the two non-rigid ones without *3-valent faces* (Wester 1984, p. 9).

of the polyhedron). Assuming that the meshes are all delimited by *n* bars and that each bar separates two and only two meshes, the following condition can be defined (Wester 1984, p. 14):

$$2E_{LS} = nF_{LS} \tag{8.15}$$

The combination of the conditions expressed by the (8.14) and the (8.15) eventually yields (Wester 1984, p. 14):

$$n \leq 3 \tag{8.16}$$

Considering that the minimum number of bars that can delimit a mesh is 3, only convex polyhedra with triangular faces (i.e. *3-valent* faces) can be used as a base for the generation of rigid spatial lattice structures (Wester 1984).

Based on this observation, if the Platonic solids are built as lattice structures (Fig. 8.7), only the triangulated polyhedra, whose faces are 3-valent, are rigid in space. That is, only the tetrahedron, the octahedron, and the icosahedron can perform as rigid lattice structures. On the contrary, the non-triangulated polyhedra such as the cube and the dodecahedron prove to be kinematically unstable if built as a lattice structure (Wester 1984).

The aforementioned conditions for the rigidity of spatial lattice structures as convex polyhedra can be extended to the case of convex polyhedral surfaces with polygonal openings, not necessarily planar (Wester 2011). In fact, the rigidity of these structures is attained by triangulating each opening with additional bars that are connected exclusively at existing nodes on the boundary of the opening.

This operation turns the convex polyhedral surface into a convex polyhedron. In case an opening has n delimiting bars on its boundary, $n - 3$ supplementary bars are necessary for its complete triangulation (Wester 2011). If the structure is supported, according to the (8.11), minimum 6 independent kinematic restrains are present. Further $n - 3$ independent kinematic restraints on the nodes along the border of the opening can then replace the additional bars.

The extension of the condition of rigidity to non-convex polyhedra is generally not possible. Although Gluck (1977) has demonstrated that almost all triangulated polyhedra, either convex or not, are infinitesimally rigid, cases can be found of non-convex triangulated polyhedra that are not rigid, such as *Steffen's flexible polyhedron* (Demaine and O'Rourke 2007).

8.2.2   Rigidity of Plate Structures

As proved by Rankine (1856), projective transformations do not modify the static and kinematic characteristics of a structure, including the infinitesimal rigidity. Moreover, as later demonstrated by Whiteley (1987), the same properties are also preserved under polar transformations. That is, considering the requirements for static rigidity of spatial lattice structures (§ 8.2.1), dual conditions can be defined for the dual plate structures.

Construction of Rigid Plate Structures   A procedure analogous to the one described in (§ 8.2.1) for the construction of *simple* lattice structures can be used for the creation of plate structures. In this regard, as dual to the condition for rigidity illustrated in (Fig. 8.6.3), a new plate can be connected to a given rigid plate structure using at least three hinge lines, resulting in (Wester 1984, p. 16):

$$E_{PS} \geq 3F_{PS} \tag{8.17}$$

where E_{PS} is the number of hinge lines, and F_{PS} is the number of plates. From a kinematic standpoint, a hinge line behaves like a kinematic restraint at the supports (i.e. support force variable). Hence (Wester 1984, p. 16):

$$E_{PS} + k \geq 3F_{PS} \tag{8.18}$$

where k is the number of independent kinematic restrains at the supports. Being six the minimum number of restraints to prevent any rigid-body motion of space, the following general condition can be defined for non-supported rigid plate structure (Wester 1984, p. 16):

$$E_{PS} \geq 3F_{PS} - 6 \tag{8.19}$$

As can be observed, the (8.19) is exactly equivalent to Maxwell's rule for non-supported spatial lattice structures (8.10), provided the hinge lines are substituted with their dual bars and the plates are replaced with their dual nodes.

Rigid Plate Structures as Polyhedra Like spatial lattice structures, also plate structures can be built in the shape of convex polyhedra. In this case (§ 8.1), the plates, hinge lines, and points of intersection of hinge lines of a plate structure correspond respectively to the faces, edges, and vertices of a polyhedron. As pointed out by Wester (1984) in analogy to what observed in the case of spatial lattice structures (§ 8.2.1), a non-supported plate structure that is constructed in this way complies with both the (8.1) and the (8.19) (Wester 1984, p. 18):

$$\begin{cases} V_{PS} - E_{PS} + F_{PS} = 2 \\ E_{PS} \geq 3F_{PS} - 6 \end{cases}$$

These conditions result in (Wester 1984, p. 18):

$$2E_{PS} \leq 3V_{PS} \tag{8.20}$$

where E_{PS} is the number of hinge lines of the plate structure (i.e. edges of the polyhedron), and V_{PS} is the number of points of intersections of hinge lines of the plate structure (i.e. vertices of the polyhedron). Assuming that in all the points of intersection concurs n hinge lines and that each hinge line is incident with two points, the following equation holds true (Wester 1984, p. 18):

$$2E_{PS} = nV_{PS} \tag{8.21}$$

Given the (8.20) and the (8.21), the following general condition can be derived (Wester 1984, p. 18):

$$n \leq 3 \tag{8.22}$$

Being three the minimum number of hinge lines at a point of intersection, only convex polyhedra that have vertices with three concurrent edges (i.e. *3-valent* vertices) can be used as a base for rigid plate structures. Hence, regarding the Platonic solids as plate structures (Fig. 8.8), only those with 3-valent vertices are rigid in space (Wester 1984), namely the tetrahedron, the cube, and the dodecahedron (Fig. 8.8).
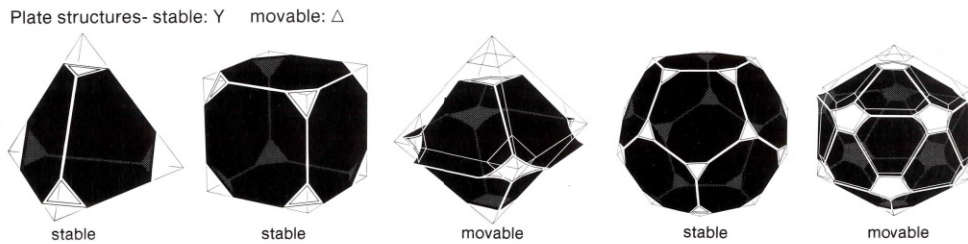

Figure 8.8: The three Platonic solids with *3-valent vertices* that are rigid as plate structures, and the two non-rigid ones without *3-valent vertices* (Wester 1984, p. 9).

8.2.3 Combined Lattice and Plate Structures

In the general case, the faces of a polyhedron may have an arbitrary number of boundary edges. Likewise, its vertices may have an arbitrary number of concurrent edges (Fig. 8.9, left). From a static rigidity standpoint, in relation to the conditions defined at (§ 8.2.1) and at (§ 8.2.2), neither a kinematically stable lattice structure nor a kinematically stable plate structure could be generally constructed based on such geometry (Wester 1984).

On the one hand, as observed by Wester (1984), a spatial lattice structure in the shape of a generic polyhedron (Fig. 8.9, centre top) is generally non-rigid since some of the meshes delimited by bars (i.e. faces of the polyhedron) may not be 3-valent and internal finite mechanisms may evolve. A possible strategy to attain the rigidity of the structure is the triangulation of all the meshes with more than three edges with the addition of extra bars. This approach, however, would break the correlation between the number of edges of the polyhedron and the number of bars of the lattice structure.

On the other hand, a plate structure generated on the geometry of a generic polyhedron (Fig. 8.9, centre bottom) may not be rigid for the possible presence of points of intersection of hinge lines (i.e. vertices of the polyhedron) that are not 3-valent. In this case, the rigidity of the structure may be attained by introducing extra shear bridges across those non-adjacent plates that are connected to the same points of intersection Wester (1984). Nonetheless, also in this case, the correlation between the number of edges of the polyhedron and the number of hinge lines of the plate structure would be altered.

To avoid these inconsistencies, Wester (1984) developed a structural model for generic polyhedra as a hybrid between the lattice and the plate models (Fig. 8.9, right). This structural model relies on the combined effects of bars, nodes, plates, and hinge lines. More specifically, those parts of the structure with 3-valent faces work as a pure lattice structure; here, if not directly loaded on their planes, the plates are not active and may be removed together with their hinge lines without compromising the overall rigidity of the system. The parts of the structure where the vertices are 3-valent work as a pure plate structure; here, if not directly loaded, the nodes are not active and may be removed together with their connected bars.

At the boundary between the two structural parts, the transfer of forces between a bar and the hinge lines located along the same polyhedral edge gives rise to *buffer forces*. Because of the presence of these buffer forces, the difference in the axial forces at the two nodes of the bar is equivalent to the difference between the shear forces along the two adjacent hinge lines (Wester 1987). It should be noted that this structural model could be extended to represent generic polyhedral surfaces after the introduction of appropriate support conditions (Wester 1987, 2011).
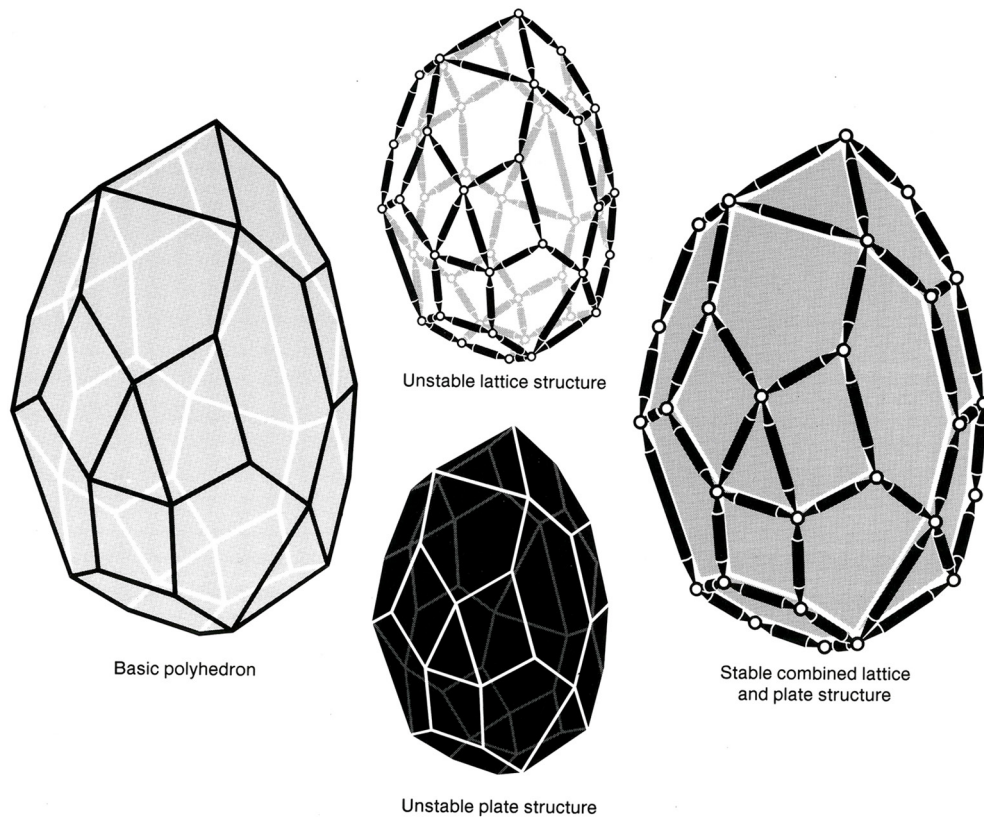
Figure 8.9: A generic polyhedron (left) is not statically rigid as a pure lattice (centre top) or as a pure plate (centre bottom) structure; it is rigid as a combination of plate and lattice structures (right) (Wester 1984, p. 25).

8.3   Strut-and-Tie Model for Folded Plate Structures

Various structural models can be found in the literature to describe the behaviour of different types of folded geometries (Chapter 2). As classified by Lebée (2015), these models include structures as *assemblies of rigid facets*, as *shells*, as *membranes*, and as *trusses*:

1. In a folded geometry as an *assembly of rigid facets*, the structure is modelled as a combination of rigid panels that are able to withstand both in-plane loads (i.e. *global plate action*) and out-of-plane loads (i.e. *global slab action*). The panels are connected to each other through hinge lines at the edges and are in general locally free to rotate around their edges. This model is equivalent to the structure system of *articulated spatial panels* introduced by Baracs (1975).

2. In a folded geometry as a *shell*, the structure is modelled as a monolithic system in which individual shell elements resist both in-plane and out-of-plane loads and are connected to each other by means of elastic hinges. In general, the elements are not locally free to rotate around their edges, and the static rigidity of the structure also depends on the rotational stiffness of the edges (Robeller et al. 2014; Roche et al. 2015; Stitic et al. 2015; Stitic et al. 2018).

3. In a folded geometry as a *membrane*, the structure is modelled as an assembly of plates rigid in their planes that are connected to each other through hinge lines, like in the plate structure system (§ 8.1). In this membrane model, the global internal stresses are transferred in-plane (i.e. *global plate action*), apart from the potential local transfer of out-of-plane loads to the edges within each individual plate (i.e. *local slab action*). Contrary to the plate structure system (§ 8.1), axial forces can be transferred along the edges.

4. In a folded geometry as a *truss*, the structure is modelled as an assembly of bars that are connected to each other by means of nodes working as pin-joints, like in the lattice structure system (§ 8.1). In case the folded geometry has non-triangular facets, these are triangulated introducing supplementary bars in the model[3].

---

[3]Belong to this category the *bar-and-hinge models*, which are specifically used in origami engineering to characterise the elastic behaviour of thin sheet origami structures (Schenk and Guest 2011; Filipov et al. 2015; Filipov et al. 2017). These models can be used to simulate the kinematic behaviour of complex rigid-foldable origami configurations, such as deployable structures. In this regard, various effects due to the elastic deformation of the plates are taken into consideration, including in-plane stretching and shear, out-of-plane bending of the facets and bending along fold lines (Filipov et al. 2017)

A folded plate structure consists of individual *folded plates* as plane polygonal elements statically rigid in their planes that are combined together along *folded edges*, which meet at common *vertices*. The resulting folded geometry performs as a statically rigid three-dimensional structure system (§ 4.1). As the topology of a folded plate structure does not have limitations regarding the number of plates shared by the same vertex, the structure is not necessarily solely made of *3-valent vertices*. As such, it cannot be generally regarded as a pure *plate structure* (§ 8.2.2). Conversely, since the number of folded edges at the border of a folded plate is not fixed, a folded plate structure does not necessarily consist entirely of *3-valent faces*. That is, it cannot generally be regarded as a pure *lattice structure* (§ 8.2.1). From the standpoint of static rigidity, a folded plate structure thus performs as a combined plate and lattice structure (§ 8.2.3)[4].

General Features of the Proposed Structural Model   Building upon the previously introduced notions of static rigidity (§ 8.2), a model for folded plate structures is here defined that is derived from the structural archetypes of space, namely the plate and lattice structure systems (§ 8.1). This proposed model complies with the above membrane structural model. Contrary to the combined model (§ 8.2.3) suggested by Wester (1984), the model proposed here does not rely on the simultaneous use of different structural elements such as bars, nodes, plates, and hinge lines to account for both plate and lattice actions. In fact, the proposal is grounded on a *strut-and-tie*[5] modelling approach (§ 10.1), where solely linear members are employed to generate a spatial network in equilibrium. These members are organized along the axes of the folded edges (*edge members*) and on the midplanes of the plates (*plate members*).

As in the lattice structure model (§ 8.1), the assumption is made that all the linear members of the strut-and-tie network are connected to each other through nodes working as pin-joints. Furthermore, the linear members can be loaded by axial forces only, either in compression (*struts*) or in tension (*ties*). Unlike the lattice structure model, the edge and plate members do not represent actual bars but rather the lines of action of internal stress resultants within the geometric boundary of the folded plate structure (§ 10.1).

In compliance with the plate structure model (§ 8.1), the assumption is made that the *out-of-plane* loads applied to the surface of a folded plate (i.e. perpendicular to the plate) are redirected to the folded edges by *local slab action*

---

[4]Similar considerations on the static rigidity of folded plate structures in relation to the duality of lattice and plate structures suggested by Wester (1984) can be found in the works of Bagger (2010), and Samuelsson and Vestlund (2015).

[5]Strut-and-tie models have been initially introduced for the analysis and design of reinforced concrete structures (Schlaich et al. 1987; Muttoni et al. 1997). Based on the lower bound theorem of the theory of plasticity (§ 10.1), they have been subsequently employed for general equilibrium-based analysis and design of structures (Block and Ochsendorf 2007; Lachauer 2014; Rippmann 2016; Ohlbrock and Schwartz 2016; Bahr 2017; Enrique and Schwartz 2017; D'Acunto et al. 2019).

(i.e. flexural action), while the ones *in-plane* (i.e. parallel to the plate) by *local plate action* (i.e. extensional action) (Almegaard and Hansen 2007; Bechthold 2008; Bagger 2010; Stitic et al. 2018). As described in details in the following paragraphs, in the proposed approach, uniformly distributed area loads on the plates can then be replaced by an equivalent system of point loads applied at the midpoints of the folded edges. As such, nodes are placed at the midpoints of every folded edge, the edge being modelled as two edge members. Plate members are arranged in the model so that each polygonal face representing a folded plate is entirely triangulated, with the plate members connected to the midpoints of the folded edges. It is assumed that external point loads are only applied at the midpoints or at the endpoints of the folded edges[6].

In relation to static rigidity, all the considerations concerning the spatial lattice structures (§ 8.2.1) are directly applicable to the proposed strut-and-tie model. In case a folded plate structure is globally and locally statically rigid (i.e. no internal finite or infinitesimal mechanisms are present in the structure), it is not necessary to mobilise the local bending resistance of the individual folded edges to secure the overall kinematic stability of the structure. As the proposed structural model relies on a statically rigid configuration, the local rotational stiffness of the folded edges is neglected, and the folded edges are treated as hinges[7].

Load Repartition on the Folded Plate Structure   The repartition of uniformly distributed area loads on a folded plate structure and the generation of a strut-and-tie network is here exemplified taking the geometry of the roof of *Stabilimento Raffo* by Musmeci (§ 4.2.2) as a reference. Given the modularity of the structure, only a subset of the entire roof is considered. Moreover, in the geometrical model, the thickness of the folded plates is not taken into account, and the folded plates are represented as two-dimensional elements located on the midplanes of the plates. Under the assumption that each folded plate is statically rigid in its own plane, the structure is kinematically stable for the given support conditions (Fig. 8.10a). The generation of the strut-and-tie network is illustrated on one of the modules, which consists of sixteen folded plates. It is here assumed that the structure is loaded under self-weight.

At first, the uniformly distributed area loads are replaced by an equivalent system of discrete point loads. This is achieved by applying at the centre of mass of each plate a point load representing the resultant of the self-weight of the plate, whose magnitude is thus proportional to the surface area of the plate itself (Fig. 8.10b). Considering each folded plate as a sub-system in equilibrium,

---

[6]A point load applied along a folded edge in a position different from the midpoint or the endpoints can be taken into consideration by adding an extra node to the model; in this case, a different triangulation of the folded plates evolves.

[7]Under the assumptions of the theory of plasticity (§ 10.1), the bending resistance of the folded edges can be then regarded as an additional local resistance capacity of the structure.
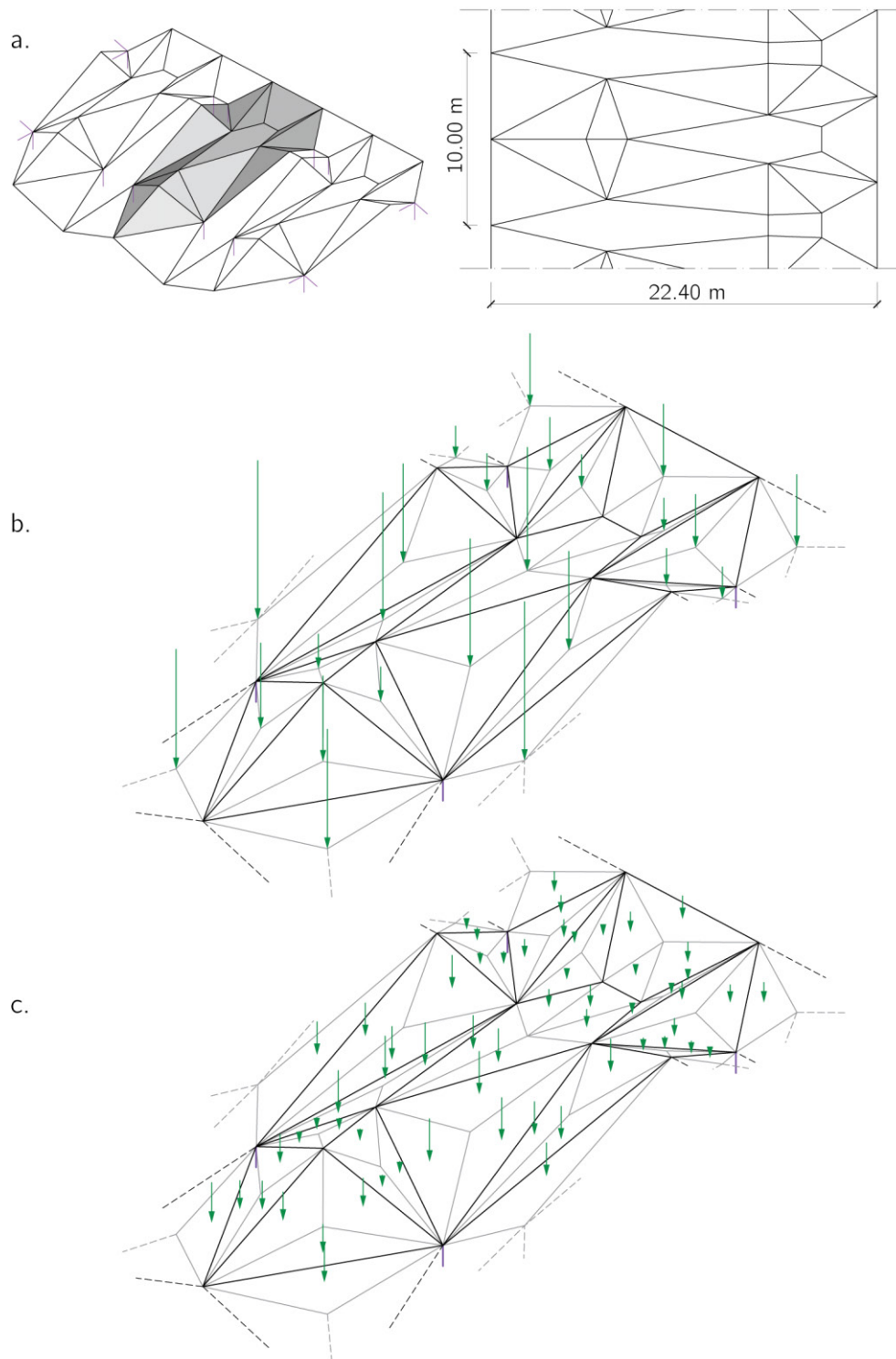
a.

10.00 m

22.40 m

b.

c.

Figure 8.10: (a) Folded plate structure based on the roof of *Stabilimento Raffo* by Musmeci (§ 4.2.2). (b) A module of the roof, regarded as a sub-system in equilibrium: system of point loads representing the resultants of the self-weight of the plates. (c) Equivalent system of point loads related to the tributary areas of the folded edges.
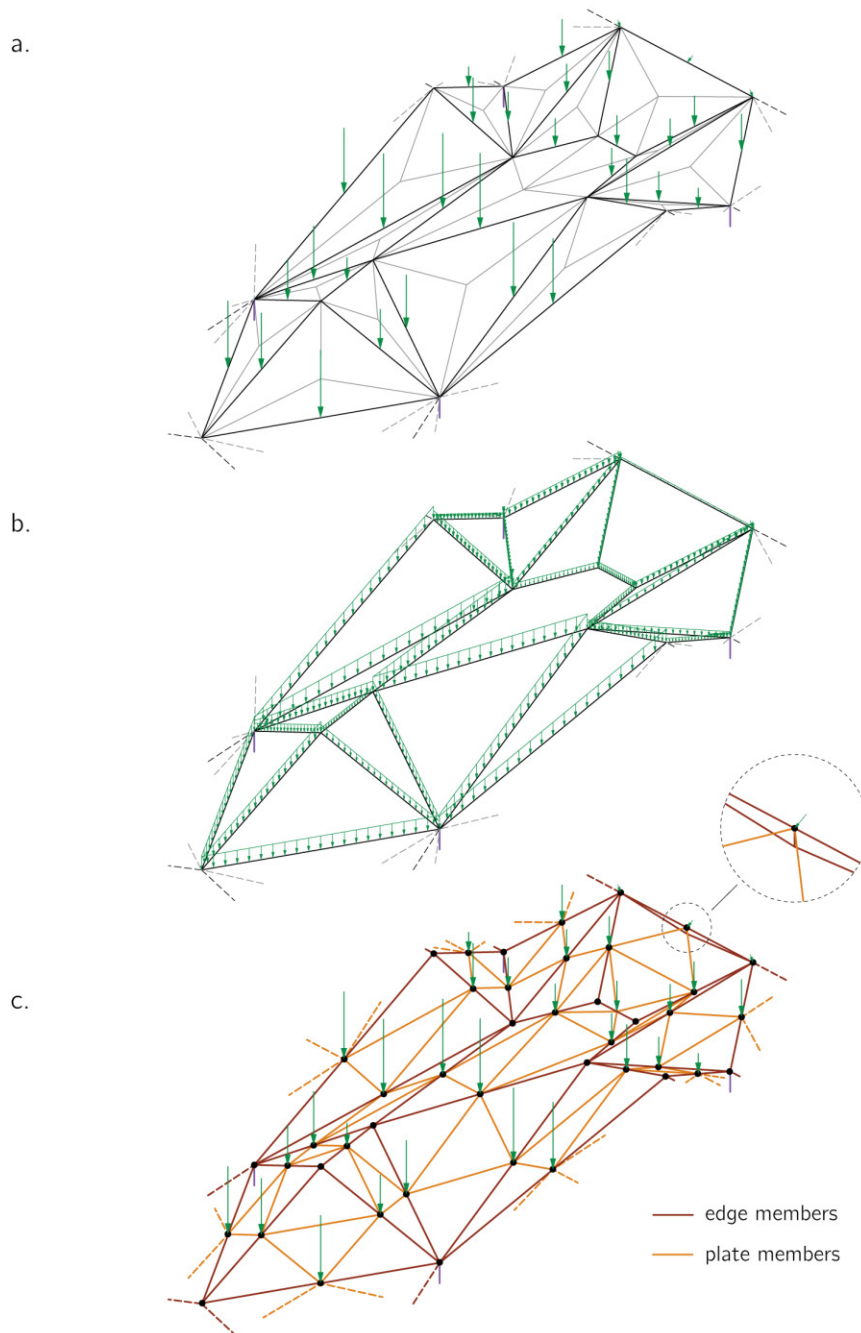
Figure 8.11: (a) Load repartition on a module of the roof based on the tributary areas of the folded edges. (b) Equivalent system of uniformly distributed line loads along the folded edges. (c) Proposed *complete strut-and-tie model* for folded plate structure: every folded edge is modelled as two linear *edge members* (brown) while the plates are entirely triangulated using linear *plate members* (orange); note the special solution adopted for the *free edge*.

through local slab and plate actions, each point load is resisted by a system of reaction forces applied at the folded edges on the border of the plate. These reaction forces can be subsequently regarded as action forces that replace the given point load and are applied to the folded plate structure. Because the plate is a statically indeterminate structural element, multiple possible configurations of load repartition can be defined in relation to the sole equilibrium conditions (Bagger 2010). Each configuration of load repartition entails the definition of a different system of reaction forces at the folded edges. As long as the assumptions of the theory of plasticity are fulfilled (§ 10.1), any load repartition is allowed that generates a system of reaction forces that are in equilibrium with the given loading (§ 9.2)[8].

In the developed approach, a load repartition related to the tributary areas of the folded edges is assumed. A possible procedure to define these areas is to subdivide each folded plate, regarded as a sub-system in equilibrium, into *triangular panels*, which have one side coinciding with a folded edge and one vertex located at the centroid of the plate. A new system of point loads, equivalent to the given one, is then generated by applying at the centroid of each triangular panel a force vector corresponding to the self-weight of that panel (Fig. 8.10c). Each force vector generates a reaction force that is opposite to the force vector itself and is applied at the midpoint of the corresponding folded edge. Each reaction force can be then regarded as an action force applied to the folded plate structure. At the folded edges, the action forces related to adjacent folded plates are composed into one resultant force (Fig. 8.11a). In the special case of a *free edge* (i.e. an edge that is not shared by two plates but is on the boundary of one plate only), the single force vector, whose magnitude is proportional to the tributary area of the free edge, is first decomposed into the in-plane and out-of-plane components. The in-plane component is placed at the midpoint of the free edge, while the out-of-plane component is split into two equivalent vectors that are placed at the endpoints of the edge (Fig. 8.11a). Hence, a new system of discrete point loads, which is equivalent to the initial uniformly distributed area loads regarding the global equilibrium (§ 9.2), is eventually defined. In fact, in terms of global equilibrium, this system of point loads is itself equivalent to a system of uniformly distributed (i.e. constant) line loads along the individual folded edges at the boundary of the folded plates (Fig. 8.11b). In the following procedure, this system of uniformly distributed line loads is assumed replacing the initial system of uniformly distributed area loads.

---

[8]Refined equilibrium solutions for the load repartition based on moment fields can be found in the literature, especially for the design of reinforced concrete slabs (Hillerborg 1996). In their simplest formulation, these approaches are mostly suitable for regular slab geometries. The application of these solutions to more complex geometries, like the ones investigated in the rest of this work, generally requires the use of the finite element method (FEM). This, however, would partly preclude the possibility of employing an intuitive structural model (Chapter 7) like the strut-and-tie model proposed in this work. Thus a simplified, but more generalizable and yet valid equilibrium-based procedure is put forward.

The proposed procedure for the repartition of the loads on folded plate structure can be directly applied to any convex polygonal geometry of the folded plates and to any orientation of the applied loads in relation to the plane of the plates. The particular case of non-convex polygonal plates is treated by subdividing the plates into convex sub-plates. For specific geometric configurations, this approach might represent an oversimplification of the actual mechanical behaviour of the structure, and a more appropriate load repartition can be taken into consideration[9].

Generation of the Strut-and-Tie Network   Once the load repartition is completed, a statically rigid strut-and-tie network can be generated as previously described (Fig. 8.11c). As such, vertices are placed at the midpoints and at the endpoints of every folded edge. Two edge members are introduced along each folded edge. In case of a free edge, three supplementary edge members are introduced to stabilise the free edge and remove the out-of-plane degree of freedom of the node at the midpoint of the free edge. These additional edge members are placed within the geometric boundary of the plate, on the plane incident to the free edge and perpendicular to the plate[10]. Plate members are then placed on the midplanes of the plates so that the plates are entirely triangulated. For plates with polygonal shapes other than the triangle, any pattern for triangulation is allowed, as long as the plate members are connected to the midpoints of the folded edges only[11]. In this way, any force vector that is applied at a node of the strut-and-tie network can be decomposed into forces along the plate and edge members.

Synthetic Strut-and-Tie Network   The strut-and-tie model described above is a *complete model*, that takes into account both lattice and plate action and complies with the previously introduced membrane model. An alternative *synthetic model*, which complies with the aforementioned truss model and employs a smaller amount of linear members, can also be defined.

For the generation of a synthetic strut-and-tie network, a repartition of the loads on the folded plate structure different from the one previously described is considered. For uniformly distributed area loads such as the self-weight, an equivalent system of discrete forces is applied to the vertices of the folded plate structure, whose magnitudes are proportional to the tributary areas of the vertices. At first, each folded plate is subdivided into *polygonal panels* (Fig. 8.12a).

---

[9]This is the case, for instance, of plates with overall elongated geometries, for which a more suitable subdivision of the plates along the long edges can be adopted, as shown in the example based on the project of *Scuola di Atletica* by Musmeci (§ 10.2).

[10]This construction relies on the assumption that any force vector applied to the midpoint of the free edge is transferred by bending action to the endpoints of the edge.

[11]As shown in the following section (§ 10.2), in this case, the strut-and-tie network requires an adjustment before an in-plane discrete stress field within the plate can be derived.
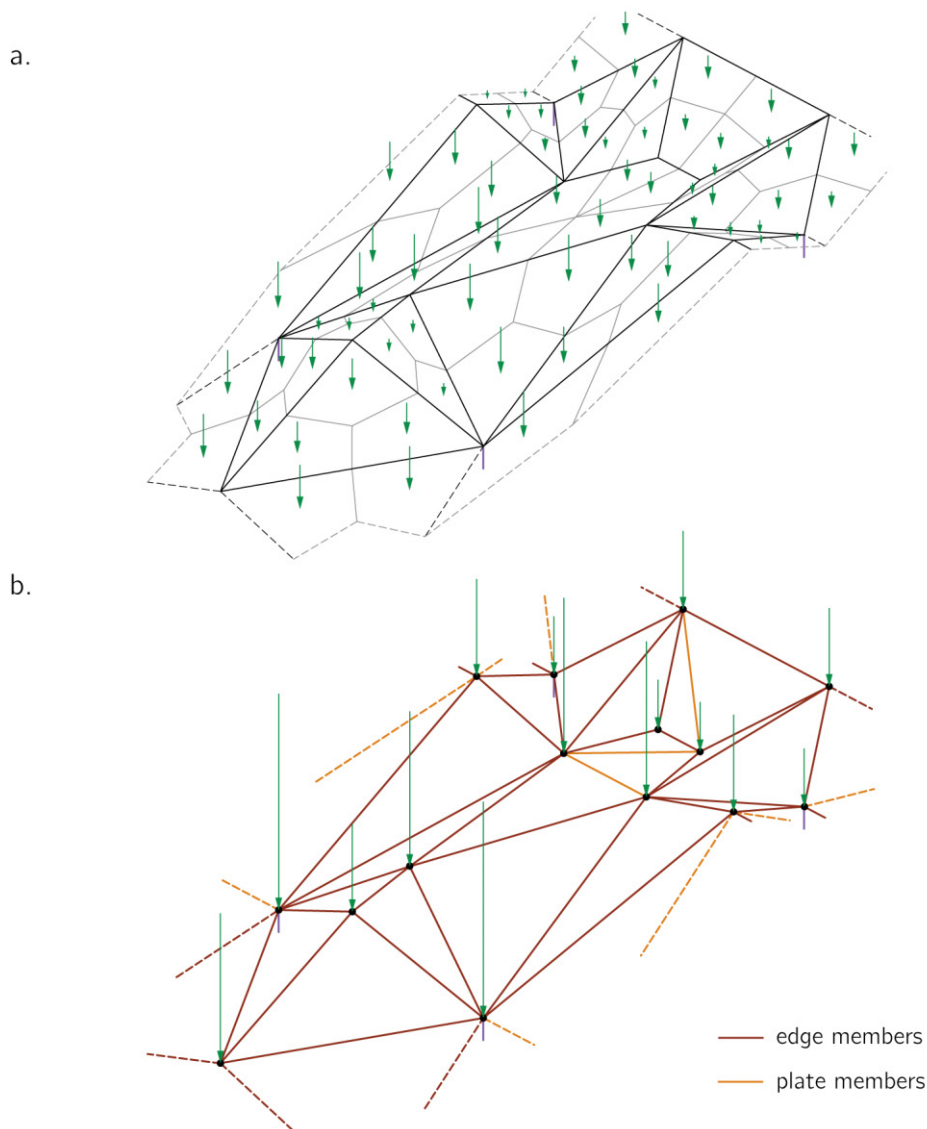
Figure 8.12: (a) Load repartition on a module of the roof according to the tributary areas of vertices of the folded plates. (b) Proposed *synthetic strut-and-tie model* for folded plate structure: every folded edge is modelled as one linear *edge member* (brown) while the non-triangular plates are triangulated using linear *plate members* (orange).

For each vertex of a given folded plate, its related panel is a polygon built on the vertex, the midpoints of the connected edges, and the centroid of the given plate. A new system of point loads, equivalent to the initial one in terms of global equilibrium (§ 9.2), is defined by placing at the centroid of each polygonal panel a force vector equal to the self-weight of that panel. Regarding each folded plate as a sub-system in equilibrium, the force vector applied to each panel produces a reaction force that is opposite to the force vector itself and is applied at the vertex of the folded plate corresponding to the panel. Each reaction force can

be then regarded as an action force applied to the folded plate structure. At the vertices of the folded plates, the action forces related to adjacent folded plates are composed into one resultant force.

For this given load repartition, a synthetic strut-and-tie model can be obtained by replacing each folded edge with one *edge member*. In this case, plates that are not triangular can be made rigid in their planes by triangulating them using *plate members* (Fig. 8.12b). In this model, the folded plate structure is thus assimilated to a spatial lattice structure (§ 8.2.1), where the internal forces are mainly present in the folded edges, and the external loads are only applied to the endpoints of the folded edges. Although this model represents a drastic simplification of the load-bearing behaviour of a folded plate structure, it still complies with the above complete model in terms of global static rigidity and global equilibrium. Because of this reason and considering the simplicity of the model due to the limited amount of elements included, this can be effectively used for early conceptual design explorations (§ 13.2).

9. Equilibrium of Folded Plate Structures

The previously introduced strut-and-tie model for folded plate structures (§ 8.3), either in the form of a complete or synthetic network, can be used to assess the equilibrium of a given loaded folded geometry. As shown in details in the following sections, this operation can be performed using *3D graphic statics* and leads to the definition of an *equilibrium-based solution*.

9.1 Graphic Statics and the Third Dimension[1]

Graphic statics is a geometry-based approach that enables to link the form of a loaded structure to the distribution of its internal forces. It is built upon a series of procedures that allows the analysis and design of structures in static equilibrium. Graphic statics relies on the use of two geometric constructions, the *form diagram* and the *force diagram*, the first one representing the geometry of a lattice structure (i.e. pin-jointed framework) including the applied external forces, and the second one the static equilibrium of the individual nodes of the structure. One of the first implementations of graphical procedures for the solution of static problems is due to Varignon, who in the 18th century introduced the notions of *funicular polygon* and *polygon of forces* to evaluate the global equilibrium of forces on the plane (Varignon 1725). During the 19th century, graphic statics developed into an autonomous discipline (Kurrer 2008). This is mainly thanks to the contributions of Rankine (1858), who addressed the analysis of structures through various graphical constructions, Culmann (1866), who firstly formalised the methodologies of graphic statics, and of Maxwell (1864) and Cremona (1872), who related graphic statics to projective geometry (Konstantatou et al. 2018).

Within two-dimensional graphic statics, fundamental is the notion of *reciprocity* between form and force diagrams. That is, form and force diagrams are interdependent geometric constructions, and the manipulation of one of the two diagrams entails a consequent direct transformation of the other one. This property has been initially researched for 2D structures by Maxwell (1864), who

---

[1]Contents of this section have been previously published in (D'Acunto et al. 2019).

developed a procedure to construct reciprocal form and force diagrams on the basis of a *polar transformation* (§ 8.1) induced by an *elliptic paraboloid* (Konstantatou and McRobie 2016; Konstantatou et al. 2018). This procedure yields diagrams in which corresponding edges are perpendicular to each other. The topic has been further investigated by Cremona (1872), who defined a strategy for the generation of reciprocal diagrams alternative to the one of Maxwell and based on Möbius's *null polarity* (Möbius 1833; Konstantatou et al. 2018). Cremona's procedure results in reciprocal diagrams with corresponding edges parallel to each other.

While the early applications of graphic statics were almost exclusively confined to the analysis and design of two-dimensional structures, recent research contributions have been focused on the development of graphic statics in the third dimension (Konstantatou et al. 2018). Three general strategies can be detected in this context, namely the *projective*, the *composite* and the *full 3D* ones (Jasienski et al. 2014). Within the full 3D approach, two main strategies have been brought forward, the *polyhedron-based* and the *vector-based* ones.

Polyhedron-based approach   The polyhedron-based approach is grounded on the initial investigations on the equilibrium of polyhedral frames by Rankine (1864). Based on this approach, for a given 3D form diagram as a polyhedral frame in static equilibrium (Fig. 9.1.a), a reciprocal 3D force diagram can be built out of individual *closed polyhedral cells* (Fig. 9.1.b), each of them defining the equilibrium of the forces acting on one specific node of the form diagram. Several computational algorithms for the construction and manipulation of polyhedral form and force diagrams, which operate on a node-by-node basis, have been developed over the last few years (Akbarzadeh et al. 2015b; Lee et al. 2016; Lee et al. 2018). An alternative direct procedure, which makes use of projective geometry and four-dimensional reciprocal stress functions, has also been recently introduced (McRobie et al. 2016; Konstantatou and McRobie 2016; Konstantatou et al. 2018).

Vector-based approach   The vector-based approach has been firstly described by Maxwell (1864) as a more pragmatic alternative to the polyhedron-based approach. It has been later further investigated by Crapo (1979), and more recently by Micheletti (2008), and D'Acunto et al. (2019) among others. Like in 2D graphic statics, vector-based 3D form and force diagrams are built out of *closed cycles of force vectors* (i.e. *force polygons*) (Fig. 9.1.c), each of them identifying the equilibrium of the forces applied to one individual node of the form diagram (Jasienski et al. 2016). Contrary to 2D graphic statics, in vector-based 3D graphic statics, the cycles of force vectors are not plane polygons but usually skew polygons. In compliance with the method of Cremona in 2D, corresponding edges in the two diagrams are parallel. Procedures for the construction of vector-based 3D force diagrams for a given 3D form diagram have
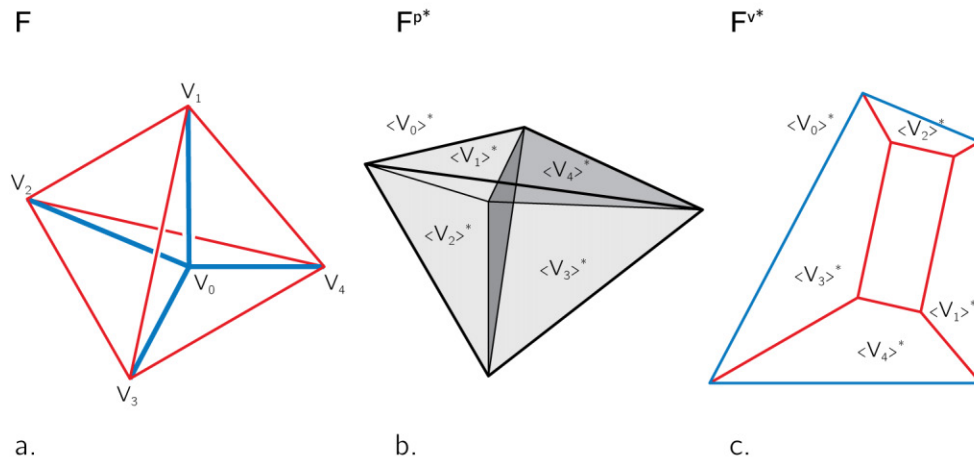
Figure 9.1: (a) 3D form diagram **F** of a self-stressed tetrahedron. (b) Polyhedron-based 3D force diagram $\mathbf{F}^{p*}$. (c) Vector-based 3D force diagram $\mathbf{F}^{v*}$ (D'Acunto et al. 2019). Note that in this thesis the convention is adopted of representing tensile forces in *red*, compressive forces in *blue* and external forces in *dark green*.

been recently described (Jasienski et al. 2016; D'Acunto et al. 2016; D'Acunto et al. 2019). These are based on the node-by-node generation of the cycles of force vectors and on their subsequent assembly into one single diagram following procedures based on graph theory. Thanks to the use of vectors in place of polyhedra, 3D vector-based diagrams generally retain the immediacy of 2D form and force diagrams. In fact, like 2D diagrams, they can be easily built manually using simple geometric constructions within a 3D software environment, without the aid of specialised algorithms. Moreover, corresponding edges in 3D form and force diagrams are usually easily recognisable. Because corresponding edges stay parallel under parallel projections, the main features of the diagrams are not lost when these are represented onto a two-dimensional plane.

Owing to its practical advantages over its polyhedron-based counterpart, in the present work, the vector-based 3D graphic statics approach is used. The latter is here regarded as a consistent framework for the evaluation and manipulation of the external and internal forces in folded plate structures, which are defined using the previously introduced strut-and-tie model (§ 8.3). At first, a geometric procedure for the evaluation of the 3D global equilibrium is described, and an equivalent algebraic formulation is suggested (§ 9.2). Subsequently, the evaluation of the equilibrium of the internal forces within the proposed strut-and-tie model is taken into consideration, following both a geometric and an algebraic approach (§ 9.3). Based on these equilibrium solutions, the construction of vector-based 3D force diagrams is explained in details (§ 9.4), and their transformation is addressed thereafter (§ 9.5).

9.2   Assessment of the External Equilibrium[2]

Given the strut-and tie model of a folded plate structure under external loading
(§ 8.3), the first step in the solution of the static problem consists in the eval-
uation of the global equilibrium of the system of applied forces. In this regard,
a procedure is here described that makes use of vector-based 3D graphic statics
and projections (D'Acunto et al. 2016). This procedure can be applied for any
configuration of the external forces, as long as the structure is statically rigid.

The procedure is exemplified on the strut-and-tie network of one of the
modules of the roof of *Cinema San Pietro* by Musmeci (§ 4.2), which is here
regarded as a standalone structure. As such, an additional plate has been added
to the bottom of the module in order to transform its geometry into a polyhedron.
This polyhedron performs like a rigid body, and it is kinematically stable (§ 8.2)
with respect to the specified support conditions (Fig. 9.2). In the proposed
example, five arbitrary forces Σ are supposed being applied as point loads to five
different nodes of the strut-and-tie network.
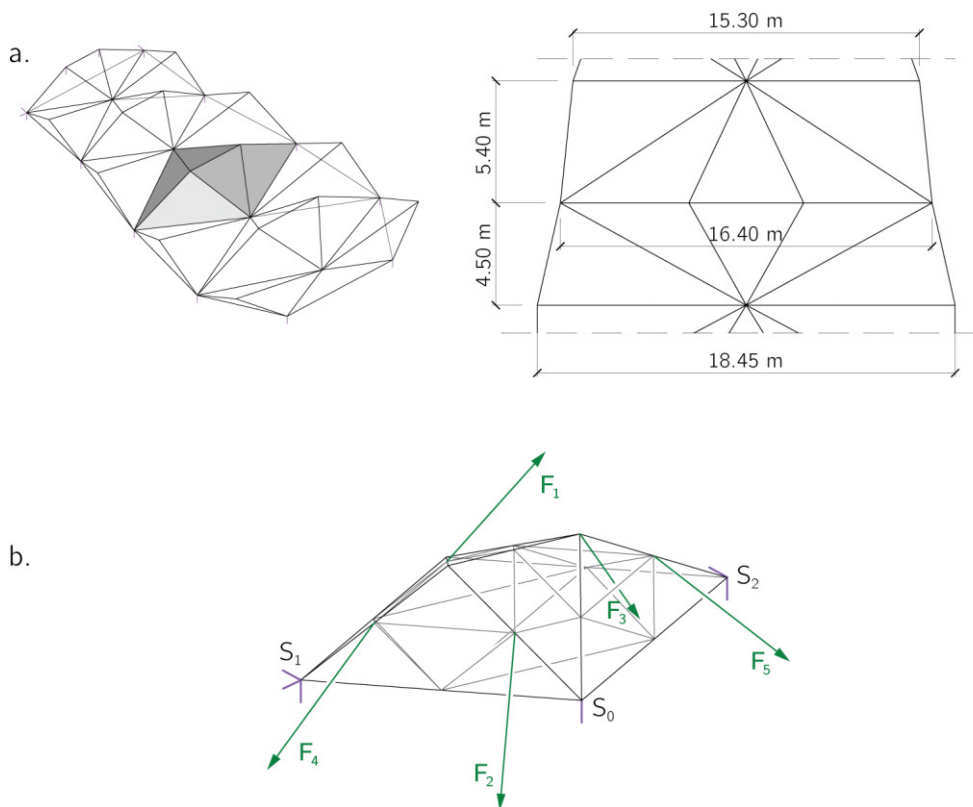
Figure 9.2: (a) Folded plate structure based on the roof of *Cinema San Pietro* by Musmeci
(§ 4.2). (b) Strut-and-tie network of one of the modules of the roof (§ 8.3), with a system Σ
of five applied arbitrary forces.

---

[2]Contents of this section have been previously published in (D'Acunto et al. 2016).

A system of n applied forces Σ can be associated to an equivalent force-couple system $\{R, M_O\}$ (Marti 2013, p. 44) with resultant force R and resultant couple M_O, being the latter evaluated in relation to an arbitrary reference point O. The resultant force R is obtained as the vector sum of the individual forces F_i that are included in the system of forces Σ:

$$R = \sum_{i=0}^{n} F_i \tag{9.1}$$

The resultant couple M_O, calculated with respect to an arbitrary reference point O, can be found as:

$$M_O = \sum_{i=0}^{n} p_i \times F_i \tag{9.2}$$

where p_i is the position vector of an arbitrary point on the line of action of the force F_i based on the chosen reference point O. Two systems of forces Σ and Σ' are equivalent if their force-couple systems are identical with respect to the same arbitrary reference point (Marti 2013, p. 44). Moreover, a system of forces is in equilibrium if its force-couple system is null, that is:

$$R = 0 \qquad M_O = 0 \tag{9.3}$$

The evaluation of the global equilibrium of a given system of external forces according to specified boundary conditions can be solved following a two-phase process (D'Acunto et al. 2016). At first, a force-couple system that is equivalent to the input system of forces is found. Then, a system of reaction forces in relation to the specified boundary conditions is obtained so that the forces are in equilibrium with the force-couple system. Based on the properties above, the system of reaction forces and the input system of forces constitute themselves a system of forces in equilibrium.

Evaluation of the Global Equilibrium using Graphic Statics and Projections
Two graphic statics procedures can be found in the literature that address the problem of global equilibrium in three dimensions, and lead to the definition of vector-based (Schrems and Kotnik 2013) and polyhedron-based (Akbarzadeh et al. 2015a) form and force diagrams respectively (§ 9.1). A third vector-based procedure, which is used in this work to assess the global equilibrium of the strut-and-tie networks (§ 8.3), is grounded on the use of graphic statics and projections (D'Acunto et al. 2016). This approach has been initially introduced by Culmann (1866, pp. 141–144) to determine the centre of a system of parallel forces in space. As explained by Mayor (1910, pp. 103–109), a similar procedure was used by Cremona to find the equilibrium of concurrent forces in space, and eventually, Saviotti (1888, pp. 57–58) described an equivalent process to compose arbitrary forces in space.
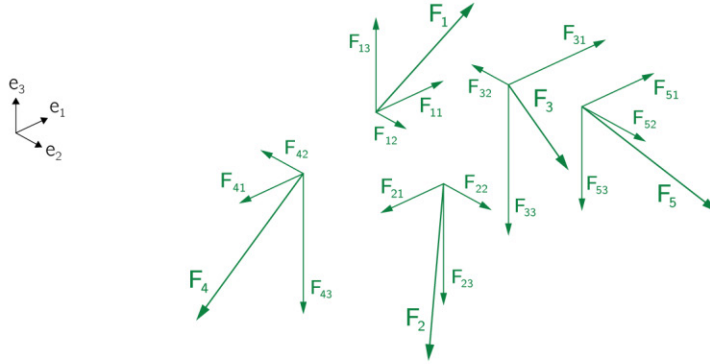
Figure 9.3: Decomposition of the system of forces Σ along e_1, e_2, and e_3.

Based on this method, a given system of n forces Σ can be represented by three skew resultants $\{R_1, R_2, R_3\}$, which are equivalent to the resultant force-couple system $\{R, M_o\}$ of Σ and which are parallel to three initially freely chosen unit vectors $\{e_1, e_2, e_3\}$. Moreover, the three resultants $\{R_1, R_2, R_3\}$ can be further composed into a pair of forces or one force and one couple $\{R, M_o\}$.

In order to evaluate the global equilibrium of the system Σ of five arbitrary skew forces $\{F_1, F_2, F_3, F_4, F_5\}$ applied to the strut-and-tie network of the example (Fig. 9.2), in the first step, three unit vectors $\{e_1, e_2, e_3\}$ not lying on the same plane are defined (Fig. 9.3); the line of actions of the forces of the sought triplet of resultants $\{R_1, R_2, R_3\}$ will be parallel to e_1, e_2, and e_3 respectively. Based on this set-up, every force F_i of Σ is decomposed into its components $\{F_{i1}, F_{i2}, F_{i3}\}$ (Fig. 9.3) along the chosen directions:

$$F_i = F_{i1} + F_{i2} + F_{i3} = F_{i1}e_1 + F_{i2}e_2 + F_{i3}e_3 \qquad (9.4)$$

where the absolute values of F_{i1}, F_{i2} and F_{i3} are the magnitudes of the components F_{i1}, F_{i2} and F_{i3} along e_1, e_2, and e_3 respectively. In this way, the initial system of forces Σ is replaced by three sets of forces Σ_1, Σ_2 and Σ_3, which are parallel to e_1, e_2, and e_3 respectively. To easily illustrate the process, in the example the unit vectors $\{e_1, e_2, e_3\}$ are chosen to be orthonormal.

In the second step, three auxiliary projection planes Π', Π'' and Π''' are set to be parallel to the vector pairs $\{e_2, e_3\}$, $\{e_1, e_3\}$, and $\{e_1, e_2\}$ respectively. Moreover, three unit vectors $\{t', t'', t'''\}$ are introduced, which define the directions of projection onto Π', Π'', and Π'''; each vector of the triplet $\{t', t'', t'''\}$ can be freely chosen, provided that it is not parallel to its corresponding projection plane. For convenience of illustration, in the example the vectors $\{t', t'', t'''\}$ are chosen to be parallel to $\{e_1, e_2, e_3\}$ respectively. The forces F_{i3} included in the set Σ_3, which are all parallel to e_3, are then projected onto Π' through a parallel projection in the direction of t', thus generating a new set Σ_3' of coplanar forces F_{i3}' (Fig. 9.4.a). In order to find the magnitude and line of action of the resultant R_3' of Σ_3', the standard procedure for the evaluation of the global equilibrium in

2D graphic statics is applied. Hence, on the plane Π', an auxiliary funicular structure is built, and the corresponding force polygons are constructed, thus generating the form $\mathbf{F_3}'$ and the force $\mathbf{F_3^{*}}'$ diagrams. The magnitude of R'_3 of Σ'_3 is then assessed graphically. The position of its line of action is found so that the moment generated by R'_3, with respect to any arbitrary reference point in Π', is equivalent to the resultant couple of Σ'_3. Likewise, the forces F_{i3} included in Σ_3 are projected onto Π'' in the direction of t'' to generate Σ''_3; by construction, the magnitude of the resultant R''_3 of Σ''_3 is equal to the one of R'_3 and its line of action is assessed following the 2D graphic statics procedure described earlier (Fig. 9.4.a). The forces R'_3 and R''_3 represent the projections on Π' and Π'' respectively of the resultant R_3 of Σ_3. The magnitude of R_3 is, therefore, the same as R'_3 and R''_3. The line of action of R_3 is the intersection between the plane containing R'_3 and parallel to the vector pair $\{t', e_3\}$ and the plane containing R''_3 and parallel to the vector pair $\{t'', e_3\}$. The moment generated by R_3 with respect to an arbitrary reference point O in space is equivalent to the resultant couple of Σ_3.

The entire process is then repeated to determine the magnitudes and the lines of action of the resultant forces R_2 of Σ_2 (Fig. 9.4.b) and R_1 of Σ_1 (Fig. 9.5.a). As a result, the magnitudes of R_1, R_2 and R_3 and their lines of action are determined to be equivalent to the resultant force-couple systems of Σ_1, Σ_2 and Σ_3 respectively (Fig. 9.5b). Moreover, considering that Σ_1, Σ_2 and Σ_3 are themselves equivalent to the given system of forces Σ, the triplet of forces $\{R_1, R_2, R_3\}$ is also equivalent to Σ. In fact, the triplet of forces here obtained represents one of the infinite triplets of forces that are all equivalent to the force-couple system $\{R, M_O\}$ of Σ. By varying the unit vectors $\{e_1, e_2, e_3\}$ other triplets can be found. Depending on the specific problem to be solved, one or more resultants of the triplet $\{R_1, R_2, R_3\}$ may be null. In this particular case, the system may also produce a couple M, whose magnitude is invariant to the choice of the reference point O.

Determination of One Resultant and One Couple The procedure previously explicated to determine three skew resultants $\{R_1, R_2, R_3\}$ equivalent to a given system of forces Σ through projections can be used to find a resultant force-couple system $\{R, M\}$ of Σ directly. In fact, if the unit vectors $\{e_1, e_2, e_3\}$ are chosen to be orthonormal and e_3 is set to be parallel to the free resultant R^* of Σ in the force diagram $\mathbf{F}^*$ (Fig. 9.6), the method of the projections yields the position of the line of action of the resultant R, which coincides with the resultant R_3 of the set of forces Σ_3 parallel to e_3. Furthermore, the set of forces Σ_1 and Σ_2, which are parallel to e_1 and e_2 respectively, if not empty, generate a resultant couple M. This can be represented by a free vector with two components, $M_\parallel$ parallel to R and $M_\perp$ perpendicular to R. Likewise, and in case the forces of the given system Σ are decomposed at the intersection points of their lines of action and a plane parallel to the projection plane Π''', which
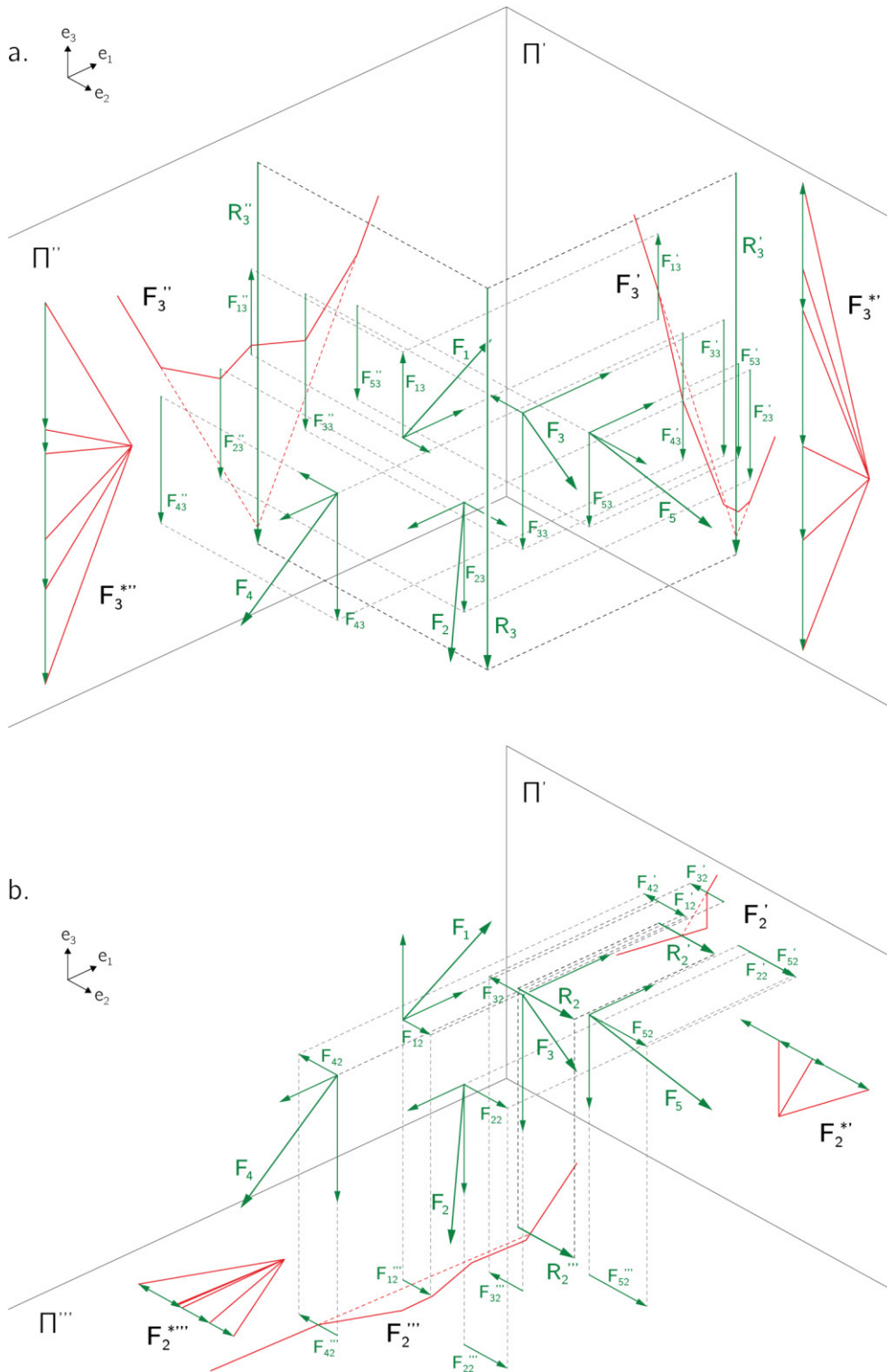
Figure 9.4: (a) Determination of $\boldsymbol{R_3}$ in relation to $\boldsymbol{R_3^{'}}$ on $\Pi^{'}$ and $\boldsymbol{R_3^{''}}$ on $\Pi^{''}$. (b) Determination of $\boldsymbol{R_2}$ based on $\boldsymbol{R_2^{'}}$ on $\Pi^{'}$ and $\boldsymbol{R_2^{'''}}$ on $\Pi^{'''}$.
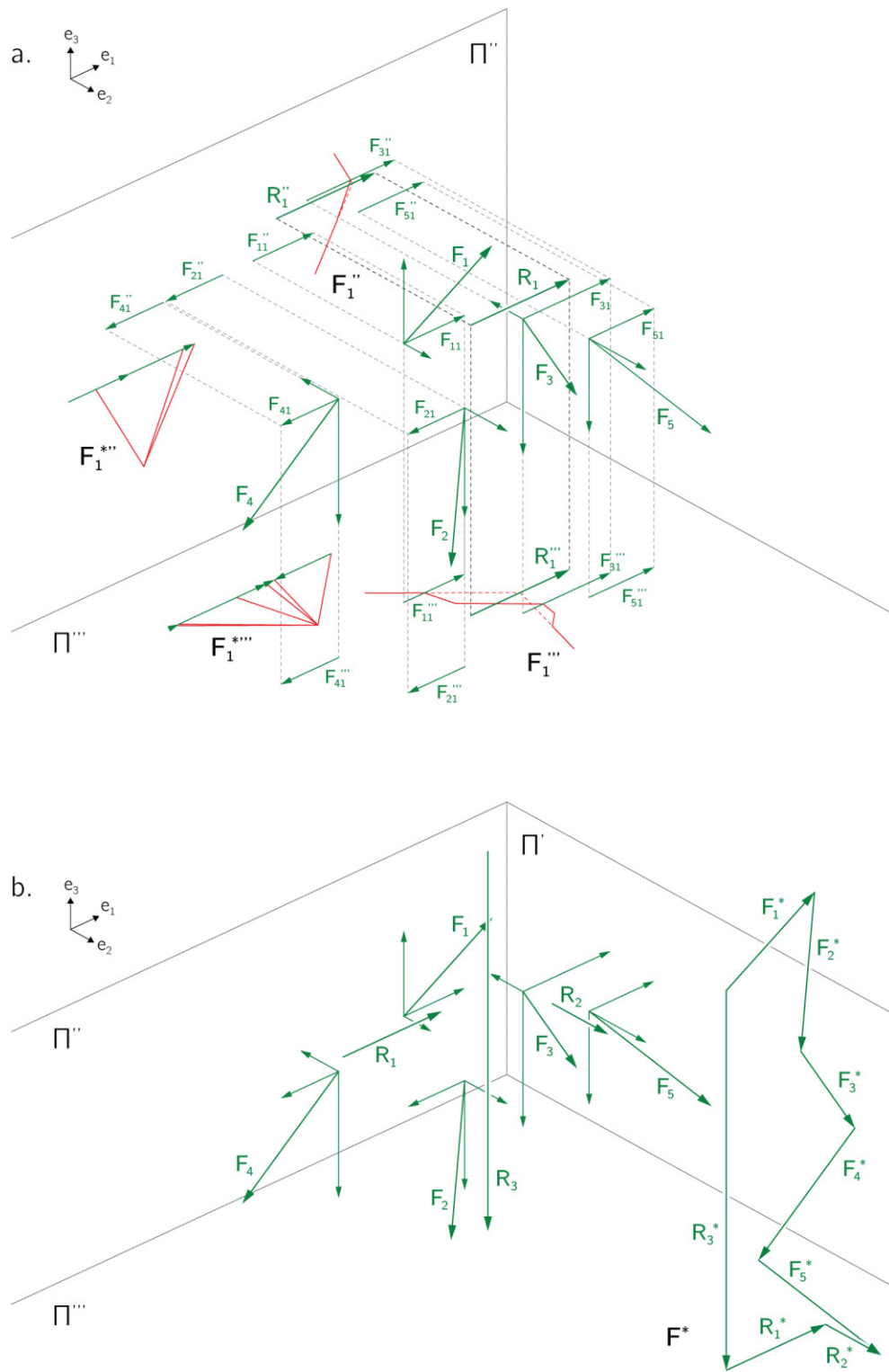
Figure 9.5: (a) Determination of R_1 in relation to $R_1^{''}$ on $\Pi^{''}$ and $R_1^{'''}$ on $\Pi^{'''}$. (b) The given system of forces Σ with the resultants $\{R_1, R_2, R_3\}$.
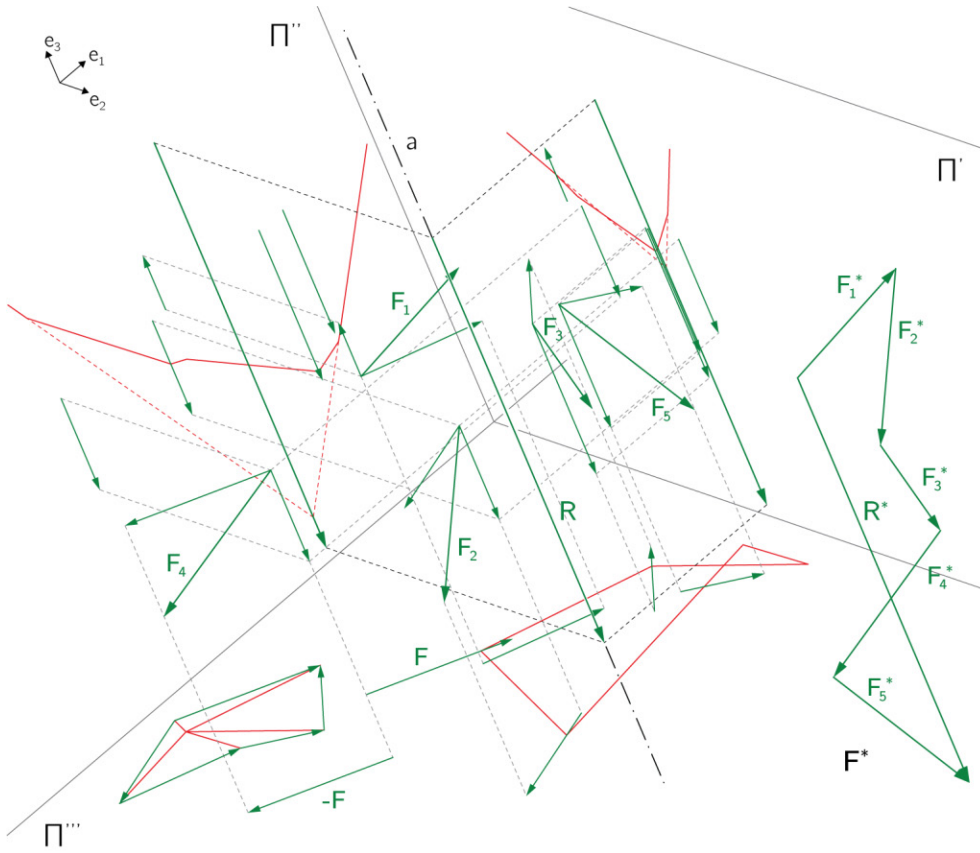
Figure 9.6: Determination of the resultant R and the couple $\{F, -F\}$ equivalent to Σ

itself is perpendicular to e_3, the method of the projections is totally equivalent to the procedure described by Akbarzadeh et al. (2015a). The line of action of the resultant R, which coincides with the resultant R_3 parallel to e_3, constitutes the *central axis a* of the system Σ, and the plane Π''' is the *orthographic plane* (Cremona 1872).

If not null, the components of the input forces Σ parallel to e_1 and e_2 generate a resultant couple M that can be represented by a free vector parallel to R and perpendicular to Π'''; hence, the component $M_\perp$ of M is null. Furthermore, if the resultant couple M is defined in the form diagram by a couple of forces $\{F, -F\}$ on Π''' and the line of action of F is made to intersect the central axis, F and R can be composed into a force F_r. The lines of action of F_r and $-F$ are *conjugate lines* in relation to a *null polarity* (Möbius 1833; Pottmann and Wallner 2001), and the system Σ is thus equivalent to the pair of forces $\{F_r, -F\}$. Given this construction, it is immediate to show that the projections of conjugate lines onto the orthographic plane are parallel lines (Cremona 1872).

Evaluation of the Support Reactions   Once the triplet of forces $\{R_1, R_2, R_3\}$ equivalent to the given system of forces Σ is found, the reactions at the supports
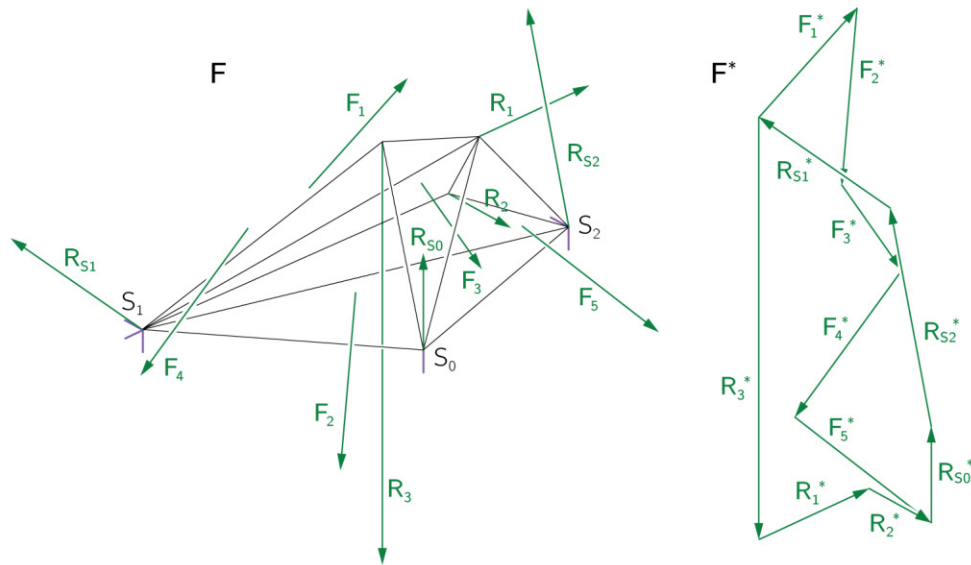
Figure 9.7: Evaluation of the reaction forces R_{S0}, R_{S1}, and R_{S2} at the supports.

can be evaluated according to the specified boundary conditions (Fig. 9.2). If the structure is statically rigid and statically determinate externally (§ 8.2), the equilibrium between the applied loads and the reactions can be resolved before the evaluation of the internal equilibrium. In case the structure is statically rigid and statically indeterminate externally (§ 8.2), those support forces other than the ones necessary to attain the static determinacy of the system can be regarded as parameters in the solution of the equilibrium problem.

In relation to the given example, which is statically rigid and statically determinate externally (Fig. 9.2), a simple auxiliary structure can be used to evaluate the reaction forces R_{S0}, R_{S1} and R_{S2} produced by the forces $\{R_1, R_2, R_3\}$ at the support points S_0, S_1 and S_2 respectively. As such, an internally statically determinate 3D truss made of three tetrahedra (6 nodes, 12 edges) is constructed (Fig. 9.7), whose nodes are the three support points S_0, S_1 and S_2 and other three freely chosen points on the lines of action of R_1, R_2 and R_3 respectively.

Global Equilibrium and Exterior Algebra   The global equilibrium of a system of forces Σ can also be assessed by means of exterior algebra (Crapo 1979; Whiteley 1987, Baniček et al. 2018). As such, forces are treated as 2-extensors, which can be represented as 6-vectors using Plücker coordinates (Plücker 1865; Grassmann 2000). As described in details by Whiteley (1987), the composition of two 2-extensors yields another 2-extensor only if the lines of action of the corresponding forces intersect each other. In the general case, the sum of 2-extensors generates a 6-vector, which is defined as *wrench* and is equivalent to the previously introduced resultant force-couple system $\{R, M\}$ of Σ.

9.3   Assessment of the Internal Equilibrium

Once the global equilibrium of the given strut-and tie network has been solved
(§ 9.2), the internal equilibrium of the structure can be evaluated. This opera-
tion leads to the identification of the magnitudes of the forces within the *edge
members* and *plate members* (§ 8.3) of the strut-and-tie network.

Assuming that the given structure is rigid and externally statically determi-
nate under the specified support conditions, based on its degree of static inde-
terminacy, the strut-and-tie network is either internally statically determinate or
indeterminate (§ 8.2). In the first case, the equilibrium problem has only one pos-
sible solution, and the assessment of the internal equilibrium can be immediately
performed. In the second case, multiple equilibrium solutions are possible for the
same given static configuration. In compliance with the theory of plasticity, as
long as the hypotheses of the lower bound theorem are fulfilled (§ 10.1), any of
these solutions is admissible. In this case, before proceeding to the evaluation
of the internal equilibrium, the redundant members of the strut-and-tie network
(i.e. the members that can be removed without compromising the kinematic
stability of the structure) have to be identified[3], and their internal forces have
to be then treated as parameters in the equilibrium problem.

9.3.1   Evaluation of the Internal Equilibrium using Graphic Statics

As a preliminary step to the solution of the internal equilibrium, the edges of
the strut-and-tie network with zero force can be detected based on simple geo-
metrical rules (Pirard 1950; Coates et al. 1987). Thanks to this operation, the
number of unknown forces in the static problem can be reduced.

Regarding the strut-and-tie network as a form diagram **F**, the equilibrium of
the internal forces within the structure can then be solved iteratively node-by-
node using vector-based 3D graphic statics (Jasienski et al. 2016).

In particular, each vertex V_i of **F** is isolated into a free body diagram (Marti
2013, p. 44) together with the forces $\boldsymbol{F}_{i-j}$ in the edge and plate members E_{i-j}
incident to V_i, and the applied external forces $\boldsymbol{F}_i$ and reaction forces $\boldsymbol{R}_{s_i}$ when
present. The unknown forces are then determined so that in the force diagram **F***
the $\boldsymbol{F}_{i-j}^*$, the applied external forces $\boldsymbol{F}_i^*$, and reaction forces $\boldsymbol{R}_{s_i}^*$ generate a *closed
cycle of force vectors*. Provided that the amount of unknown forces at every
node is no more than three, the closed cycle of force vectors can be constructed
geometrically (Jasienski et al. 2016). At every iteration, the nodes V_i of **F** are
sorted in ascending order in relation to the number of unknown forces.

---

[3]When possible, this operation can be performed by detecting first a statically determinate
sub-system of the given strut-and-tie network and then locating the redundant members. A
more general algebraic procedure involves the singular value decomposition of the ($3V - k$ by
E) *equilibrium matrix A* of the structure (§ 8.2.1) as described by Pellegrino (1993).

The procedure described above is here illustrated using a strut-and-model based on the geometry of one of the modules of the roof of *Cinema San Pietro* by Musmeci (§ 4.2; § 9.2). A *synthetic strut-and-tie network* (§ 8.3) is considered, which meets the requirement of the geometric procedure[4]. A supplementary edge has been introduced at the bottom of the structure to generate a statically determinate configuration in relation to the specified support conditions (Fig. 9.8, top). The structure is loaded with two external forces (F_2 and F_4).

After the global equilibrium is evaluated (§ 9.2), the reactions at the supports (R_{S0}, R_{S1} and R_{S2}) are found, and the cycle of external force vectors $\langle V_E \rangle^*$ is built in $\mathbf{F}^*$. The internal equilibrium of the strut-and-tie network can then be solved, starting from a vertex with no more than three unknown forces, such as V_1. The equilibrium at the other five vertices is then assessed iteratively considering, for example, the sequence $\{V_1, V_2, V_4, V_5, V_0, V_3\}$. Hence, six cycles of force vectors $\{\langle V_1 \rangle^*, \langle V_2 \rangle^*, \langle V_4 \rangle^*, \langle V_5 \rangle^*, \langle V_0 \rangle^*, \langle V_3 \rangle^*\}$ are generated in $\mathbf{F}^*$ other than the one of the external forces $\langle V_E \rangle^*$ (Fig. 9.8, bottom).

Internal Equilibrium and Linear Algebra From an algebraic standpoint, the above geometric procedure is equivalent to the following equilibrium condition applied at every vertex V_i of $\mathbf{F}$:

$$\sum_j (F_{i-j}) + F_i + R_{si} = 0 \tag{9.5}$$

where j iterates on the indexes of the vertices V_j of $\mathbf{F}$ connected to V_i. In particular, for each vertex V_i of $\mathbf{F}$, the unknown force magnitudes μ_{i-j} are found so that:

$$\sum_j (F_{i-j}) + F_i + R_{si} = \sum_j (\mu_{i-j} d_{i-j}) + F_i + R_{si} = 0 \tag{9.6}$$

where the unit vector d_{i-j} is equivalent to:

$$d_{i-j} = \frac{p_j - p_i}{\|p_j - p_i\|} \tag{9.7}$$

being p_i the position vector of V_i and the p_j the position vectors of the vertices V_j of $\mathbf{F}$ connected to V_i[5]. A more general procedure for the assessment of the equilibrium of a given structure relies on the solution of a system of linear equations based on the ($3V - k$ by E) *equilibrium matrix* $\mathbf{A}$ of the structure (§ 8.2.1), as explained in details by Pellegrino and Calladine (1986), Micheletti (2008) and Van Mele and Block (2014).

---

[4]Note that in case the folded plate structure has only triangular plates and the external forces are applied only at the endpoints of the folded edges like in the proposed example, the plate members are not loaded; in this occurrence, complete and synthetic strut-and-tie networks (§ 8.3) are equivalent.

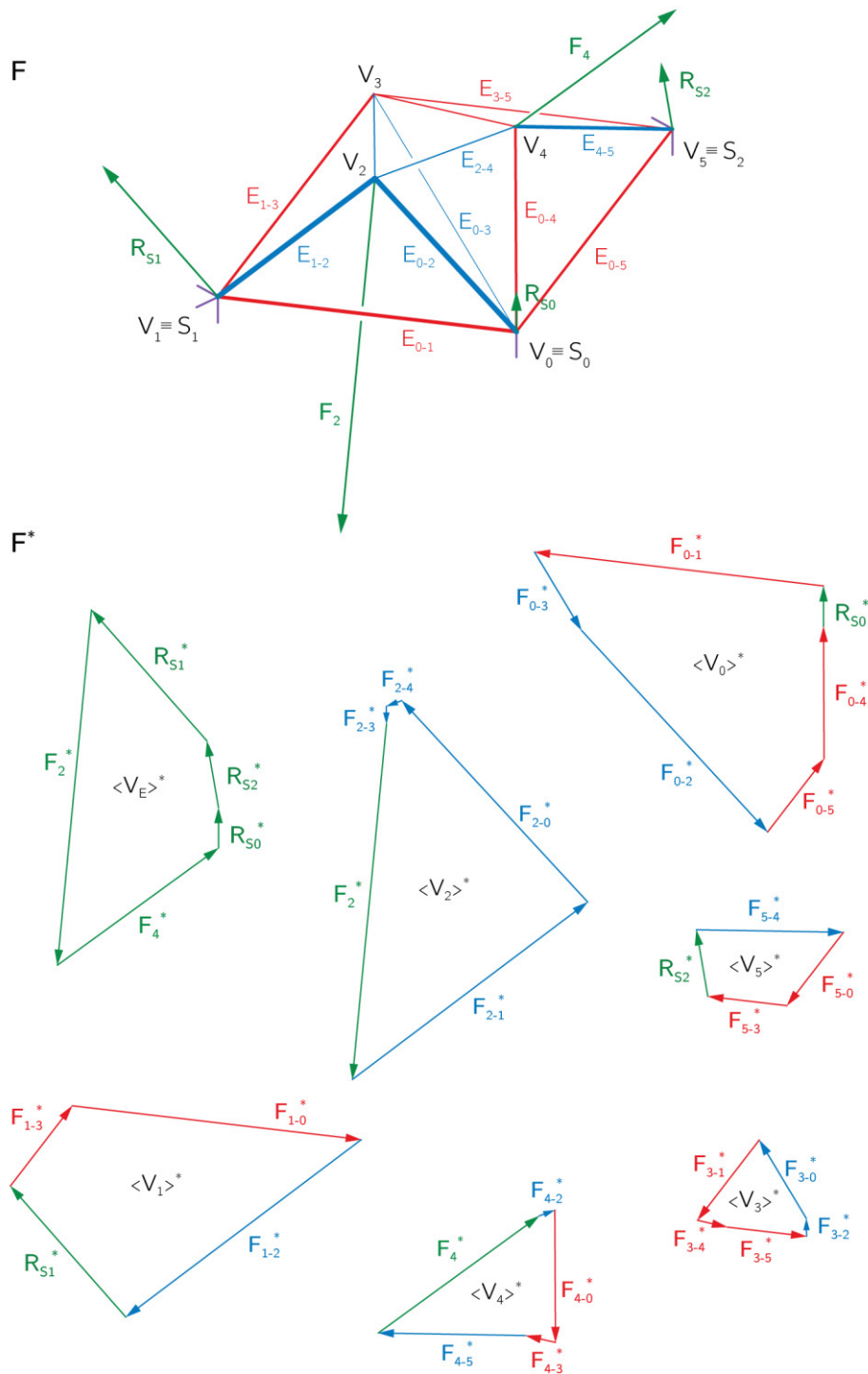[5]The values of the μ_{i-j} are positive for tension and negative for compression forces.

Figure 9.8: Assessment of the internal equilibrium of the 3D form diagram **F** of the strut-and-tie model related to the roof of *Cinema San Pietro* by Musmeci (§ 4.2; § 9.2). The graphical node-by-node procedure (Jasienski et al. 2016) results in the generation of seven cycles of force vectors $\{\langle V_E \rangle^*, \langle V_0 \rangle^*, \langle V_1 \rangle^*, \langle V_2 \rangle^*, \langle V_3 \rangle^*, \langle V_4 \rangle^*, \langle V_5 \rangle^*\}$.

9.4 Construction of 3D Force Diagrams[6]

A vector-based 3D force diagram is built out the assembly of *closed cycles of force vectors*, each of them representing the equilibrium of a node of the 3D form diagram (§ 9.1). As a result, each edge of the form diagram corresponds to a *pair of opposite force vectors* in the force diagram. In the diagram, these two force vectors have to be overlapped to define a single *edge*. Form and force diagrams are *reciprocal* if all the pairs of opposite force vectors can be overlapped without generating any duplicate edge. Conversely, when a pair of opposite force vectors cannot be directly overlapped (i.e. *a pair of non-overlapping vectors*) (Jasienski et al. 2016), an additional pair of opposite vectors have to be introduced in the force diagram, thus creating a *pair of duplicate edges* (D'Acunto et al. 2019). The presence of duplicate edges in the force diagram, other than preventing it from being reciprocal to the form diagram, reduces its legibility.

In the general case, vector-based 3D force diagrams have one or more pairs of duplicate edges. The same can also occur for certain two-dimensional structures. As highlighted by Cremona (1872) and Maxwell (1876), configurations of non-reciprocal form and force diagrams can be already found in the work of Culmann (1866).

9.4.1 On the Reciprocity of Vector-based 3D Form and Force Diagrams

As demonstrated by Whitney (1933) within the domain of graph theory, the necessary and sufficient condition for a graph to have its dual (§ 8.1), is that the graph should not contain any of the Kuratowski's graphs as a subgraph - i.e. a subgraph that is a subdivision of K_5 or $K_{3,3}$ being the former the complete graph on five vertices and the latter the complete bipartite graph on six vertices (Harary 1969). This is equivalent to the condition that the graph is *planar*[7]. According to Crapo and Whiteley (1993), the necessary and sufficient condition for a given truss to have a reciprocal on its dual graph is that its underlying graph is planar and that the structure supports a non-null self-stress state[8]. The planarity of the underlying graph of a structure can be tested by using one of the many algorithms available in the literature, such as the one by Boyer (2001).

In the case of three-dimensional structures, only specific configurations of lattice structures have underlying planar graphs. Belong to this category, for example, surface structures made of bars in space (Sauer 1970; Wallner and Pottmann 2008; Tachi 2012b; Tachi 2012a), some classical tensegrity structures

---

[6]Contents of this section have been previously published in (D'Acunto et al. 2019).

[7]A graph is planar if it can be embedded in the plane, without the edges crossing each other except at the vertices (§ 8.1). After the embedding, the graph is defined *plane graph* (Harary 1969, p. 102).

[8]This consists in a self-stress that is non-zero on all edges of the structure (Crapo and Whiteley 1993).

(Micheletti 2008), or the dependent cube and octahedron (Crapo 1979). The reciprocal vector-based force diagrams of these structures have been defined as *Cremona Reciprocals* (Crapo 1979). However, as in the general case the underlying graph of a 3D structure is non-planar, reciprocity between 3D form and force diagrams is generally not achieved (Jasienski et al. 2016). Several strategies to generate 2D and 3D reciprocal form and force diagrams, when their underlying graphs are non-planar, can be found in the literature. Particularly relevant are the strategy of Bow (1873) of introducing a supplementary node at the crossing of bars in 2D trusses, the proposal of Crapo and Whiteley (1993) of reciprocals as infinite frameworks and the approach of Micheletti (2008) of point-symmetric reciprocal diagrams of specific self-stressed structures. When reciprocal form and force diagrams cannot be constructed, multiple alternative configurations of the force diagram can be generated for a given form diagram (D'Acunto et al. 2019).

In the next section, several geometric procedures are described to construct different vector-based 3D force diagram configurations $\mathbf{F}^*$ for a given 3D form diagram $\mathbf{F}$ with underlying non-planar graph $\mathbf{T}$ (D'Acunto et al. 2019). These approaches can be regarded as a generalisation to the third dimension of the conventional graphic statics procedures explicated by Bow (1873) and Saviotti (1888) for the solution of 2D trusses with underlying non-planar graphs. The procedures are exemplified using the strut-and-tie model of the roof of *Cinema San Pietro* by Musmeci (§ 4.2; § 9.3) as an externally loaded 3D form diagram $\mathbf{F}$ with underlying non-planar graph $\mathbf{T}$ (Fig. 9.9).
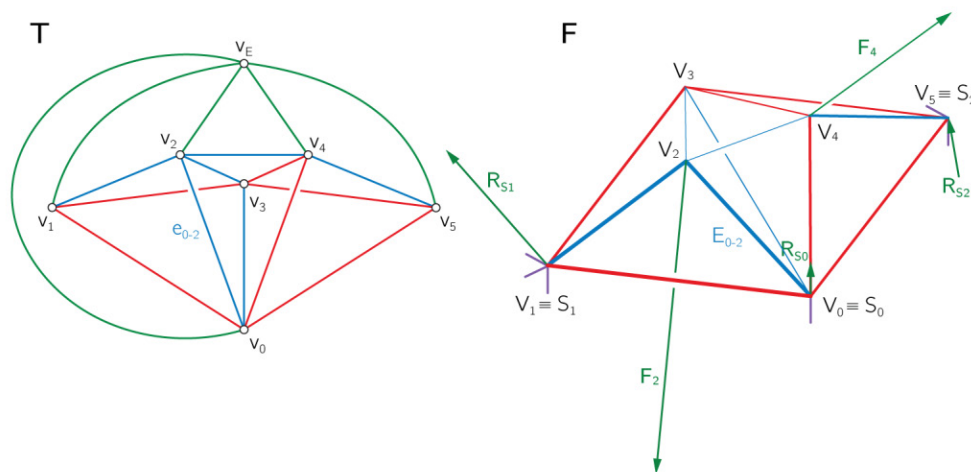

Figure 9.9: Graph $\mathbf{T}$ and 3D form diagram $\mathbf{F}$ of the strut-and-tie model based on the geometry of *Cinema San Pietro* by Musmeci (Fig. 9.8). Because of the presence of two pairs of crossing edges in $\mathbf{T}$, the graph is non-planar. Note the presence of the *vertex of the external forces* v_E in $\mathbf{T}$, to which all the edges of the external forces are connected. This vertex does not correspond to any node in $\mathbf{F}$.

.

9.4.2   Vector-based 3D Force Diagrams Configurations

In the following paragraphs, four different vector-based 3D force diagram configurations are presented (D'Acunto et al. 2019). Each configuration is characterised by a diverse organisation of the cycles of force vectors within the force diagrams, which in turn implies a different number of duplicated edges. The choice of the configuration depends on the specific design problem to be solved.

Double-layered Configuration   For the construction of a double-layered 3D force diagram (Jasienski et al. 2016), in the first step all the vertices of $\mathbf{T}$, corresponding to the nodes of $\mathbf{F}$ where external forces are applied, are connected to a newly created vertex of the external forces v_E through edges e_{Ei} (Fig. 9.9, left). The v_E is an ideal element and does not correspond to any node of $\mathbf{F}$.

Without changing the topology of $\mathbf{T}$, in the second step its vertices are repositioned in a way that the e_{Ei} do not cross any other edge of $\mathbf{T}$. In the third step, the non-planar graph $\mathbf{T}$ (Fig. 9.9, left) is transformed into a plane graph $\mathbf{T_P}$ (Fig. 9.10.a, left), without altering the static equilibrium of the structure. That is, each crossing edge e_{s-t} is split into two new edges e_s and e_t that are respectively connected to the vertices v_s and v_t of e_{s-t} and to one newly created ideal vertex v_D, avoiding any crossing between the new edges and the e_{Ei}. The corresponding edge E_{s-t} of $\mathbf{F}$, connected to the nodes V_s and V_t, is substituted by a pair of opposite force vectors $\boldsymbol{F_s}$ and $\boldsymbol{F_t}$, representing respectively the internal forces $\boldsymbol{F_{s-t}}$ and $\boldsymbol{F_{t-s}}$ (§ 9.3). In the fourth step, the cycle of force vectors $\langle V_E \rangle^*$ and the $\langle V_i \rangle^*$ are constructed. The sequence of the force vectors in each cycle is the one of the corresponding edges in $\mathbf{T_P}$ when following a *cyclic order* around the vertex of $\mathbf{T_P}$ corresponding to that cycle. Note that the order of the force vectors in $\langle V_E \rangle^*$ (e.g. counter-clockwise) is opposite to the one of the force vectors in the $\langle V_i \rangle^*$ (e.g. clockwise). An additional closed cycle $\langle V_D \rangle^*$ is created out of the force vectors corresponding to the edges of $\mathbf{T_P}$ connected to v_D.

In the last step, the $\langle V_E \rangle^*$, $\langle V_i \rangle^*$ and $\langle V_D \rangle^*$ are assembled into a force diagram $\mathbf{F}^*$ (Fig. 9.10.a, right), based on the connectivity of the corresponding vertices in $\mathbf{T_P}$. That is, any two cycles of force vectors $\langle V_m \rangle^*$ and $\langle V_n \rangle^*$ are connected to each other if their corresponding nodes v_m and v_n in $\mathbf{T_P}$ share the same edge e_{m-n}. The connection between the cycles is attained by overlapping the opposite force vectors of $\langle V_m \rangle^*$ and $\langle V_n \rangle^*$, which relate to the common edge e_{m-n}, into one single edge E_{m-n}^* in $\mathbf{F}^*$. The topology of $\mathbf{F}^*$ is thus represented by $\mathbf{T_P}^*$, which is the dual graph (§ 8.1) of $\mathbf{T_P}$ (Fig. 9.10.a, left).

As a result, the external force vectors in the $\langle V_i \rangle^*$ that are overlapped to the ones in $\langle V_E \rangle^*$ generate a closed cycle of external force edges. Likewise, the force vectors of the cycles $\langle V_i \rangle^*$ that are overlapped to the ones of the cycle $\langle V_D \rangle^*$ generate a closed cycle of duplicate edges. $\langle V_E \rangle^*$ and $\langle V_D \rangle^*$ constitute the first and second layers of $\mathbf{F}^*$. According to the initial repositioning of the vertices in $\mathbf{T}$, various possible double-layered force diagrams can be produced.
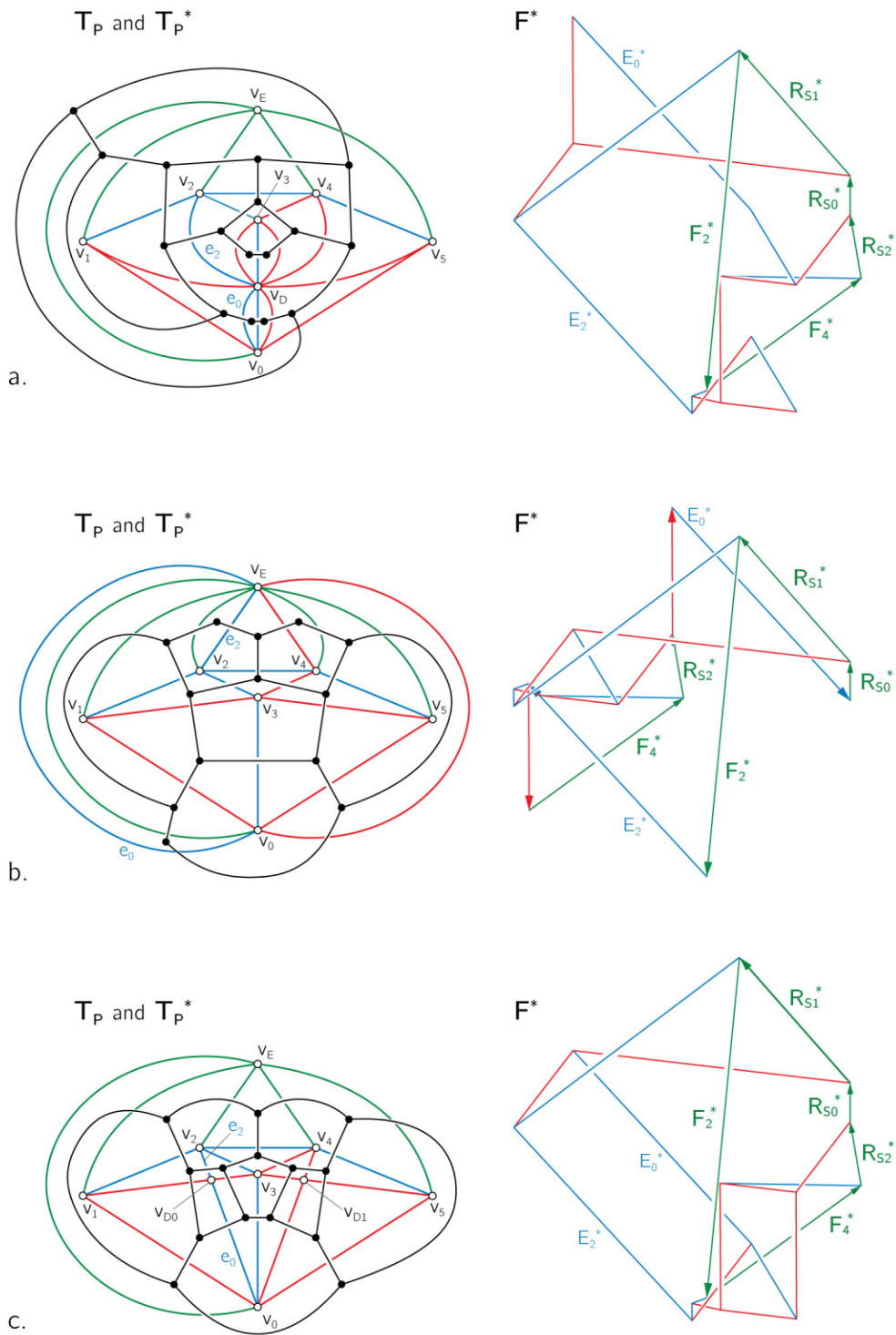
Figure 9.10: (a) Double-layered configuration: plane graph $\mathbf{T_P}$ of $\mathbf{T}$ (Fig. 9.9) and its dual graph $\mathbf{T_P}^*$; corresponding 3D force diagram $\mathbf{F}^*$. (b) Single-layered configuration: plane graph $\mathbf{T_P}$ of $\mathbf{T}$ (Fig. 9.9) and its dual graph $\mathbf{T_P}^*$; corresponding 3D force diagram $\mathbf{F}^*$. (c) Multiple-quads configuration: plane graph $\mathbf{T_P}$ of $\mathbf{T}$ (Fig. 9.9) and its dual graph $\mathbf{T_P}^*$; corresponding 3D force diagram $\mathbf{F}^*$.

.

Single-layered Configuration   A single-layered vector-based 3D force diagram (D'Acunto et al. 2017) can be obtained after modifying the previously described procedure (Fig. 9.10.b). In the third step, the two new edges e_s and e_t that are generated after splitting each crossing edge e_{s-t}, are here connected to v_E (Fig. 9.10.b, left). The edge E_{s-t} of **F** connected to the nodes V_s and V_t is then substituted by a pair of opposite external force vectors F_s and F_t. A closed cycle of external force vectors $\langle V_E \rangle^*$ is thus generated in which a pair of non-overlapping vectors (F_s^* and F_t^*) is created for each pair of newly introduced external forces (F_s and F_t). In comparison to other configurations, the single-layered one generally allows producing a more compact force diagram $\mathbf{F}^*$ (Fig. 9.10.b, right).

Multiple-quads Configuration   To construct a multiple-quads vector-based 3D force diagram, **T** (Fig. 9.9) is transformed into a plane graph $\mathbf{T_P}$ (Fig. 9.10.c, left) through *planarization* (Buchheim et al. 2014) by adding a new vertex v_{Di} at every crossing of edges in **T**. Hence, every pair of crossing edges of **T** are split into four edges. Although this strategy does not alter the equilibrium of the structure, contrary to the 2D case (Bow 1873), the new vertices v_{Di} are not related to any node in **F**. In fact, the edges of **F** corresponding to the crossing ones in **T** generally do not intersect in one point in space. For every new vertex v_{Di}, a new quadrilateral cycle $\langle V_{Di} \rangle^*$ constituted by two pairs of opposite force vectors is generated in $\mathbf{F}^*$ (Fig. 9.10.c, right). This force diagram configuration usually leads to a high amount of duplicate edges. In this regard, specific algorithms can be used to minimise the number of crossing edges in **T** (Chimani 2008).

Case-specific Configuration   As an alternative to the procedures described in the previous paragraphs, the general strategy of transforming the graph **T** of **F** into a plane graph $\mathbf{T_P}$, without altering the static equilibrium of the structure, can be applied. In this way, **T** can be transformed into $\mathbf{T_P}$ by splitting the crossing edges in **T** and connecting them to any number of new vertices v_{Di} or to any existing vertex v_i. The equilibrium of the structure is kept unchanged by respecting the condition that the two edges (e_s and e_t) generated after splitting an existing one (e_{s-t}) are connected to the same vertex. Vector-based force diagrams of this type can always be constructed but they are case-specific: their features cannot be characterised in the same way as the ones previously described.

To test the applicability of the aforementioned procedures to a more complex structural configuration, a double-layered vector-based 3D force diagram is constructed on the basis of the complete strut-and-tie network of a module of the roof of *Stabilimento Raffo* by Musmeci (§ 4.2; § 8.3). The module is here regarded as a standalone structure, which is globally statically determinate with respect to the specified support conditions (Fig. 9.11).
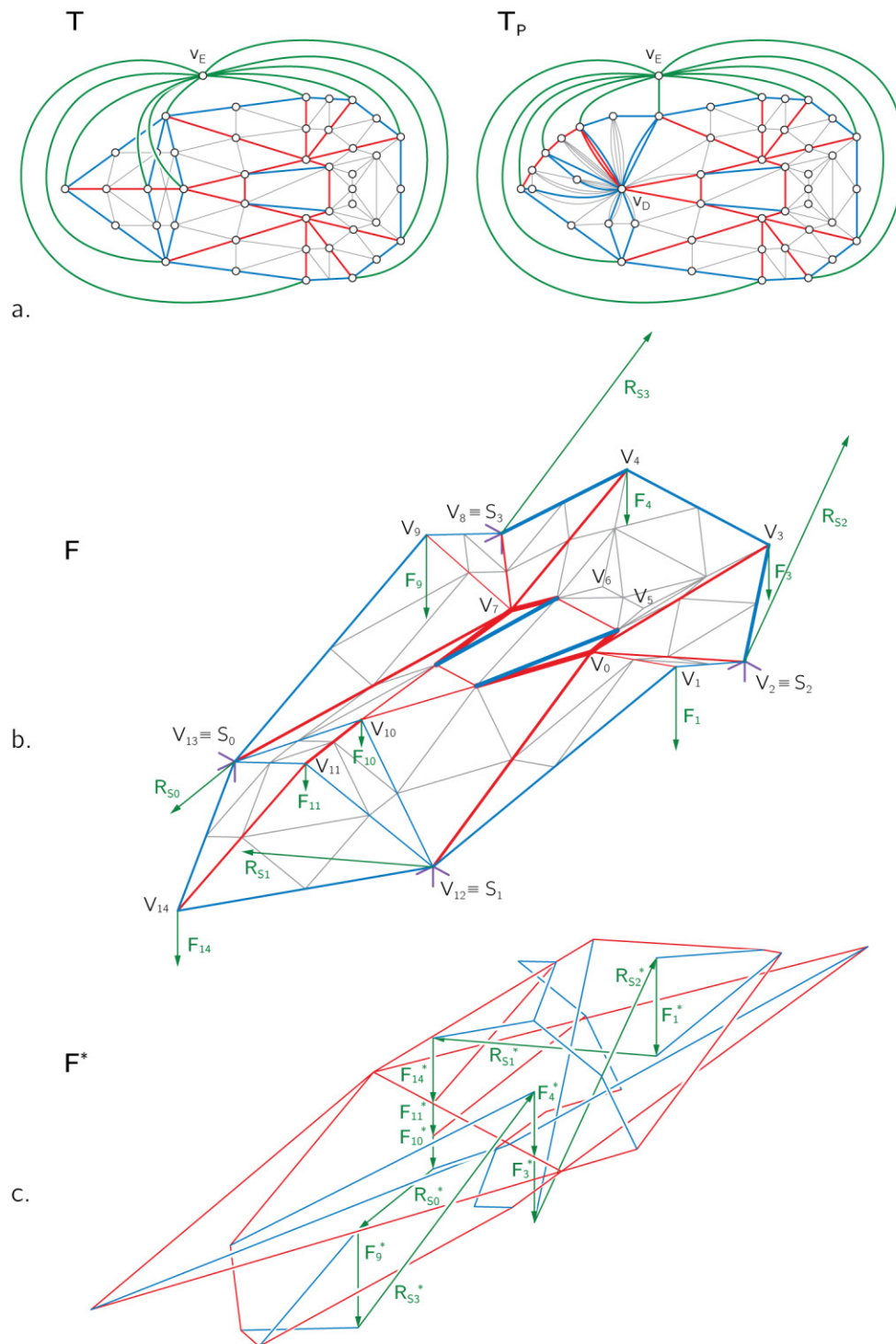
Figure 9.11: (a) Graph **T** and plane graph **T$_P$** based on the complete strut-and-tie model of a module of the roof of *Stabilimento Raffo* by Musmeci (§ 4.2). (b) 3D form diagram **F**. (c) 3D force diagram **F*** built according to the double-layered configuration.

.

9.5   Transformation of 3D Force Diagrams[9]

This section presents several transformations that can be applied to a vector-based 3D force diagram without breaking its interdependence to its corresponding 3D form diagram (D'Acunto et al. 2017). These transformations ensure the parallelism between corresponding edges in the two diagrams and keep their topology unchanged. The transformations can be applied to any of the force diagram configurations described earlier (§ 9.4). The possibility of manipulating the force diagram by means of geometric transformations is particularly relevant within the design process. Thanks to this opportunity, the designer is able to control the distribution of the forces within a given structure directly and steer its load-bearing behaviour towards a desired one. In this way, the adjustment of the magnitude and the direction of the forces in a vector-based 3D force diagram can be used as an active operation. Two categories of manipulations of force diagrams are described: global transformations, which affect all the elements of the diagram simultaneously, and local transformations, which permit the manipulation of individual elements of the diagram (D'Acunto et al. 2017).

9.5.1   Global Transformations

In compliance with the classification introduced by Fivet (2016), a series of global transformations of a vector-based 3D force diagram $\mathbf{F}^*$ is here presented that can be applied no matter the presence of duplicate edges in $\mathbf{F}^*$ (§ 9.4) and regardless of the static and kinematic determinacy of the structure (§ 8.2.1).

Global Parallel Transformations   Global parallel transformations in space are also known as *affine transformations*. Apart from Euclidean transformations (rotation, translation, reflection), these include, among others, *spatial uniform scaling*, *non-uniform scaling*, and *shear*. Affine transformations are characterised by three peculiar properties (Pottman et al. 2007): straight lines (planes) are transformed into straight lines (planes); parallel lines (planes) are mapped into parallel lines (planes); the ratio of the lengths of two line segments on parallel lines is invariant throughout the transformation. Based on the first property, an affine transformation converts $\mathbf{F}^*$ into a new vector-based diagram $\mathbf{F}^{*'}$; the same applies to $\mathbf{F}$, which is transformed into $\mathbf{F'}$. Thanks to the second property, corresponding edges in $\mathbf{F}^*$ and $\mathbf{F}$ stay parallel to each other if the same affine transformation is applied to both. The third property, which is particularly relevant in the case $\mathbf{F}^*$ has duplicate edges, ensures that these edges stay parallel and have the same length after the transformation. The application of global parallel transformations is exemplified using the multiple-quads 3D force diagram $\mathbf{F}^*$ (Fig. 9.10.c, right) related to the 3D form diagram $\mathbf{F}$ (Fig. 9.9, right) of the strut-and-tie network of *Cinema San Pietro* by Musmeci (§ 4.2).

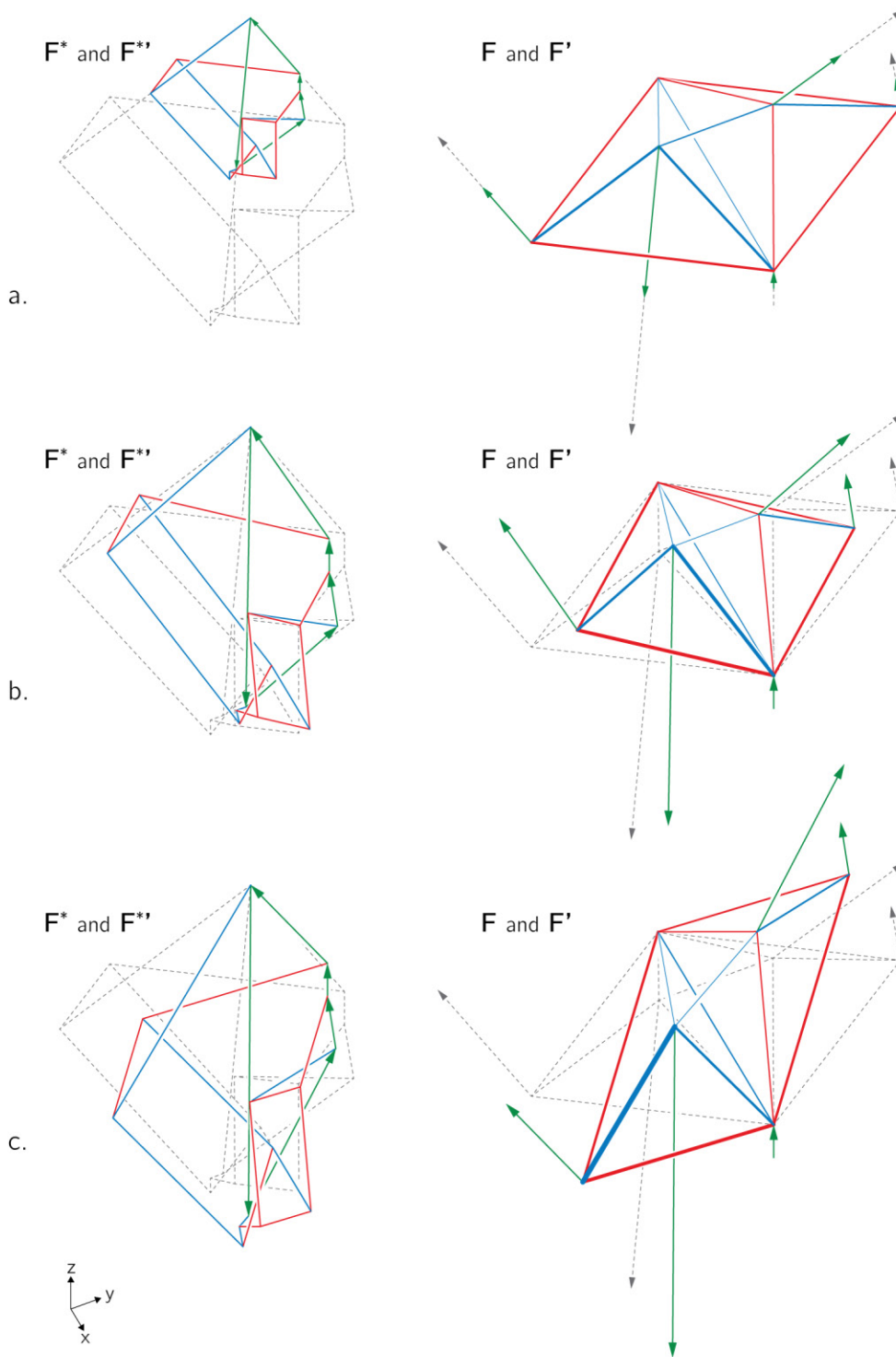[9]Contents of this section have been previously published in (D'Acunto et al. 2017).

F* and **F*'**   **F** and **F'**

a.

F* and **F*'**   **F** and **F'**

b.

F* and **F*'**   **F** and **F'**

c.

Figure 9.12: (a) Spatial uniform scaling applied to the strut-and-tie network of Fig. 9.9: initial 3D force diagram **F*** (dashed grey) and transformed one (colours) **F*'**; corresponding initial **F** and transformed **F'** 3D form diagrams. (b) Non-uniform scaling along the *y*-axis: initial **F*** and transformed **F*'** 3D force diagrams; initial **F** and transformed **F'** 3D form diagrams. (c) Shear transformation along the *x*-axis: initial **F*** and transformed **F*'** 3D force diagrams; initial **F** and transformed **F'** 3D form diagrams.

Semi-global Parallel Transformations   Under specific geometric or static conditions, it is possible to define *semi-global parallel transformations* that affect only a subset of the 3D force diagram while leaving the rest unchanged (D'Acunto et al. 2017). Belong to this category the transformation of the 3D force diagram of a statically indeterminate structure. In this static condition, to every degree of static indeterminacy, one infinity of internal forces distribution in equilibrium can be found (§ 9.3). As shown by Mitchell et al. (2016) and by McRobie et al. (2016) in 2D, also in the 3D force diagram $\mathbf{F}^*$ of a statically indeterminate strut-and-tie network, an *offset transformation* can be used to modify a subset of the geometry of $\mathbf{F}^*$, while keeping the direction of all the E^*_{i-j} unchanged. Hence, considering each degree of static indeterminacy as a parameter, the space of all possible internal forces distribution can be explored (Rondeaux et al. 2017).

The application of this semi-global transformation is exemplified using the previously defined multiple-quads 3D force diagram $\mathbf{F}^*$ (Fig. 9.10.c, right) and the related form diagram $\mathbf{F}$ (Fig. 9.9, right). The strut-and-tie network has been made statically indeterminate to one degree after adding an edge at the bottom of the structure (Fig. 9.13, right). The external forces are kept constant, and therefore the nodes V^*_a, V^*_b, V^*_c, V^*_d, and V^*_e of $\mathbf{F}^*$ are fixed (Fig. 9.13, left). The relative position x of the node V^*_x along the line of E^*_{0-1} is regarded as a parameter. Given the position of V^*_x, the positions of the remaining nodes of $\mathbf{F}^{*}{}'$ are unequivocally determined. This parametric transformation can be directly used for the limit state analysis (§ 10.1) of the given strut-and-tie network (Rondeaux et al. 2017). As long as the hypotheses of the lower bound theorem of the theory of plasticity are fulfilled (§ 10.1), an optimisation process can be used to minimise the length of the longest force edge E^*_{i-j} in $\mathbf{F}^{*}{}'$, which consents to determine the *limit load factor* λ_u (§ 10.1).
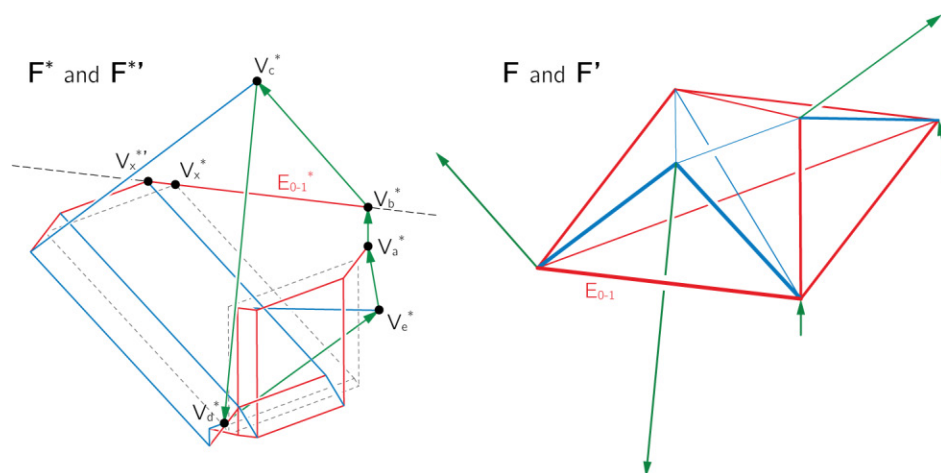

Figure 9.13: Semi-global parallel transformation applied to a strut-and-tie network with one degree of static indeterminacy, related to the example of Fig. 9.9: initial 3D force diagram $\mathbf{F}^*$ (dashed grey) and transformed one (colours) $\mathbf{F}^{*}{}'$; corresponding initial $\mathbf{F}$ and transformed $\mathbf{F}'$ 3D form diagrams.

9.5.2 Local Transformations

Contrary to global transformations, which affect all the elements of the 3D force diagram $\mathbf{F}^*$ simultaneously, *local transformations* allow the manipulation of individual elements of the diagram while keeping the others unaffected. Thanks to these transformations, it is possible to adjust the magnitude and direction of specific forces in $\mathbf{F}^*$ and assess the corresponding transformation of $\mathbf{F}$ (D'Acunto et al. 2017).

A series of geometric constraints have to be defined to secure the interdependence between $\mathbf{F}^*$ and $\mathbf{F}$ during the transformation. More specifically, corresponding edges in the two diagrams (E_{i-j}^* and E_{i-j}) are kept parallel to each other, while the duplicate edges in $\mathbf{F}^*$ are kept parallel and equal in length. Such a constrained non-linear problem entails the use of a numerical simulation since it cannot be solved with direct geometric constructions only.

Numerical methods can be effectively used for the solution of specific structural problems, especially in the case of form-finding. Significant examples of numerical approaches adopted in this field are the force density method (Schek 1974) and dynamic relaxation (Barnes 1977). In comparison to direct geometric constructions, like the ones used in all the previously described transformations, numerical approaches are based on iterative numerical approximations, and they normally require that computational tools be used. In the approach presented here, local transformations are applied within the commercial CAD platform *McNeel Rhinoceros 3D*[10] thanks to the use of customised *IronPython*[11] and *C#*[12] scripts. These scripts make use of the *Kangaroo2* library by Piker (2017), whose solver is built around a specific implementation of position-based dynamics (Bender et al. 2015).

As an example, local transformations are applied to the multiple-quads 3D force diagram $\mathbf{F}^*$ (Fig. 9.11.c) and to the related 3D form diagram $\mathbf{F}$ (Fig. 9.11.b) of the strut-and-tie network based on the geometry of the roof of *Stabilimento Raffo* by Musmeci (§ 4.2). These transformations have been implemented with the goal of reducing the magnitudes of the internal forces $\mathbf{F}_{i-j}$ in the edge and plate members of the top pentagonal plate of the structure (Fig. 9.14). Throughout the transformations, specific constraints have been applied other than the aforementioned general constraints. In particular, the magnitudes of the external applied loads $\mathbf{F}_i$ have been kept constant, thus allowing only the reaction forces $\mathbf{R}_{s_i}$ to change their magnitudes. Moreover, the geometry of the 3D form diagram $\mathbf{F}$ has been kept symmetrical along its longitudinal axis. Finally, edge and plate members related to the same plate have been constrained to stay on the same plane.

---

[10] McNeel Rhinoceros: `http://www.rhino3d.com/` (Accessed 05.06.2018).

[11] .NET Foundation IronPython: `https://ironpython.net/` (Accessed 05.06.2018).

[12] Microsoft .NET C# language: `https://docs.microsoft.com/en-us/dotnet/csharp` (Accessed 05.06.2018).
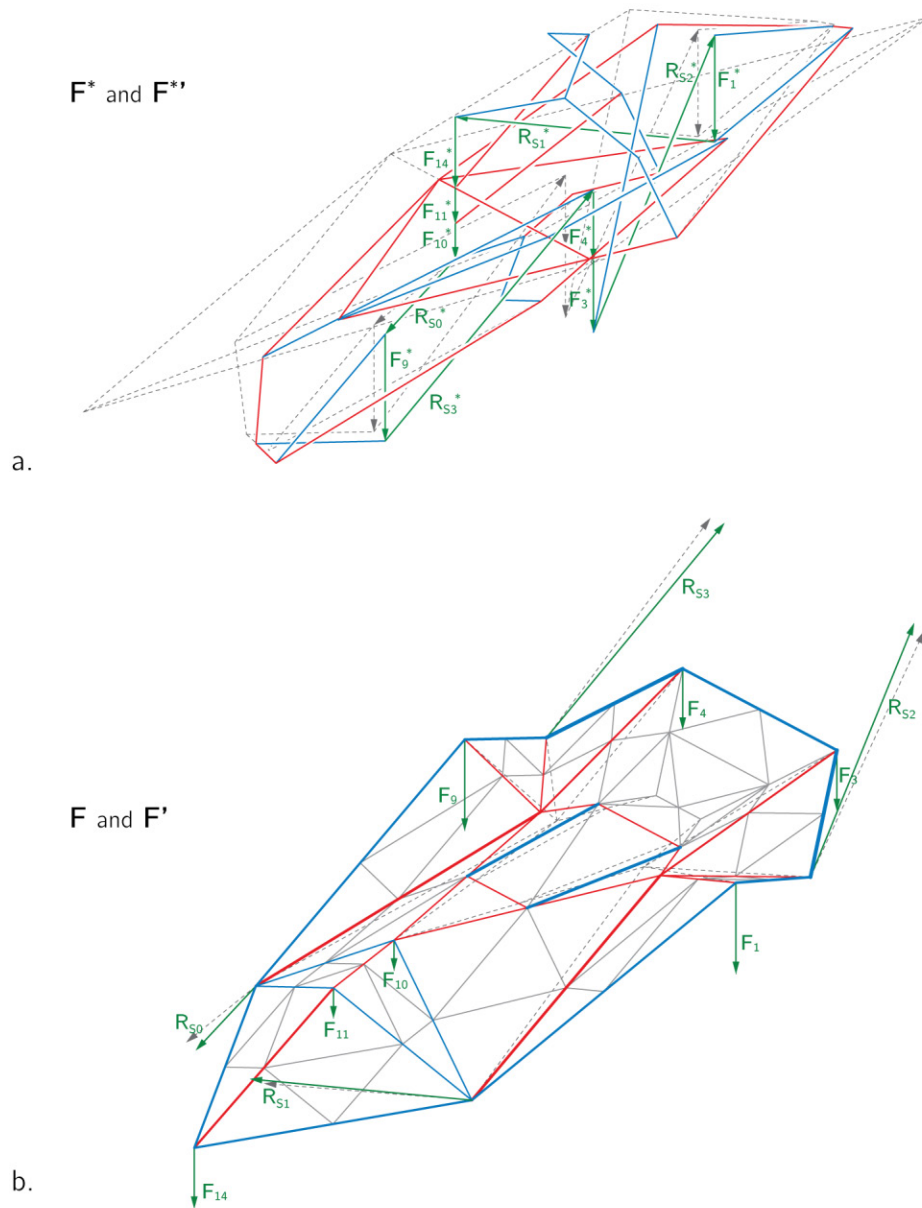
Figure 9.14: Local transformation applied to a strut-and-tie network based on the geometry of the roof of *Stabilimento Raffo* by Musmeci (Fig. 9.11). Initial 3D force diagram **F*** (dashed grey) and transformed one (colours) **F***'. Initial form diagram **F** and transformed one **F**'.
.

As can be observed, the transformed 3D force diagram **F***' shows a high degree of variation in comparison to the initial one **F*** (Fig. 9.14, top). On the other hand, by comparing the initial state of the of the 3D form diagram **F** with the final state **F**' (Fig. 9.14, bottom), the concurrent modifications to the geometry of the strut-and-tie network are less relevant.

10. Stress State in Folded Plate Structures

In this chapter, a strategy to derive in-plane stress fields in folded plate structures is described. This relies on the equilibrium-based solution of the strut-and-tie model defined through the application of vector-based 3D graphic statics (Chapter 9). The fundamental concepts of the theory of plasticity, upon which the presented approach is built, are first introduced.

10.1 Fundamental Concepts of the Theory of Plasticity

At the end of the 19th century, an innovative methodology for the analysis of statically indeterminate reinforced concrete beams subjected to shear and bending was introduced by Hennebique (Kurrer 2008), and later further developed by Ritter (1899) and Mörsch (1908). According to this approach, a reinforced concrete beam loaded in its own plane develops an internal load-bearing mechanism that can be associated to the one of a planar truss, whose elements are subjected to axial forces of tension or compression. Based on this *truss model*, the stress resultants within a loaded reinforced concrete beam can be then found after solving an equilibrium problem. This method was later extended by Rausch (1938) to take into account torsion. Further developments in the second half of the 20th century are grounded on the works of Rüsch (1964), Kupfer (1964), and Leonhardt (1965), among others (Schlaich et al. 1987; Kurrer 2008). A major contribution to the application of the truss model to reinforced concrete structures is due to Thürlimann et al. (1983), who consistently framed the model within the domain of the *theory of plasticity* (Prager and Hodge 1951; Drucker 1961).

Strut-and-Tie Models   A generalisation of the truss analogy to the analysis and design of any part of reinforced and pre-stressed concrete structures, including those with static and geometrical discontinuities, was put forward by Schlaich et al. (1987). Their comprehensive theory is built upon the use of *strut-and-tie models* (STM) to represent the interaction between the compressive stress fields distributed within the concrete mass (whose resultants are modelled as struts) and the tensile stress fields in the steel reinforcement (ties). STM can be directly

used to design the so-called *D-regions*, parts of reinforced concrete where the hypotheses of the Bernoulli beam theory are not fulfilled because of the presence of discontinuities (Schlaich et al. 1987).

A synthetic and complete methodology for the analysis and design of reinforced and pre-stressed concrete structures entirely grounded on the theory of plasticity is due to Muttoni et al. (1997). One of the main advantages offered by this approach is the possibility to solve, using the proposed unified approach, analysis and design problems in reinforced concrete at various scales, from the definition of the global layout of the structure to the detailing of the structural components. Strut-and-tie models are used to represent the equilibrium of compressive and tensile stress resultants based on the underlying *stress field* within reinforced concrete. Hence, the methodology primarily employs equilibrium-based tools, such as graphic statics, for the evaluation of the internal forces in the structural elements (Muttoni et al. 1997).

Limit State Theorems of the Theory of Plasticity   While the theory of elasticity can be generally applied to evaluate the serviceability of a structure subjected to elastic deformations[1], the theory of plasticity can be used to assess the ultimate load-bearing capacity of a structure. In the theory of plasticity, only those material parameters that define the resistance capacity of a structure are considered (Muttoni et al. 1997). This approach relies on a rigid-plastic formulation of material behaviour. That is, a sufficient ductile capacity of the material is assumed, which consents to ignore the elastic deformations, being such deformations considerably smaller than the plastic ones (Muttoni et al. 1997). The further assumptions are also observed that the mechanical behaviour of the structure is not modified by excessive plastic deformations and the loaded structural members are not affected by instability (Heyman 2008).

Within the context of the theory of plasticity, *limit analysis* can be used to evaluate the ultimate capacity of a given externally loaded structure (Greenberg and Prager 1952; Gvozdev 1960; Drucker 1961; Rondeaux et al. 2017). In particular, the system of loads $\{Q_u\}$ that induces the collapse of the structure is obtained by multiplying the *limit load factor* λ_u with the intensities of the forces defining the actual loading $\{Q\}$ on the structure (Marti 2013, p. 410):

$$\lambda_u\{Q\} = \{Q_u\} \tag{10.1}$$

Considering the relation between the value of the actual load factor λ and the limit load factor λ_u, the following theorems of limit analysis are established (Muttoni et al. 1997; Heyman 2008; Marti 2013):

---

[1]In its simplest formulation, the theory of elasticity relies on a perfect linear elastic model of material behaviour. The solution of a statically indeterminate problem using the theory of elasticity leads to the identification of one specific configuration of stress distribution. This requires the simultaneous evaluation of three systems of equations related to static equilibrium, kinematic compatibility, and constitutive relationships (Marti 2013).

- *Lower bound theorem* (static theorem): a load factor λ_s based on a statically admissible stress field[2], which does not violate anywhere the yield conditions, is not higher than the limit load factor λ_u.

- *Upper bound theorem* (kinematic theorem): a load factor λ_k based on a kinematically admissible displacement field[3], which transforms the structure into a mechanism, is not lower than the limit load factor λ_u.

- *Uniqueness theorem*: the limit load factor is unique.

The three theorems above can be formulated using the following expression (Marti 2013, p. 411; Rondeaux et al. 2017):

$$\lambda_{k,i} \geq \lambda_u \geq \lambda_{s,j} \tag{10.2}$$

where $\lambda_{k,i}$ is the load factor related to the ith kinematically admissible collapse mechanism and $\lambda_{s,j}$ the load factor of the jth statically admissible stress field.

Grounded on the lower bound theorem, *static methods* of limit analysis can be defined (Marti 2013; Rondeaux and Zastavni 2018). These methods imply a successive formation of plasticised sections and a redistribution of the internal stresses in a given structure under an increment of the load factor λ_s. When the full plastic resistance of the structure is reached, the static load factor λ_s coincides with the limit one λ_u. Using static procedures for the evaluation of λ_u is in general *safe* since the determination of only a subset of all possible equilibrium solutions can only result in an underestimation of the actual load-bearing capacity of the structure (Rondeaux et al. 2017).

Because of its consistency and direct correlation to graphic statics, the approach proposed by Muttoni et al. (1997), grounded on the lower bound theorem of the theory of plasticity, is employed in the present work as a coherent theoretical basis for the determination of stress fields within folded plate structures. In this way, the solution of the static problem can be confined to the sole evaluation of the equilibrium of the stress field resultants within the structure and the fulfilment of the hypotheses of the lower bound theorem.

10.2   Discrete Stress Fields in Folded Plate Structures

The complete strut-and-tie model for folded plate structures (§ 8.3) consists in a discrete representation of the folded plates entirely made of linear members, which are arranged along the folded edges (*edge members*) and within the folded

---

[2]A statically admissible stress field requires that the equilibrium and the static boundary conditions be respected (Muttoni et al. 1997).

[3]A kinematically admissible displacement field (velocity field) requires that the geometrical boundary conditions be respected and that the resistances and deformations fulfil the yield condition and the flow rule (Muttoni et al. 1997).

plates (*plate members*). It is assumed that these linear members are connected to each other at their nodes through pin-joints. Thanks to the overall triangulation of the model and due to the condition that the nodes are placed at the midpoints and at the endpoints of the folded edges, the proposed strut-and-tie model is equivalent to its underlying folded plate structure in terms of static rigidity (§ 8.2). Given the kinematic stability of the structure, the local bending stiffness of the folded edges can be neglected, and the edges can be treated as hinges. Placed within the framework of the theory of plasticity (§ 10.1), the equilibrium solution of the strut-and-tie model of a given folded plate structure obtained using vector-based 3D graphic statics (Chapter 9) is used to derive in-plane discrete stress fields on the midplanes of the folded plates.

10.2.1   In-Plane Discrete Stress Field in a Single Plate

For a given plane polygonal element in equilibrium under constant in-plane stresses applied along its edges, a discrete stress field can be generated within the element, based on the assumption of rigid-plastic material behaviour. The stress field consists of a combination of triangular sub-fields, each with a constant planar bi-axial stress state (Hajdin 1990; Bahr 2017). Each sub-field is separated from an adjacent sub-field by a discontinuity line, where only the stresses of the two sub-fields perpendicular to the line must respect the equilibrium condition (Nielsen 1984, p. 13; Bahr 2017).

   Given a folded plate structure in equilibrium and based on the proposed strut-and-tie model (§ 8.3), each folded plate can be regarded as a sub-system in equilibrium under in-plane boundary reaction forces applied at the midpoints of its edges. Each boundary reaction force is equivalent to the opposite of the resultant of the forces carried by those plate members that meet at the midpoint of the edge where the reaction force is applied. In case of a uniformly distributed area load on the plate (§ 8.3), the reaction forces on the boundary of the plate can be regarded as the resultants of in-plane uniformly distributed line loads along the edges of the plate.

Simple Triangular Plate Element   Considering the form diagram $\mathbf{F}$ of a simple triangular plate element (Fig. 10.1a, left), its boundary reaction forces (F_1, F_2, F_3) can be found via the force diagram $\mathbf{F}^*$ (Fig. 10.1a, right), knowing the internal forces in the plate members. The boundary reaction forces can be regarded as the resultants of in-plane uniformly distributed line loads (f_1, f_2, f_3) (Fig. 10.1b, left). For a plate with constant thickness t, constant stresses are generated along the edges. The global equilibrium (§ 9.2) of the plate requires that the boundary reaction forces fulfil the conditions (Hajdin 1990, p. 19):

$$F_1 + F_2 + F_3 = 0 \tag{10.3}$$
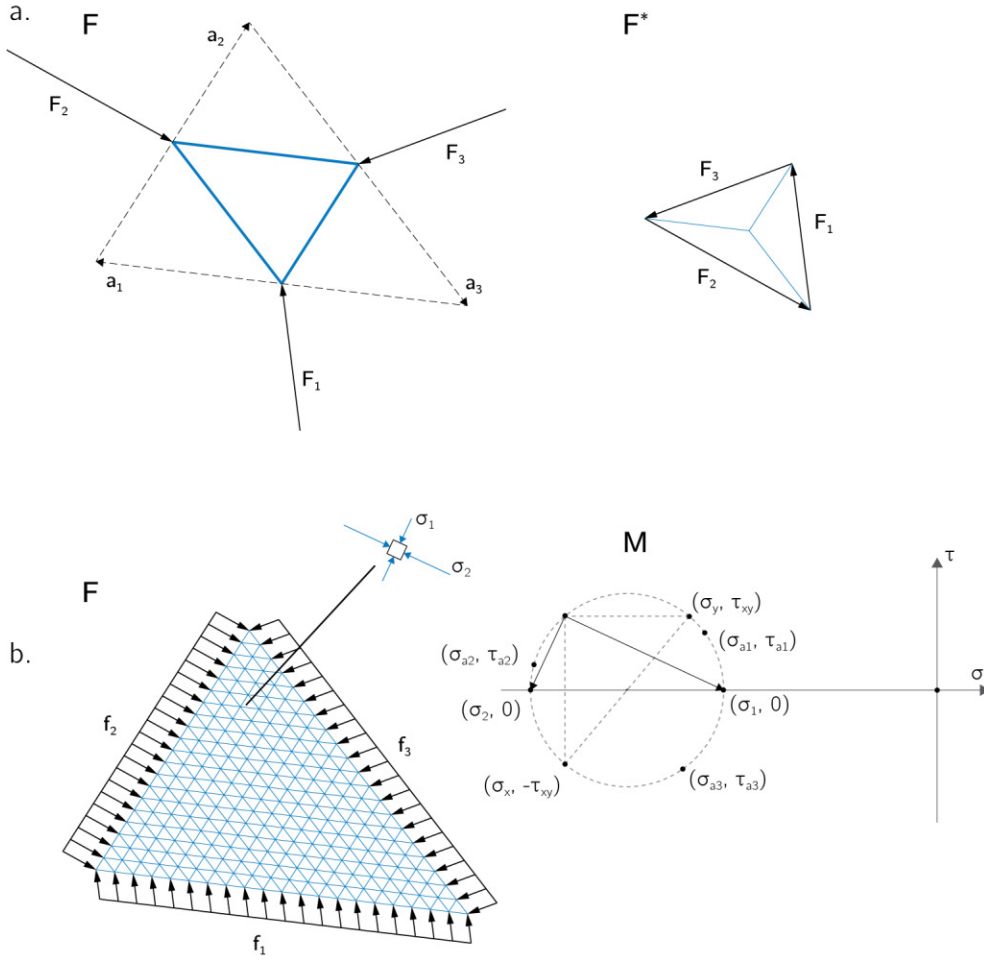
$$F_1 \times a_2 - F_2 \times a_1 = 0 \tag{10.4}$$

Figure 10.1: Constant Stress field in a simple triangular plate. (a) Determination of the boundary reaction forces (F_1, F_2, F_3) using form **F** and force **F***** diagrams. (b) Equivalent in-plane uniformly distributed line loads (f_1, f_2, f_3) and diffused strut-and-tie model representing the stress field in the plate; determination of the principal stresses using the Mohr circle **M**.

Under these boundary conditions, on the midplane of the plate a constant bi-axial stress field evolves, whose stress tensor T results (Hajdin 1990, p. 19):

$$T = \left[\widehat{F_1} a_2 - \widehat{F_2} a_1 \right] \frac{1}{a_1 \times a_2} \tag{10.5}$$

where $\widehat{F_1} = F_1 / t$ and $\widehat{F_2} = F_2 / t$. Given a Cartesian orthogonal coordinate system, T can be formulated as:

$$T = \begin{bmatrix} \sigma_x & \tau_{xy} \\ \tau_{yx} & \sigma_y \end{bmatrix} = \frac{1}{a_{1x} a_{2y} - a_{1y} a_{2x}} \begin{bmatrix} \widehat{F}_{1x} a_{2x} - \widehat{F}_{2x} a_{1x} & \widehat{F}_{1x} a_{2y} - \widehat{F}_{2x} a_{1y} \\ \widehat{F}_{1y} a_{2x} - \widehat{F}_{2y} a_{1x} & \widehat{F}_{1y} a_{2y} - \widehat{F}_{2y} a_{1y} \end{bmatrix} \tag{10.6}$$

The corresponding principal stresses can be found graphically after constructing the *Mohr circle* **M** based on the known stress states at the boundary of the plate (Fig. 10.1b, right).

General Polygonal Plate Element   In case of a polygonal plate with an arbitrary number of edges and constant stress state at its boundary, an iterative approach can be used to generate a discrete stress field within the midplane of the plate, which is made of triangular sub-fields as the one previously described. As explained in details by Hajdin (1990, pp. 42–53), the following procedure is repeated until all the triangular sub-fields are generated:

1. Two, three, or four adjacent edges on the boundary of the plate are selected.

2. Based on the previous selection, respectively two, three, or four triangles are constructed over the selected edges so that they all share one common vertex inside the boundary of the plate. Each triangle defines a sub-field with constant stress state and constant stresses along its boundary. The respect of the equilibrium conditions at the shared edges of adjacent triangles requires that the position of the vertex meet specific geometric conditions; it can be freely chosen, it is bounded to a line, or it is constrained to a point if the initially chosen edges are respectively two, three, or four.

3. The stress tensor in each triangular sub-field is calculated.

4. The resulting two edges, which are not shared between adjacent triangles, are regarded as part of a new boundary.

For example, given the form diagram $\mathbf{F}$ of a pentagonal plate (Fig. 10.2a, left), the corresponding boundary reaction forces $(F_1, F_2, F_3, F_4, F_5)$ are initially obtained through the force diagram $\mathbf{F}^*$ (Fig. 10.2a, right). The three boundary edges (a_1, a_2, a_3) corresponding to the boundary forces (F_1, F_2, F_3) are selected, and three triangular fields are generated after choosing the vertex V_1 (Fig. 10.2b, left). This vertex must lie along the line r_1, which is found by imposing the following condition (Hajdin 1990, p. 49):

$$b_1 \times [(a_2 \times a_3)\, F_1 - (a_1 \times a_3)\, F_2 + (a_1 \times a_2)\, F_3] - (a_1 \times a_2)\,(F_2 \times a_3 - F_3 \times a_2) = 0$$

(10.7)

The magnitudes of the boundary forces (R_1, R_2, S_1, S_2) at the edges of the three triangles can be found using graphic statics. The same procedure is iterated a second time, now taking into consideration the three boundary edges (c_1, c_2, a_4) and the corresponding boundary forces (S_1, S_2, F_4) (Fig. 10.2b, right). The vertex V_2 is chosen along the line r_2, which is found based on a condition analogous to the (10.7). Once all the triangular sub-fields are determined, a new strut-and-tie network can be generated (Fig. 10.2c, left), which represents the stress resultants of the discrete stress field within the plate. The field can be then visualised with a diffused strut-and-tie network (Fig. 10.2c, right). The principal stresses within each triangular sub-field can be found graphically using the Mohr circle.
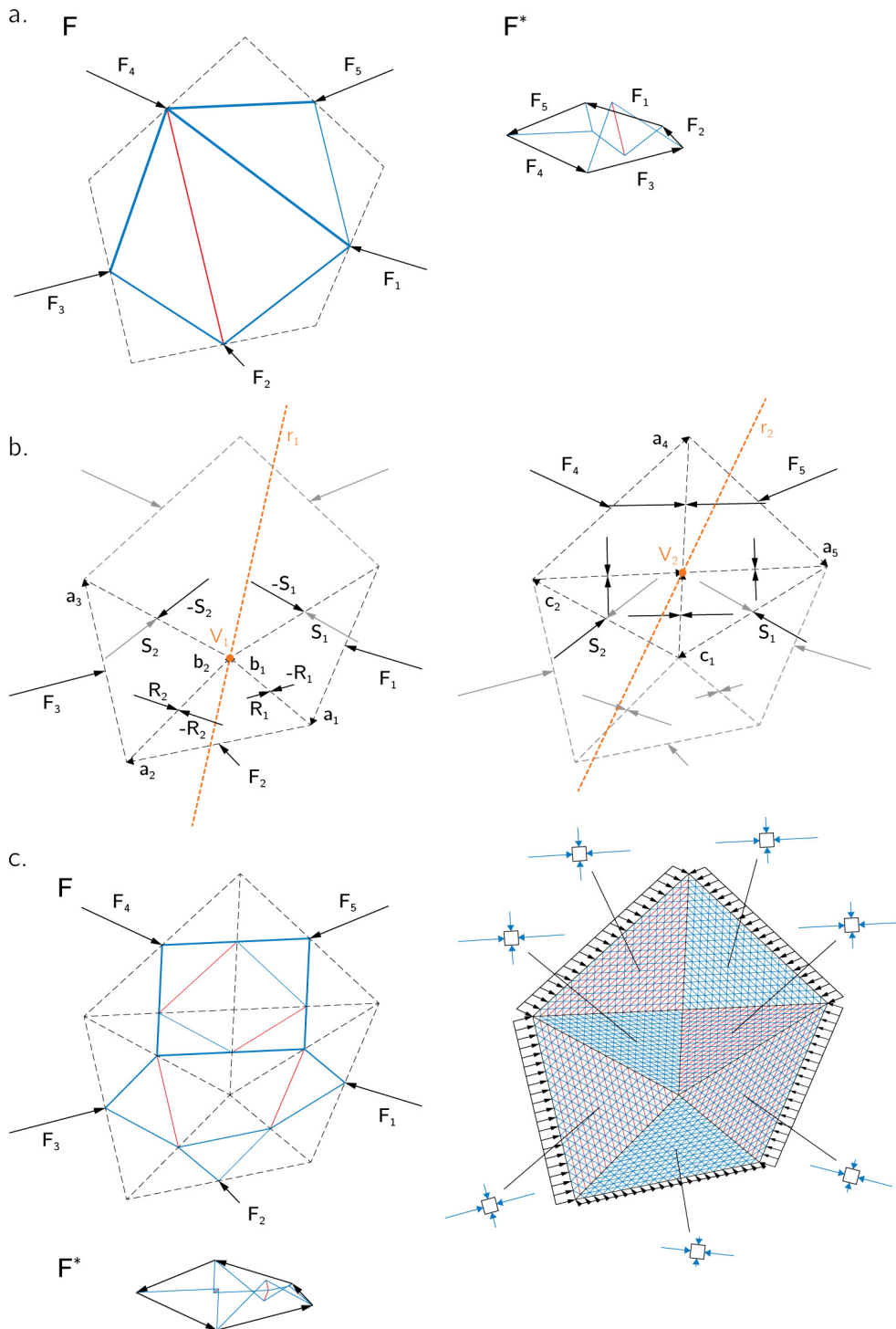
Figure 10.2: Discrete stress field in a polygonal plate as a combination of triangular sub-fields with constant bi-axial stress state. (a) Determination of the boundary reaction forces (F_1, F_2, F_3, F_4, F_5) using form **F** and force **F*** diagrams. (b) Determination of the first three triangular sub-fields based on the boundary edges (a_1, a_2, a_3); determination of the remaining four triangular sub-fields in relation to the boundary edges (c_1, c_2, a_4). (c) Form **F** and force **F*** diagrams of the adjusted strut-and-tie network inside the plate. Diffused strut-and-tie model representing the stress field in the plate and principal stresses in the triangular sub-fields.

10.2.2   General Procedure for the Determination of Stress Fields in a Folded Plate Structure

In the definition of the complete strut-and-tie model for folded plate structures (§ 8.3), the assumption has been made that uniformly distributed area loads on the surface of the folded plates (Fig. 8.10) can be replaced by an equivalent system of point loads applied at the midpoints of the folded edges. These loads are proportional to the tributary areas of the edges and represent the resultants of uniformly distributed line loads along the edges (Fig. 8.11). Considering the folded plates as sub-systems in equilibrium, this assumption implies that in-plane and out-of-plane components of the uniformly distributed area load are locally transferred to the folded edges respectively by plate and slab actions. As explained in the following paragraphs, these two loading components define two local stress states on the folded plate, the first one being an in-plane stress field on the midplane of the plate and the second one a combined shear and moment field on the midplane of the plate, or equivalently, two *curved stress fields* (Bahr 2017).

At the folded edges, the aforementioned point loads are then decomposed into in-plane components into the adjacent folded plates. In turn, these originate an in-plane stress field within the plates (§ 10.2.1). In order to obtain a complete distribution of the stresses within a folded plate, the previously described stress fields can be coupled to produce an overall combined stress, shear, and moment field applied on the midplane of the plate (Bahr 2017). Because the behaviour of a folded plate structure is not necessarily that of a pure plate structure (§ 8.3), concentrated stresses may also evolve along the folded edges.

The effects of uniformly distributed area loads applied to a folded plate structure are here analysed in terms of individual stress fields. The analysis is performed using the geometry of the roof of *Scuola di Atletica* by Musmeci (§ 4.2) as a reference. Since the roof consists of the repetition of the same basic module, the analysis is carried out on only one of these modules, which is itself composed of two rectangular folded plates (Fig. 10.3.a). Each plate has dimensions of $l = 19.40\,\text{m}$ by $h = 2.60\,\text{m}$ and constant thickness $t = 100\,\text{mm}$. In this example, the folded plate roof is supposedly made of an ideal isotropic material with density $\rho = 2500\,\text{kg/m}^3$ and with compressive and tensile yield strengths of $f_{yc} = -20\,\text{MPa}$ and $f_{yt} = 20\,\text{MPa}$ respectively. Considering that each plate is statically rigid in its own plane, the structure is kinematically stable for the given support conditions.

Local Transfer of Loading to the Folded Edges   Contrary to the general approach described in § 8.3, due to the specific rectangular geometries of the folded plates and their overall elongated shapes, the plates are subdivided along their long edges into nine rectangular panels (Fig. 10.3.a). After the subdivision, the applied uniformly distributed loading, which in this example is equivalent to
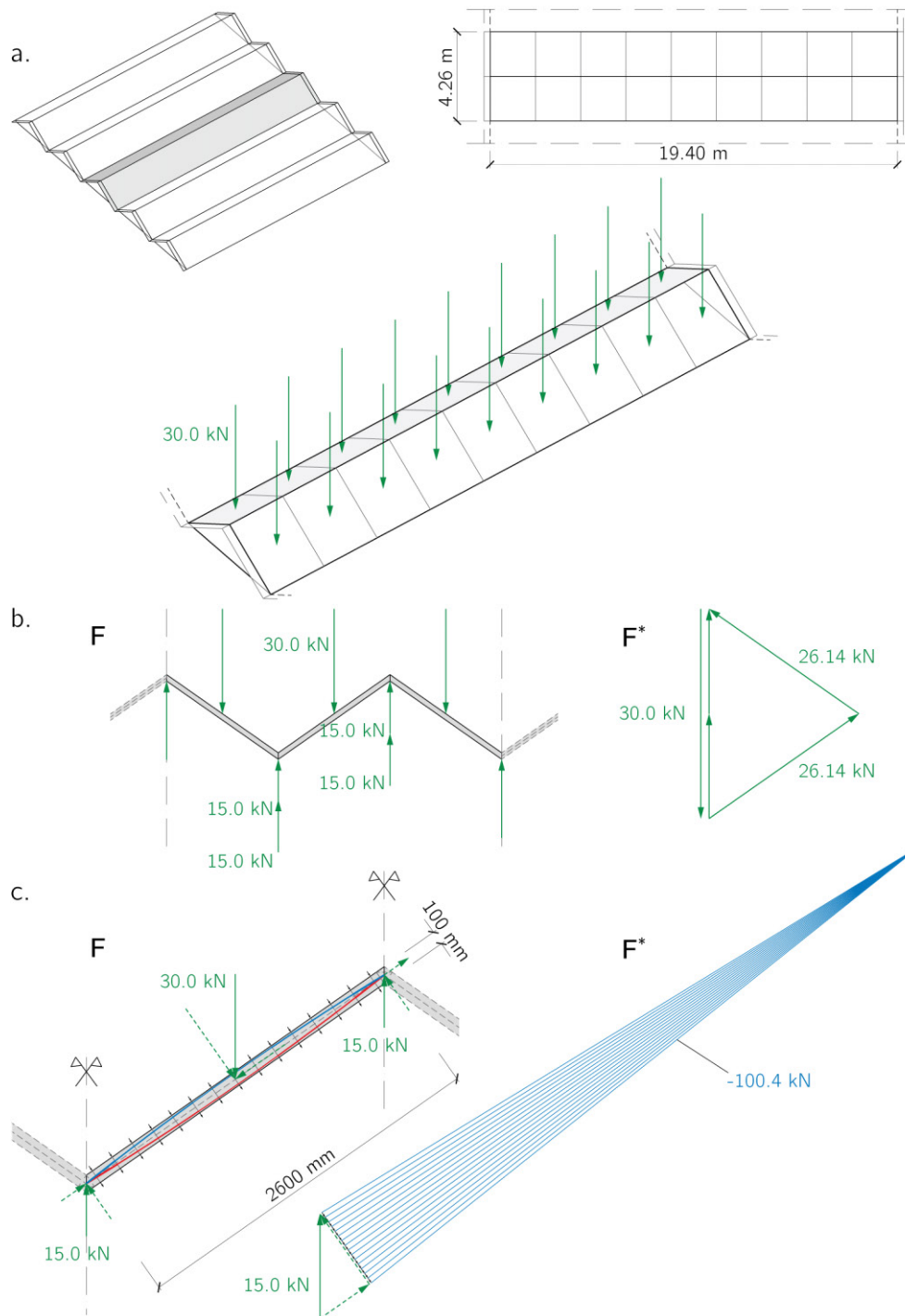
Figure 10.3: (a) Folded plate structure based on the roof of *Scuola di Atletica* by Musmeci (§ 4.2): geometry of the structure and system of point loads as resultants of uniformly distributed area loads. (b) Global repartition of the point loads to the folded edges: form diagram **F** of a section through a panel and related force diagram **F***. (c) Local slab and plate actions on a panel of the folded plate regarded as a sub-system in equilibrium: form diagram **F** representing the stress resultants of two curved stress fields produced by the out-of-plane component of the load; force diagram **F*** of the portion of the curved stress field in compression.

three-times the self-weight of the structure, is replaced by a system of discrete point loads $F_i = 30\,$kN, which are applied to the centres of mass of the panels. In the first phase of the analysis, the effects of the local transfer of the loading to the folded edges are taken into consideration.

On a global level, regarding a module of the roof as a sub-system in equilibrium and taking into account a vertical section through a panel of the folded plate structure (Fig. 10.3.b, **F**), the point load $F_i = 30\,$kN applied on one panel generates two reaction forces $R_{si} = 15\,$kN at the folded edges. Here, the reaction forces of two panels belonging to adjacent plates are combined together into one resultant force $F_i = 30\,$kN, which is subsequently decomposed into two in-plane components $F_{Pi} = 26.14\,$kN into the adjacent plates (Fig. 10.3.b, **F***).

On a local level (Fig. 10.3.c, **F**), after isolating a folded plate as a sub-system in equilibrium, the point load $F_i = 30\,$kN applied at the centre of mass of a panel is first decomposed into in-plane and out-of-plane components. As previously described, the in-plane component produces an in-plane stress field on the midplane of the folded plate. The stress resultant of this field generates reaction forces at the folded edges that are parallel to the plate (Fig. 10.3.c, **F**). The out-of-plane component can be regarded as the resultant of a distributed loading that is perpendicular to the plane of the plate (Fig. 10.3.c, **F**). As highlighted earlier, this loading gives rise to two curved stress fields (Bahr 2017), one in compression and one in tension respectively at the top and the bottom of the plate. In this specific example, the stress resultants of the curved stress fields can be represented as a two-dimensional funicular strut-and-tie network on the section of the panel, whose internal forces can be assessed using graphic statics (Fig. 10.3.c, **F***)[4]. Based on these forces, the stress resultants of the combined stress, shear, and moment field on the midplane of the plate can be eventually found (Bahr 2017) as a combination of the local in-plane and the curved stress fields.

Discrete In-Plane Stress Field in a Folded Plate   In the second phase of the analysis, considering a folded plate as a sub-system in equilibrium (Fig. 10.4) the effects produced by the previously described in-plane components $F_{Pi} = 26.14\,$kN applied at the top and bottom boundary edges of each panel are investigated. These forces have to be regarded as the resultants of uniformly distributed line loads $f_P = 12.1\,$kN/m applied at the top and bottom boundary edges of the folded plate.

In the first step, a complete strut-and-tie network (§ 8.3) is generated to represent the stress resultants of the internal forces in the folded plate. Edge members are introduced along the top and bottom folded edges and plate members on the midplane of the folded plate. The nodes of the strut-and-tie network

---

[4]In case of panels with more complex geometries, a spatial strut-and-tie network has to be generated in order to define the curved stress fields on the plate (Bahr 2017).
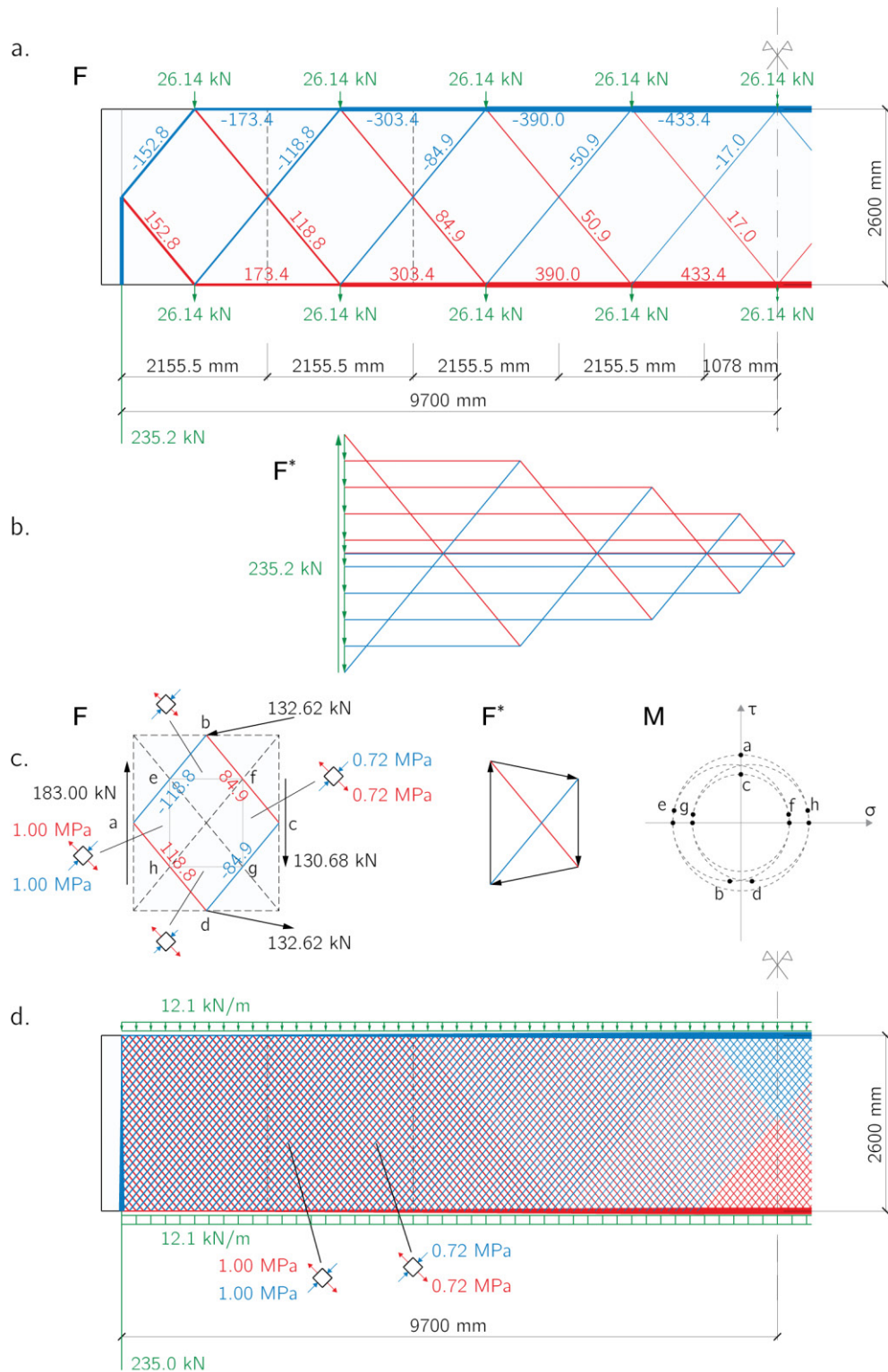
Figure 10.4: Definition of discrete in-plane stress fields in a folded plate made of an ideal isotropic material, based on the roof of *Scuola di Atletica* by Musmeci (§ 4.2): first iteration. (a) Complete strut-and-tie network as a form diagram **F**. (b) Related force diagram **F***. (c) Analysis of a panel of the folded plate regarded as a sub-system in equilibrium to derive a discrete in-plane stress field: form diagram **F**, force diagram **F*** and Mohr circle **M**. (d) Diffused strut-and-tie network representing the stress field in the plate.

are placed at the midpoint of the boundary edges of the panels, where the point loads are applied (Fig. 10.4.a).

In the second step, regarding the strut-and-tie network as a form diagram **F**, the equilibrium of its external and internal forces is assessed after generating the related force diagram **F*** (Fig. 10.4.b). An initial assumption is here made that the edge members coincident with the top and bottom boundary edges of the panels behave like stringers with zero width and infinite resistance capacity. It is thus supposed that the concentration of stresses along the folded edges can be directly resolved at the boundary of the plate, without the necessity of mobilising part of the resistance capacity of the plate. As a result, the lever arm h_l between the top struts and the bottom ties is regarded as equal to the full height of the plate (i.e. $h_l = h = 2600\,\text{mm}$). This assumption obviously leads to an overestimation of the resistance capacity of the folded plate structure. As explained later, further adjustments to the strut-and-tie network have to be taken into consideration.

In the third step, regarding each panel as a sub-system in equilibrium (Fig. 10.4.c, **F**), its boundary reaction forces are determined with the aid of a force diagram (Fig. 10.4.c, **F***), based on the known internal forces within the plate members (§ 10.2.1). Since the thickness of the folded plate is constant, these boundary reaction forces imply the presence of constant in-plane stresses along the boundary of the panel. Given these reaction forces, a discrete in-plane stress field in the plane of the panel can be derived as a combination of triangular sub-fields, each with a constant planar bi-axial stress state (§ 10.2.1). The Mohr circle (Fig. 10.4.c, **M**) can be used to determine the principal stresses associated with each triangular sub-field. After repeating the same procedure for all the panels of the folded plate, a first instance of the stress field on the midplane of the folded plate can be eventually visualised in the form of a diffused strut-and-tie network (Fig. 10.4.d). Note that this in-plane stress field has to be combined with the local in-plane and curved stress fields defined in the first phase of the analysis to obtain a complete stress distribution on the plate.

To take into account the effects of the accumulation of stresses along the top and bottom folded edges, an iterative analysis process is necessary (Muttoni et al. 1997). More specifically, at each iteration, a strut-and-tie network is developed, and its internal forces are assessed. Based on the yield strength of the material f_{yc} (respectively f_{yt}) and plate thickness t, the widths w_{ij} of the struts and ties at the folded edges are calculated as $w_{ij} = \boldsymbol{F}_{ij}/(f_{yc}t)$, respectively $w_{ij} = \boldsymbol{F}_{ij}/(f_{yt}t)$, with $\boldsymbol{F}_{ij}$ being the internal forces in the struts and ties. The assumption is made that a uniaxial stress field with constant stress intensity f_{yc}, respectively f_{yt}, is generated along the folded edges. The geometry of the strut-and-tie network is then adjusted to accommodate for the required widths w_{ij}. The procedure is iterated until the resistance capacity of the folded plate is entirely exploited, thus allowing to maximise the lever arm h_l between the top struts and the bottom ties. Using the configuration depicted in Fig. 10.4 as a

starting point, the outcome of the analysis after four iterations (Fig. 10.5) shows a final lever arm of $h_l = 2153\,$mm at the middle axis of the folded plate.

10.2.3   Influence of Material and Geometry on the Stress Field

The procedure described above for the definition of in-plane discrete stress fields in folded plates is now applied to other case studies in order to highlight, on the one hand, the effects of the material properties and the adopted construction technology, and on the other hand, the influence of the geometry of the plates.

Application to Reinforced Concrete Folded Plates   In the previous example based on the roof of *Scuola di Atletica* by Musmeci, the assumption was made that the folded plate was constituted of an ideal isotropic material with compressive and tensile yield strengths of $f_{yc} = -20\,$MPa and $f_{yt} = 20\,$MPa respectively. Following the approach described by Muttoni et al. (1997), the analysis is here repeated on the same case study (i.e. same loading and support conditions), now considering that the folded plate is in reinforced concrete. In this regard, the density of the composite material is assumed to be $\rho = 2500\,$kg/m^3, the effective concrete strength is set to $f_{ce} = -20\,$MPa, while the plastic limit of the reinforcing bars is set to $f_{sy} = 460\,$MPa. The load-bearing behaviour of the folded plate is assimilated to the one of a deep beam with uniformly distributed line loading. The reinforcement is constituted by longitudinal bars along the bottom edge of the folded plate and vertical stirrups distributed along the plate.

An initial strut-and-tie network is defined to represent the distribution of the internal forces within the plate. In this case, the struts along the top boundary edge of the plate represent the longitudinal concrete zone under compression, while the ties along the bottom boundary edge represent the reinforcing steel bars under tension. The transfer of forces between the struts and ties at the top and bottom of the plate is attained through a load-bearing mechanism that involves inclined compression concrete struts and vertical stirrup reinforcement. Due to the high slenderness ratio of the plate, a solution with multiple suspensions, equivalent to the combination of five structural systems (Muttoni et al. 1997) is adopted. In analogy to the previous example, the analysis process is iterated four times, and the result is illustrated in Fig. 10.6. The comparison between the in-plane stress fields of three modules (i.e. six folded plates) of the roof for the above and current examples (Fig. 10.7) allows identifying the influence of the material properties and the adopted construction technology on the definition of the stress fields.

Application to Folded Plates with General Geometries   The application of the procedure explained above is here further exemplified on two folded plate structures with generic plate geometries. In particular, the first example is related to the roof of *Cinema San Pietro* by Musmeci (§ 4.2); the analysis is applied to
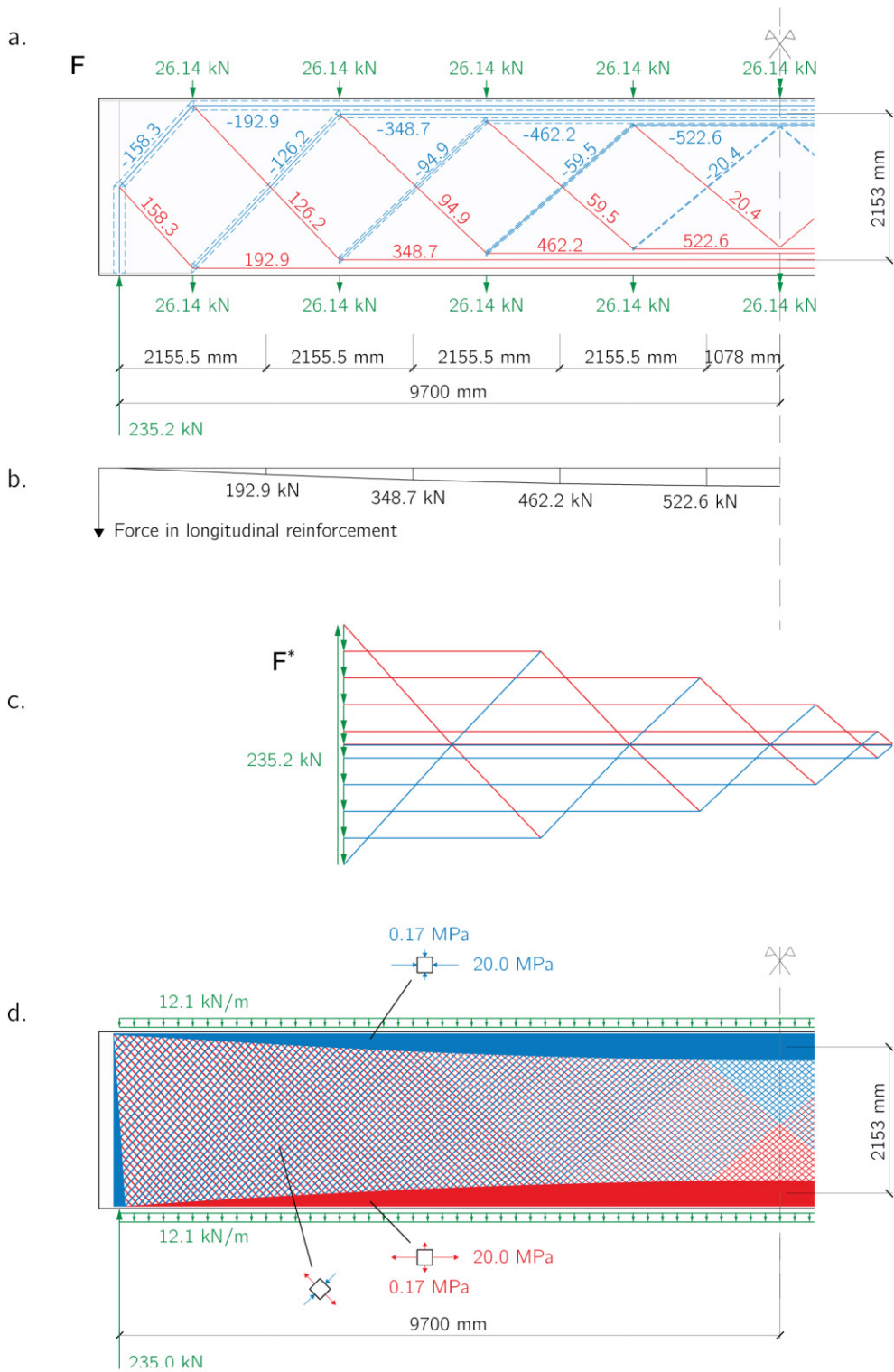
a.

b.

c.

d.

Figure 10.5: Definition of discrete in-plane stress fields in a folded plate made of an ideal isotropic material, based on the roof of *Scuola di Atletica* by Musmeci (§ 4.2): fourth iteration. (a) Complete strut-and-tie network as a form diagram **F**. (b) Distribution of the forces along the longitudinal reinforcement. (c) Force diagram **F*** of the strut-and-tie network. (d) Diffused strut-and-tie network representing the stress field in the plate.
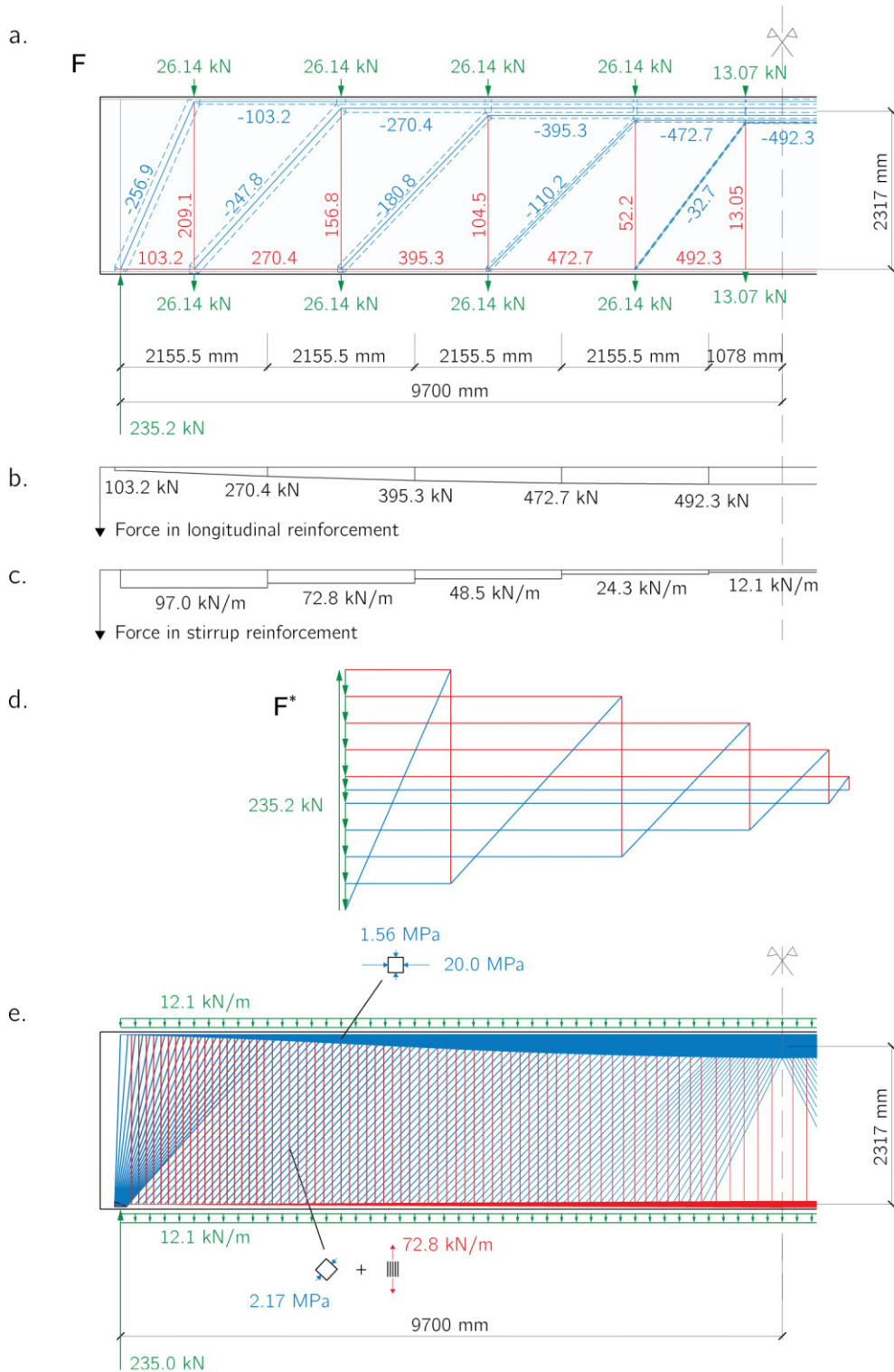
a.

F

26.14 kN   26.14 kN   26.14 kN   26.14 kN   13.07 kN

−103.2   −270.4   −395.3   −472.7   −492.3

−256.9   209.1   −247.8   156.8   −180.8   104.5   −110.2   52.2   −32.7   13.05

103.2   270.4   395.3   472.7   492.3

26.14 kN   26.14 kN   26.14 kN   26.14 kN   13.07 kN

2317 mm

2155.5 mm   2155.5 mm   2155.5 mm   2155.5 mm   1078 mm

9700 mm

235.2 kN

b.

103.2 kN   270.4 kN   395.3 kN   472.7 kN   492.3 kN

▼ Force in longitudinal reinforcement

c.

97.0 kN/m   72.8 kN/m   48.5 kN/m   24.3 kN/m   12.1 kN/m

▼ Force in stirrup reinforcement

d.

F*

235.2 kN

1.56 MPa

20.0 MPa

e.

12.1 kN/m

12.1 kN/m   72.8 kN/m

2.17 MPa

9700 mm

2317 mm

235.0 kN

Figure 10.6: Definition of discrete in-plane stress fields in a folded plate made of reinforced concrete, based on the roof of *Scuola di Atletica* by Musmeci (§ 4.2): fourth iteration. (a) Complete strut-and-tie network as a form diagram **F**. (b) Forces along the longitudinal reinforcement. (c) Forces in the stirrup reinforcement. (d) Force diagram **F*** of the strut-and-tie network. (e) Diffused strut-and-tie network representing the stress field in the plate.
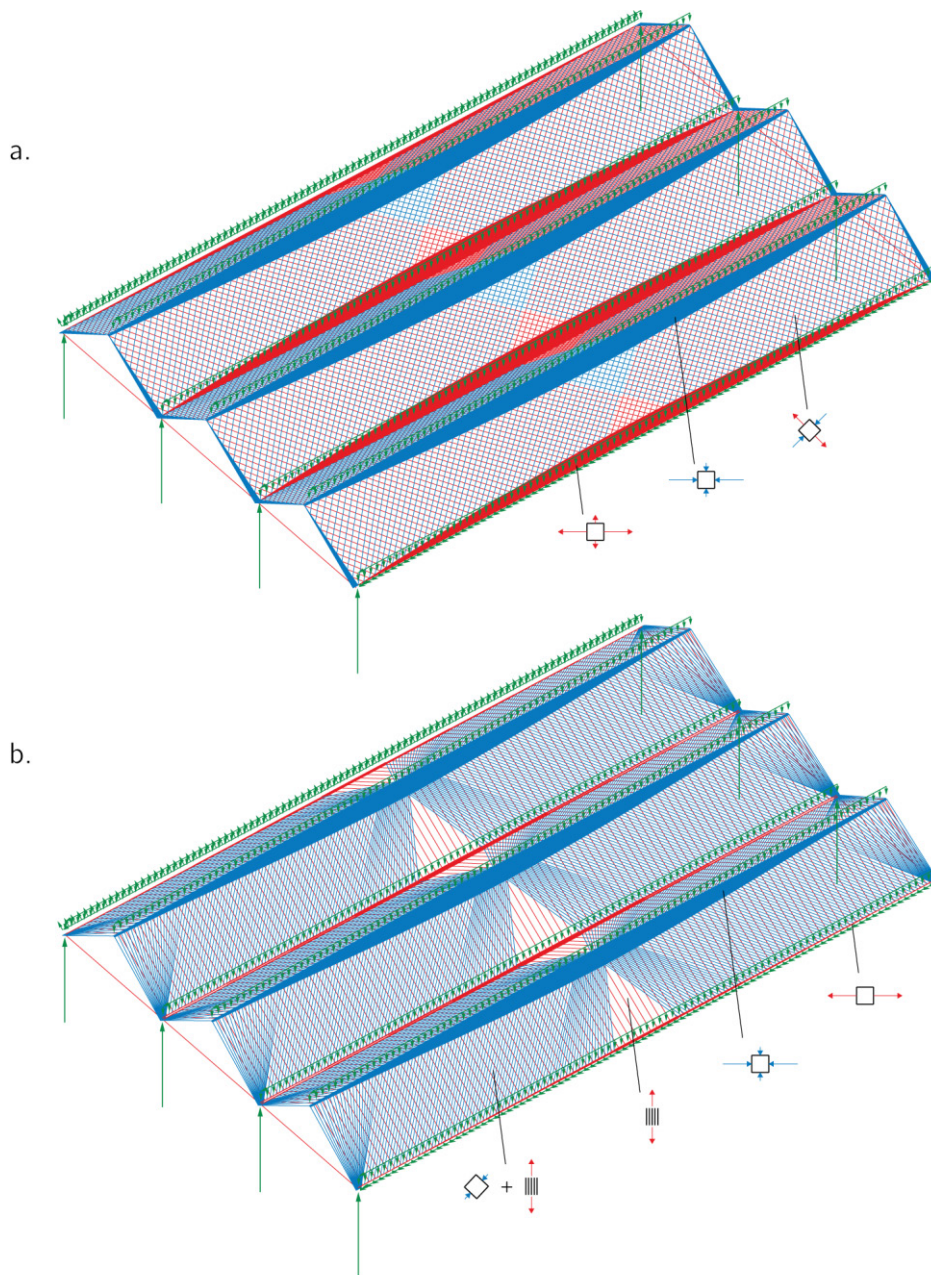
Figure 10.7: Axonometric view of the in-plane stress fields as diffused strut-and-tie networks in the folded plate structure of the roof of *Scuola di Atletica* by Musmeci (§ 4.2). (a) Ideal isotropic material. (b) Reinforced concrete.

one of the modules of the roof, which is itself composed of ten triangular folded plates (Fig. 10.8). The second example is related to the roof of *Teatro Regio* by Musmeci (§ 4.2); in this case, the analysed module consists of eleven folded plates with various polygonal shapes (Fig. 10.10.a). In both examples, a constant thickness $t = 100$ mm for the folded plates is assumed. Moreover, the plates are regarded as made of an ideal isotropic material with density $\rho = 2500$ kg/m³ and

with compressive and tensile yield strengths of $f_{yc} = -20\,\text{MPa}$ and $f_{yt} = 20\,\text{MPa}$ respectively. The structures are kinematically stable in relation to the specified support conditions, and they are loaded under self-weight. Moreover, in these examples, the assumption is made that the struts and ties along the folded edges behave like stringers with infinite resistance capacity.

In both examples, the generation of the complete strut-and-tie networks relies on the general procedure described in § 8.3 (Fig. 10.9.a and Fig. 10.10.b). As such, the folded plates are entirely triangulated with nodes only at the midpoints and endpoints of the folded edges, where the point loads that replace the uniformly distributed area loads due to the self-weight are applied. It is then assumed that these point loads represent the resultants of uniformly distributed line loads along the folded edges (§ 8.3). In order to define in-plane discrete stress fields in the folded plates, the initial strut-and-tie networks are adjusted on a plate basis (Fig. 10.9.b and Fig. 10.10.c), following the procedure described in § 10.2.1. Grounded on the specific strut-and-tie network defined for each plate, multiple possible equilibrium solutions can be developed. First instances of the stress fields on the midplanes of the folded plates are shown as diffused strut-and-tie networks (Fig. 10.9.c and Fig. 10.11).

As mentioned before, because of the initial assumptions, these results generally represent an overestimation of the resistance capacity of the structures. Hence, they should be considered only as a qualitative representation of the discrete in-plane stress fields in the folded plates. Results that are more accurate can be obtained with an iterative analysis process. It should also be noted that the definition of the stress fields at the nodes of the strut-and-tie model with concurrently loaded edge members (i.e. at the endpoints of the folded edges) requires the development of specific nodal solutions (Bahr 2017). Finally, as previously highlighted, these in-plane stress fields have to be combined with the local in-plane and curved stress fields to obtain a complete stress distribution on the folded plates.
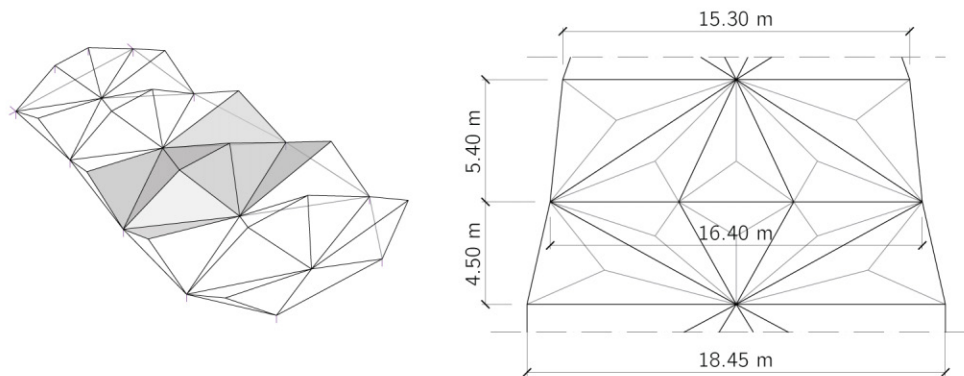

Figure 10.8: Folded plate structure whose geometry is based on the roof of *Cinema San Pietro* by Musmeci (§ 4.2).
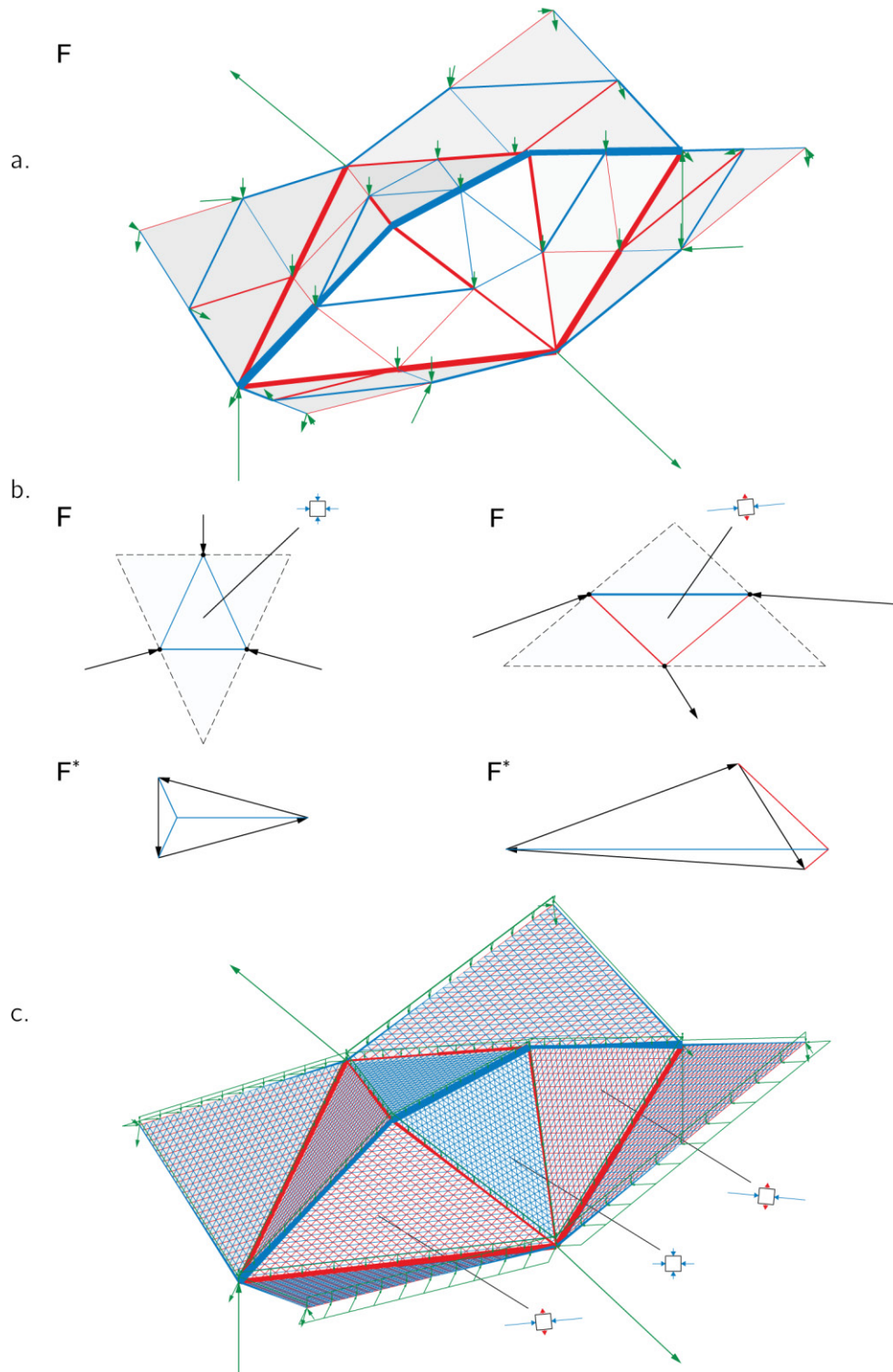
Figure 10.9: Definition of discrete in-plane stress fields in a folded plate module made of an ideal isotropic material, based on the roof of *Cinema San Pietro* by Musmeci (§ 4.2): first iteration. (a) Complete strut-and-tie network as a form diagram **F**. (b) Analysis of two plates regarded as sub-systems in equilibrium: form **F** and force diagrams **F***. (c) Diffused strut-and-tie network of the stress field in the folded plate module.
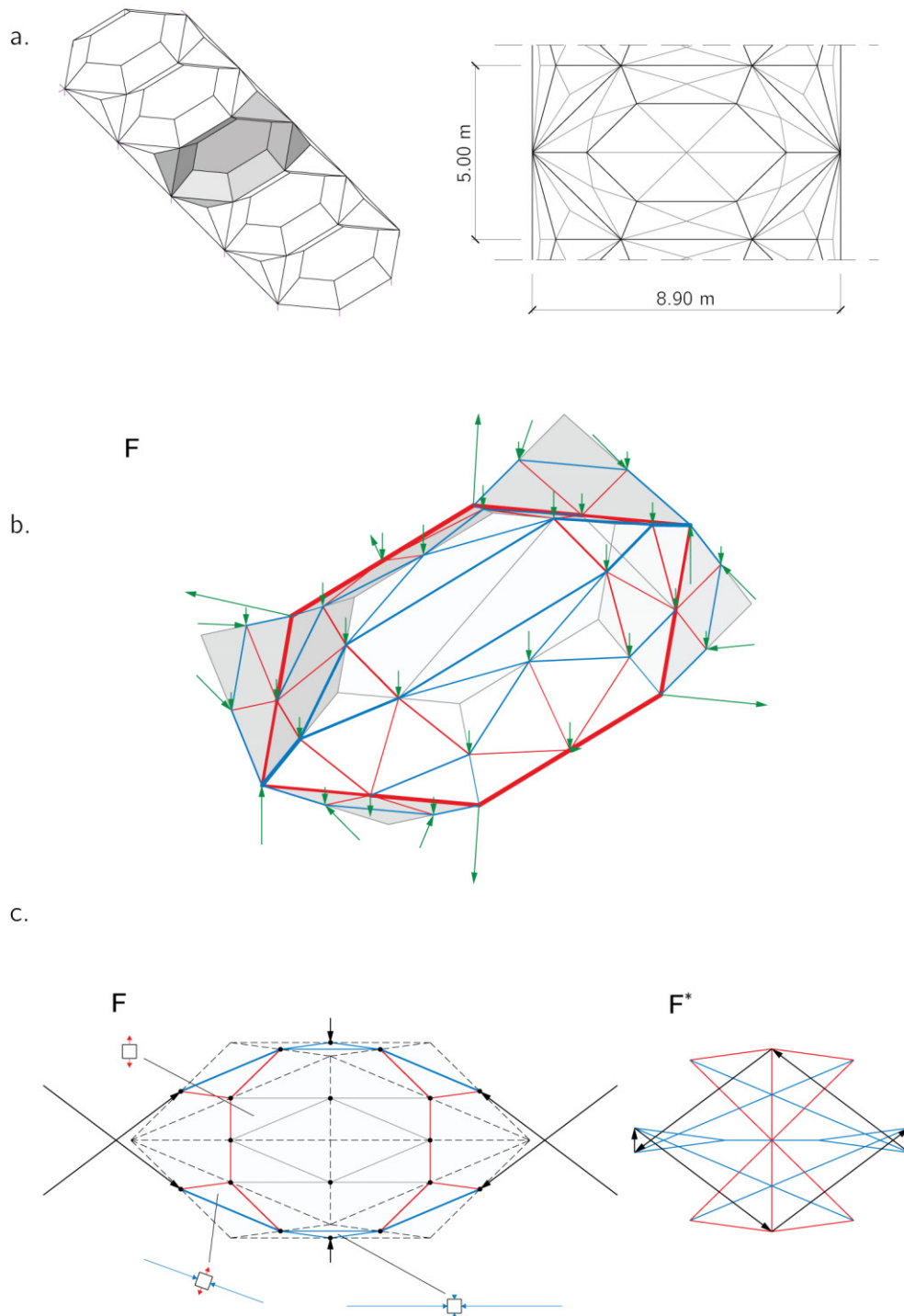
a.

5.00 m

8.90 m

F

b.

c.

F

F*

Figure 10.10: (a) Folded plate structure whose geometry is based on the roof of *Teatro Regio* by Musmeci (§ 4.2). (b) Complete strut-and-tie network of a folded plate module as a form diagram **F**. (c) Analysis of a polygonal folded plate regarded as a sub-system in equilibrium to derive a discrete in-plane stress field on the midplane of the plate as a combination of triangular sub-fields: form diagram **F**, force diagram **F***.
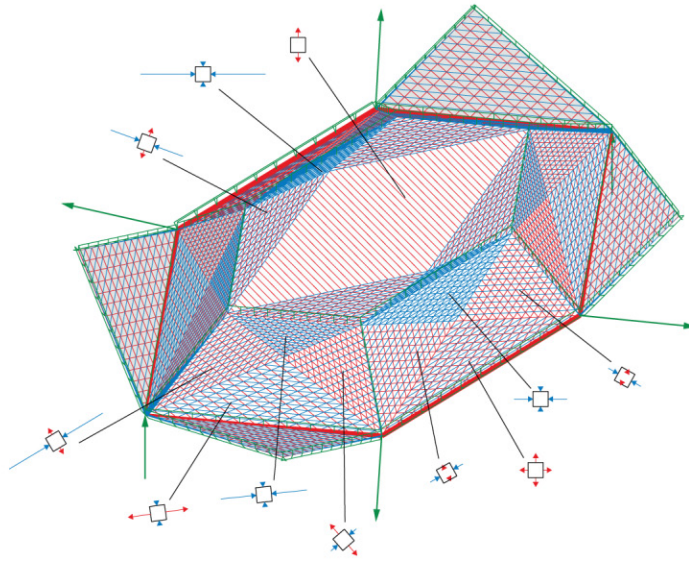
Figure 10.11: Visualization of the in-plane stress field as a diffused strut-and-tie network in a folded plate module from the project *Teatro Regio* by Musmeci (§ 4.2).

Design Method

11. General Framework

The design method for structural folding in architecture here presented relies on the previously defined structural model for folded plate structures (§ 8.3). The method is implemented within a software-based computational toolkit that makes use of the resources offered by contemporary digital tools for architectural and structural design. Hence, contrary to other design practices that are directly based on physical folding, in the proposed approach folding is regarded as a *virtual design operation* (D'Acunto and Castellón 2015), as in the works of Buri and Meyer (Chapter 6). Even though the method can be easily used to produce *folded surface structures* (Chapter 2), such as the previously analysed roofs designed by Musmeci (§ 4.2, § 8.3, Chapter 9, Chapter 10), its main scope is the generation of *folded volumetric structures* (Chapter 2), which enclose architectural spaces, as in the case of the buildings designed by Sancho and Madridejos (§ 5.2).

The developed approach aims to offer the designer, either architect or engineer, the possibility to make use of the structural and spatial potentials of folding simultaneously. In fact, it is intended to support the designer throughout the design process, starting from the initial phase. As such, this approach put a specific focus on the relationship between architecture and engineering, considering folding as a mediator between load-bearing capacity and design intention.

The developed method addresses various aspects of the design of folded plate structures in architecture, starting from the initial topological organisation of the structure and the architectural space generated by the folded plates, to the subsequent definition of their geometry. The method is grounded on a three-dimensional design process (D'Acunto and Castellón 2015), in which the plate geometry is virtually folded within a previously designed statically rigid reference grid as a spatial lattice structure (§ 8.2.1). As a result, a folded plate structure is generated that is also the building envelope of an architectural space. Without compromising its intrinsic structural properties in terms of static rigidity and its inner spatial organisation, the geometry of the folded plate structure can be transformed. Furthermore, by relying on the previously illustrated strut-and-tie model (§ 8.3), the internal forces within the folded plate structure can be controlled and adjusted (Chapter 9, Chapter 10).

Because of the use of geometric operations only, the proposed approach is generally material and scale-independent. As explained in the next sections, restraints concerning specific material properties, fabrication or scale-related de-

TOPOLOGY

| STRUCTURE
Static Rigidity | ⟷ | SPACE
Internal Organisation |

EUCLIDEAN GEOMETRY

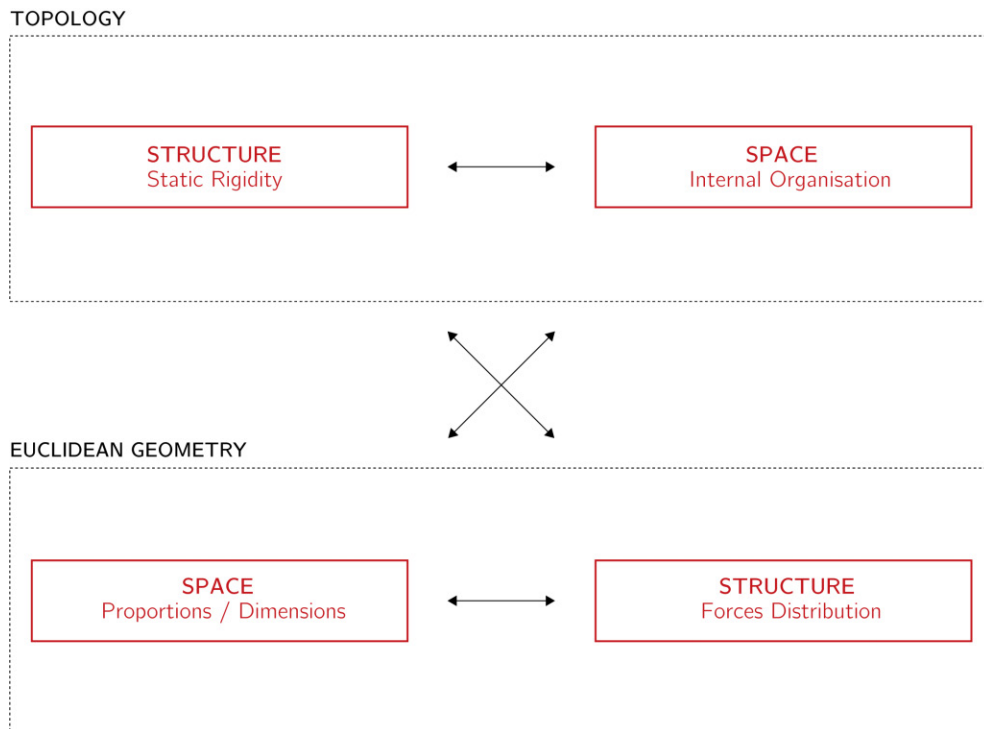| SPACE
Proportions / Dimensions | ⟷ | STRUCTURE
Forces Distribution |

Figure 11.1: Overview of the proposed design method for structural folding in architecture, concerning both levels of topology and Euclidean geometry and dealing with matters related to both space and structure.

pendencies can be adequately taken into consideration within the design process in the form of geometric constraints (D'Acunto and Castellón 2015). The developed design method relies on two general procedures: a topological one and a metric one. Each of them includes two main operations that allow the designer to deal with matters related to both space and structure (Fig. 11.1).

Level of Topology: Structure and Space   The topological and projective geometric procedure comprises the two operations *T1–grid generation* and *T2–virtual folding*. It is through these two operations that the static rigidity of the folded plate structure is attained and the general organisation of its enclosed architectural space is controlled.

In particular, the first operation (*T1–grid generation*) supports the designer in defining the topology of a statically rigid grid as a lattice structure that is made out of individual tetrahedra or more general triangulated polyhedra (§ 8.2.1). This grid is subsequently used as a reference for the generation of the folded plate structure (§ 8.3). Hence, this first operation mainly pertains to the structural aspects of the design.

The second operation (*T2–virtual folding*) gives the designer the opportunity to define the topology and outline the geometry of the folded plate structure and of its enclosed architectural space. As such, this second operation is com-

plementary to the first one as it also addresses questions related to architecture. Moreover, the reference grid and the folded plate structure are topologically interdependent. Different topologies of the folded plate structures can be generated based on the same initial reference grid.

Level of Euclidean Geometry: Space and Structure   The metric procedure includes the two operations *M1-form manipulation* and *M2–force manipulation*. Given a kinematically stable folded plate structure with its enclosed architectural space as generated using the first procedure, the second procedure allows the designer to adjust both its form and the distribution of its inner forces.

In particular, the third operation (*M1–form manipulation*) can be used to modify the geometry of the structure and thus of its enclosed architectural space. Therefore, this operation gives the designer control on the proportions and dimensions of the architectural space in order to meet specific design requirements.

The fourth operation (*M2–force manipulation*), which is complementary to the third one, permits the load-bearing behaviour of the structure to be steered towards a desired one. Based on the proposed strut-and-tie model for folded plate structure (§ 8.2), this operation makes use of vector-based 3D graphic statics (Chapter 9) to construct the force diagram of the structure and to enable its direct transformation based on specific structural requirements. Stress fields in the folded plates can be then derived (Chapter 10). Modifications to the metric properties of the force diagram affect in turn the geometry of the structure, making the *M1* and *M2* interdependent.

It is important to point out that it is not necessary to apply the four operations following a predefined sequential order. That is, after a first complete execution of the process (*T1–T2–M1–M2*), any of these operations can be implemented in a non-sequential way. This can be attained without losing the consistency of the folded plate structure being designed (D'Acunto and Castellón 2015).

For example, the topology of the reference grid or the one of the folded plate structure can be modified again with the operations *T1* or *T2* after its geometry has been already transformed by means of the operation *M1* or *M2*, without the necessity to reinitialise the entire design process. In the same way, the form of the structure can be adjusted again using the operation *M1* after its force diagram has been transformed using the operation *M2*. Furthermore, the same operation can be re-executed multiple times throughout the process in a linear or hierarchical way, based on the specific design necessities (D'Acunto and Castellón 2015).

This non-sequential character is a peculiarity of the proposed design method, which distinguishes it from other procedures for architectural and structural design, such as those based on form-finding. Contrary to form-finding, the output of the developed design approach is not clearly determined for a given set of

inputs, but it is instead a negotiation between both structural and architectural requirements, which are directly managed by the designer. In this way, the method enables architects and engineers to engage with the different aspects related to the design of folded plate structures. Moreover, it empowers them with a synthetic approach to explore the relationship between structure and space (Fig. 11.2).

Software Implementation The implementation of the design method into a parametric digital toolkit has facilitated the applicability of the proposed approach to the solution of actual design tasks (Kotnik and D'Acunto 2013). This software implementation allows the designer to operate with the previously introduced topological and metric procedures in a completely interactive way. Thanks to the robustness of the toolkit, each operation and its related sub-operations can be applied at will, while keeping the geometry of the folded plate structure consistent. In fact, through the toolkit, the designer is given the opportunity to switch in real time from one operation to another, while having constant feedback on the consequences of this operation on the geometry of the folded plate structure and the repartition of its internal forces (Kotnik and D'Acunto 2013).

Because of the parametric nature of the toolkit, the folded geometry is generated as a variable object, like an *objectile* (§ 5.1), which is constructed through a set of geometric relationships and which is potentially able to express multiple forms at the same time. In this way, the designer can explore at once diverse design solutions and easily adapt them to different design scenarios (D'Acunto and Castellón 2015).

Since all the previously introduced operations are geometry-based, it has been possible to develop the toolkit as a software package within a single 3D modelling environment. For its flexibility and intuitive graphical interface, the commercial CAD software *McNeel Rhinoceros 3D*[1] and the parametric plug-in *Grasshopper*[2] have been chosen for the development. Besides, the implementation of the design operations is based on a set of customised computational definitions developed using the programming languages *IronPython*[3] and *C#*[4]. For the solution of non-linear problems such as constraint-based transformations, the *Kangaroo2* library by Piker (2017) has been implemented.

---

[1] McNeel Rhinoceros: `http://www.rhino3d.com/` (Accessed 05.06.2018).

[2] McNeel Grasshopper: `http://www.grasshopper3d.com/` (Accessed 05.06.2018).

[3] .NET Foundation IronPython: `https://ironpython.net/` (Accessed 05.06.2018).

[4] Microsoft .NET C# language: `https://docs.microsoft.com/en-us/dotnet/csharp` (Accessed 05.06.2018).

OPERATION T1
grid generation

OPERATION T2
virtual folding

OPERATION M1
form manipulation
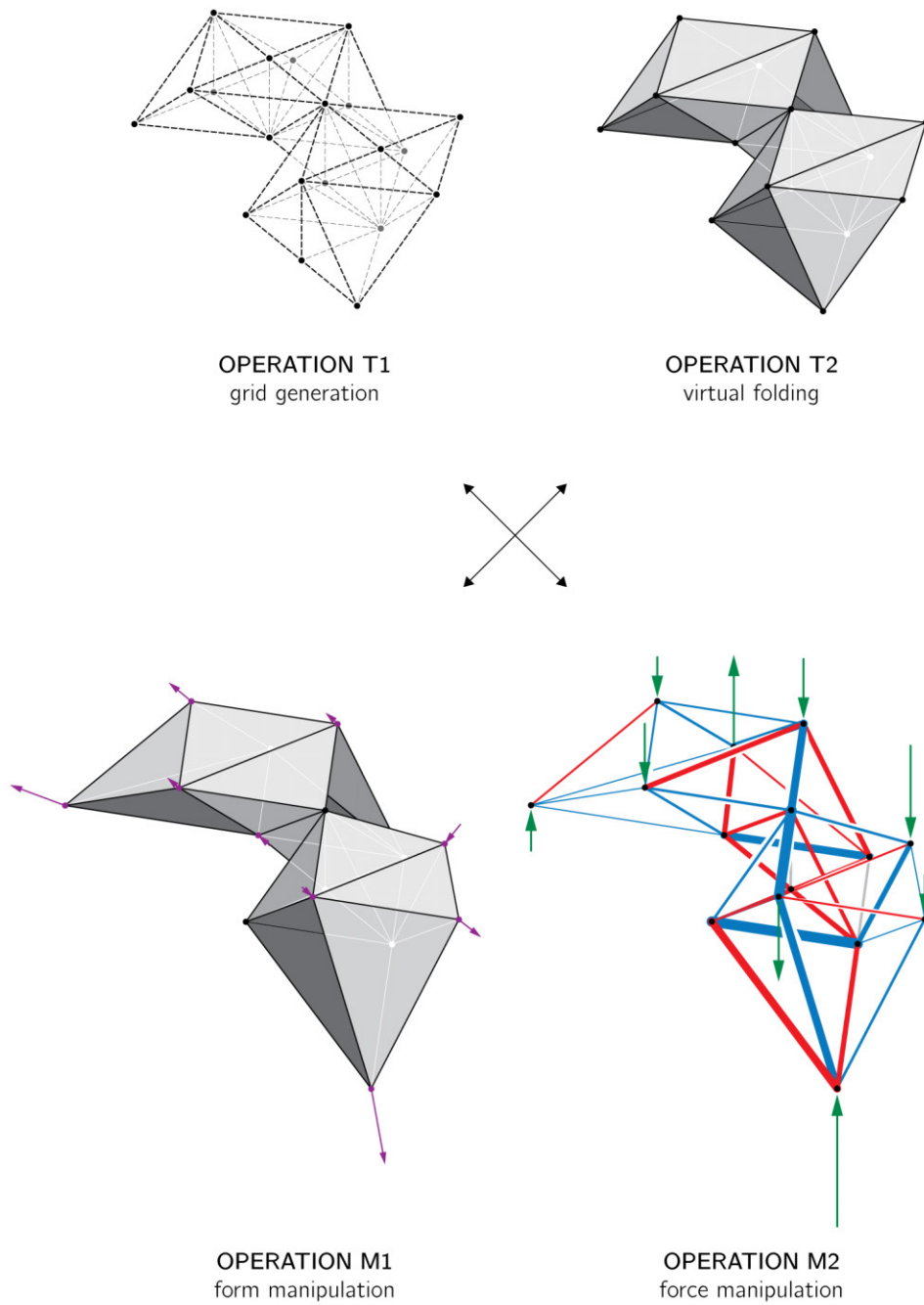
OPERATION M2
force manipulation

Figure 11.2: Overview of the proposed design method for structural folding in architecture, based on four main non-hierarchical operations: *T1–grid generation*, *T2–virtual folding*, *M1–form manipulation*, and *M2–force manipulation*.

12. Level of Topology

12.1 Generation of the Reference Grid

Operation *T1–grid generation* allows the designer to generate a reference grid constituted by a cluster of space-filling non-regular tetrahedra. This reference grid can be regarded as a virtual spatial lattice structure, not supported to the ground, made of edges connected to each other at common vertices by means of pin-joints (§ 8.1). The edges of the grid are the edges of the tetrahedra, which in turn coincide with the edges of the folded plate structure that is generated in the subsequent operation *T2–virtual folding*.

From a topological point of view, the grid works as a structural and spatial reference for the overall design process. That is, the topology of the grid controls the static rigidity (§ 8.2) of the folded plate structure and the organisation of its enclosed architectural space as created using the operation *T2–virtual folding* (D'Acunto and Castellón 2015). Hence, through operation *T1* the topology of the folded plate structure is set by specifically defining the amount of the tetrahedra within the grid and their mutual connectivity. The grid is assembled following a *bottom-up* strategy in which individual tetrahedra are used as elementary rigid bodies that are clustered into a larger overall rigid lattice structure. In order to perform structurally as rigid bodies, these tetrahedra must be non-degenerate[1].

This bottom-up strategy for the creation of kinematically stable structures is a specific application of the procedure for the generation of *simple* rigid structures made of successive linkages (§ 8.2). Similar procedures for the sequential construction of kinematically stable spatial structures can be found in the literature. Among others, the *Stringer System* (Almegaard 2003) for the definition of triangulated spatial networks, the *Tetraedermethode* (Schrems 2016) for the assembly of tetrahedral trusses and the approach suggested within the *Load Path Network Method* (Enrique and Schwartz 2017) for the construction of spatial strut-and-tie networks.

---

[1]A tetrahedron is non-degenerate if its four vertices are not all incident to the same plane. In fact, in this specific projective geometric configuration, the tetrahedron is not a rigid body, as it is not infinitesimally rigid. The edges of the tetrahedron are linearly dependent on each other, and they have a lower *rank* (§ 8.2) than the one that would be expected from solely topological considerations (Crapo 1979, p. 28).

Construction of the Grid   The first step in the generation of the reference grid consists in the creation of a non-degenerate tetrahedron B_0 (Fig. 12.1.a), working as a spatial lattice structure, with vertices V_i, edges E_{i-j} and faces f_{i-j-k}. This constitutes the initial seed of the grid. Starting from the seed, the grid can be then extended through the sub-operation *T1-A*, by adding a new tetrahedron at a time, thus resulting in a cluster of tetrahedra (Fig. 12.1.b). Tetrahedra can be removed through the sub-operation *T1-R*. An underlying *tetrahedral volume mesh* is used to represent the grid, whose individual elements are *tetrahedral mesh cells* that can be visualised in the projective space in a form diagram $\mathbf{F_G}$[2].

In principle, any rigid linkage could be used to connect a new tetrahedron to an existing one (§ 8.2). Since the continuity between faces of any two connected tetrahedra is necessary for the operation *T2*, the ordinary way to connect two tetrahedra of the grid is by sharing a contact face; in turn, this implies that the two tetrahedra share three contact edges and three contact vertices[3]. In fact, with regard to static rigidity, connecting two completely disconnected tetrahedra by means of a shared face is analogous to linking two tetrahedra through six linearly independent edges. Likewise, the same configuration can be achieved by linking a point to the three vertices of an existing tetrahedron using three new edges (§ 8.2). In this case, the point and the three edges constitute one of the vertices and three of the edges of a second tetrahedron that shares its three other vertices and its three other edges with the existing tetrahedron in the grid.

Static Rigidity   As mentioned above, the reference grid performs structurally as a spatial lattice structure not supported to the ground. Based on the *extended Maxwell's rule* (8.12) the number s_G of independent states of self-stress of the grid can be found as follows:

$$s_G = E_G - 3V_G + m_G + 6 \tag{12.1}$$

with E_G the number of grid edges, V_G the number of grid vertices, m_G the number of internal mechanisms and 6 the number of rigid body motions of space. Being rigidly assembled, $m_G = 0$ and the grid is either statically determinate ($s_G = 0$) or statically indeterminate ($s_G > 0$). In the latter case, s_G corresponds to the number of edges of the grid other than the minimum necessary ones to attain the static determinacy of the structure, i.e. the *degree of static indeterminacy* of the structure *n* as expressed in (8.11).

---

[2]It should be noted that all the metric properties of the diagram $\mathbf{F_G}$ are irrelevant and only the topological and projective properties of incidence among geometric elements have to be taken into consideration.

[3]To prevent the eventuality of self-intersection among the individual tetrahedral mesh cells of the reference grid, no more than two tetrahedra are allowed to share the same face. Moreover, considering the face normals of each underlying tetrahedral mesh cell *outward-pointing*, the two face normals, corresponding to a face shared between two tetrahedra, are always opposite to each other.
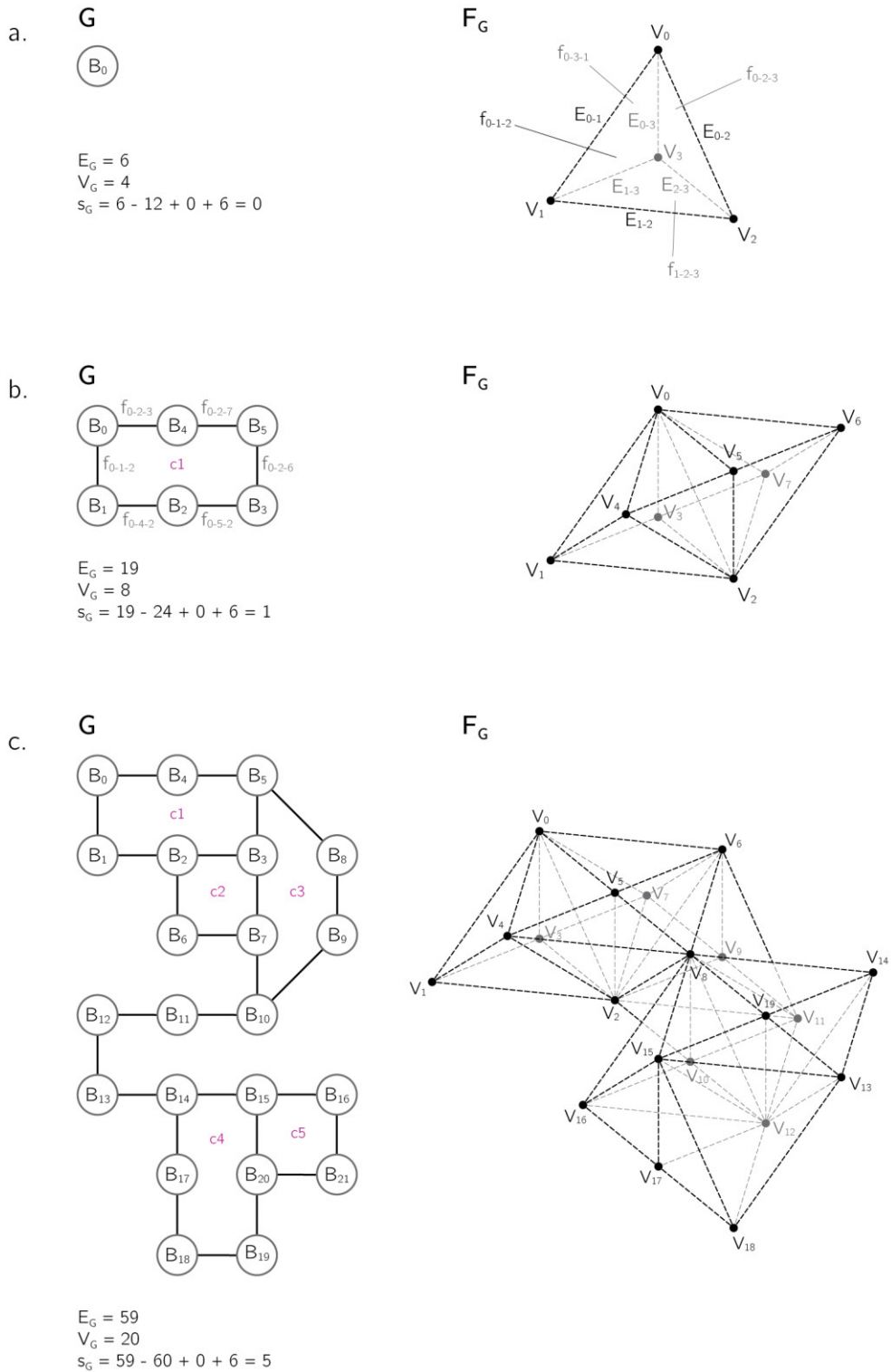
a.

G

(B_0)

$E_G = 6$
$V_G = 4$
$s_G = 6 - 12 + 0 + 6 = 0$

F$_G$

b.

G

$E_G = 19$
$V_G = 8$
$s_G = 19 - 24 + 0 + 6 = 1$

F$_G$

c.

G

$E_G = 59$
$V_G = 20$
$s_G = 59 - 60 + 0 + 6 = 5$

F$_G$

Figure 12.1: Operation T1–grid generation: graph **G**, showing the connectivity of the individual rigid bodies, and form diagram **F**$_G$, depicting the reference grid. (a) Initial seed as a tetrahedron B_0 with vertices V_i, edges E_{i-j} and faces f_{i-j-k}. (b) Creation of a loop of rigid bodies $(B_0, B_1, B_2, B_3, B_5, B_4)$ in **F**$_G$, resulting in a cycle $(c1)$ in **G**. (c) Sequential assembly of the reference grid as a combination of rigid bodies.

The grid is statically determinate as long as its constituting tetrahedra are connected to each other to form linear chains of rigid bodies. In this case, as previously described, adding a new tetrahedron implies the addition of one new vertex and three new edges to the grid, so that s_G in the (12.1) does not change. The grid becomes statically indeterminate to one or more degrees when the connected tetrahedra generate loops of rigid bodies (Fig. 12.1.b). In the simplest case, a loop is achieved after adding to the grid a new tetrahedron that shares two of its faces with two existing tetrahedra, thus adding a new edge to the grid and one degree of static indeterminacy. In the occurrence that the additional tetrahedron shares three faces with three existing tetrahedra of the grid, s_G stays invariant. Moreover, in the special case of a loop of tetrahedra forming a toroidal polyhedron, at least three new tetrahedra are necessary to close the initially disconnected chain, and six new degrees of static indeterminacy are added to the grid. While building the grid, it is possible to keep track of its degree of static indeterminacy by counting how many new vertices and edges are added in relation to the (12.1).

A graph **G** can be laid out to depict synthetically the connectivity of the individual rigid bodies (Fig. 12.1, left)[4]. In **G** each rigid body B_h is represented as a vertex and each face f_{i-j-k} shared by any two rigid bodies is represented as an edge. As such, loops of rigid bodies in the grid define elementary cycles in **G**.

Subdivision and Combination Adding (*T1-A*) and removing (*T1-R*) tetrahedra are the basic sub-operations for the generation of the reference grid (Fig. 12.1.c). Two supplementary sub-operations can be used to transform the topology of the grid, namely subdivision (*T1-S*) and combination (*T1-C*).

On the one hand, through subdivision (*T1-S*), an existing tetrahedron can be replaced by a cluster of two or more tetrahedra that are enclosed within the existing one. For example, by introducing a new vertex inside a given tetrahedron, the tetrahedron can be subdivided into four new tetrahedra, each of them sharing the newly introduced vertex and having as a face one of the faces of the given tetrahedron (Fig. 12.2.a). After this sub-operation is applied, a new degree of static indeterminacy is added to the grid since the four new tetrahedra generate themselves a closed chain of rigid bodies (Fig. 12.2.b). Likewise, by inserting a new vertex along one of the edges of a given tetrahedron, the tetrahedron can be subdivided into two new tetrahedra. In case the edge where the new vertex is inserted is shared with other tetrahedra, these have to be subdivided accordingly in order to keep face-to-face connectivity between all the tetrahedra. The sub-operation (*T1-S*) can be repeated hierarchically, and each of the tetrahedra resulting from the subdivision of an initially given tetrahedron can be further subdivided to obtain a refined grid.

---

[4]A related approach based on the use of graph theory for the construction of statically determinate strut-and-tie networks in space is found in (Enrique and Schwartz 2017).

On the other hand, through combination (*T1-C*), a cluster of tetrahedra can be joined (Fig. 12.2.a) to produce a convex triangulated polyhedron (Fig. 12.2.b). According to Alexandrov's theorem (Alexandrov 1958), a convex triangulated polyhedron, with no vertex having its connected edges coplanar, performs itself as a rigid body (§ 8.2) and therefore it is rendered in the graph **G** as an individual vertex (Fig. 12.2.b). A degree of static indeterminacy is removed from the grid for any simple closed chain of tetrahedra that is combined into a triangulated polyhedron.

Topological and Projective Constraints Specific constraints can be imposed on the reference grid according to the given design requirements. These are then retained throughout the entire design process and are applied on top of any other constraint introduced within the subsequent design operations. From a topological standpoint, rules can be applied on the number of tetrahedra within the grid, the number of connections per tetrahedron and the number of closed chains of tetrahedra (i.e. the degree of static indeterminacy of the structure).

From the point of view of projective geometry, constraints of incidence can be established among different elements of the grid and applied sequentially while the reference grid is being constructed. These constraints are applicable as long as the tetrahedra or triangulated polyhedra constituting the grid do not degenerate into a *critical form* (Baracs 1975), thus creating an internal finite or infinitesimal mechanism (§ 8.2). Provided that the tetrahedra are not connected to each other to generate loops, the linearity of the constraints of incidence is attained.

For example, it is possible to enforce the incidence of two adjacent faces f_{s-j-k} and f_{t-k-j} with the same plane $\pi_{s-j-t-k}$ or the incidence of two connected edges E_{s-j} and E_{j-t} with a common line l_{s-j-t}. Based on the axioms of incidence of projective geometry (Coxeter 1987) and given the relationship between faces f_{i-j-k}, edges E_{i-j} and vertices V_i of the grid, these rules of incidence can be formulated as constraints applied directly to the V_i. If no constraints are applied, a vertex V_i has three *degrees of freedom* (DOFs) with regard to its position in space. Enforcing a vertex to be incident with one plane (respectively two or three), reduces its DOFs to only two (respectively one or zero). No more than three incident planes can be assigned to the same vertex to avoid the system being over-constrained. The dependencies between the vertices V_i can be illustrated and controlled using a *directed graph* as suggested by Fivet and Zastavni (2015).
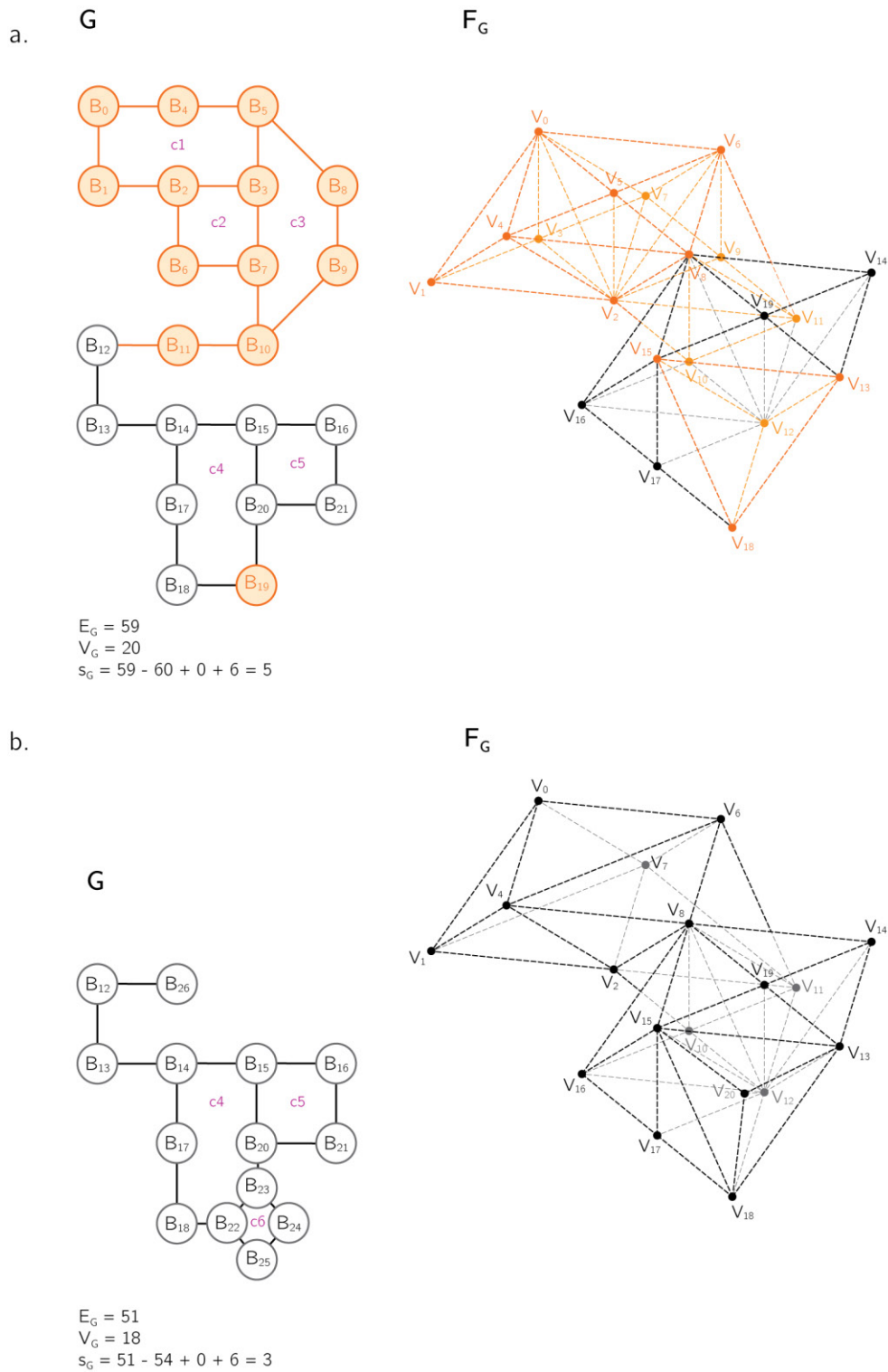
a. **G**   **F**_{**G**}

$E_G = 59$
$V_G = 20$
$s_G = 59 - 60 + 0 + 6 = 5$

b.   **F**_{**G**}

G

$E_G = 51$
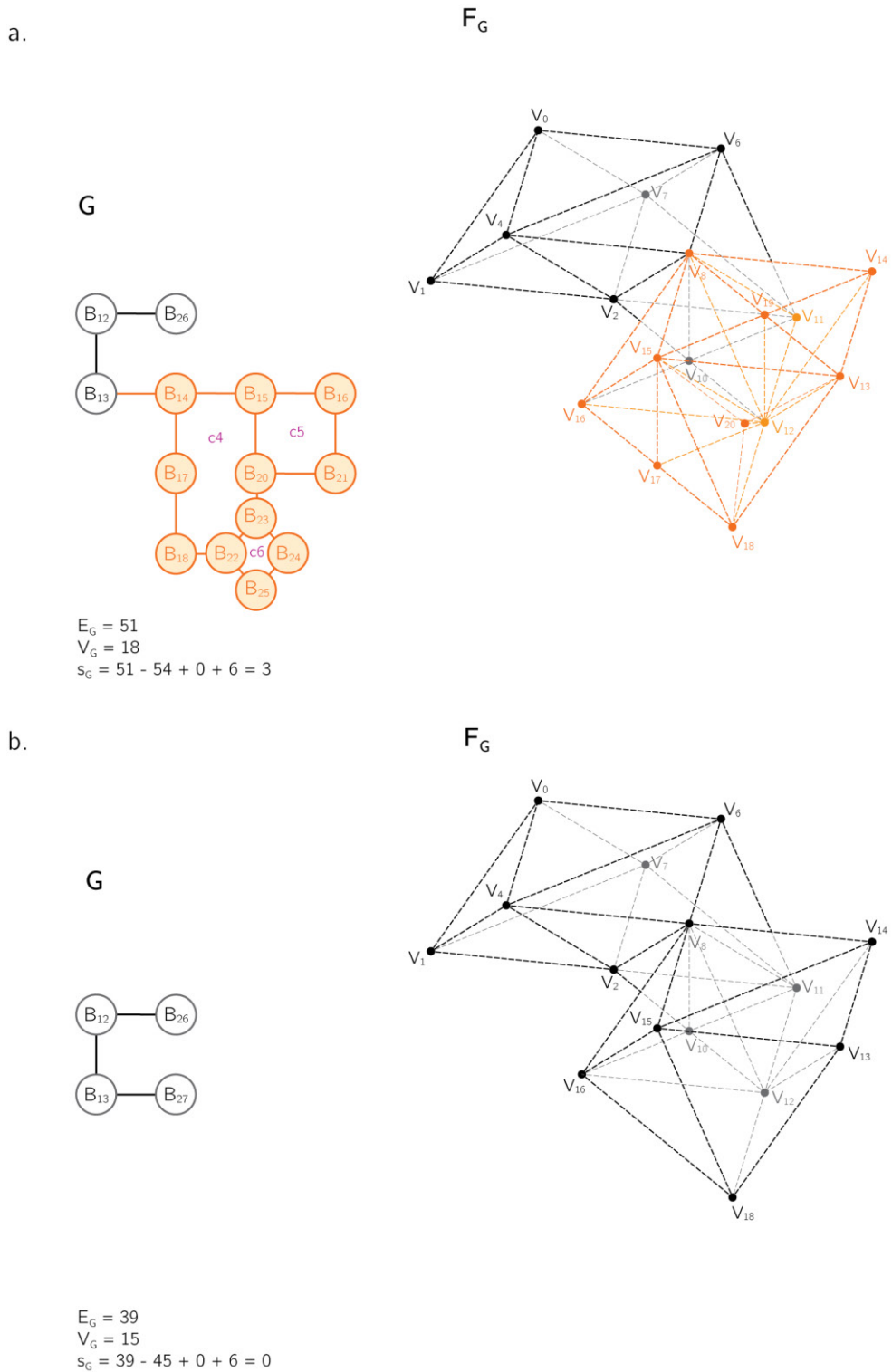$V_G = 18$
$s_G = 51 - 54 + 0 + 6 = 3$

Figure 12.2: Operation T1–grid generation: graph **G**, showing the connectivity of the individual rigid bodies, and form diagram **F**_{**G**}, depicting the reference grid. (a) (b) Subdivision (T1-S) of a tetrahedron (B_{19}) into four tetrahedra (B_{22}, B_{23}, B_{24}, B_{25}); combination (T1-C) of a cluster of tetrahedra ($B_0 - B_{11}$) into a triangulated polyhedron (B_{26}).

a.

$\mathbf{F_G}$

G

$E_G = 51$
$V_G = 18$
$s_G = 51 - 54 + 0 + 6 = 3$

b.

$\mathbf{F_G}$

G

$E_G = 39$
$V_G = 15$
$s_G = 39 - 45 + 0 + 6 = 0$

Figure 12.3: Operation T1–grid generation: graph **G**, showing the connectivity of the individual rigid bodies, and form diagram $\mathbf{F_G}$, depicting the reference grid. (a) (b) Combination (T1-C) of a cluster of tetrahedra ($B_{14} - B_{25}$) into a triangulated polyhedron (B_{27}).

12.2   Creation of the Folded Plate Structure

Operation *T2–virtual folding* allows the designer to delineate the geometry of the folded plate structure, which is virtually folded within the spatial reference grid generated via operation *T1–grid generation* (Fig. 12.1). That is, through the sub-operation *T2-A* a subset of mesh faces from the polyhedral volume mesh representing the reference grid are actualised into a continuous triangulated mesh, which outlines the geometry of the folded plate structure. Using the form diagram $\mathbf{F_G}$ as a base (Fig. 12.3.b), the triangulated mesh can be visualised with the aid of a form diagram $\mathbf{F_P}$ (Fig. 12.4.a).

Architectural Considerations   While creating the geometry of the folded plate structure through operation *T2*, an enclosed architectural space is also produced. In this way, the developed design approach overturns the traditional tectonic separation among the walls, the floor, and the ceiling of a building (D'Acunto and Castellón 2015). In compliance with the proposal of Sancho and Madridejos (§ 5.2), the folded plate geometry generates a continuous and differentiated architectural space. In fact, it is through operation *T2* that the main topological features of the architectural space can be outlined and controlled. These aspects include the general organisation of the interior space in terms of the number of floors of the building, the distribution of the rooms according to a given architectural programme, as well as the main internal circulation. Moreover, while creating the folded plate structure also the topological relationship between interior space and external context can be addressed by defining the amount and the location of the openings to the outside (D'Acunto and Castellón 2015).

Structural Behaviour   The folded plate structure relies on the combination of lattice and plate actions (§ 8.2.3) and the folded edges work at the same time as axially loaded bars and hinge lines (§ 8.3). Different possible folded plate structures can be actualised based on the same initial reference grid. The topology of the folded plate structure can be outlined using a graph $\mathbf{P}$, in which each folded plate f_{i-j-k} is represented by a vertex and each folded edge E_{i-j} shared by adjacent folded plates is shown as an edge (Fig. 12.4, left). Based on the *extended Maxwell's rule* (8.12), a relationship analogous to the (12.1) can be defined for the number m_P of internal mechanisms in the folded plate structure regarded as system supported on the ground:

$$m_P = -E_P + 3V_P + s_P - k_P \qquad (12.2)$$

with E_P the number of folded edges, V_P the number of folded plate vertices, s_P the number of self-stresses and k_P the number of kinematic restraints at the supports (6 minimum to prevent any rigid body motion of space).

For a given statically determinate grid ($s_G = 0$ and $m_G = 0$) as defined through operation *T1* (Fig. 12.3.b), its full set of grid edges E_G (and as such

grid vertices V_G) have to be actualized into folded edges E_P (respectively folded plate vertices V_P) in order to achieve the static determinacy of the folded plate structure ($s_P = 0$ and $m_P = 0$), provided $k_P = 6$ (Fig. 12.5.a). That is, if one or more grid edges are not converted into folded edges ($E_P < E_G$), one or more internal rotational mechanisms can be found within the folded plate structure ($m_P > 0$). In this occurrence, the static rigidity of the folded plate structure can be achieved by introducing supplementary kinematic restraints at the supports ($k_P > 6$). Alternatively, the rotational degrees of freedom due to the internal mechanisms can be eliminated by regarding one or more appropriate folded edges as rotationally rigid connections rather than hinges. From the point of view of the sole static rigidity, the effect of these rigid connections can be taken into account in the (12.2) by supposing the missing edges in the structure as actually present, until $E_P = E_G$. In case one or more faces of the reference grid are constrained to be incident with the same plane (§ 12.1), a single folded plate can be built on these faces as a triangulated mesh polygon. Note that both the exterior and the interior edges of the triangulated mesh polygon have to be taken into account when evaluating E_P.

Continuity of the Folded Plate Geometry In order to guarantee the geometric continuity of the generated folded plate structure, a series of topological rules have to be respected in the definition of the underlying triangulated mesh in $\mathbf{F_P}$ throughout the application of the sub-operation *T2-A*. In particular, any two triangular mesh faces or triangulated mesh polygons are not allowed to share a single vertex but at least two, which should belong to the same mesh edge. Besides, more than two mesh faces or mesh polygons can share the same mesh edge. In this case, the edge is defined as *non-manifold*, and it is shown in **P** as many times as the number of mesh faces or mesh polygons connected to it. Holes are allowed within the mesh and can be produced by removing selected mesh faces of mesh polygons via the sub-operation *T2-R*. This implies the generation of *naked edges* (i.e. edges belonging to only one mesh face) along the boundaries of the holes as *free edges*. After the removal of mesh faces or mesh polygons, the static rigidity of the modified folded plate structure has to be re-evaluated, and additional kinematic restraints or rotationally rigid connections have to be introduced when required.

Unfolding of the Folded Geometry Following the approach suggested by Nejur and Steinfeld (2017), the graph **P** can be used to identify a valid sequence of folded plates (i.e. triangular mesh faces or a triangulated mesh polygons) to be rotated in order to unfold the entire folded plate structure onto one plane $\mathbf{F_U}$ (Fig. 12.5.b). Through the sub-operation *T2-U*, a folded plate that lies on the target unfolding plane is first chosen. Selected edges of **P** are then cut until all cycles in the graph are removed while keeping the graph connected. This results in the creation of a *directed rooted tree* $\mathbf{P_U}$ (Fig. 12.5.b), whose paths

are all branching out from the vertex corresponding to the chosen initial mesh face. The order of the vertices in $\mathbf{P_U}$ defines the sequence of folded plates to be rotated for the unfolding.
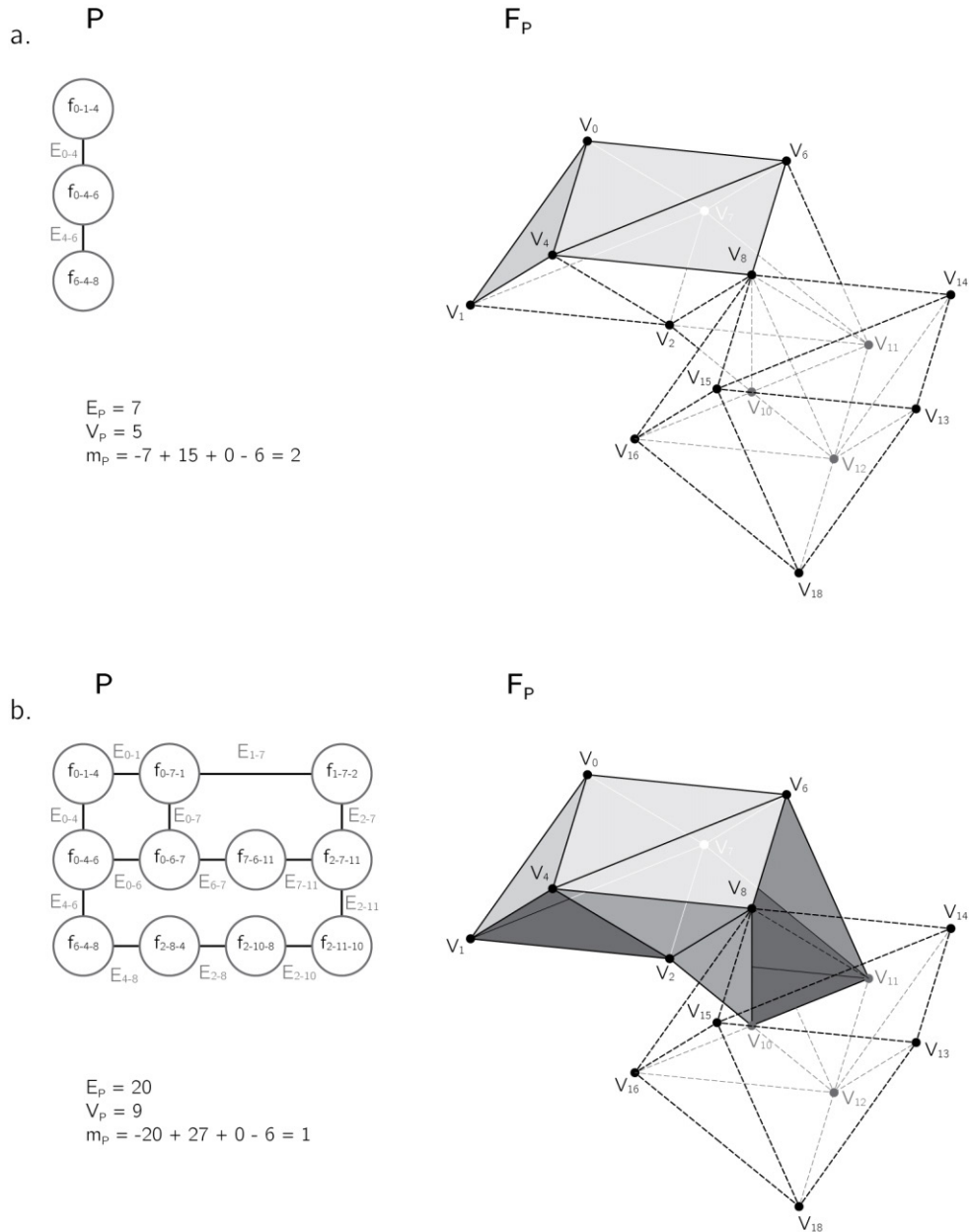
a.

b.

Figure 12.4: Operation T2–virtual folding. (a) (b) Sequential construction of the folded plate structure $\mathbf{F_P}$ and related graph $\mathbf{P}$.
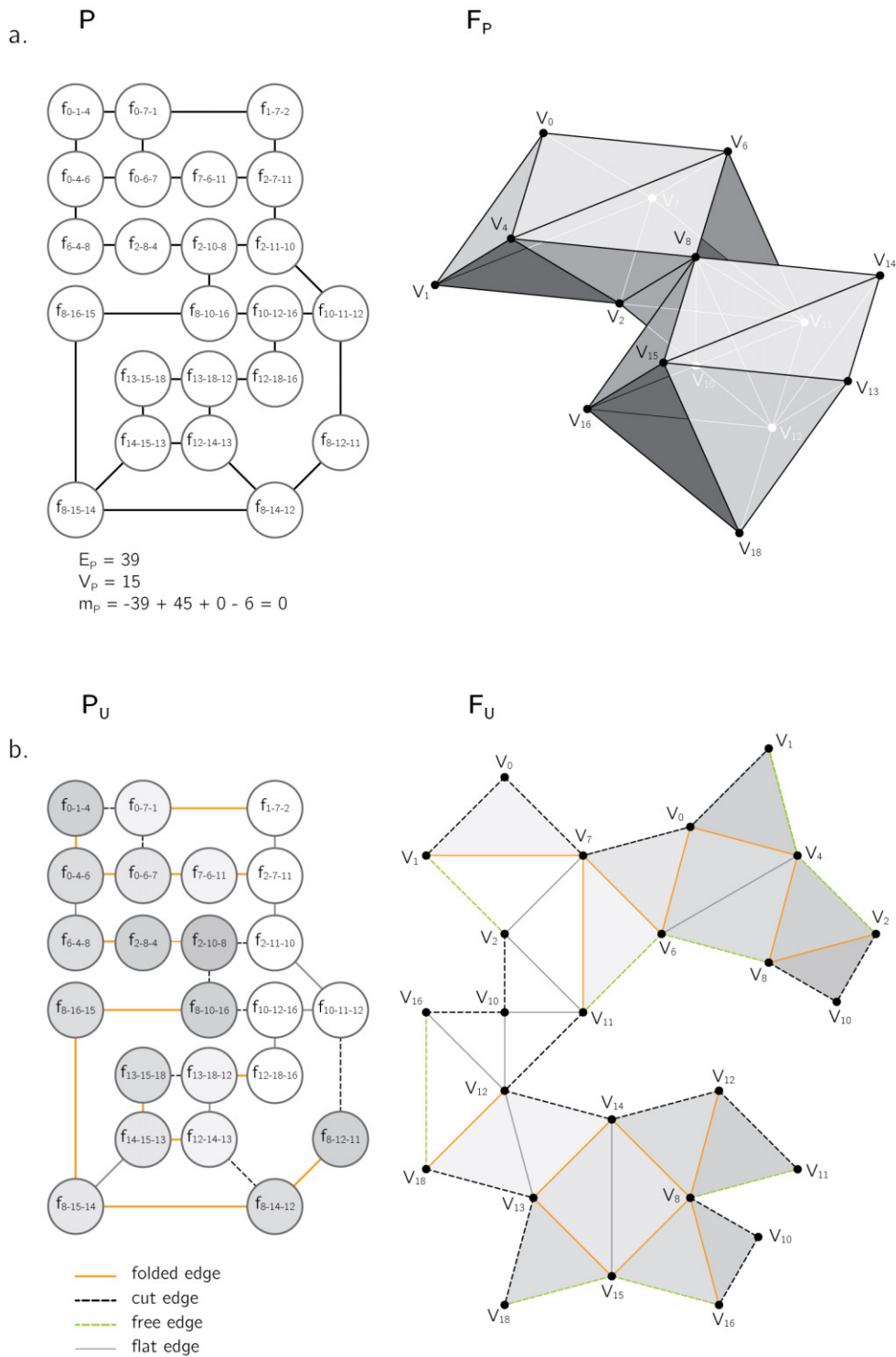
Figure 12.5: Operation T2–virtual folding. (a) Statically determinate folded plate structure F_P and related graph P. (b) Unfolded plate structure F_U and related graph P_U as a *directed rooted tree*. The colour of the faces of F_U (respectively vertices of P_U), from white to dark grey, is related to the number of rotations necessary for the unfolding of the faces.

13. Level of Euclidean Geometry

13.1   Transformation of the Form

With operation *M1–form manipulation*, the metric properties of the reference
grid (§ 12.1) and of the folded plate structure (§ 12.2) can be specified and
modified without altering their topological features, as defined through the previ-
ously described operations. Hence, operation *M1* enables the designer to explore
diverse metric design solutions that are grounded on the same topological layout.
As such, variation can be introduced into the design development (D'Acunto and
Castellón 2015).

   In particular, with operation *M1* the proportions and dimensions of the folded
plate structure and the ones of its enclosed architectural space can be controlled
and adjusted. The designer can thus inform the process in relation to the specific
design needs to obtain the desired spatial qualities. As a result, using operation
M1, the architectural opportunity of folding to combine diverse spatial conditions
within the same continuous variation of the form (Lynn 1993b; Carpo 2004) can
be exploited (D'Acunto and Castellón 2015).

Introduction of Metric Properties   In the form diagram $\mathbf{F_P}$ (§ 12.2), the refer-
ence grid and the folded plate structure are depicted respectively as a polyhedral
volume mesh and a continuous triangulated mesh. In the Euclidean 3D space,
$\mathbf{F_P}$ is converted into the metric form diagram $\mathbf{F_M}$.

   A Cartesian coordinate system is defined by choosing an origin $O = (0, 0, 0)$
and three coordinate axes $\{x_1, x_2, x_3\}$. A set of position vectors $\boldsymbol{p}_i = \{p_{i1}, p_{i2}, p_{i3}\}$
are then assigned to the vertices V_i of the polyhedral volume mesh, which are
themselves coincident with the vertices of the triangulated mesh. As previously
observed (§ 12.1), based on the degree of freedom (DOFs) of the V_i, the heads
of the $\boldsymbol{p}_i$ are either free in space, bounded to a plane[1], bounded to a line (i.e.
intersection of two planes)[2], or fixed in a point (i.e. intersection of three planes).

---

[1] In this case, $\boldsymbol{p}_i$ can also be outlined as $\boldsymbol{p}_i = \{p_\perp, p_{\|1}, p_{\|2}\}$, where $p_\perp$ is a fixed component
perpendicular to the constraint plane while $p_{\|1}$ and $p_{\|2}$ are two variable components parallel to
the plane and perpendicular to each other.

[2] With $\boldsymbol{p}_i = \{p_\perp, p_\|\}$, where $p_\perp$ is a fixed component perpendicular to the constraint line,
and $p_\|$ is a variable component parallel to the line.

Global and Local Transformations   Through operation *M1*, each vertex V_i of the reference grid (respectively folded plate structure) can be adjusted by adding a translation vector $\boldsymbol{t}_i$ to its position vector $\boldsymbol{p}_i$. A grid edge E_{i-j} (respectively folded edge) can be transformed by applying two translation vectors to its vertices. Likewise, a grid face f_{i-j-k} (respectively folded plate) can be transformed using three translation vectors applied to its vertices. Since the vertices of the reference grid and those of the folded plate structure are coincident, any geometric transformation of the reference grid implies the concurrent modification of the folded plate structure. Two categories of transformations can be employed, namely global and local transformations.

Among the global transformations, particularly useful with regard to the design process are the global parallel transformations (§ 9.5). These manipulations are applied at the same time to all the vertices V_i (Fig. 13.1.a). Because of the underlying properties of this class of transformations (Pottman et al. 2007), not only the topology but also the previously defined constraints of incidence between elements of the reference grid (§ 12.1) are preserved throughout the transformation. Moreover, the kinematic stability of the folded plate structure is also secured after the transformation (Rankine 1856). These properties can help the designer to adapt the geometry of the folded plate structure to specific design requirements, such as given boundary constraints.

Local transformations can be applied to the vertices V_i (Fig. 13.1.b) by means of direct geometric operations as long as the transformation is compatible with the degrees of freedom (DOFs) of the V_i. When present, the previously defined constraints of incidence (§ 12.2) have to be updated based on the dependencies between the V_i. The application of constraint-based global and local transformations (Fig. 13.2.a) entails the use of numerical simulations, which are here dealt with the *Kangaroo2* library by Piker (2017).

Application of Extra Metric Constraints   A series of extra metric constraints can be applied along with the operation *M1*. These constraints allow for the shape and the dimension of the folded geometry to be adjusted to meet given programmatic and static needs or to adapt to certain architectural and structural boundary requirements (D'Acunto and Castellón 2015). Metric constraints may also reflect specific design necessities, such as material properties, construction and fabrication needs, or scale-dependent requisites. In order to introduce constraints within the proposed design method, these have to be formulated in terms of metric restrains imposed on the surface area $|A_f|$ of the folded plates, on the length $|E|$ of the folded edges, or on the angle α between adjacent folded plates (D'Acunto and Castellón 2015). Metric constraints generally introduce non-linearity into the system, and therefore their application necessitates the use of numerical simulations, as highlighted above.
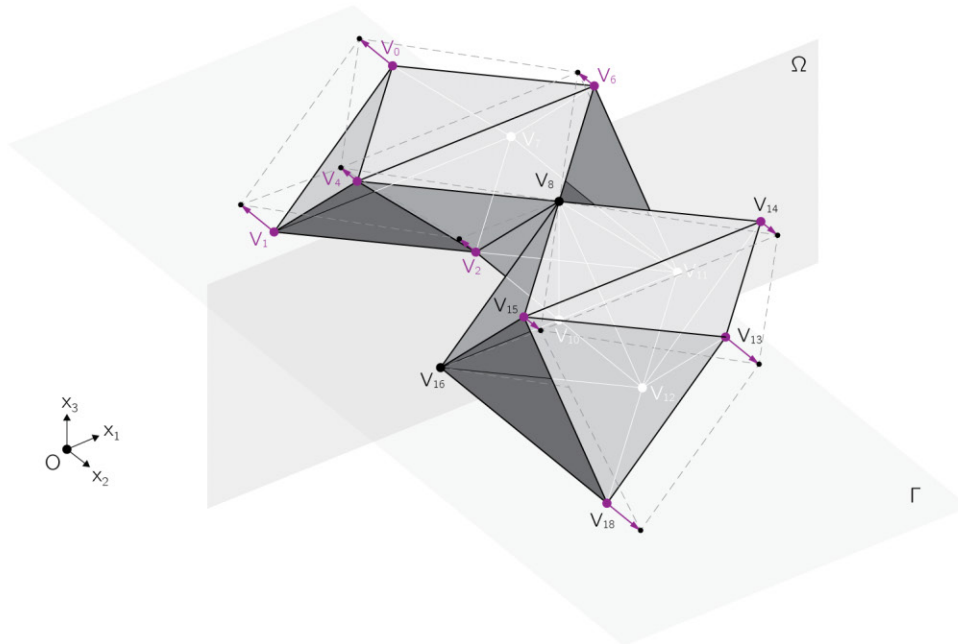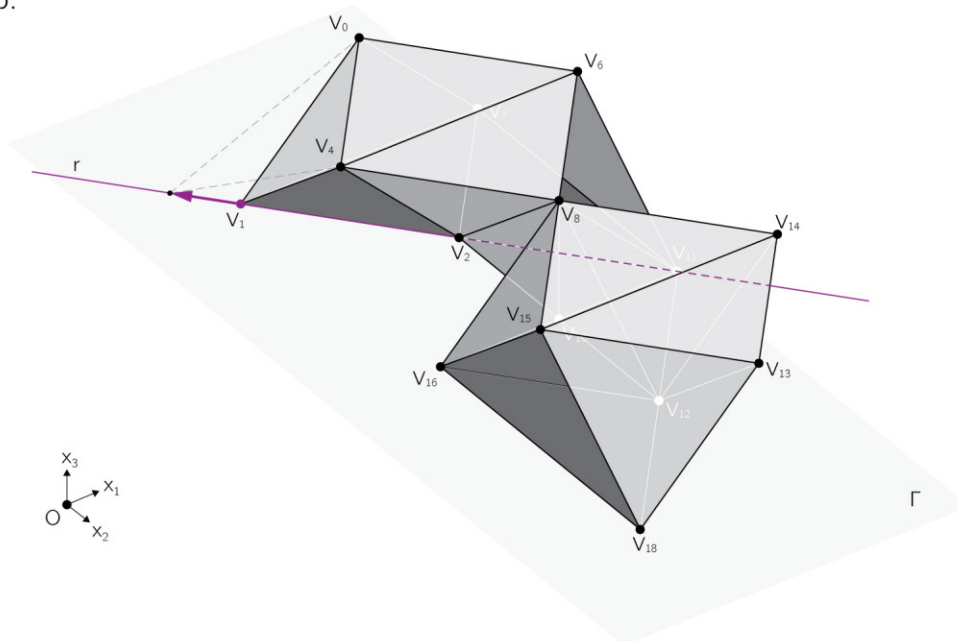
Figure 13.1: Operation M1–form manipulation. (a) Application of a global transformation to the folded plate structure ($\mathbf{F_M}$): non-uniform scaling along the x_2 coordinate axis and with origin plane $\Omega = \{V_8, V_{10}, V_{16}\}$. (b) Application of a local transformation to $\mathbf{F_M}$': translation of the vertex V_1 along the line $r = \{V_1, V_2\}$.
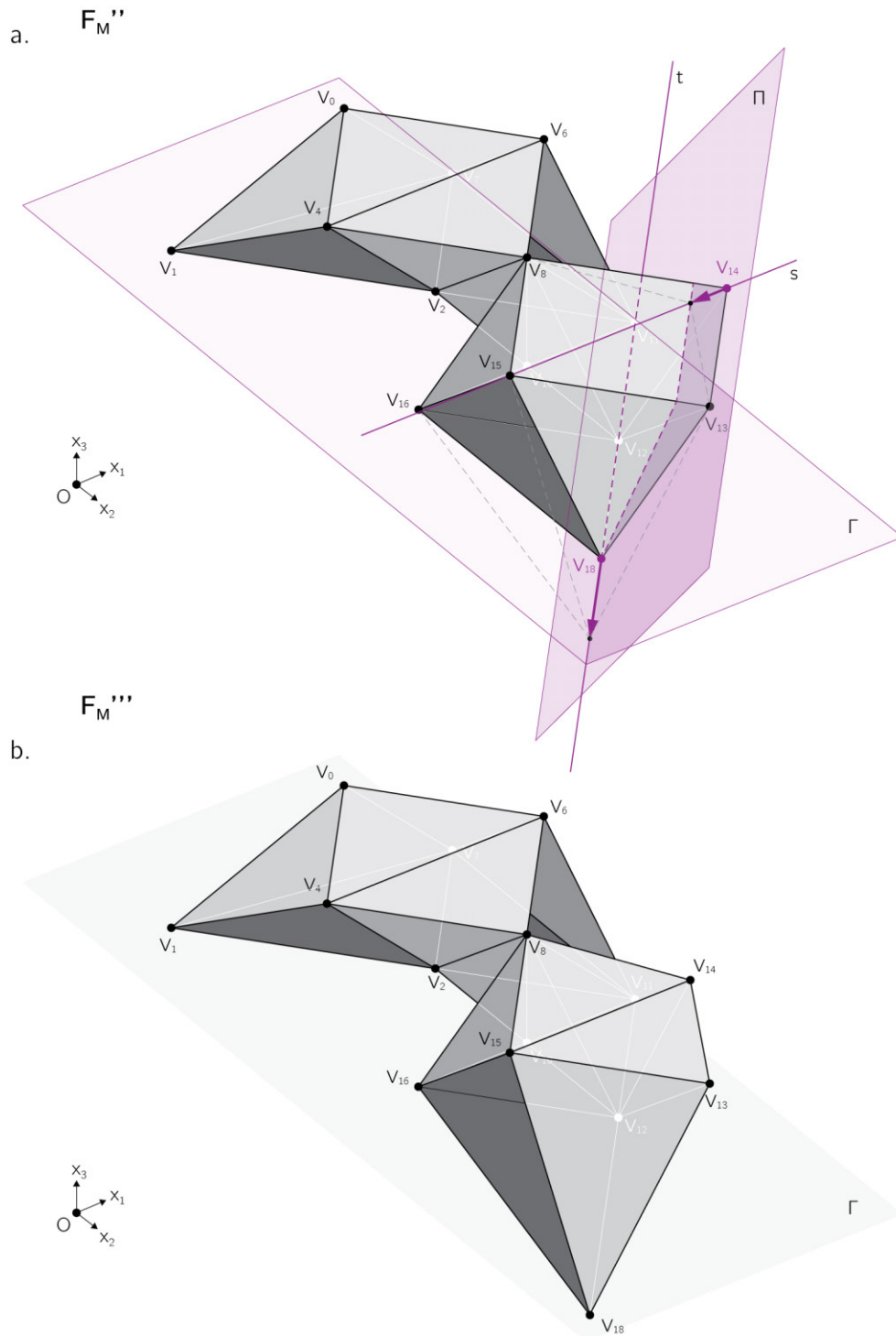
Figure 13.2: Operation M1–form manipulation. (a) Constraint-based local transformation of the folded plate structure ($\mathbf{F_M}$"): translation of the vertex V_{18} along the line t of intersection between the plane $\Gamma = \{V_{12}, V_{16}, V_{18}\}$ and the given plane Π; translation of the vertex V_{14} to the point of intersection between the plane Π and the line $s = \{V_{14}, V_{15}\}$. (b) Transformed folded plate structure $\mathbf{F_M}$"'.

13.2   Manipulation of the Internal Forces

Through operation *M2–force manipulation*, the integration between structure and architecture is eventually attained. In fact, this operation allows for the inherent structural logic of the previously created folded plate structure to be revealed. Given the form diagram $\mathbf{F}_M$ (§ 13.1), where the reference grid and the folded plate structure are represented respectively by a polyhedral volume mesh and a triangulated mesh, operation *M2* can be used to automatically generated the related strut-and-tie network. In relation to the scope of the design task, a complete strut-and-tie network or a synthetic one (§ 8.3) can be created.

Complete Strut-and-Tie Model   A complete strut-and-tie model (Fig. 13.4.a) can be automatically assembled according to the procedure described in § 8.3. Hence, each folded edge is replaced by two *edge members*, while the folded plates by an appropriate triangulation of *plate members*[3]. Considering the strut-and-tie network as a 3D form diagram $\mathbf{F}$, its corresponding 3D force diagram $\mathbf{F}^*$ can be constructed according to any of the approaches described in § 9.4 and transformed as explained in § 9.5 to meet specific design requirements.

It is worth noting that the usual high amount of linear members in a complete strut-and-tie network together with the large number of external forces potentially applied to any node of the network may result in the generation of a vector-based 3D force diagram with several duplicate edges (§ 9.4). Although the construction of the 3D force diagram is always possible, in some instances a clear visual correlation between 3D form and force diagrams may be prevented. Hence, the vector-based 3D force diagrams may be difficult to be handled during the design process, and the benefit of using vector-based 3D graphic statics for the control of the internal forces in the structure reduced. In this occurrence, it may be more convenient to use instead a synthetic strut-and-tie network with a reduced number of linear members.

As previously described (§ 10.2), a complete strut-and-tie model can be used to automatically derive in-plane discrete stress fields within the folded plates (Fig. 13.4.b), in compliance with the lower bound theorem of the theory of plasticity (§ 10.1).

Synthetic Strut-and-Tie Model   A synthetic strut-and-tie network can be automatically generated directly from the triangulated mesh (Fig. 13.3.a). Such a strut-and-tie network has a reduced amount of linear members in comparison to the one described above. In particular, each folded edge is replaced by an *edge member* and each internal edge in a triangulated mesh polygon is substituted with a *plate member*. In this strut-and-tie network, loads can be applied at the

---

[3]Folded plates as triangulated mesh polygons are triangulated based on the rules described in § 8.3; as such, the plate members are connected exclusively at the midpoints of the folded edges located along the borders of the mesh polygons.

endpoints of the folded edges only. Given its simplified nature, such a model does not completely take into account the load-bearing capacity of the folded plate structure, since the transfer of the internal forces is confined almost exclusively to the folded edges and the plates are not entirely active (§ 8.3). Nonetheless, the model still constitutes a valid equilibrium-based solution. Because of this reason, such a model can be particularly useful during the conceptual design stage, when a synthetic model can facilitate the process of testing several different design options. That is, fundamental structural input for the early stage of the design process is supplied to the designer by this synthetic strut-and-tie model in a comprehensible and coherent way.

Thanks to the use of vector-based 3D graphic statics (§ 9.4), regarding the strut-and-tie model as a 3D form diagram $\mathbf{F}$ (Fig. 13.3.a), its corresponding 3D force diagram $\mathbf{F}^*$ (Fig. 13.3.b) can be constructed to reveal the inherent relationship between the geometry of the folded plate structure and the distribution of its internal forces. As a result, similarly to the design approach suggested by Musmeci (§ 4.2), the capability of the structure to resist the externally applied loads through its form is made explicitly evident. Contrary to Musmeci's solution, in this case, the geometry of the folded plate structure not necessarily has to be described through projections. This aspect permits the proposed synthetic strut-and-tie model and its related 3D force diagram to be constructed for any folded plate structure, either in the form of a *folded surface structure* or a *folded volumetric structure* (Chapter 2).

Due to the dependency between $\mathbf{F}^*$ and $\mathbf{F}$ (§ 9.5), while the former is adjusted to control the magnitudes of the internal forces in the folded plate structure, the latter is modified accordingly. Both global and local transformations can be used to manipulate the force diagram. Furthermore, the inherent relationship among the various operations of the proposed design method makes it possible to apply any valid transformation to the topology and metrics of the reference grid or of the folded plate structure (§ 12.1; § 12.2; § 13.1) without losing the dependency between $\mathbf{F}^*$ and $\mathbf{F}$. In fact, after applying any of those topological or metric transformations the geometry of the strut-and-tie network is updated accordingly.

For example, in case the strut-and-tie network has some edge or plate members loaded with high internal forces, the network can be modified not only metrically, but also topologically through a subdivision of the related reference grid (§ 12.1). In turn, this operation results in the creation of subdivided edge or plate members and the consequent redistribution of the high-magnitude forces into more elements. Similarly, in case the folded plate structure has free edges under compression, a modification to the topology of the structure (§ 12.2) can be introduced as an effective design solution to remove the free edge and avoid the risk of buckling (Kotnik and D'Acunto 2013).
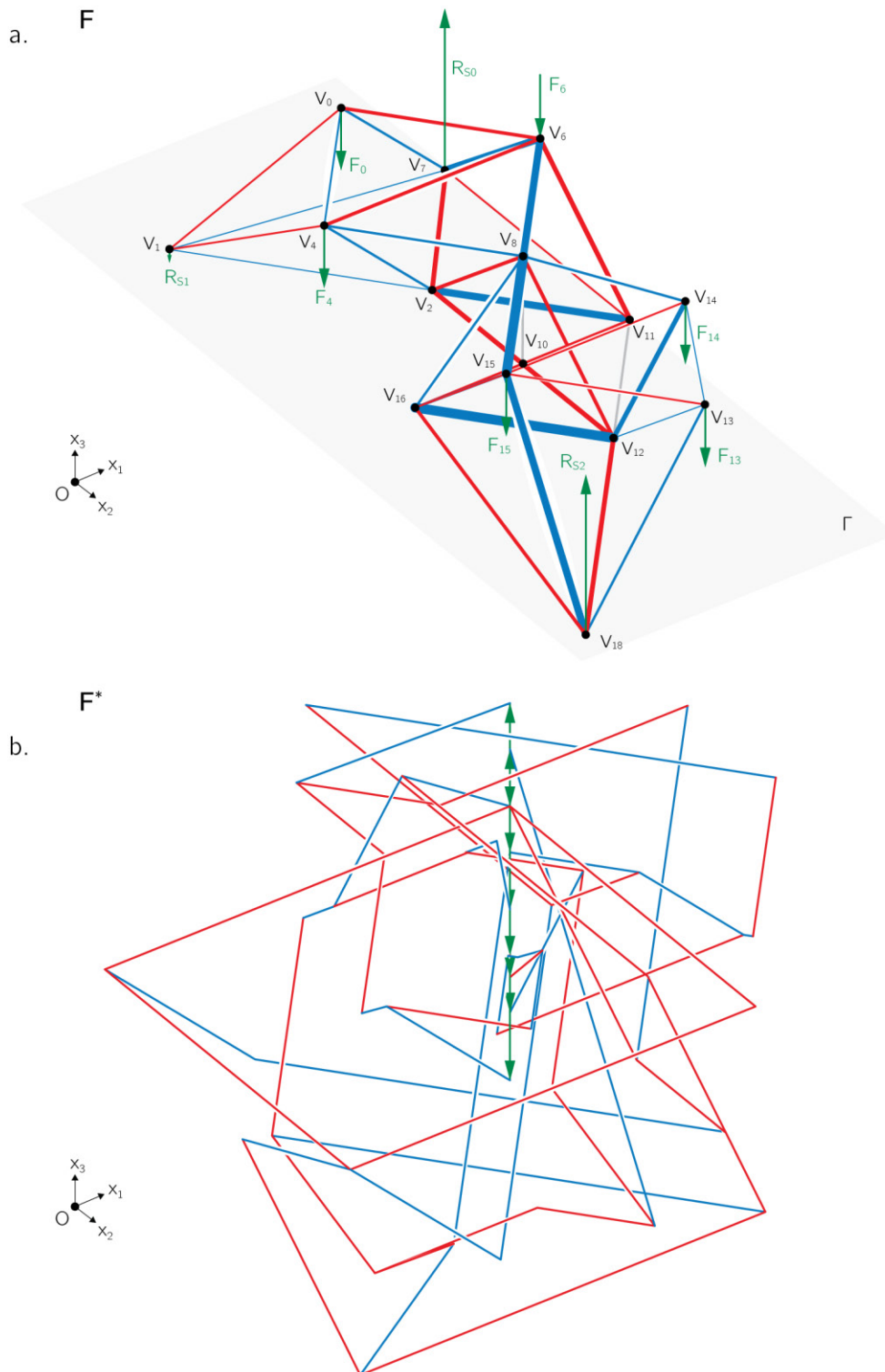
Figure 13.3: Operation M2–force manipulation. (a) Synthetic strut-and-tie network of the folded plate structure as a 3D form diagram **F** with 6 applied loads and 3 support points. (b) Corresponding 3D force diagram **F***. Given the complexity of the force diagram, its manipulation necessarily requires the use of a 3D software environment.
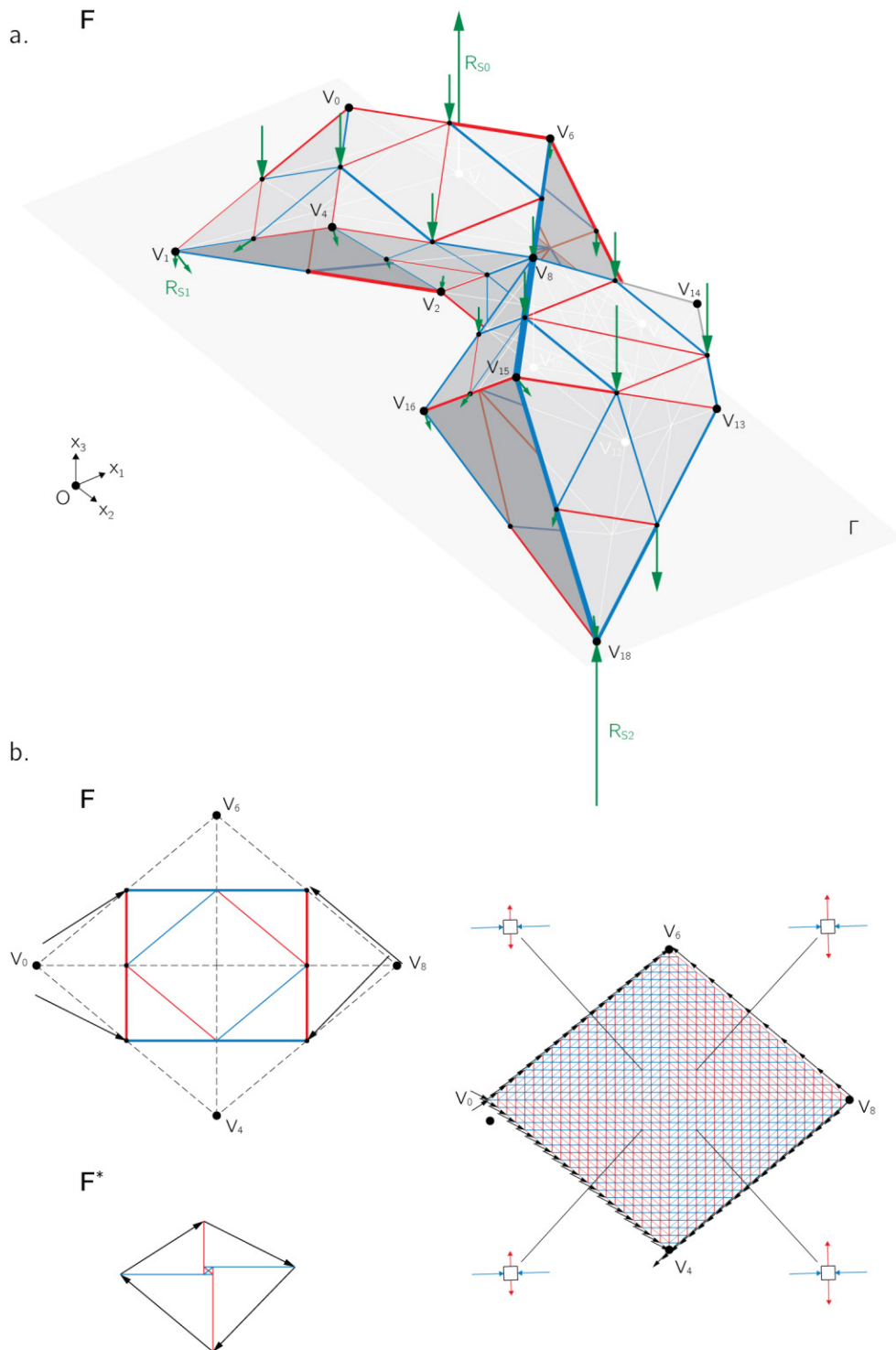
Figure 13.4: Operation M2–force manipulation. (a) Complete strut-and-tie network of the folded plate structure as a 3D form diagram **F**. (b) Discrete in-plane stress field in a polygonal plate as a combination of sub-fields with constant bi-axial stress states (§ 10.2). The assumptions are made that the plate is constituted of an ideal isotropic material with rigid-plastic behaviour and that the edges behave like stringers with infinite resistance capacity (§ 10.2.2).

Case Studies

14. Folded Plate Prototypes at Various Scales

A series of design experiments as case studies have been carried out to inform the theoretical advancement of the proposed design method for structural folding in architecture (Chapter 11). With the aim to prove the validity of the approach in real design scenarios, each of these experiments has been associated with a specific design task, with a given brief and clear boundary conditions. The primary goal of this part of the investigation was to explore the potentials offered by the proposed design method to define and materialise architectural and structural concepts that go beyond the conventional typological boundaries. Accordingly, in the creation of a series of folded plate prototypes, folding has been used as an effective way to address simultaneously multiple design objectives while finding a negotiation between load-bearing capacity and architectural idea. Grounded on a holistic view on design, these design experiments reflect an integrated approach to structural folding that is alternative to most of the current ones, which are usually based either on formal exploration or on structural optimisation.

Although the primary target of the developed method is the design of folded plate structures at the scale of architecture (Chapter 11), design experiments have been carried out also at smaller scales, thus offering the possibility to build real-size physical prototypes. In fact, the general rules and procedures defined within the design method can be applied at any scale, as long as scale-dependent factors are taken into account in the form of geometric constraints (i.e. limitations on the surface area of the folded plates, on the length of the folded edges, or on the dihedral angle between the plates) (§ 13.1). The construction of full-scale prototypes has represented a fundamental opportunity to assess the strengths and limitations of the method while gathering relevant information for its further development. The experiments have been chosen to address various contexts regarding function and use. Moreover, different materials and construction technologies have been selected for the different case studies, with the objective of testing the adaptability of the proposed design operations to various design settings.

In the definition of the case studies, the method has been applied throughout the entire design process, starting at the outset of the design development. From an operative standpoint, the design has been carried out using the digital imple-

mentation of the method in the form of the parametric toolkit (Chapter 11). Overall, three case studies have been completed (Fig. 14.1): a cantilevering table, a hanging structure, and a small building within the envelope of an existing building. In the next chapters, the most relevant aspects of the design development of the three case studies are described. In particular, after a first introduction on the specific design brief and context related to each design experiment, the implementation of the design method to each case study is explicated.

A CANTILEVERING TABLE

A HANGING STRUCTURE

A BUILDING IN A BUILDING

Figure 14.1: Series of folded plate prototypes at various scales designed using the proposed method for structural folding in architecture (Chapter 11).

15. A Cantilevering Table[1]

Over the last few years, the desire to give the Chair of Structural Design at ETH Zurich a clear and identifiable image has supported the idea of designing a series of customized pieces of furniture (Schwartz 2016b) that could evidently express the specific position of the Chair within the context of structural design. In fact, this occasion has represented an opportunity to engage with the topic of structural folding in the form of a design experiment. Thanks to its versatility as a design operation, folding has been employed for the creation of a multi-purpose meeting table, the *foldDESK*[2] with the aim to produce a piece of furniture that could also embody additional functions other than the usual ones for which a table is generally designed. Based on the inherent properties of folding (Fig. 15.1), it has been possible to establish a direct correlation between the form of the load-bearing structure and the flow of the internal forces.
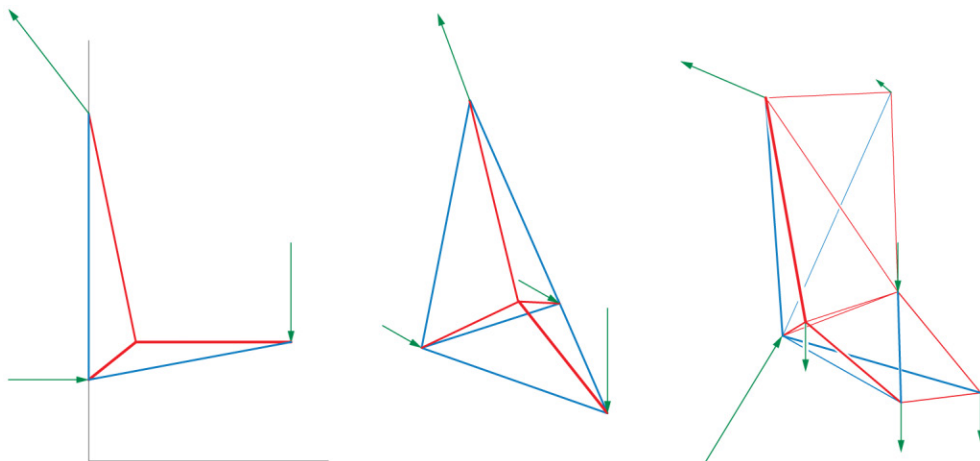
Figure 15.1: Structural concept of the foldDESK: from 2D to 3D, gaining structural integrity through folding.

---

[1]Contents of this chapter have been previously published in (Kotnik and D'Acunto 2013) and (D'Acunto 2016).

[2]The project foldDESK was developed in 2013 by the author in collaboration with Özgür Keles (ETH Zurich, Chair of Structural Design), based on a first design proposal developed in 2011 by the latter. Special thanks go to the student assistant Simon Wolfensberger for his support in the construction of the physical prototypes.

15.1   Design Development

The project *foldDESK* is the response to the request of providing the professor's office with a new meeting area for the discussions with the students. The initial design proposal (Fig. 15.3.A) was built upon the redefinition of the traditional meeting table typology. More specifically, a multi-functional table was proposed based on the combination of two diverse and generally disjointed elements, namely a tabletop and a whiteboard, into one single piece of furniture. Due to the limited amount of space in the professor's office, the idea has arisen to reduce the footprint area of the table to the minimum, thus supporting it using a sub-structure cantilevering directly from the wall.

Although innovative from a functional point of view, the design proposal was nevertheless based on a conventional load-bearing solution. This solution relied on the presence of a sub-structure made of two standard steel I-beams hidden beneath a cladding surface in the form of a steel sheet that could be used at the same time as the tabletop and the whiteboard.

While seeking the goal of making the load-bearing system of the table explicit and correlating the form to the distribution of the internal forces, in a second stage of the design process structural folding has been introduced as the guiding principle for the design development. Hence, the hidden sub-structure conceived in the initial design proposal has been subsequently eliminated, while the steel sheet defining the tabletop and the whiteboard has been converted into a folded plate structure and elevated to be the actual load-bearing system of the table. It is through this operation of synthesis and reduction to the essential that programmatic functions and structural aspects have been integrated into the very same element, thus reaching the essence of the new design idea (Fig. 15.2).

Based on the initial design proposal (Fig. 15.3.A), geometric studies were first conducted in order to define the overall topology of the table. These resulted in two opposite solutions, the first one consisting in a non-regular closed polyhedron (Fig. 15.3.B) and the second one in an open polyhedral surface (Fig. 15.3.C). If in the first case the folded plate nature of the structure was not explicitly shown and this was rather perceived as a solid volume, in the second case the structure had to rely on the bending stiffness of the folded edges to achieve its static rigidity (§ 8.2.2, § 12.2). To overcome these limitations, a third solution (Fig. 15.3.D), as a combination of the first two, has been then put forward in compliance with the proposed design method for folded plate structures (Chapter 11).

The topology of the table has been initially delineated by arranging in space an assembly of four tetrahedra (Fig. 15.4, $\mathbf{F_G}$) through operation *T1* (§ 12.1). Using operation *T2* (§ 12.2), the statically rigid folded plate structure of the table has been subsequently virtually folded within the reference grid (Fig. 15.4, $\mathbf{F_P}$). In terms of geometry, the proportions and dimensions of the table have been defined using operation *M1* (§ 13.1) after setting up three constraint planes (Fig. 15.4, $\mathbf{F_M}$). These have been introduced to take into account the boundary

Figure 15.2: The foldDESK viewed from the professor's desk (photo © Karin Gauch and Fabien Schwartz).
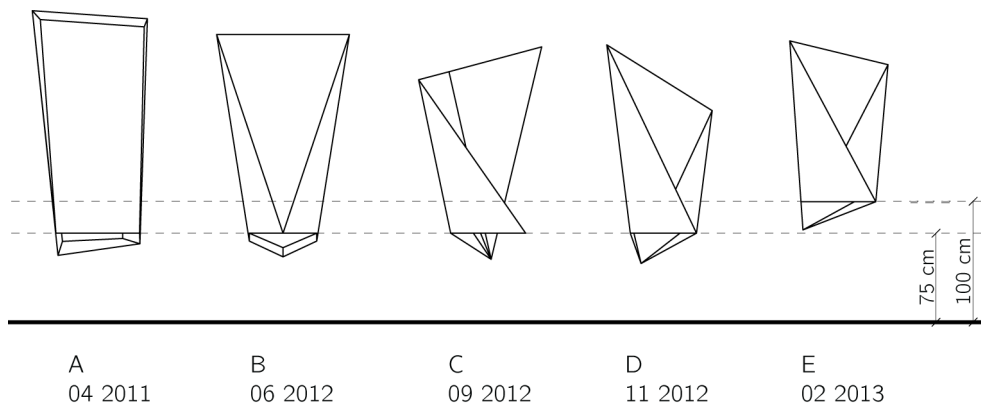
Figure 15.3: Evolution of the geometry of the foldDESK throughout the design process (front views).

constraints at the site and the functional constraints dictated by the use of the table. Hence, on the one hand, a vertical plane has been used to restrain one of the plates to lie onto the surface of the office's wall. On the other hand, a horizontal plane has been employed to define the position of the tabletop and a tilted plane to control the spatial arrangement of the plate doubling as the whiteboard. By intersecting the three planes together, the lines corresponding to the folded edges of the table could be generated at once. Being grounded on this geometrical construction, the shapes of the plates depended on a series of interrelated parameters. Hence, the modification of one parameter in the model, such as the height of the plane containing the tabletop or the angle of inclination of the whiteboard to the horizontal, had direct influence on the geometries of the plates, based on the mutual dependencies between the vertices of the folded plate structure (§ 12.2, § 13.1).

An iterative process using the operations *M1* and *M2* (§ 13.2) has been subsequently carried out while mediating between the functional and structural needs prescribed by the project. In this case, a *synthetic* strut-and-tie network (§ 8.3; § 13.2), with vertical loads applied only to the endpoints of the edges at the boundary of the tabletop, has been initially set up. Such a model has been employed to gain a qualitative understanding of the global mechanical behaviour of the structure while subjected to a typical loading on the tabletop. Hence, regarding the strut-and-tie network as a 3D form diagram, its corresponding vector-based 3D force diagram has been generated (Fig. 15.5). The latter has allowed assessing the relative magnitudes of the internal forces in the folded plate structure (§ 9.3) and adjusting them by means of appropriate local trans- formations of the force diagram (§ 9.5) while respecting the previously imposed constraint planes.
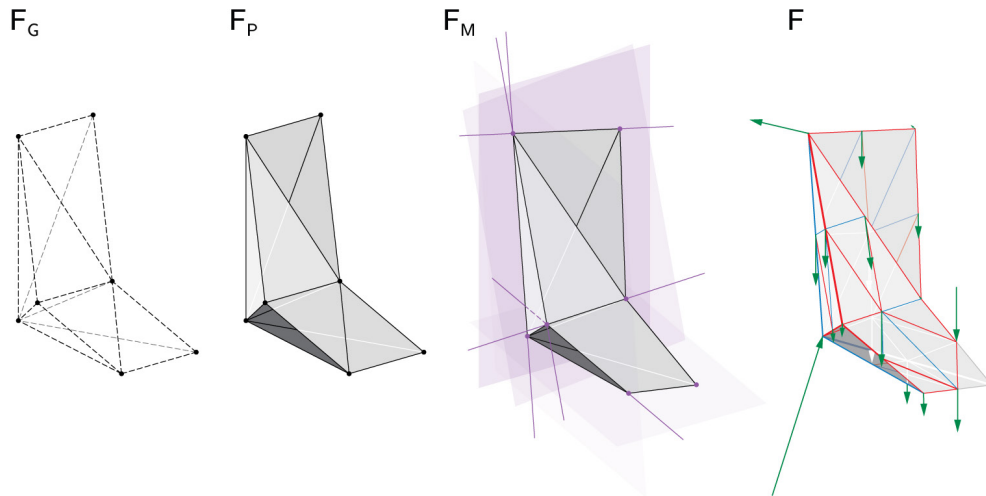
Figure 15.4: Application of the proposed design method for folded plate structure (Chapter 11) to the design of the foldDESK: definition of the reference grid F_G; creation of the folded plate structure F_P; adjustment of the geometry of the folded plate structure F_M; definition of the strut-and-tie model F.
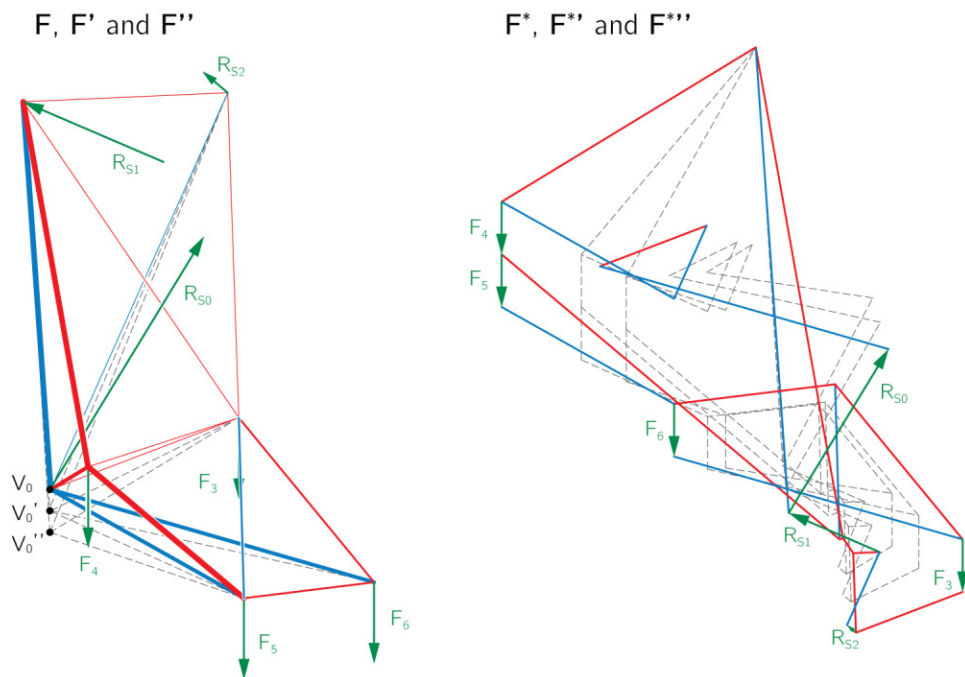

Figure 15.5: Local constraint-based transformation of the synthetic strut-and-tie network (§ 8.3; § 13.2) of the foldDESK: variations of the 3D form diagram (F, F', F'') and the corresponding 3D force diagram (F^*, $F^{*'}$, $F^{*''}$).

Since at the time of the design of the foldDESK the procedure to derive stress fields using a *complete* strut-and-tie network (§ 10.2) was not yet developed, a stress analysis has been then carried out using a conventional FEM solver (Fig. 15.6). The resulting stress field generated with this analysis is qualitatively
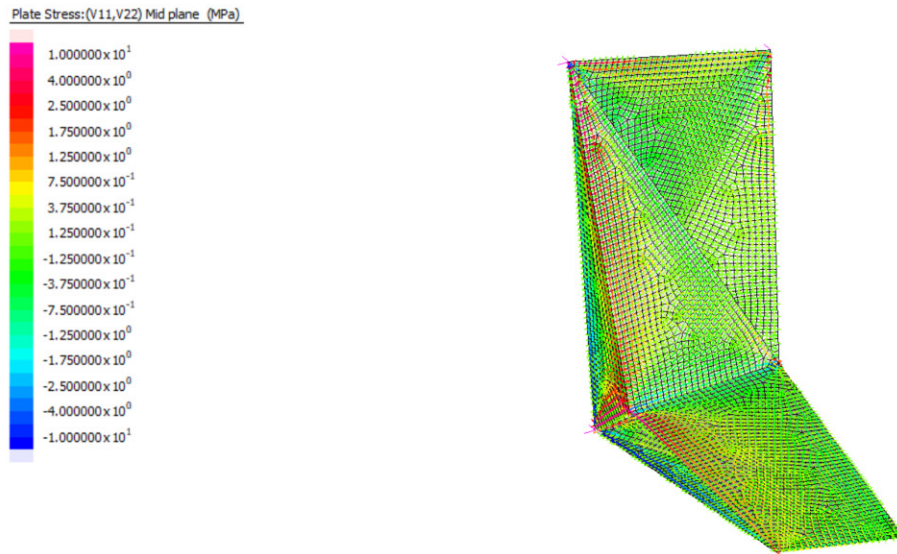
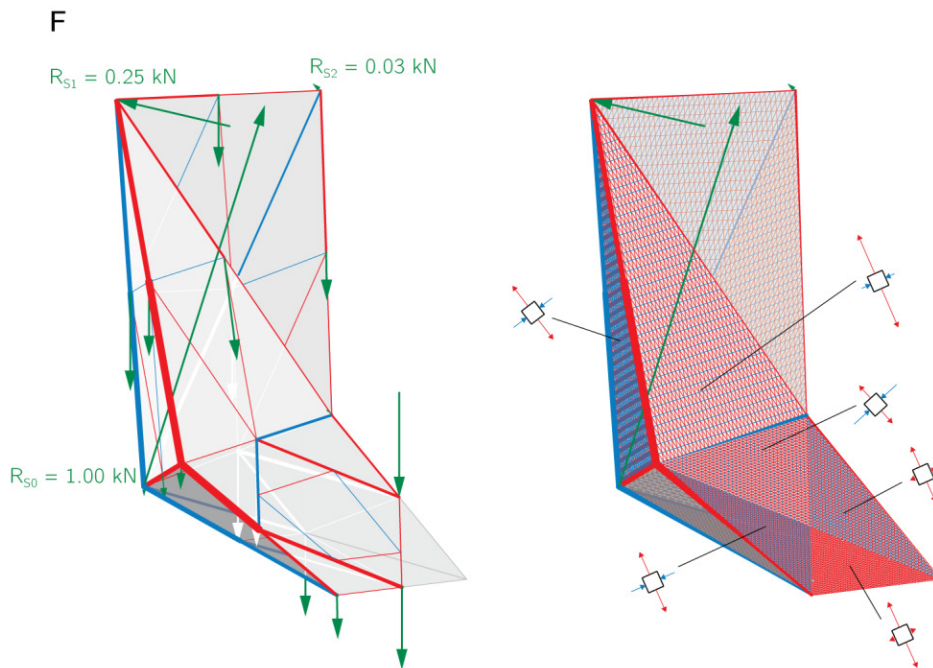Figure 15.6: Midplane principal stresses under self-weight based on FEM analysis.

Figure 15.7: Complete strut-and-tie network of the foldDESK under self-weight and visualisation of the stress field as a diffused strut-and-tie network.

comparable to the force distribution in the synthetic strut-and-tie network (Kotnik and D'Acunto 2013), leading to the dimensioning of the thickness of the steel plates at 3.0 mm. A complete strut-and-tie network, which takes into account both lattice and plate action under self-weight, is illustrated in Fig. 15.4, **F**. This network can be used to derive in-plane discrete stress fields as a combination of triangular sub-fields, each with a constant bi-axial stress state (Fig. 15.7).

Figure 15.8: 1:50 cardboard model of the foldDESK.

Figure 15.9: 1:1 cardboard model of the foldDESK mounted on site.

15.2   Manufacturing

Based on the geometry of the table resulting from the previously described design
process, physical models at various scales were produced to investigate further
the design solution (Fig. 15.8; Fig. 15.9). For the construction of the full-scale
steel prototype of the foldDESK (Fig. 15.11), a collaboration was established
with an industrial partner specialised in high-tech metal manufacturing[3].   An
unfolded layout of the folded plates (Fig. 15.10, $\mathbf{F_U}$) was generated through the
sub-operation T2-U (§ 12.2). This was then used as the cutting layout for the
manufacturing of the 3.0 mm-thick steel plates, which have been laser cut using
an automated (CNC) metal laser cutter.

Considering the variable dihedral angles between adjacent plates, two differ-
ent techniques have been employed for the connection of adjacent plates in the
final prototype. More specifically, for dihedral angles larger than 90°, the edges
between two adjacent plates have been physically bent using a high-tonnage hy-
draulic press brake with a V-die, resulting in rounded edges (Fig. 15.12, left).
For angles smaller than 90°, the connections between plates have been obtained
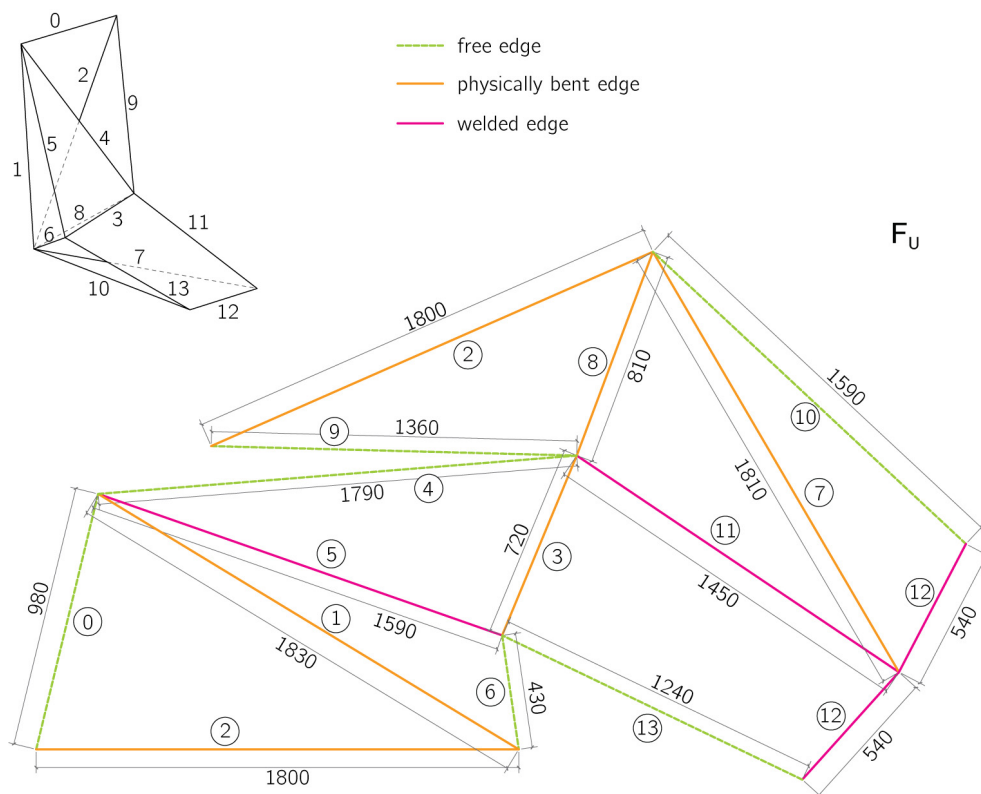through welding, thus generating sharp edges (Fig. 15.12, right).

Figure 15.10: Unfolded configuration of the foldDESK ($\mathbf{F_U}$) and classification of the edges.

---

[3]Gysi AG, Baar (Switzerland): `https://www.gysi.ch/` (Accessed 15.06.2018).

Figure 15.11: The foldDESK under construction. (Left) Overall view. (Right) Detail of the connection between the plates.
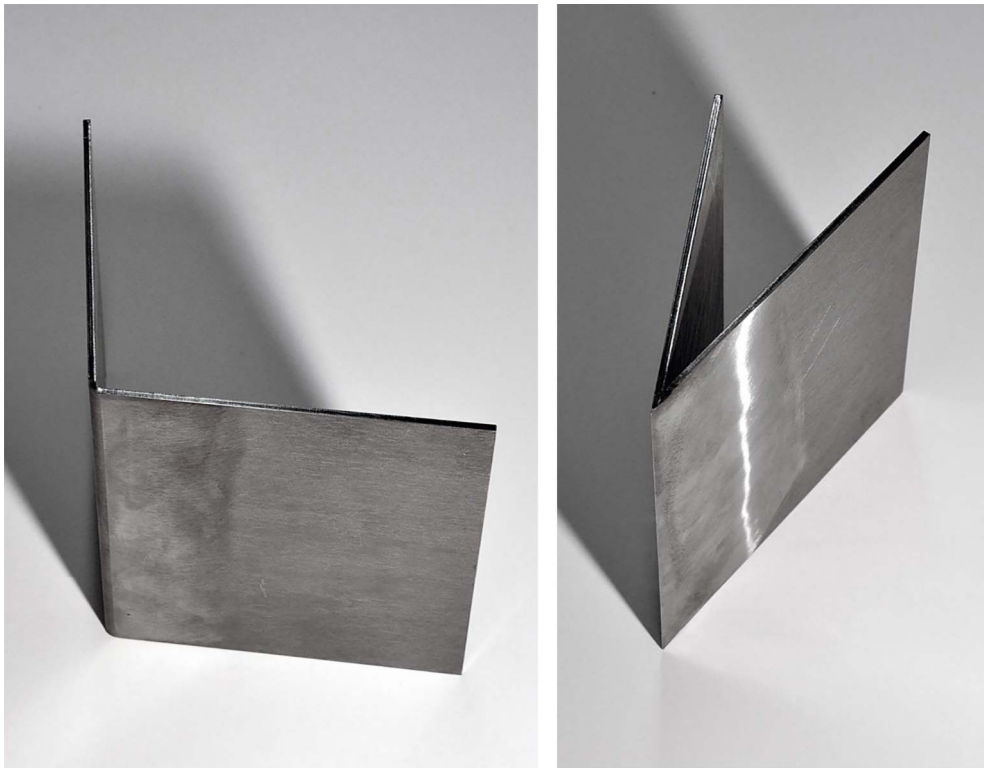

Figure 15.12: Detail samples showing the two types of edges in the foldDESK. (Left) Physically bent edge with a rounded profile. (Right) Welded edge with a sharp profile.

15.3   Continuity and Differentiation

Thanks to the use of folding, the final design of the foldDESK (Fig. 15.15) integrates functional requirements, structural necessities and the research for creative expression into one object. Indeed, the table is a neat and elegant form that fills the available space at the site consistently, while at the same time becoming a new focal point within the office (Fig. 15.13).

Despite the simplicity of its form, the table manifests a high level of complexity. Being a three-dimensional object generated through a continuous and differentiated folded plate geometry, the table has to be observed from diverse points of view in order to experience completely its presence. Due to its variable openness, the folded plate structure of the table is perceived either as a semi-enclosed volume (Fig. 15.14) or as a semi-open surface (Fig. 15.2) according to the position of the observer. Such a dichotomy is emphasised by the position of the table within the office, as it directly faces the two possible ways to access the room (Fig. 15.15.b) respectively with its front and its side elevations (Fig. 15.15.a). This position enforces the foldDESK to be initially seen from either one or the other of these two sides and encourages the observer to walk around it to comprehend entirely its three-dimensionality.

From a visual point of view, the foldDESK naturally establishes an active dialogue between solid and void. The nature of this porous structure is highlighted by the play of lights and shadows on the surface of the folded plates. It is especially because of this effect that the table appears to levitate above the ground, regardless of its mass of 98.0 kg. Moreover, as in the case of the Chapel in Valleacerón by Sancho and Madridejos (§ 5.2.1), each side of the table reacts in a completely different way to the lighting conditions. This is particularly strengthened by the two diverse treatments of the folded edges (§ 15.2), some of them creating a clear contrast between light and shadow and other ones producing a soft transition. Yet, as in the case of the architectural pieces of Sancho and Madridejos, through the unifying action of the fold, the different parts of the foldDESK are still connected visually into one single geometry thus generating differentiation through continuity (§ 5.1). Such visual qualities have been especially tested using the cardboard models (Fig. 15.8; Fig. 15.9). These have been built at different scales up to the full-scale size in order to thoroughly investigate the appearance of each side of the table in relation to the mutable lighting conditions at the site.

With regard to the structure, as highlighted in the case of the work of Musmeci (§ 4.2), it is through the statics that the expressiveness of the form of the table is declared. As such, the load-bearing behaviour of the foldDESK is directly exposed to the observer who can immediately read the flow of the internal forces in its geometry. In this way, the table constitutes a clear materialisation of the principle of resistance through form by structural folding (§ 4.1).

Figure 15.13: The foldDESK in use (photo © Karin Gauch and Fabien Schwartz)

Figure 15.14: The foldDESK in use (photo © Lukas Schaffhuser)

a.

Lateral View   Front View

b.

Lateral View   Front View
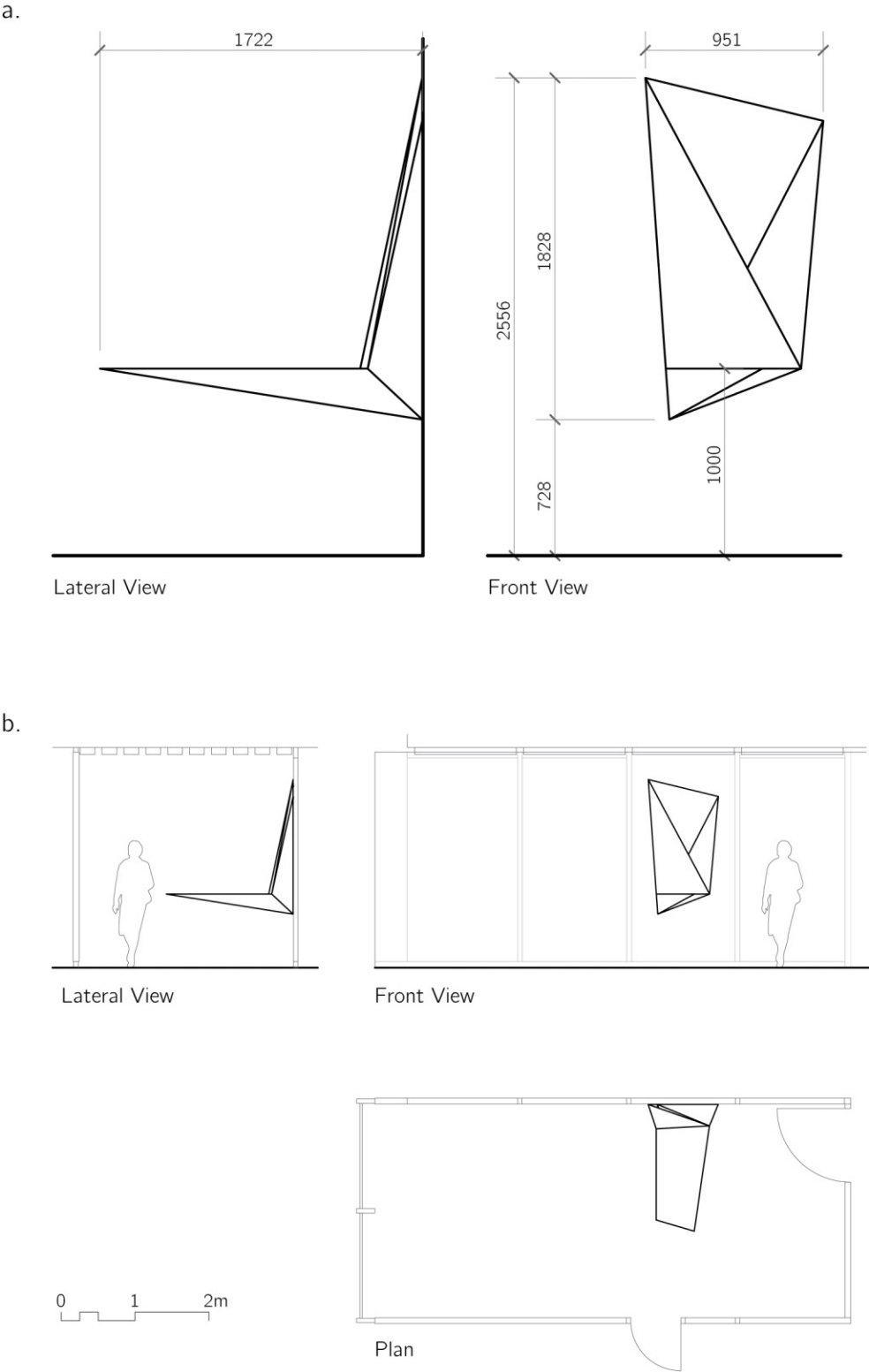
0   1   2m

Plan

Figure 15.15: Final design solution of the foldDESK. (a) Lateral and front views of the table and overall dimensions. (b) Lateral, front and plan views of the table on site.

16. A Hanging Structure[1]

Being developed as an entry for the International Association for Shell and Spatial Structures (IASS) Expo 2015 out of a collaboration between ETH Zurich and Arup Amsterdam, the project *foldKITE* aimed to explore the potentials of folded plate structures in the field of ultra-lightweight design[2].

Given the lack of bounding functional requirements, the project *foldKITE* represented a good occasion to test the limits of the proposed design method for folded plate structures (Chapter 11) in terms of complexity of the geometric and structural solutions. Yet, as an entry for the IASS Expo 2015, the foldKITE had to comply with the regulation introduced by the organisers of the exhibition. These required the constituent parts of the structure to be prefabricated off-site and transported to the site, the *Muziekgebouw* at Amsterdam, using no more than six containers, each with maximum dimensions of 1.00 m x 0.75 m x 0.65 m and a mass lower than 32.0 kg. Moreover, once built, the structure had to fit into an assigned virtual bounding box of maximum dimensions of 8.00 m x 4.00 m x 4.00 m and be able to be suspended from the ceiling of the Muziekgebouw using no more than three cables. Given these guidelines, a design concept has been put forward to challenge the aforementioned rules with the introduction of even more radical restraints. With the intention of reducing the mass of the system to the minimum, the number of boxes allowed for the transportation of the parts to the site has been decreased from six to one. In addition, to maximise the overhang of the structure, the three suspension cables have been allowed being connected to the structure at the vertices of one plate only.

During the conceptual stage of the design process, the global geometry of the foldKITE has been generated using the proposed design method (Chapter 11). Based on this geometry, in a second phase, detailed solutions have been developed for the individual plates that constituted the folded plate structure. The design has been eventually materialised into a full-scale prototype.

---

[1]Contents of this chapter have been previously published in (D'Acunto et al. 2015).

[2]The design experiment here presented has been conceived and developed between December 2014 and May 2015 by the author in collaboration with Juan José Castellón González (ETH Zurich, Chair of Structural Design), Alessandro Tellini (ETH Zurich, Raplab) and Shibo Ren (Arup Amsterdam). Special thanks go to the student assistants Jonas Hodel and Leo Kleine for their support during the manufacturing process.
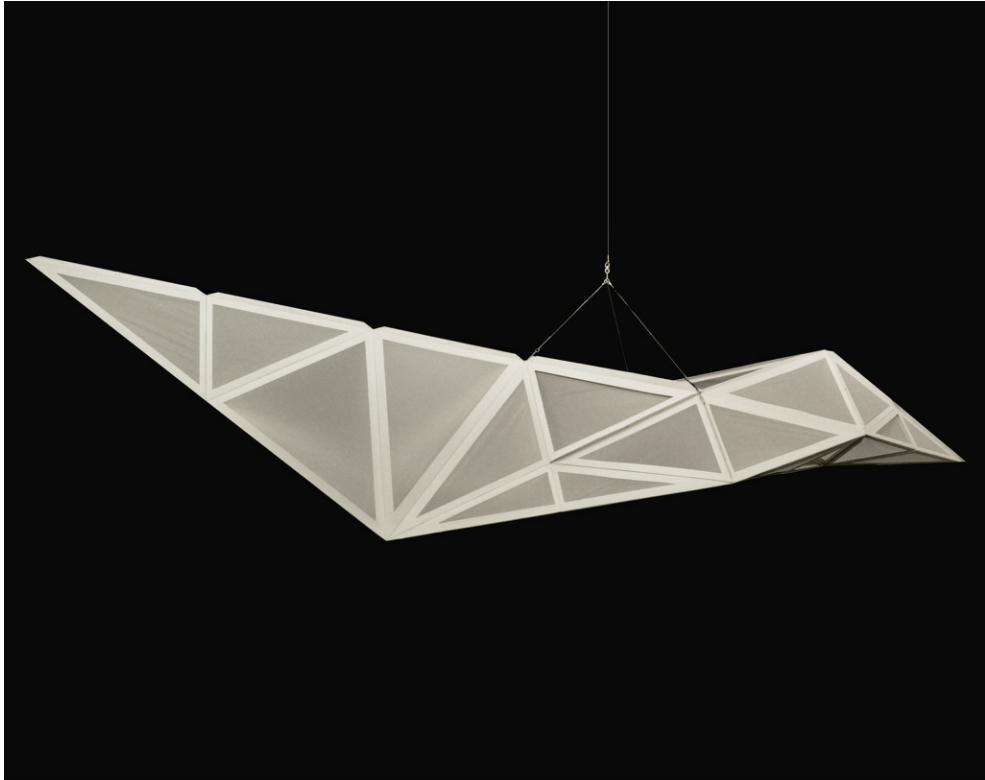
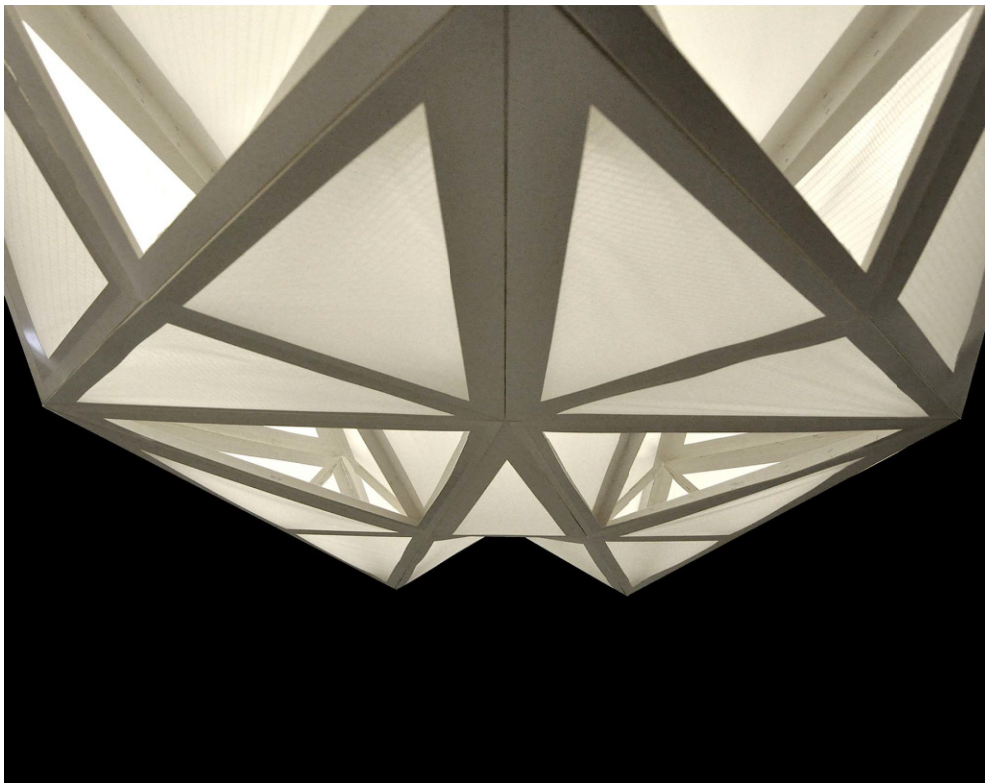Figure 16.1: Overall view of the hanging structure foldKITE.

Figure 16.2: Close-up view of the hanging structure foldKITE.

16.1   Generation of the Global Geometry

The global geometry of the foldKITE has been designed throughout a process involving three main design iterations. At each iteration, the geometry of the folded plate structure has been gradually refined, to address specific structural, manufacturing, and transportation constraints.

In the first design iteration, through operation *T1* (§ 12.1) a grid made of 11 tetrahedra has been generated as a spatial reference for the subsequent design steps (Fig. 16.3, **F**$_\mathrm{G}$). With operation *T2* (§ 12.2), the topology of the folded plate structure has been then delineated (Fig. 16.3, **F**$_\mathrm{P}$). Hence, properties such as the organisation of the space enclosed by the folded plates and the amount and location of openings have been here defined. Various design solutions have been investigated in order to introduce spatial differentiation in the folded geometry while keeping the continuity of the form. Moreover, specific rules of incidence (§ 12.2) related to the alignment of certain vertices of the folded plate structure have been defined and used as underlying constraints in the subsequent transformations of the geometry.

Through the repeated application of operations *M1* (§ 13.1) and *M2* (§ 13.2), the position of the individual vertices of the reference grid, and thus of the folded plate structure, has been adjusted in space until the desired design intentions and the necessary structural requirements have been fulfilled, in compliance with the above rules of incidence among the vertices (Fig. 16.3, **F**$_\mathrm{M}$ and **F**). In particular, a *synthetic* strut-and-tie model (§ 8.3; § 13.2), with the internal forces transferred exclusively along the folded edges, has been used to obtain a qualitative insight on the mechanical behaviour of the structure. Being the foldKITE meant to be suspended indoor, its self-weight has been the only loading taken into consideration. For each plate, a weight proportional to its surface area has been regarded as redistributed to the corresponding vertices by local bending action. Three supports, related to the suspension cables, have been placed at the vertices of one of the middle plates of the folded plate geometry. Based on this set-up the internal forces have been evaluated with operation *M2* and the folded plate structure transformed to improve its structural behaviour. Hence, through operation *M1* the static height of the structure has been increased at the supports to reduce the magnitudes of the internal forces. To avoid local instability due to buckling, the length of the free edges under compression has been reduced. With the same aim, the dihedral angles between the plates have been adjusted in relation to the magnitude of the forces in the folded edges. In a subsequent step, the reference grid has been subdivided into 20 tetrahedra using the sub-operation *T1-S* to increase the number of folded plates at the back of the structure. Thanks to this topological transformation, the centre of mass of the structure has been shifted toward the back, and the internal forces have been spread evenly (Fig. 16.4, **F**).
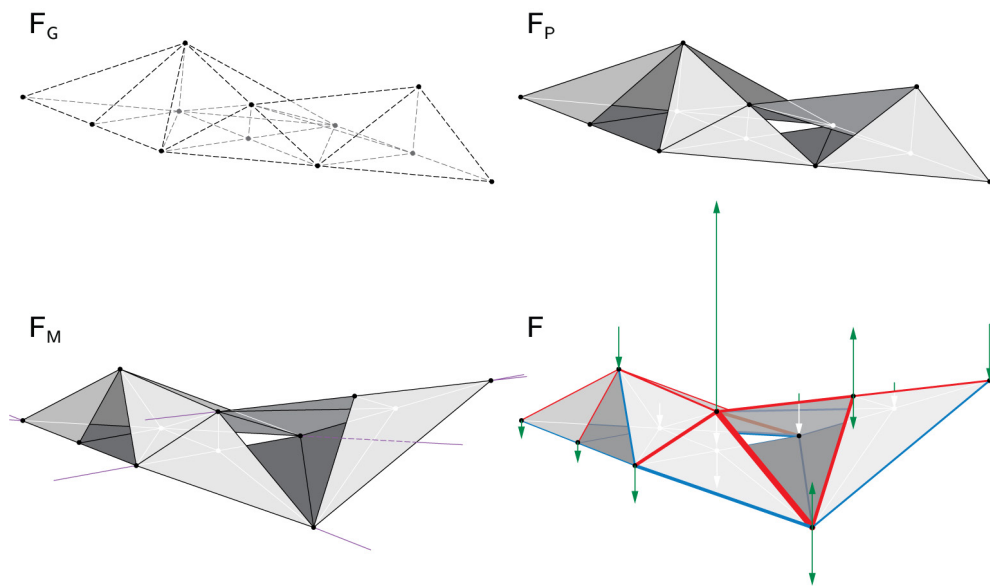
F_G

F_P

F_M

F

Figure 16.3: Application of the proposed design method for folded plate structure (Chapter 11) to the generation of the global geometry of the foldKITE: definition of the reference grid F_G; creation of the folded plate structure F_P; adjustment of the geometry of the folded plate structure F_M; definition of the strut-and-tie model F.
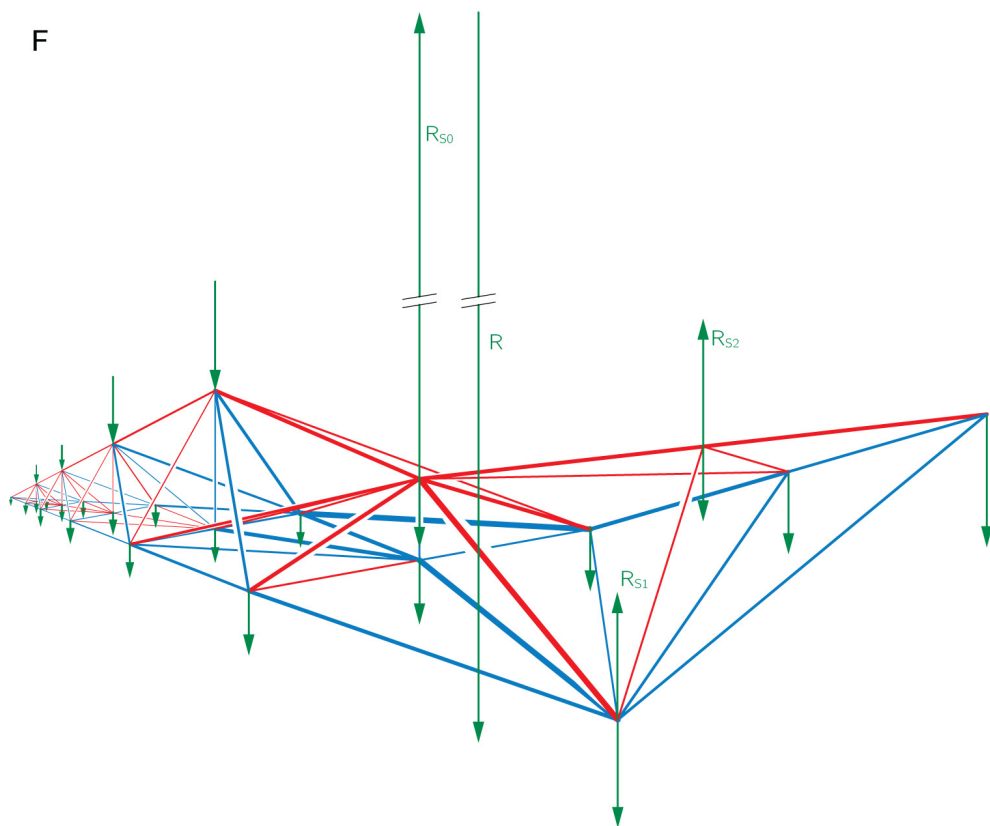
F

R_{S0}

R

R_{S2}

R_{S1}

Figure 16.4: Synthetic strut-and-tie network of the foldKITE under self-weight.

a.   b.   c.

number of plates: 49   number of plates: 85   number of plates: 65

number of edges: 80   number of edges: 129   number of edges: 100

dimensions: dimensions: dimensions:
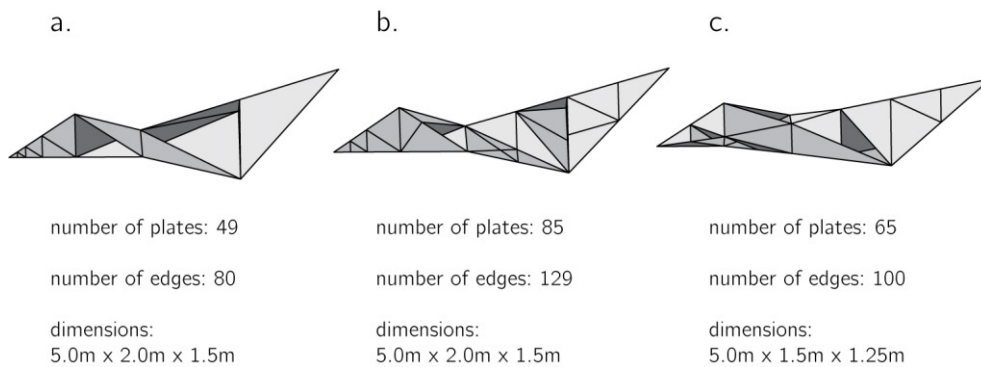5.0m x 2.0m x 1.5m   5.0m x 2.0m x 1.5m   5.0m x 1.5m x 1.25m

Figure 16.5: Evolution of the design solution. (a) First design iteration. (b) Second design iteration. (c) Final design solution.

The first proposal for the global geometry of the foldKITE resulted in an asymmetric structure of 5.00 m x 2.00 m x 1.50 m in size and composed of 49 triangular plates of various dimensions (Fig. 16.5.a). In order for this solution to comply with the aforementioned constraint according to which the entire structure had to fit within a container of 1.00 m x 0.75 m x 0.65 m, most of the plates would have had to be necessarily split into sub-parts. Due to the disadvantages of this procedure, especially in terms of reduced static rigidity (§ 8.2.2) for the presence of extra inner hinges within the plates, an alternative design solution has been searched for to keep the individual plates as single parts.

Hence, a second iteration of the design process was run, this time introducing the dimensions of the container as an extra metric constraint (§ 13.2) in the first place. With operation *T1*, the initial tetrahedral grid composed of 20 tetrahedra has been re-subdivided into 40 tetrahedra. While keeping a global geometrical configuration similar to the one of the previous design proposal, with operation *M1* the vertices of the reference grid have been adjusted through a constraint-based local transformation in order for the size of each plate to fit within the given container's dimensions. A second design proposal with 85 triangular plates was generated in this design iteration (Fig. 16.5.b). Although this solution avoided the plates to be split into smaller parts, this new proposal relied on a relatively high number of plates to be manufactured and later assembled.

A new global geometry of the foldKITE was finally developed in a third iteration of the design process, which combined the advantages of both first and second proposals. In particular, using the latter as a starting point, a longitudinal vertical plane of symmetry has been introduced to reduce the total amount of bespoke plates. This overall simplification of the system has been applied without compromising the sculptural quality of the design solution. The final proposal resulted in a geometry composed of 65 triangular plates and 100 edges, with global dimensions of 5.00 m x 1.50 m x 1.25 m (Fig. 16.5.c).

16.2   Detailed Design and Materialization

Based on the final proposal for the global geometry of the foldKITE (Fig. 16.5.c), a detailed design has been initiated for the engineering of the plates constituting the folded plate structure. This phase has been carried out using digital and physical models. In this second phase of detail design, explicit questions related to materials and construction technologies have been addressed. Given the initial intention of designing the foldKITE as an ultra-lightweight structure, thorough research on lightweight materials has been conducted. Indeed, an important reference in this phase has been found in the sport kite sector; the necessity to produce flying objects able to resist severe wind conditions has pushed this sector to develop high-strength materials that are, at the same time, ultra-lightweight. Because of its mechanical properties and its ethereal and translucent materiality that fitted particularly well with the design concept, the hydrophobic kite fabric *Icarex* (PC-31)[3] has been selected as the main material for the production of the plates of the foldKITE.

In compliance with the synthetic strut-and-tie model (§ 16.1), a strategy has been put forward to reinforce the kite fabric along the edges of the folded plate structure with frames, whose dimensions have been made proportional to the length of the edges and to the intensity of the internal forces. A first solution has been explored using fibreglass strips. The strips could be directly laminated onto one side of the PC-31 fabric using two-component epoxy resin. A physical prototype of a generic plate has been then developed as a test (Fig. 16.6). Although the prototype showed an adequate degree of lightness and structural stability, due to manufacturing limitations such as the impracticability to handle the epoxy resin safely and to cut the fibreglass strips easily with the available machinery, other solutions have been looked for. After testing various alternatives, frames made of 1.0 mm-thick solid bleached board (SBB) with an area density of 600 g/m^2 have been eventually chosen to replace the fibreglass strips as the reinforcement of the edges of the triangular plates. Contrary to the fibreglass strips, the SBB could be easily glued to the PC-31 fabric using common multi-purpose solvent-based spray adhesive. While satisfactory in relation to the structural requirements, the employment of SBB also gave the possibility of using a digital cutter to produce the individual frames.

In order to join the triangular plates to generate the folded plate structure, a solution based on a flap-to-flap connection has been developed by adding folded flaps along the edges of the plates, thus creating actual hinge connections. Other than providing an adequate way for the joining of the plates, the introduction of the folded flaps improved the local structural stability of the edges against their self-weight, while reducing their risk to buckle under high compressive normal forces. Special attention has been paid to the fabrication of the flaps. To keep

---

[3]The *Icarex Ripstop Polyester* (PC-31) fabric is a polycarbonate film reinforced with polyester strands with an area density of 31 g/m^2.
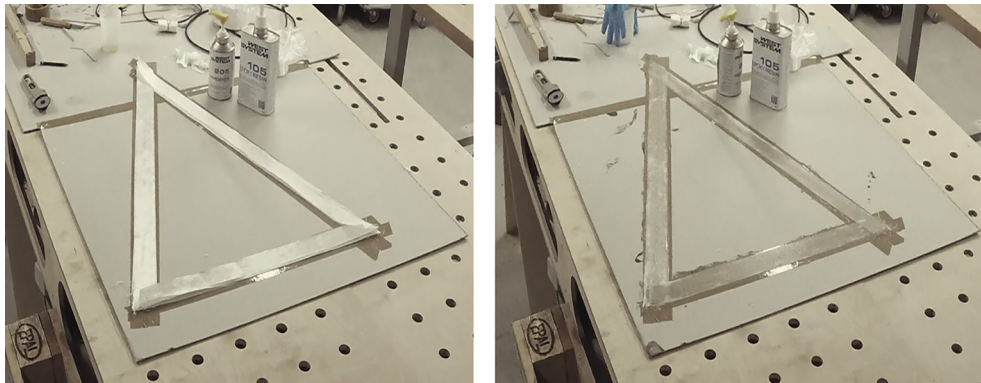
Figure 16.6: Manufacturing of a plate using the lamination technique. (Left) Arrangement of the fibreglass strips along the edges of the plate. (Right) Application of the two-component epoxy resin.
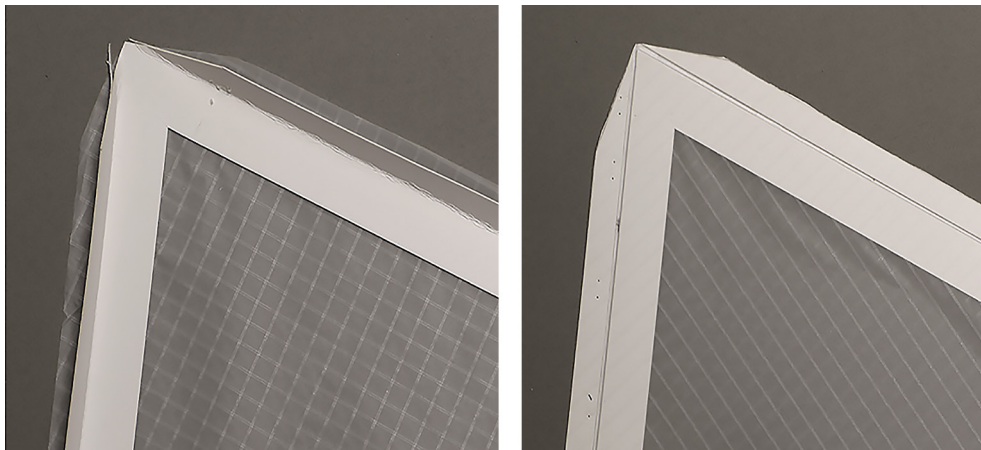

Figure 16.7: Detail design of the plates. (Left) Connection of the flaps through binding. (Right) Connection of the flaps by scoring.

the manufacturing process simple, a first design alternative has been evaluated where the flaps were cut at once with the frames, and the SBB was scored on one side along the edges to generate the required hinge (Fig. 16.7, left). However, this solution had to be rejected soon after experiencing severe problems of delamination of the SBB along the scored lines, in those tests where the flaps were loaded with local shear forces perpendicular to the axis of the scored lines.

A definitive solution has been found by looking at the bookbinding industry and precisely at the hardcover binding technique that allowed a robust yet neat connection system to be deployed. In this way, unlike the previous alternative, the flaps have been first cut as independent elements from the frames and subsequently connected to them along their edges using $160 \, \text{g/m}^2$ white paper strips with poly-vinyl acetate (PVA) glue on one side and kite fabric with spray adhesive on the other side (Fig. 16.7, right).

16.3   Construction

As imposed by the rules of the organisers of the IASS Expo 2015, the fabrication of the plates of foldKITE has been carried out entirely off-site, taking advantage of the use of the digital manufacturing machines of the Rapid Prototyping Architectural Laboratory (Raplab) at ETH Zurich. The plates have been consequently arranged into one single container of prescribed dimensions and shipped to the Muziekgebouw at Amsterdam, where the final assembly and the rigging of the full-scale structure have taken place.

The manufacturing process of the plates has been organised in four main steps: generation of the cutting drawings of the plates based on the global geometry of the foldKITE; cutting of the SBB frames and flaps using a digital cutter; mounting of the frame onto the PC-31 kite fabric; joining of the flaps to the frames. At first, the cutting layouts of the 65 triangular frames have been produced (Fig. 16.8) after unfolding the geometry of the folded plate structure using the sub-operation *T2-U* (§ 12.2). Each flap attached to each frame has been then labelled with a univocal code specifying the number of its corresponding edges in the global geometry, along with the numbers of the plates directly connected to it. This operation has been developed based on the underlying topological data-structure embedded in the graphs **G** (§ 12.1) and **P** (§ 12.2) related to the previously defined reference grid and folded plate structure respectively (§ 16.1). Using a digital cutter, the SBB frames and flaps have been then cut out of the SBB according to the cutting layouts (Fig. 16.9, top left), and automatically marked based on the previously defined codes.

Before mounting the SBB frames onto the PC-31 fabric using the multipurpose solvent-based spray adhesive, the fabric has been first laid out onto a vacuum table (Fig. 16.9, bottom left). Apart from facilitating the gluing operation, this operation also allowed the fabric to be perfectly stretched to avoid the presence of undesirable wrinkles. Furthermore, because of this procedure, after the frames have been connected to the fabric, a minimum level of pre-stressing has been introduced into the plates, with the intention of generating a structural system working similarly to a stressed skin.

The flaps have been eventually connected to the frames following the previously described hardcover binding technique (Fig. 16.9, top right). In this phase, special attention has been paid in keeping an adequate distance between the flaps and the frames, for these connections to work effectively as hinges (Fig. 16.9, bottom right). Moreover, the water content of the PVA glue has been constantly monitored to avoid unsought effects of soaking in the SBB.

Overall, for the manufacturing process $14.42\,m^2$ of PC-31 fabric have been employed along with $9.40\,m^2$ of SBB. The total mass of the foldKITE has then resulted in $7.15\,kg$, well below the maximum allowable mass prescribed by the regulation of the exhibition.
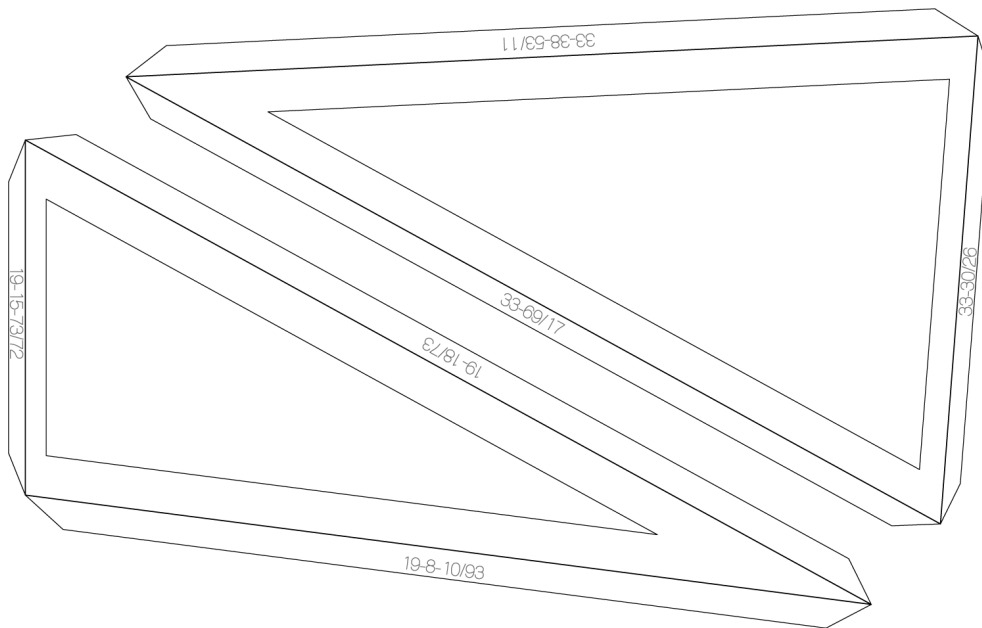
Figure 16.8: Cutting layout of two frames with flaps and identifying codes.
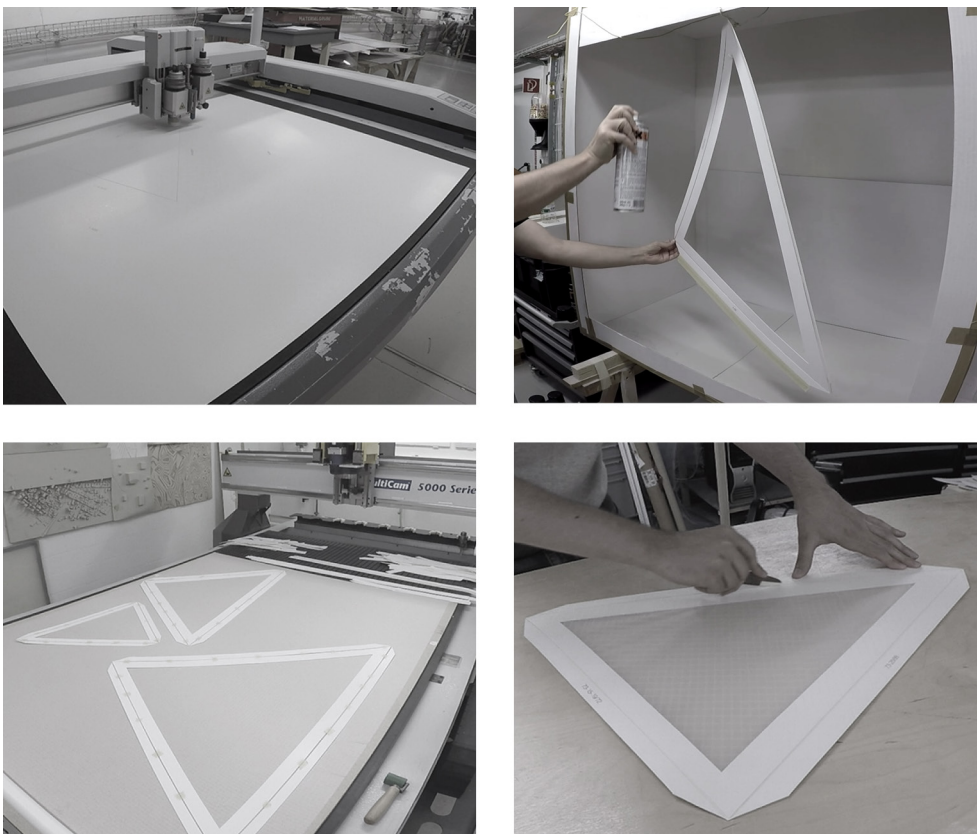

Figure 16.9: Manufacturing process of a plate. (Top left) Cutting of the SBB frames. (Bottom left) Mounting of the SBB frames onto the PC-31 fabric. (Top right) Connection of the flaps to the frames. (Bottom right) Creation of the hinges between the flaps and the frame.

16.4   Final Assembly

The final assembly of the full-scale folded plate structure has been carried out entirely on site near the Muziekgebouw at Amsterdam (Fig. 16.10). After sorting and grouping the plates based on their mutual topological connectivity, the assembly process has been accomplished by joining the adjacent plates through the previously described flap-to-flap connections (§ 16.2). Thanks to the versatility of this connection system, the assembly of the plates has been manually executed, using only ordinary hand tools. Cyanoacrylate (CA) fast-acting adhesive has been used to pair the corresponding flaps of adjacent plates together; for safety reasons, 6.0 mm and 8.0 mm-wide metal staples have also been added to prevent possible unexpected creep over time along the glued connections.

Due to the high complexity of the geometry, a precise assembly sequence has been followed with the aim of keeping the construction process easily manageable. This sequence had been generated beforehand as the result of a series of extensive assembly tests carried out on 1:10, 1:2 and 1:1 prototypes of the foldKITE to guarantee that all the parts of the structure that had to be connected to each other could be easily accessible by the operators. In fact, a strategy has been developed to erect the structure based on four main sub-clusters (Fig. 16.11). In particular, the possibility to assemble at first each sub-cluster in its unfolded two-dimensional configuration and to fold it afterwards in three dimensions has allowed for the complexity of the system to be broken down. That is, given the list of the plates belonging to each sub-cluster and the sequence how to connect these plates to each other, the three-dimensional geometry of the folded plate structure has been unambiguously determined, thus completely avoiding the need for measuring the dihedral angles between the plates.

After the entire folded plate structure has been completely built, the rigging construction necessary for hanging the structure has been produced. Eventually, the foldKITE has been suspended from the ceiling using one cable only, which had to be inevitably aligned to the resultant of the self-weight and thus to the centre of mass of the system in order to fulfil the global equilibrium (§ 9.2). In particular, a steel wire rope with a diameter of 4.0 mm in conjunction with a cable gripper has been used for this purpose. Moreover, a swivel has been inserted to permit the free rotation of the structure around the suspension cable. To allow for an even distribution of the tensile stresses from the cable to the structure, three secondary wire ropes with a diameter of 2.0 mm have been employed to join the main suspension cable to the vertices of one of the folded plates. The entire assembly process has been completed in around 9 working hours by 3 people. Despite its dimensions of 5.00 m x 1.50 m x 1.25 m, thanks to its extremely low mass of 7.15 kg, the foldKITE has been easily transported from the assembly area to the Muziekgebouw and eventually suspended from the ceiling at 4.0 m from the ground.

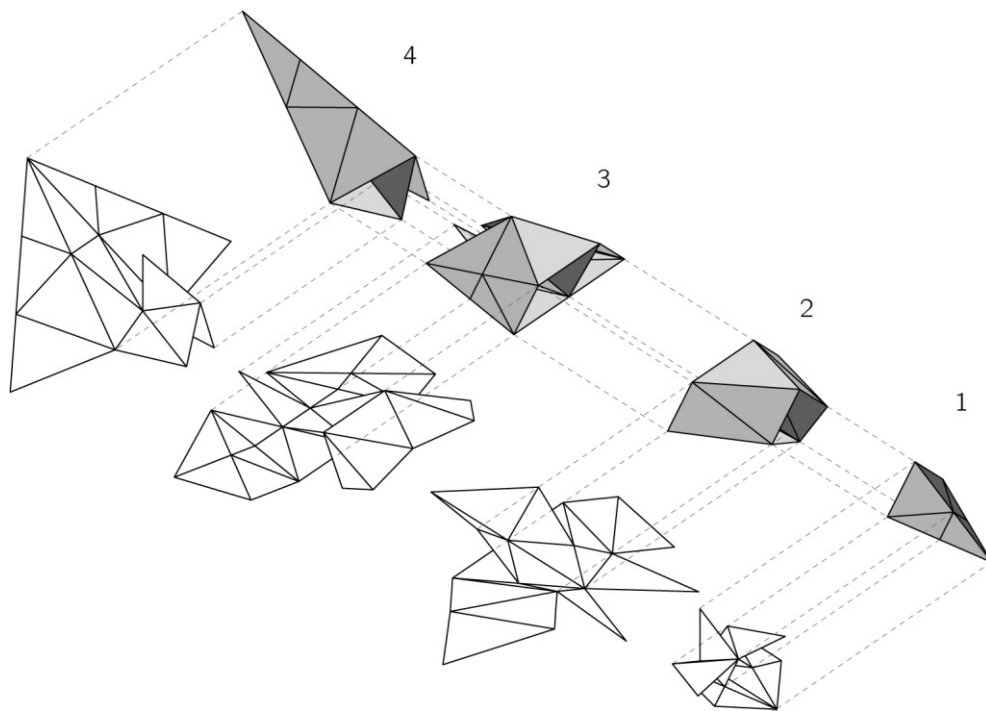Figure 16.10: On-site assembly process of the foldKITE.

Figure 16.11: Assembly logic showing the four clusters.

The foldKITE is the result of a process of negotiation between design intentions, structural, manufacturing, and transportation constraints. The three-dimensional geometry of the foldKITE is rather complex but still clearly intelligible. While folding itself from the outside to the inside, the folded plate geometry generates a porous space that is continuously variable. It is thanks to its ethereal materiality and its lightweight construction that the foldKITE is perceived as floating in the air (Fig. 16.12, Fig. 16.13, Fig. 16.14).

With regard to its load-bearing behaviour, the structure has been designed using a synthetic strut-and-tie model (§ 16.1), where the main internal forces are transferred via the folded edges. Although less precise than a complete strut-and-tie model (§ 8.3) this synthetic model has allowed to easily test different design variations during the early design phase. From a construction standpoint, owing to the flap-to-flap hinge connection between the folded plates (Fig. 16.15), the necessity to build customised three-dimensional nodes has been completely avoided. In turn, this has allowed employing a simple manufacturing process. Moreover, the possibility to assemble the foldKITE starting from two-dimensional sub-cluster has facilitated its installation on site. As a result, while pushing the boundaries of folded-plate structures into the field of ultra-lightweight constructions, the project has epitomised how structural folding can be effectively employed to achieve structural integrity and spatial differentiation within a coherent formal system.

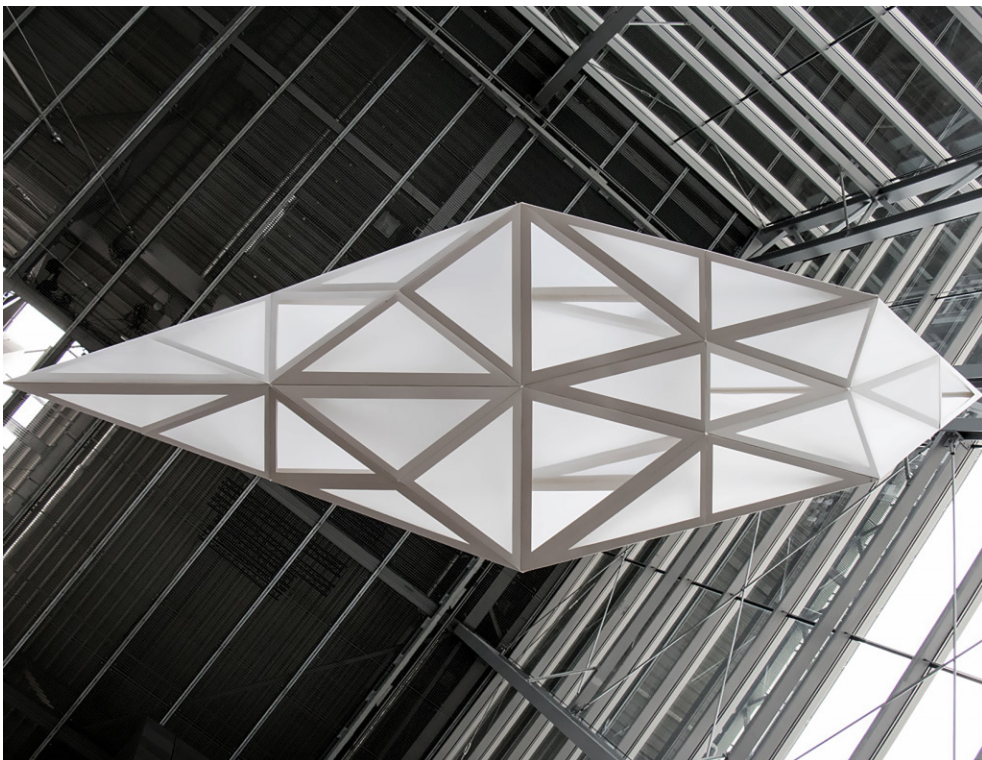Figure 16.12: Global view of the foldKITE in the Muziekgebouw (Amsterdam).

Figure 16.13: The foldKITE in the Muziekgebouw (Amsterdam) seen from underneath.

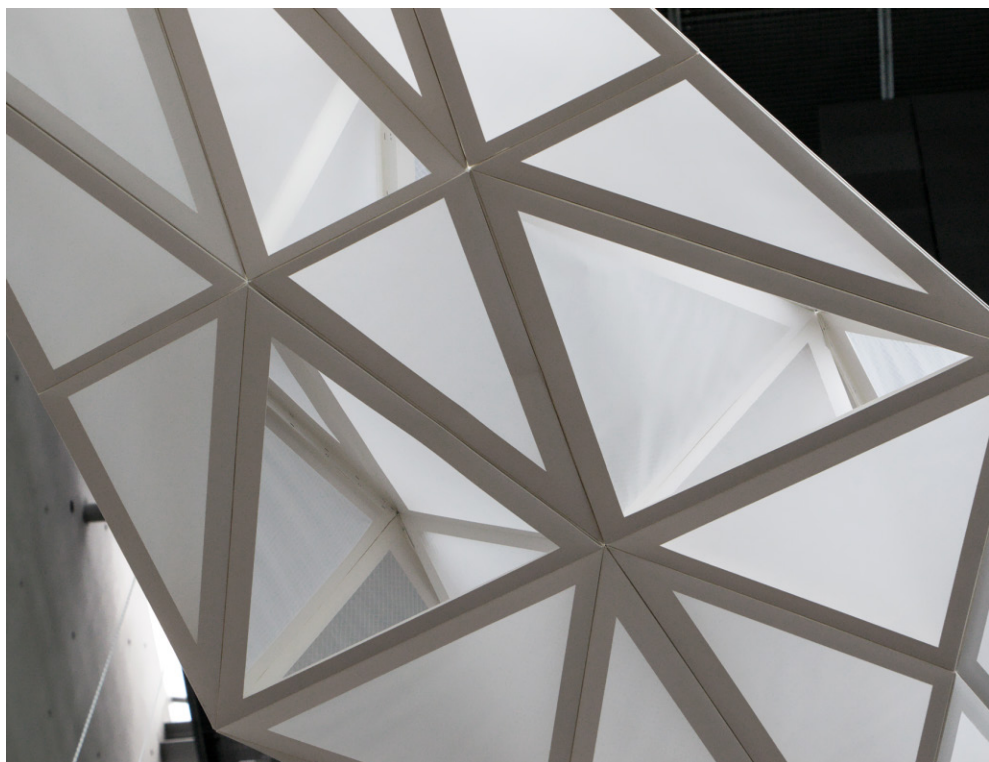Figure 16.14: Lateral view of the foldKITE in the Muziekgebouw (Amsterdam).

Figure 16.15: Close-up view of the foldKITE in the Muziekgebouw (Amsterdam).

17. A Building in a Building

This chapter presents an exemplary application of the proposed design method at the architectural scale (Chapter 11). The aim is to show how the method could be possibly used for the preliminary design of a building where space and structure are seamlessly integrated, thus giving rise to a so-called *strong structure* (Schnetzer et al. 2012; Chapter 1). In order to illustrate the proposed approach, a fictitious design brief has been taken into consideration to tackle a series of architectural and engineering questions within the conceptual stage of the design process. The design brief has been derived from a design exercise suggested within the elective course *Experimental Exploration on Space and Structure* at ETH Zurich[1], in which architecture students were asked to develop a simple architectural design using the proposed method for structural folding in architecture.

In particular, the site for this proposed design experiment has been chosen in the town of Schlieren, in the western outskirts of Zurich, an area that used to host a strategical industrial hub during the late 19th and early 20th centuries. Over the last few years, many of the industrial facilities located at Schlieren have been abandoned, and the entire site is nowadays undergoing a process of urban reconversion. The strategy of the town of Schlieren for this site is to preserve all the historical industrial constructions, while allowing for new public venues, mostly related to cultural and leisure activities, to be integrated therein.

Given this context, a fictitious task has been set to design a compact building in reinforced concrete with a maximum volume of 2000 m^3 housing a public art gallery. In order to create a dialogue with the built environment and to give new use to the existing facilities, the new building had to be placed within the envelope of one of the former industrial storehouses of Schlieren (Fig. 17.1). In the design experiment, only a portion of the storehouse has been taken into consideration and regarded as the plot for the new building (Fig. 17.2). The plot is accessible from the main entrance on the East facade of the storehouse and a secondary entrance along the North facade.

---

[1]The course *EEoSS*, from which the design brief is derived, has been taught by the author together with Juan José Castellón González, Prof. Dr. Joseph Schwartz (ETH Zurich, Chair of Structural Design), and Alessandro Tellini (ETH Zurich, Raplab) during the Winter Semester 2015.
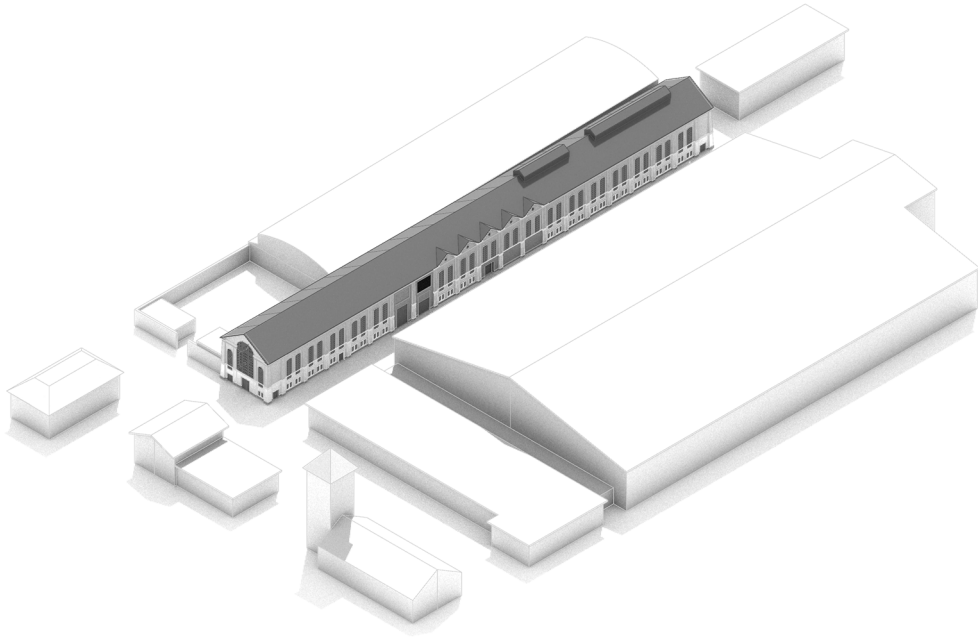
Figure 17.1: Axonometric view of the former industrial storehouse, located in Schlieren (Zurich) chosen as the site of the design experiment.
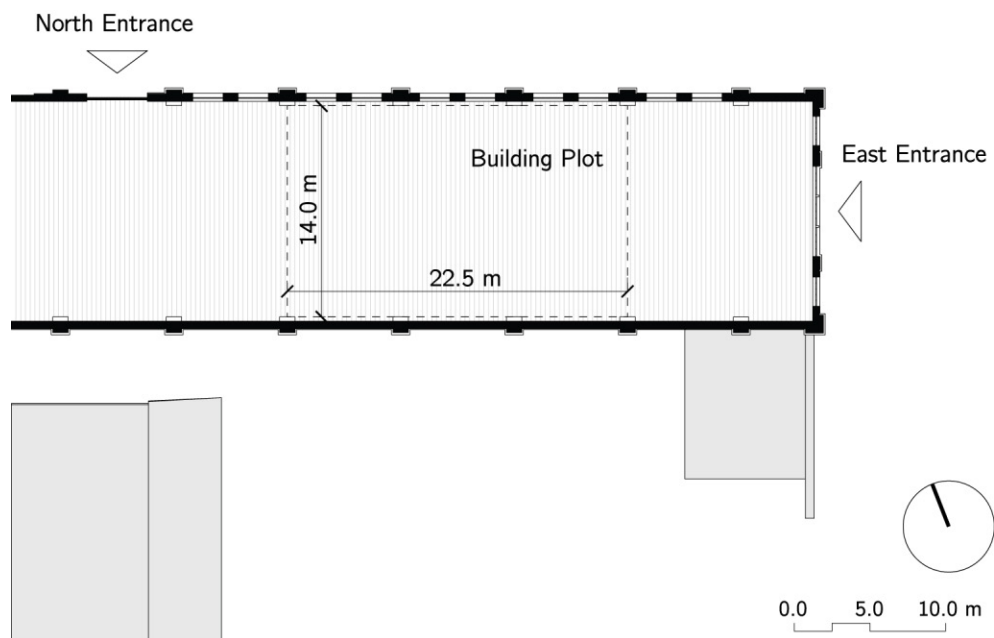

Figure 17.2: Site plan: portion of the industrial storehouse, located in Schlieren (Zurich) regarded as the plot of the new public art gallery.

17.1 Design Development

Considering the previously introduced boundary conditions, to avoid any physical interference between the new building and the existing one, the art gallery has been conceived as an independent volume, with a continuous and differentiated internal space that develops vertically and is organised along a spiral ramp. To facilitate the circulation of the visitors between the two accesses to the storehouse on the ground floor, the objective to reduce the footprint of the building to the minimum has been additionally taken into consideration.

Given the above design intentions, a conceptual design of the new building has been undertaken. Using operation *T1* (§ 12.1) an initial reference grid has been generated as a statically determinate lattice structure made of a linear chain of triangulated polyhedra. This grid has been used to delineate the topology of the aforementioned spiral ramp (Fig. 17.3, F_G a–d). With the aim of reducing the footprint of the building to the minimum, the reference grid has been defined to have only one of its triangular faces in contact with the ground. Given this initial grid, supplementary edges have been then introduced to obtain the topology of a box as an overall statically indeterminate lattice structure (Fig. 17.3, F_G e–f). Based on the reference grid, with operation *T2* (§ 12.2) the topology of the folded plate structure has been defined. Accordingly, the spiral ramp has been initially created inside the grid (Fig. 17.3, F_P a–d). To achieve the static rigidity of the folded plate structure, additional folded plates have been placed (Fig. 17.3, F_P e–f) until all the edges of the reference grid have been actualised into folded edges (§ 12.2). From an architectural standpoint, this has resulted in the creation of a porous envelope containing an enclosed architectural space. While generating the folded plate structure, the main topological features of this enclosed architectural space have been outlined, such as the number of levels of the building, the layout of the internal circulation and the organisation of the openings in the building envelope.

By applying operations *M1* (§ 13.1) and *M2* (§ 13.2) iteratively, the geometry of the reference grid and of the related folded plate structure have been defined based on the architectural and structural requirements. In relation to the architecture (Fig. 17.4, F_M), the dihedral angles between the plates have been adjusted to control the slope of the spiral ramp. This operation, together with the respect of a clearance of at least 2.20 m along the ramp, has resulted in the creation of an internal space with four main levels at 0.00 m, +2.00 m, +5.00 m and +10.00 m. The proportions and dimensions of the internal space have been then further adjusted to allow the creation of two main exhibition areas at the levels +2.00 m and +5.00 m. Furthermore, an open rooftop at the level +10.00 m has been produced to establish a direct relationship between the top of the new building and the ceiling of the existing storehouse.

With regard to the structure, considering the self-weight as the primary load case, a complete strut-and-tie network (Fig. 17.4, **F**) has been generated to get
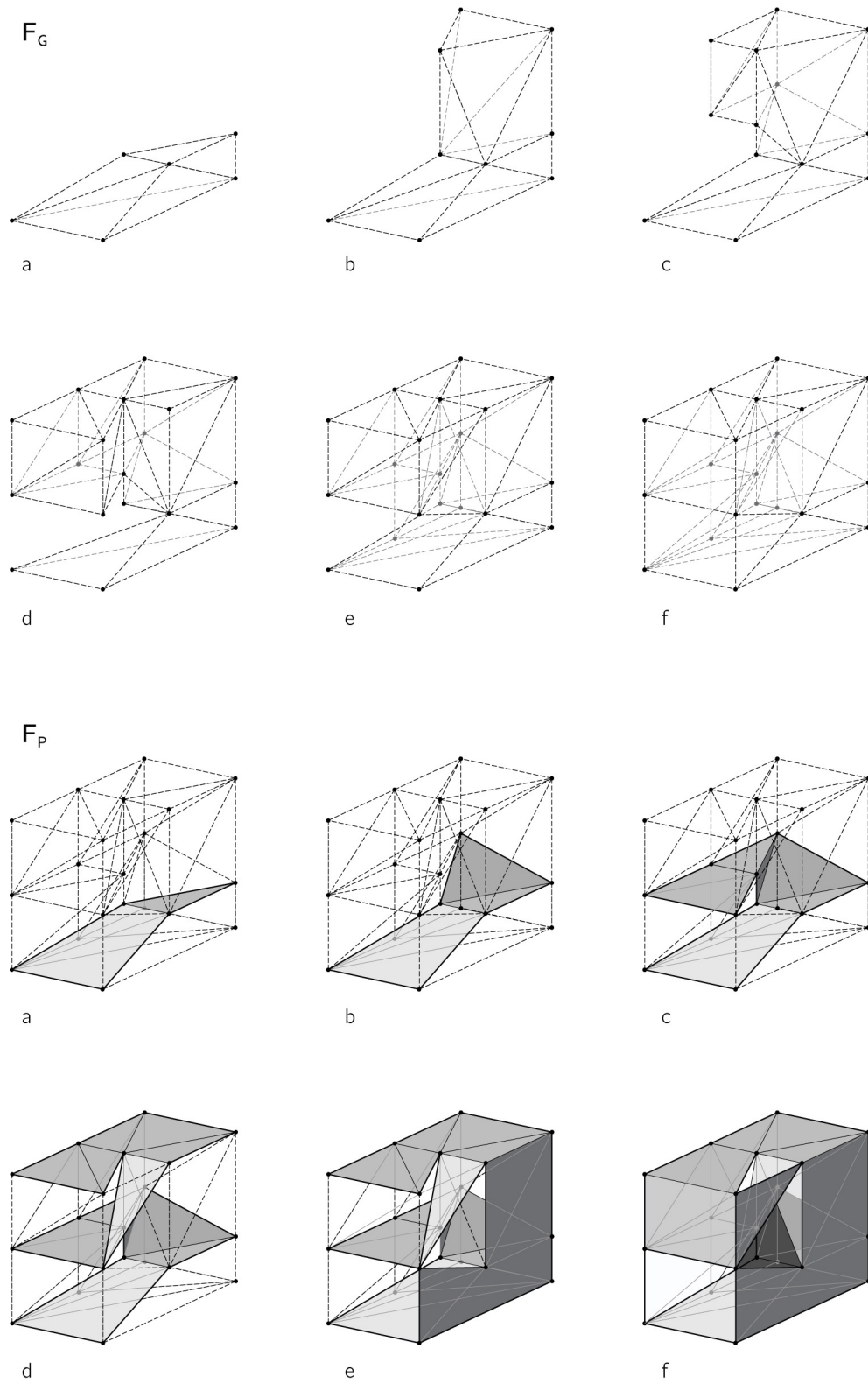
F_G

a

b

c

d

e

f

F_P

a

b

c

d

e

f

Figure 17.3: Construction of the reference grid F_G and definition of the topology of the folded plate structure F_P.
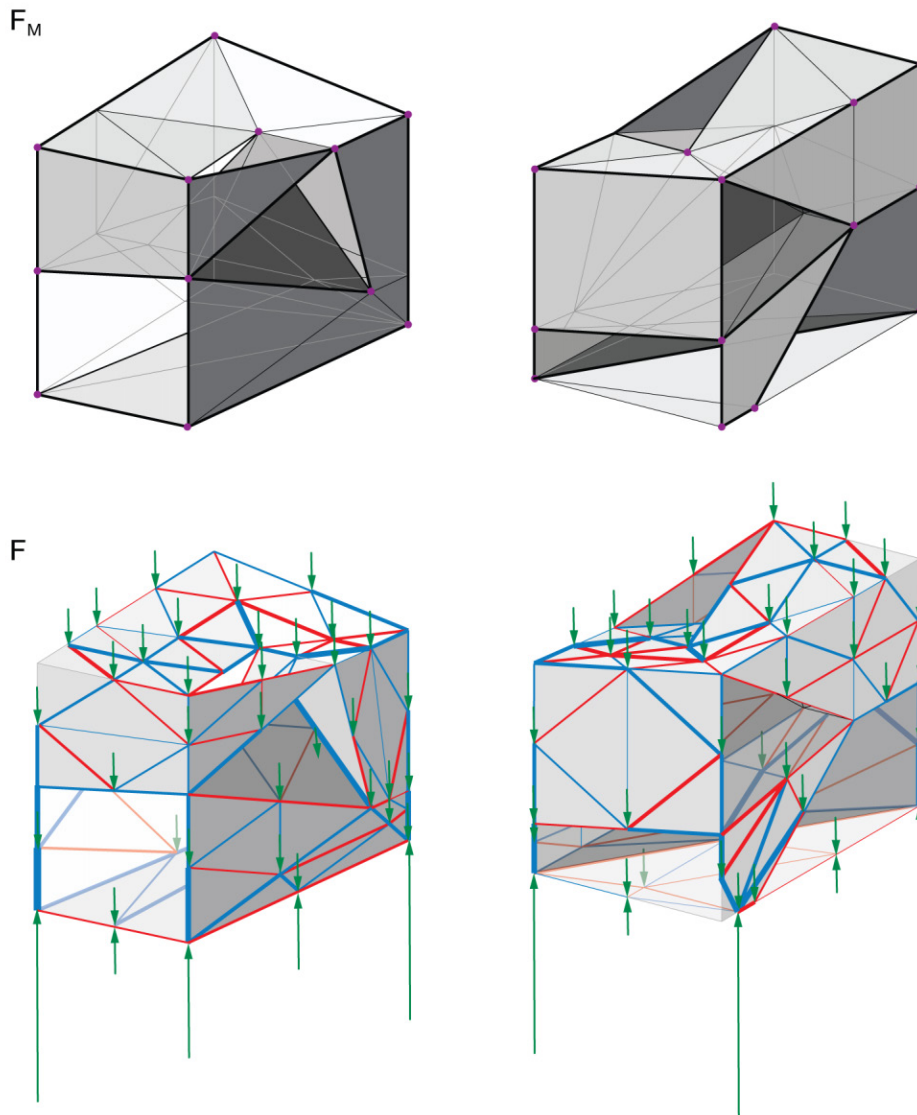
$\mathbf{F_M}$

$\mathbf{F}$

Figure 17.4: Transformation of the folded plate structure $\mathbf{F_M}$ (front, back) and definition of the strut-and-tie model under self-weight $\mathbf{F}$ (front, back).

an insight on the distribution of the internal forces in the folded plates (§ 8.3). In this initial phase of the design, it has been assumed a constant thickness of the plates of 250 mm. Considering the internal and external static indeterminacy of the strut-and-tie network, in compliance with the theory of plasticity (§ 10.1), the magnitudes of the redundant internal and external forces have been regarded as parameters. As such, these values have been adjusted through an optimisation process (Rondeaux et al. 2017) to achieve an overall uniform distribution of the forces in the structure.

17.2   Integration of Space and Structure

Based on the above application of the proposed design method, a preliminary design of the new building housing the art gallery has been put forward that offers seamless integration between space and structure (Fig. 17.5, Fig. 17.6). In fact, it is not possible to make a distinction between the structural system and the architectural envelope, as these two elements are unified within the same single object.

In this design experiment, the architectural potentials of the proposed design approach have been put forward to create a continuous folded plate geometry that folds into space to generate the spiral ramp and then unfolds back to delineate the exterior walls of the building. In line with the design approach of Sancho and Madridejos (§ 5.2), the architectural space results from the three-dimensional articulation of the folded plate structure that generates a coherent architectural formal system. As a result, the tectonic distinction between the individual elements of the building is completely dissolved (§ 12.2).

In analogy to the case of the Chapel in Valleacerón by Sancho and Madridejos, the art gallery is perceived differently (Fig. 17.8, Fig. 17.9), based on the point of view from which the building is observed. In fact, as highlighted in the previous case studies of the foldDESK (§ 15.3) and the foldKITE (§ 16.4), the complex geometry of the folded plate structure can be only comprehended by looking at it from various perspectives. In this case, an extra dimension is added, since it is possible to enter the building and observe it from the inside. While moving along the spiral ramp (Fig. 17.7), the different parts of the building can be experienced, and its relationship to the surrounding context evaluated. Consequently, a dialogue between the new building and the existing one can be established, which is mediated by the presence of the folded plate geometry.

From a structural standpoint, similarly to the approach of Musmeci (§ 4.2), the form of the building offers a direct manifestation of its static behaviour, being an expression of the principle of resistance through form. Thanks to the static rigidity of the reference grid that is inherent to the folded plate structure, the internal forces are transferred exclusively through the folded edges and the folded plates, thus avoiding activating a less effective resistance mechanism that relies on the bending stiffness of the folded edges.

Even though the design experiment here presented is limited at the level of the conceptual design phase, the use of the proposed design method has given the opportunity to address significant architectural and engineering questions. Supplementary architectural and engineering requirements, such as material and construction constraints, may be included in the design workflow as extra geometric constraints (§ 13.1). As such, the result here presented can be regarded as a starting point for further design development.
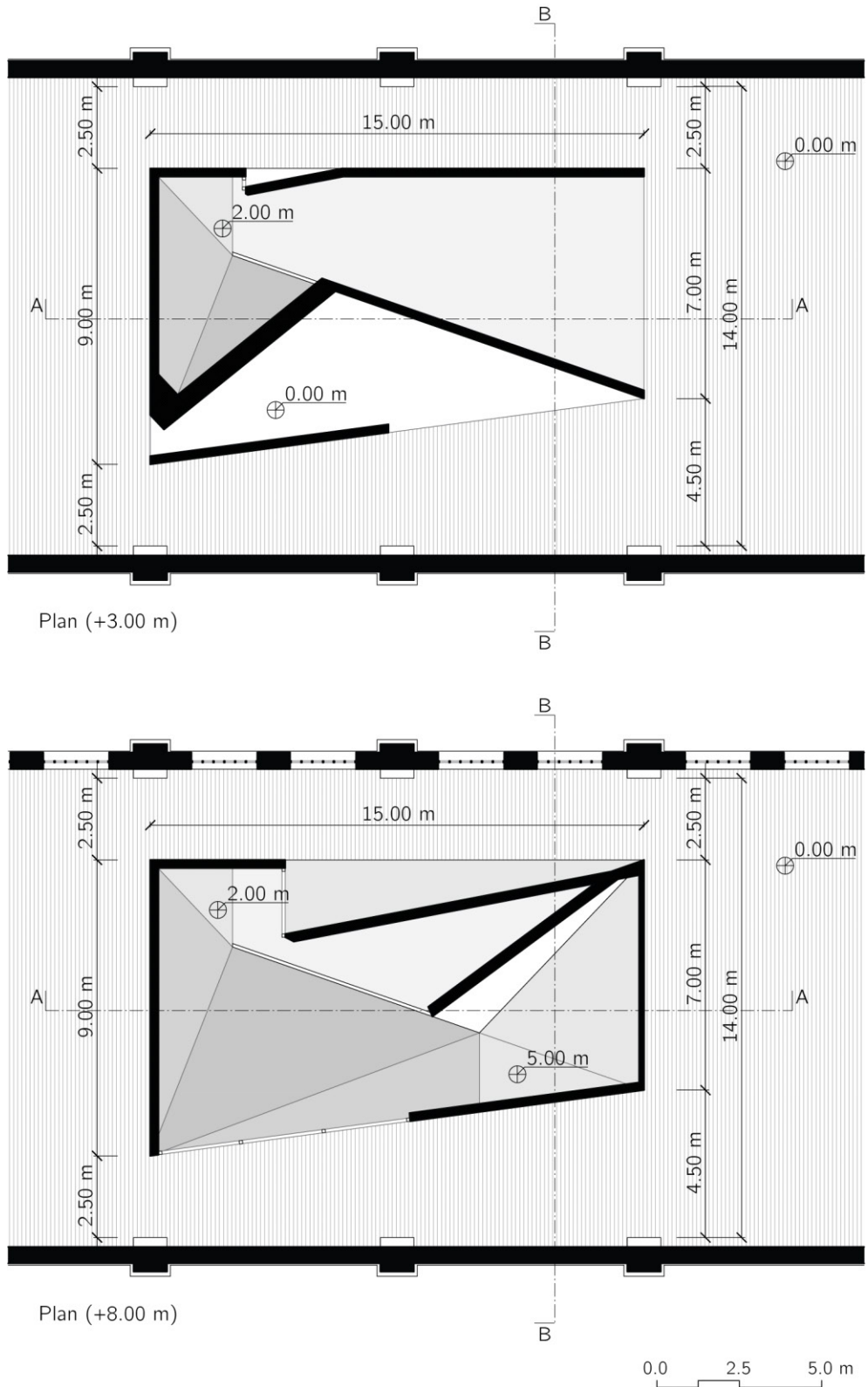
Figure 17.5: Plans at +3.00m and +8.00m of the proposed new building hosting an exhibition space.
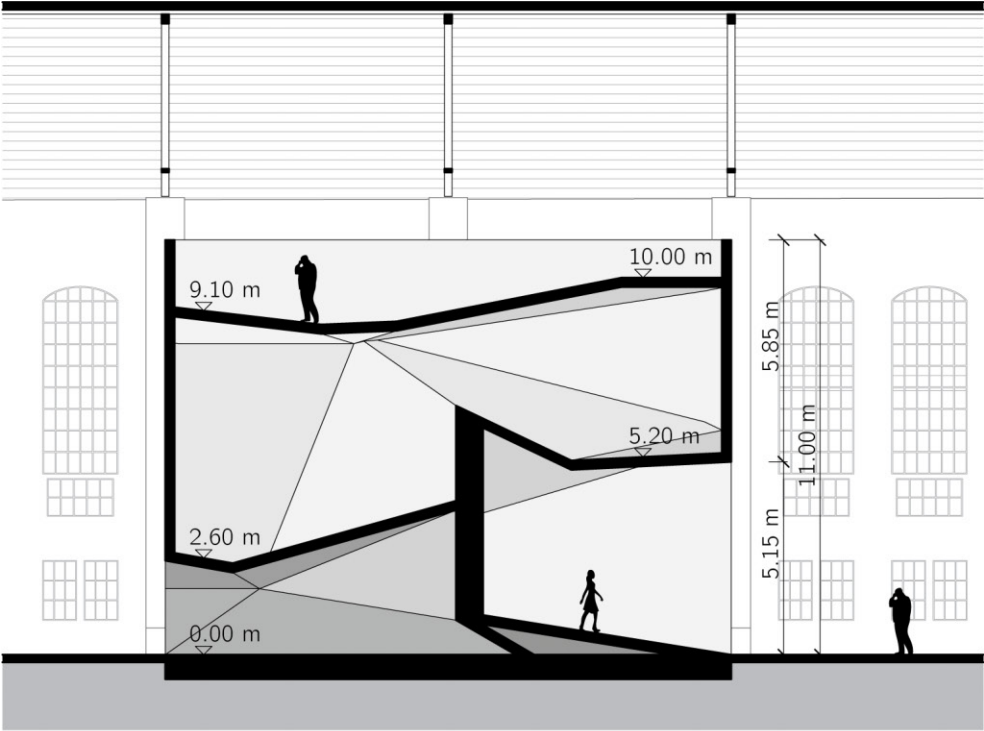
Section A-A
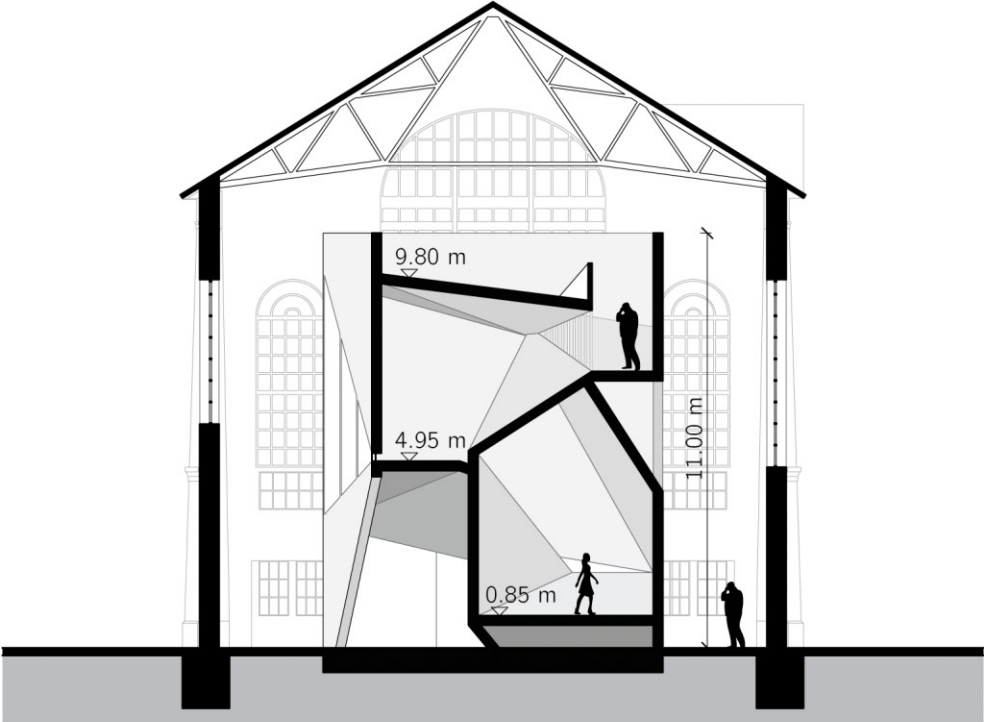
Section B-B
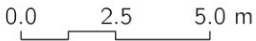
Figure 17.6: Longitudinal section (A-A) and cross-section (B-B) of the proposed new building hosting an exhibition space.
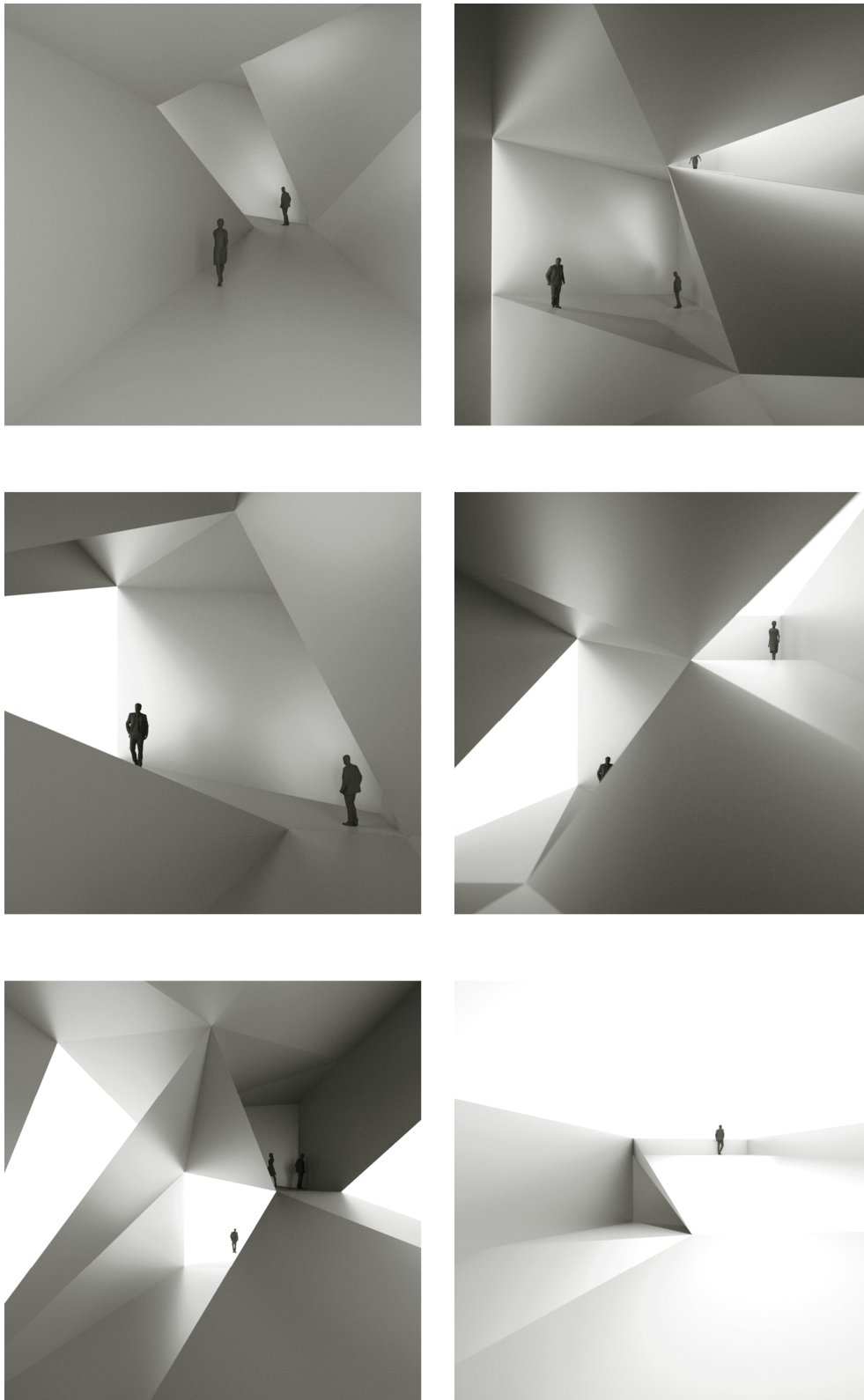
Figure 17.7: Sequence of conceptual interior views along the spiral ramp of the proposed new building hosting an exhibition space.

Figure 17.8: Conceptual view of the main entrance of the proposed new building hosting an exhibition space.

Figure 17.9: Conceptual view of the back of the proposed new building hosting an exhibition space.

Conclusions

18. Discussion

This thesis has investigated the potentials of folding as a design operation that enables exploring the interaction between the disciplines of architecture and engineering. In this context, folding has been regarded as a medium to promote the collaboration between architects and engineers, starting from the early stage of t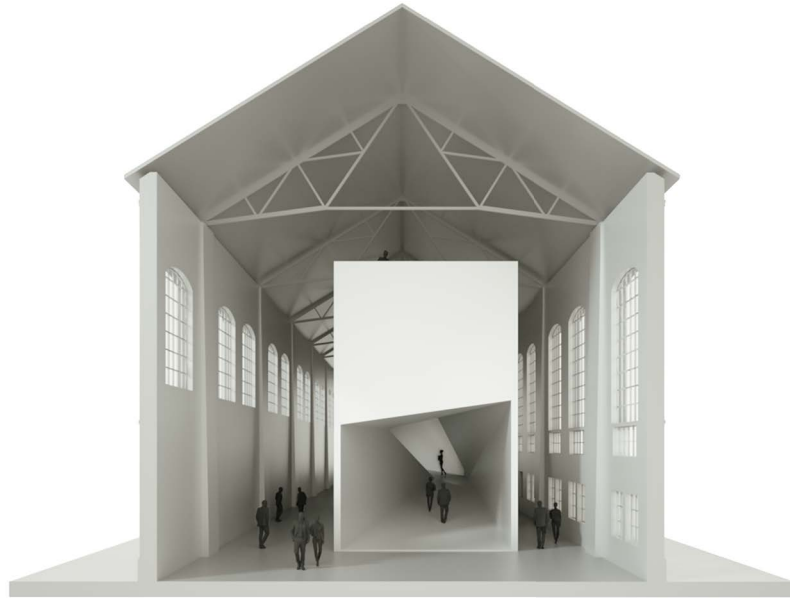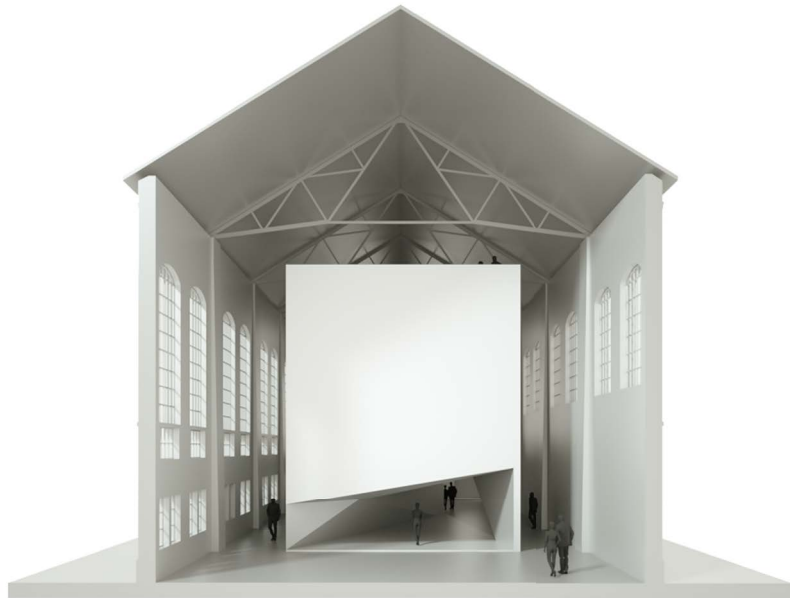he design process. In the following sections, a summary of the unique contributions of this research is presented, together with an overview of the current limitations of the proposed approach and an outlook on further developments.

18.1 Contributions

Considering the existing methodologies for the design of folded plate structures in architecture (Chapter 7), up to now a few solutions have been proposed that can deal with both spatial and structural aspects and address them simultaneously starting from the conceptual phase of the design development. On the one hand, existing strategies permit the design of folded geometries based on structural considerations (§ 4.2.2) but with a limited scope in terms of the spatial solution. On the other hand, approaches have been put forward to explore more articulated spatial configurations (§ 5.2.1); however, these solutions require the analysis of the structural performances of the folded forms to be performed in an advanced step of the design process, mostly using numerical models like the finite element method (FEM).

With the aim to overcome the limitations of the existing approaches, the main contribution of this research is the introduction of a *novel design method for structural folding in architecture* that enables both architects and engineers to take advantage of the spatial and structural opportunities of folding (Chapter 11). By establishing a unified design framework, this mode of operation brings together architectural and engineering thinking through the mediation of geometry. In fact, it is thanks to the use of geometry, and the possibility to work with topological and metric operations, that the developed approach gives the designer the chance to address questions related to both space and structure in a consistent and integral way.

The elaboration of the proposed design method has involved the development of several models and procedures, including the formulation of a structural model for folded plate structures (§ 8.3), the definition of a set of rules for designing (Chapter 11), and the development of design experiments as case studies (Chapter 14). In the following subsections, individual contributions for each of these points are listed and discussed.

18.1.1   Structural Model

Different structural models have been proposed in the literature to describe the behaviour of folded geometries (§ 8.3): structures as assemblies of rigid facets, as shells, as membranes, or as trusses (Lebée 2015). These models are generally treated within the theory of elasticity and implemented using FEM, which implies a series of limitations especially during the first steps of the design development (§ 7.1).

An alternative structural model based on *graphic statics* and the *theory of plasticity* has been here proposed; this model has been implemented in the form of a *complete strut-and-tie network* and a *synthetic strut-and-tie network* (§ 8.3):

- The *complete strut-and-tie network*, which complies with the membrane model (§ 8.3), has been defined as an integration of the *lattice* and the *plate* structure systems (Wester 1984; § 8.1). Thanks to this strut-and-tie network, fundamental properties of a folded plate structure such as static rigidity, equilibrium of the internal forces and stress distribution can be represented in a single and coherent model. This model can be easily adapted to any geometric configuration of the folded plate structure, regardless of the complexity of its topology or of its metric properties.

- The *synthetic strut-and-tie network*, which complies with the truss model (§ 8.3) and can be derived from the complete strut-and-tie model, has been defined as a simplified network that nonetheless represents a valid solution in terms of static rigidity, and equilibrium of the internal forces. This model is specifically intended for the early stage of the design process, to have a quick understanding of the global mechanical behaviour of the structure.

In order to evaluate and control the static equilibrium of the complete and synthetic strut-and-tie networks regarded as 3D form diagrams, a series of procedures involving the use of vector-based 3D graphic statics have been introduced, as part of a broader ongoing research on the development of graphic statics in the third dimension (D'Acunto et al. 2019):

- A graphical procedure for the *evaluation of the external equilibrium* of forces in space (§ 9.2), which makes use of graphic statics and projections, has been formalised (D'Acunto et al. 2016) and integrated within

the proposed design method, based on a traditional graphical construction (Culmann 1866).

- A general methodology grounded on graph theory has been proposed for the *construction of vector-based 3D force diagrams* (§ 9.4) whose corresponding 3D form diagrams are not planar (Jasienski et al. 2016; D'Acunto et al. 2019). This mode of operation extends the applicability of vector-based 3D graphic statics to any 3D strut-and-tie network in static equilibrium while making clear the fundamental relationship between form and internal forces. In this context, various topological configurations of 3D force diagrams have been introduced (double-layered, single-layered, multiple-quads, and case-specific), which can be alternatively used according to the specific design requirements.

- A series of procedures have been introduced for the global and local *transformation of vector-based 3D force diagrams* (§ 9.5) that secure their interdependency with the corresponding 3D form diagrams. These procedures permit the bi-directional manipulation of 3D form and force diagrams, thus allowing for the fundamental relationship between form and internal forces in a 3D strut-and-tie network to be used as an active design parameter (D'Acunto et al. 2017).

With regard to the complete strut-and-tie network, an approach to the evaluation of stress fields in folded plate structures has been introduced (§ 10.2):

- An existing procedure for the evaluation of discrete stress fields in two-dimensional structures (Hajdin 1990) has been adapted to derive in-plane discrete stress fields in folded plate structures, as a combination of triangular sub-fields, each with a constant planar bi-axial stress state.

18.1.2   Design Method

Built upon the above structural model, a general procedure for the design of folded plate structures in architecture has been conceived (Chapter 11). More specifically, a statically rigid folded plate structure is created within a reference grid. While generating the folded plate structure, an enclosed architectural space is produced at once. Without losing its inherent topological properties, the form of the folded plate structure and the distribution of its internal forces can be adjusted by the designer to meet specific architectural and structural requirements (D'Acunto and Castellón 2015). In relation to the proposed method, the following contributions have been made:

- A three-dimensional design process based on the use of four main operations (*T1–grid generation*, *T2–virtual folding*, *M1–manipulation of the form*, *M2–manipulation of the forces*) has been introduced that allows the

design of both *folded surface structures* and *folded volumetric structures* (Chapter 11) while operating at the levels of *topology* (Chapter 12) and *Euclidean geometry* (Chapter 13).

- The design method has been implemented within a *parametric digital toolkit* that permits the design of folded plate structures in a three-dimensional digital modelling environment. The toolkit allows for the interactive use of the proposed design operations in a non-sequential and non-destructive way.

- Considering the topological and projective geometric procedure of the proposed method (*T1–grid generation* and *T2–virtual folding*), an approach has been defined that takes advantage of structural topology and graph theory (§ 8.2) for the direct control of the kinematic and static determinacy of a folded plate structure. Topological operations of subdivision (*T1-S*) and combination (*T1-C*) have been implemented, and a strategy to deal with projective constraints has been proposed based on the work of Fivet and Zastavni (2015).

- Considering the metric procedure of the proposed method (*M1–form manipulation* and *M2–force manipulation*), the above global and local transformations of the vector-based 3D form and force diagrams have been integrated into the developed approach. These allow the designer to modify the geometry of the folded plate structure interactively while having a real-time overview of the distribution of the internal forces. A procedure to apply metric constraints to the surface area of the folded plates, to the length of the folded edges, and to the dihedral angle between folded plates has been proposed, which makes use of the work of Piker (2017).

18.1.3   Case Studies

The proposed design method for structural folding in architecture has been tested by means of a series of design experiments (Chapter 14). In particular, three case studies have been developed: a cantilevering table, a hanging structure, and a small building. Each of these experiments has been associated with a specific design task, with a given brief and clear boundary conditions. Overall, the case studies have proved the flexibility of the proposed approach when applied to real design scenarios. In this domain, two main contributions have been made:

- Demonstration of the validity of the developed method to materialise architectural and structural concepts that go beyond the conventional typological boundaries in terms of both space and structure.

- Demonstration of the flexibility of the proposed approach when applied to the design of architectural and structural projects at various scales and involving the use of different materials.

18.2   Limitations and Future Work

Although the application of the proposed design approach for structural folding in architecture to a series of case studies has demonstrated the strengths of the developed approach, several limitations in the current implementation of the method can be detected. In the following subsections, these limitations are discussed at the level of the structural model, the design method, and the case studies. Moreover, various possibilities for improvement are put forward.

18.2.1   Structural Model

The proposed strut-and-tie model (§ 8.3) is based on a series of assumptions on the mechanical behaviour of folded plate structures. On the one hand, these assumptions allow the model to be easily comprehensible while also adaptable to complex spatial configurations. On the other hand, some of these assumptions may limit its range of applicability. Regarding the strut-and-tie network, the following limitations can be detected, and further developments can be suggested:

- In the complete strut-and-tie network, vertices are placed only at the mid-points and endpoints of the folded edges. This configuration relies on the hypothesis that for a given folded plate, the uniformly distributed area load on the plate can be replaced by an equivalent system of uniformly distributed (i.e. constant) line loads along the folded edges that are proportional to the triangular tributary areas of the edges. Although this solution is valid in terms of global equilibrium, for a more precise repartition of the loads, uniformly varying loads with linear distributions (Hajdin 1990) can be considered along the folded edges. These loads can be then replaced by two resultant forces along each folded edge, yet requiring a different layout of the strut-and-tie network to be generated in comparison to the one currently proposed.

- The presented approach for the repartition of the loads is based on the subdivision of the plates into triangles. For specific geometric configurations, this procedure may represent an oversimplification of the actual mechanical behaviour of the structure. In future developments of this research, alternative strategies for the subdivision of the plates will be explored.

Regarding the introduced vector-based 3D graphic statics procedures, observations can be made as follows:

- The vector-based 3D force diagram of a complete strut-and-tie network may present a high number of duplicate edges (§ 9.4), thus compromising the possibility for a clear and direct correlation between form and distribution of internal forces in a folded plate structure. For this reason, a synthetic strut-and-tie network has been developed with a reduced number

of linear members. Further developments will explore the possibility for an interactive forward and backward conversion between the former and the latter. This possibility would allow the designer to choose the level of resolution of the strut-and-tie model based on the specific design task at hand.

- In the case of folded plate structures with complex three-dimensional geometries, also synthetic strut-and-tie networks may produce vector-based 3D force diagrams that are difficult to be visualised and handled. More research is required on the construction procedures of the force diagrams, especially to develop strategies for the minimisation of the number of duplicate edges (§ 9.4). Possible approaches in this context may involve the implementation of techniques of graph drawing (Buchheim et al. 2014).

- In the current implementation of the design method, the local constraint-based transformation of a vector-based 3D force diagram is solved using numerical simulations (Piker 2017). To avoid the necessity for this time-consuming iterative process to be run at every modification of the force diagram and to prevent any potential instability issue related to the numerical approach adopted, future research will explore other procedures. A possible strategy could be the use of machine learning applied to 3D graphic statics (Fuhrimann et al. 2018). By deploying algorithms based on neural networks, the underlying non-linear function that relates the geometries of the 3D force and form diagrams could be learned by the machine, and subsequently, the two diagrams could be interactively transformed in real time by the designer. An alternative solution may involve the direct mathematical formulation of the constraints between the diagrams (Fivet 2013).

- Because of its practical advantages (§ 9.1), in the proposed method the vector-based strategy to 3D graphic statics has been preferred over the polyhedron-based one. Considering that the folded plate structures generated using the developed approach are built on reference grids as polyhedral frames, the applicability of the polyhedron-based strategy for the construction and transformation of the 3D force diagrams (Lee et al. 2018; Konstantatou et al. 2018) will also be investigated in future work.

Regarding the solution introduced for the evaluation of the stress fields in the folded plate structures (§ 10.2), the following considerations can be made:

- In the general implementation of the proposed design method, under the assumption that the struts and ties along the folded edges behave like stringers with infinite resistance capacity, an in-plane discrete stress field can be automatically generated in a folded plate as a combination of triangular sub-fields. This approach generally leads to an overestimation of the

resistance capacity of the structure since it does not take into account the diffusion of the stresses along the folded edges. In future developments of the design method, a solution has to be implemented that considers this effect, such as the automatic procedure proposed by Hajdin (1990).

- The local repartition of a uniformly distributed area load from a folded plate to the folded edges generates two local stress states on the plate. The first one is an in-plane stress field on the midplane of the plate and the second one is a combined shear and moment field on the midplane of the plate, or equivalently, two *curved stress fields* (Bahr 2017). Future work will explore the implementation in the design approach of the procedure suggested by Bahr (2017) to calculate the curved stress fields on the folded plates.

- The definition of the stress fields at the nodes of the strut-and-tie model with concurrently loaded edge members (i.e. at the endpoints of the folded edges) has not been investigated in this work. In fact, these three-dimensional discontinuities of the structure require the development of specific nodal solutions using, for example, the procedure suggested by Bahr (2017).

18.2.2   Design Method

In relation to the set of rules defined within the scope of the proposed design method (Chapter 11), the following limitations can be highlighted, and possible improvements suggested:

- Although a solution to implement scale-dependent and material-dependent constraints within the design method has been proposed (§ 13.1), at present these constraints have to be formalised according to the specific design task. In future developments of this work, an explicit formulation of these constraints will be introduced. Possible solutions in this context may be found in the works of Buri (2010) and Meyer (2017).

- The geometry of the folded plate structure generated using the developed approach is represented using a triangulated mesh with no thickness (§ 13.1). If this simplification is helpful at the conceptual design level, in subsequent steps of the design process the possibility to control this parameter could be of fundamental importance. Further improvements of this research will introduce a new operation that allows transforming the triangulated mesh into a thick solid geometry. In this regard, the procedure suggested by Meyer (2017) can be taken into consideration.

- Using the operations defined within the proposed design method, the designer can create and control the topology and the geometry of the folded

plate structure directly. For specific design applications, however, form-finding may be more convenient. In this regard, future developments of the research will explore the integration of other frameworks for analysis and design of structures in static equilibrium, such as the Combinatorial Equilibrium Modelling (CEM) (Ohlbrock and Schwartz 2016; Ohlbrock et al. 2017). The use of the CEM would make it possible to generate a first instance of the reference grid through form-finding.

- The proposed design approach promotes the continuous interaction of the designer with a series of operations for the generation and transformation of the folded plate structure. The current digital implementation of the method involves the use of a series of customised tools, which have been defined within a common CAD software environment but developed in the form of separate scripts. To enhance the consistency of the digital implementation, a unified software package has to be developed. In this context, the open source *COMPAS* library (Van Mele et al. 2017) may be used.

18.2.3 Case Studies

Although the case study related to the design of an art gallery within the envelope of an existing building (Chapter 17) has demonstrated the potentials of the method for conceptual architectural design, a more refined example may be developed to further assess the effectiveness of the proposed approach at the scale of architecture. In fact, in this case study, many important aspects have not been taken into consideration, such as material and construction constraints.

In this context, the design and construction of a full-scale architectural project in the form of a pavilion or a small building would be useful. This additional case study would offer the chance to test the proposed design strategy at the building scale and in a real design setting while dealing with design questions that go beyond the conceptual design level.

19.   Final Reflections

Through the investigation of the diverse understandings of structural folding in architectural design, this research has explored the relationship between the load-bearing capacity and the space making potential of folded plate structures. A novel design method to incorporate structural folding in architectural design has been presented. In particular, the method allows the designer to generate a folded plate structure that forms the building envelope of an enclosed architectural space. Grounded on a new structural model for folded plate structures that relies on 3D graphic statics and the theory of plasticity, the developed approach gives the possibility to evaluate and control simultaneously the load-bearing behaviour of the structure at three different levels: static rigidity, equilibrium of the internal forces, and stress distribution. These aspects can then be used as drivers for the design development.

The broader scope of the proposed method is to foster a non-hierarchical exchange between the two interconnected disciplines of architecture and engineering. In fact, the method suggests an operative approach that supports the dialogue between architects and engineers, while guiding them throughout the entire design process, starting from the conceptual stage. In this way, essential design decisions related to space and structure can be taken at the same time, in a consistent and informed way. In this regard, as highlighted by the structural engineer Musmeci:

> "We cannot be satisfied with a design method that limits the use of rational tools to the sole process of analysis, leaving the creation of the form to arbitrary acts supported only by intuition and experience [...] Eventually, we want to earn and use our freedom as designers; not the freedom of who can go anywhere but does not know where to go, but the freedom of who knows what to look for, and also how and where to find it."[1] (Musmeci 1979b, p. 40)

The hope of the author is that the proposed holistic approach to design could contribute to the development of a design culture where freedom of architectural expression and engineering thinking are seamlessly combined, in order to trigger a paradigmatic shift in the current practices of building design.

---

[1]Translation of the quotation from Italian to English by the author.

Bibliography

Addis, B.: 2007, *Building: 3000 Years of Design Engineering and Construction*, Phaidon, London - New York.

Adriaenssens, S., Schmidt, K., Katz, A., Gabriele, S., Magrone, P. and Varano, V.: 2015, Early Form Finding Techniques of Sergio Musmeci Revisited: the Basento Viaduct Project, *Proceedings of the IASS Symposium 2015 - Future Visions*, Amsterdam.

Akbarzadeh, M., Van Mele, T. and Block, P.: 2015a, 3D Graphic Statics: Geometric Construction of Global Equilibrium, *Proceedings of the IASS Symposium 2015 - Future Visions*, Amsterdam.

Akbarzadeh, M., Van Mele, T. and Block, P.: 2015b, On the Equilibrium of Funicular Polyhedral Frames and Convex Polyhedral Force Diagrams, *CAD Computer Aided Design* **63**, 118–128.

Albers, J.: 1952, Concerning Fundamental Design, *Bauhaus 1919-1928*, Branford, Boston, pp. 114–121.

Alexandrov, A. D.: 1958, *Konvexe Polyeder*, Akademie-Verlag, Berlin.

Almegaard, H.: 2003, *Skalkonstruktioner*, PhD thesis, Statens Byggeforskningsinstitut.

Almegaard, H. and Hansen, K.: 2007, Skiveskaller: Statisk virkemåde og stabilitet, *Bygningsstatiske Meddelelser (Proceedings of the Danish Society for Structural Science and Engineering)* **78**(2), 29–54.

Bagger, A.: 2010, *Plate Shell Structures of Glass Studies Leading to Guidelines for Structural Design*, PhD thesis, Technical University of Denmark.

Bahr, M.: 2017, *Form Finding and Analysis of Shells and Slabs based on Equilibrium Solutions*, PhD thesis, ETH Zürich.

Baniček, M., Fresl, K. and Kodrnja, I.: 2018, Some Examples of Static Equivalency in Space Using Descriptive Geometry and Grassmann Algebra, *Proceedings of the IASS Symposium 2018 - Creativity in Structural Design*.

Baracs, J. J.: 1975, Rigidity of Articulated Spatial Panel Structures, *Bullettin IASS* **16**(59), 37–52.

Barazzetta, G. (ed.): 2004, *Aldo Favini: Architettura e Ingegneria in Opera*, Libreria Clup, Milano.

Barnes, M. R.: 1977, *Form-finding and Analysis of Tension Space Structures by Dynamic Relaxation*, PhD thesis, City University London.

Bechthold, M.: 2008, *Innovative Surface Structures: Technologies and Applications*, Taylor & Francis, Abingdon.

Bender, J., Müller, M. and Macklin, M.: 2015, Position-Based Simulation Methods in Computer Graphics, *in* M. Zwicker and C. Soler (eds), *Eurographics 2015*, The Eurographics Association.

Block, P. and Ochsendorf, J.: 2007, Thrust Network Analysis: a New Methodology for Three-dimensional Equilibrium, *Journal of the International Association for Shell and Spatial Structures* **48**, 167–173.

Bouquiaux, L.: 2005, Plis et Enveloppements chez Leibniz., *in* G. Cormann, S. Laoureux and J. Piéron (eds), *Différence et identité*, Georg Olms Verlag, Hildesheim, pp. 39–55.

Bow, R. H.: 1873, *Economics of Construction in Relation to Framed Structures*, E. & F. N. Spon, London.

Boyer, J. M.: 2001, *Simplified O(n) Algorithms for Planar Graph Embedding, Kuratowski Subgraph Isolation, and Related Problems*, PhD thesis, University of Victoria.

Brodini, A.: 2013, Le Coperture a Grande Luce nell'Opera di Sergio Musmeci, *in* P. Desideri, A. De Magistris, C. Olmo, M. Pogacnik and S. Sorace (eds), *La Concezione Strutturale*, Umberto Allemandi & Co., Torino, pp. 253–264.

Buchheim, C., Chimani, M., Gutwenger, C., Jünger, M. and Mutzel, P.: 2014, Crossings and Planarization, *in* R. Tamassia (ed.), *Handbook of Graph Drawing and Visualization: Discrete Mathematics and its Applications*, CRC Press, Boca Raton.

Buri, H. U.: 2010, *Origami: Folded Plate Structures*, PhD thesis, PhD Thesis. École Polytechnique Fédérale de Lausanne.

Cache, B.: 1995, *Earth Moves, The Furnishing of Territories*, The MIT Press, Cambridge, MA. Speaks, M. (ed.).

Calatrava, S.: 1981, *Zur Faltbarkeit von Fachwerken*, PhD thesis, ETH Zürich.

Calladine, C.: 1978, Buckminster Fuller's Tensegrity Structures and Clerk Maxwell's Rules for the Construction of Stiff Frames, *International Journal of Solids and Structures* **14**, 161–172.

Carpo, M.: 2004, Ten Years of Folding, *in* G. Lynn (ed.), *Folding in Architecture (Revised Edition)*, Architectural Design, John Wiley & Sons, London, pp. 14–18.

Carpo, M.: 2013, *The Digital Turn in Architecture 1992–2012*, John Wiley & Sons, London.

Cauchy, A.-L.: 1813, Sur les Polygones et Polyèdres: Second Mémoire, *Journal de École Polytechnique* **19**(9), 87–98.

Chimani, M.: 2008, *Computing Crossing Numbers*, PhD thesis, Technical University of Dortmund.

Coates, R. C., Coutie, M. G. and Kong, F. K.: 1987, *Structural Analysis*, CRC Press, London.

Coxeter, H. S. M.: 1987, *Projective Geometry (Second Edition)*, Springer Verlag, New York.

Coxeter, H. S. M.: 1989, *Introduction to Geometry (Second Edition)*, John Wiley & Sons, London.

Coxeter, H. S. M.: 1998, *Non-Euclidean Geometry (Sixth Edition)*, The Mathematical Association of America, Washington DC.

Crapo, H.: 1979, Structural Rigidity, *Structural Topology* **1**, 26–45.

Crapo, H. and Whiteley, W.: 1993, Plane Self Stresses and Projected Polyhedra: the Basic Pattern, *Structural Topology* **20**, 55–78.

Cremona, L.: 1872, *Le Figure Reciproche nella Statica Grafica*, Tipografia Bernardoni, Milano.

Culmann, K.: 1866, *Die graphische Statik*, Meyer & Zeller, Zürich.

D'Acunto, P.: 2016, Folddesk, *in* J. Schwartz (ed.), *Kleine Tragwerksobjekte (Small Structural Objects)*, Park Books, Zürich, pp. 25–37.

D'Acunto, P. and Castellón, J. J.: 2015, Folding Augmented: a Design Method for Structural Folding in Architecture, *in* K. Miura, T. Kawasaki, T. Tachi, R. Uehara, R. Lang and P. Wang-Iverson (eds), *Origami 6*, American Mathematical Society, Providence, pp. 479–488.

D'Acunto, P., Castellón, J. J., Tellini, A. and Ren, S.: 2015, foldKITE. An Ultra-Lightweight Folded Structure, *Proceedings of the IASS Symposium 2015 - Future Visions*, Amsterdam.

D'Acunto, P. and Ingold, L.: 2016, The Approach of Sergio Musmeci to Structural Folding, *Proceedings of the IASS Symposium 2016 - Spatial Structures in the 21st Century*, Tokyo.

D'Acunto, P., Jasienski, J., Ohlbrock, P. O. and Fivet, C.: 2017, Vector-based 3D Graphic Statics: Transformations of Force Diagrams, *Proceedings of the IASS Symposium 2017 - Interfaces: Architecture Engineering Science*, Hamburg.

D'Acunto, P., Jasienski, J. P., Ohlbrock, P. O., Fivet, C., Zastavni, D. and Schwartz, J.: 2019, Vector-Based 3D Graphic Statics: a Framework for the Design of Spatial Structures based on the Relation between Form and Forces, *International Journal of Solids and Structures* . In Press (https://doi.org/10.1016/j.ijsolstr.2019.02.008).

D'Acunto, P., Ohlbrock, P. O., Jasienski, J. and Fivet, C.: 2016, Vector-based 3D Graphic Statics (Part I): Evaluation of Global Equilibrium, *Proceedings of the IASS Symposium 2016 - Spatial Structures in the 21st century*, Tokyo.

Deleuze, G.: 1988, *Le Pli: Leibniz et le Baroque*, Editions de Minuit, Paris.

Deleuze, G.: 1993, *The Fold: Leibniz and the Baroque*, The Athlone Press, London.

Demaine, E. D. and O'Rourke, J.: 2007, Flexible Polyhedra, *Geometric Folding Algorithms: Linkages, Origami, Polyhedra*, Cambridge University Press, New York.

Drucker, D. C.: 1961, On Structural Concrete and the Theorems of Limit Analysis, *International Association for Bridge and Structural Engineering (IABSE)* **21**, 49–59.

Dureisseix, D.: 2012, An Overview of Mechanisms and Patterns with Origami, *International Journal of Space Structures* **27**(1), 1–14.

Eisenman, P.: 1991, Unfolding Events: Frankfurt Rebstock and the Possibility of a New Urbanism, *in* A. S. Eisenman Architects, Partners and Hanna/Olin (eds), *Unfolding Frankfurt*, Ernst & Sohn, pp. 8–18.

Eisenman, P.: 1992, Visions Unfolding: Architecture in the Age of Electronic Media, *Domus* **734**, 17–24.

Engel, H.: 2013, *Tragsysteme - Structure Systems (Fifth Edition)*, Hatje Cantz Verlag, Ostfildern.

Enrique, L. and Schwartz, J.: 2017, Load Path Network Method, an Equilibrium-based Approach for the Design and Analysis of Structures, *Structural Engineering International* **27**(2), 292–299.

Favini, A.: 1962, Chiesa del Sacro Cuore ad Ivrea (Torino), *Atti del IV Congresso Internazionale del Precompresso (F.I.P.). Realizzazioni Italiane in Cemento Armato Precompresso*, Associazione Italiana Tecnico-Economica del Cemento, Roma - Napoli, pp. 313–316.

Fernandez Ordoñez, J. A.: 1979, *Eugène Freyssinet*, 2C, Barcelona.

Filipov, E. T., Liu, K., Tachi, T., Schenk, M. and Paulino, G. H.: 2017, Bar and Hinge Models for Scalable Analysis of Origami, *International Journal of Solids and Structures* **124**(1), 26–45.

Filipov, E. T., Tachi, T. and Paulino, G. H.: 2015, Toward Optimization of Stiffness and Flexibility of Rigid, Flat-Foldable Origami Structures, *in* K. Miura, T. Kawasaki, T. Tachi, R. Uehara, R. Lang and P. Wang-Iverson (eds), *Origami 6*, American Mathematical Society, Providence, pp. 409–419.

Fivet, C.: 2013, *Constraint-Based Graphic Statics - A Geometrical Support for Computer-aided Structural Equilibrium Design*, PhD thesis, Université Catholique de Louvain.

Fivet, C.: 2016, Projective Transformations of Structural Equilibrium, *International Journal of Space Structures* **31**(2-4), 135–146.

Fivet, C. and Meng, X.: 2017, Digital Graphic Statics – Shared Design Tools for Architects and Engineers, *Architectural Journal China* **590**, 20–25.

Fivet, C. and Zastavni, D.: 2015, A Fully Geometric Approach for Interactive Constraint-based Structural Equilibrium Design, *CAD Computer-Aided Design* **61**, 42–57.

Flury, A.: 2012, Inquisitive Openness, *in* A. Flury (ed.), *Cooperation: The Engineer and the Architect*, Birkhäuser, Basel, pp. 9–15.

Fortuna, E., Frigerio, R. and Pardini, R.: 2016, *Projective Geometry, Solved Problems and Theory Review*, Springer International Publishing, Cham.

Frichot, H.: 2013, Deleuze and the Story of the Superfold, *Deleuze and Architecture*, Edinburgh University Press, Edinburgh.

Fuhrimann, L., Moosavi, V., Ohlbrock, P. O. and D'Acunto, P.: 2018, Data-Driven Design: Exploring new Structural Forms, *Proceedings of the IASS Symposium 2018 - Creativity in Structural Design*, Boston.

García-Abril, A.: 2003, The Chapel in Valleacerón, *DA Documentos de Arquitectura: Sancho-Madridejos - Pliegues* pp. 1–2.

Gargiani, R. and Bologna, R.: 2016, *The Rethoric of Pier Luigi Nervi. Concrete and Ferrocement Forms*, EPFL Press/Routledge, Lausanne - London.

Gioia, F., Dureisseix, D., Motro, R. and Maurin, B.: 2012, Design and Analysis of a Foldable/Unfoldable Corrugated Architectural Curved Envelop, *Journal of Mechanical Design* **134**(3), 031003.

Gluck, H.: 1977, Almost all Simply Connected Surfaces are Rigid, *Geometric Topology, Lecture Notes in Mathematics*, Vol. 438, Springer-Verlag, Berlin, pp. 225–239.

Grassmann, H.: 2000, *Extension Theory*, American Mathematical Society, London Mathematical Society. (translation of Die Ausdehnungslehre 1862).

Greco, C.: 2008, *Pier Luigi Nervi: dai Primi Brevetti al Palazzo delle Esposizioni di Torino 1917-1948*, Quart Verlag, Luzern.

Greenberg, H. J. and Prager, W.: 1952, Design of Beams and Frames, *Transactions ASCE* **117**, 447–484.

Grünbaum, B.: 1967, *Convex Polytopes*, Wiley-Interscience, London.

Guest, S. D. and Hutchinson, J. W.: 2003, On the Determinacy of Repetitive Structures, *Journal of the Mechanics and Physics of Solids* **51**(3), 383–391.

Gvozdev, A. A.: 1960, The Determination of the Value of the Collapse Load for Statically Indeterminate Systems Undergoing Plastic Deformations, *International Journal of Mechanical Sciences* **1**, 322–335.

Hajdin, R.: 1990, *Computerunterstützte Berechnung von Stahlbetonscheiben mit Spannungsfeldern (Computer-aided Calculation of Reinforced Concrete Slabs with Stress Fields)*, PhD thesis, ETH Zürich.

Harary, F.: 1969, *Graph theory*, Addison-Wesley Publishing, Reading, MA.

Heyman, J.: 2008, *Basic Structural Theory*, Cambridge University Press, Cambridge.

Hillerborg, A.: 1996, *Strip Method Design Handbook*, CRC Press, London.

Hunt, G. W. and Airo, I.: 2005, Twist Buckling and the Foldable Cylinder: an Exercise in Origami, *International Journal of Non-Linear Mechanics* **40**, 833–843.

Ingold, L. and D'Acunto, P.: 2017, Structural Folding as a Source of Research for Sergio Musmeci, *Proceedings of the IASS Symposium 2017 - Interfaces: Architecture Engineering Science*, Hamburg.

Ingold, L. and Rinke, M.: 2015, Sergio Musmeci's Search for New Forms of Concrete Structures, *Proceedings of the Fifth International Congress on Construction History*, Chicago.

Iori, T.: 2011, La Storia Italiana del Cemento, *in* T. Iori and A. Marzo Magno (eds), *150 Anni di Storia del Cemento in Italia*, Gangemi, Roma, pp. 18–21.

Iwamoto, L.: 2009, *Digital Fabrications: Architectural and Material Techniques*, Princeton Architectural Press, New York.

Jackson, P.: 2011, *Folding Techniques for Designers: from Sheet to Form*, Laurence King Publishing, London.

Jasienski, J. P., D'Acunto, P., Ohlbrock, P. O. and Fivet, C.: 2016, Vector-based 3D Graphic Statics (Part II): Construction of Force Diagrams, *Proceedings of the IASS Symposium 2016 - Spatial Structures in the 21st Century*, Tokyo.

Jasienski, J.-P., Fivet, C. and Zastavni, D.: 2014, Various Perspectives on the Extension of Graphic Statics to the Third Dimension, *Proceedings of the IASS-SLTE Symposium 2014 - Shells, Membranes and Spatial Structures: Footprints*, Brasilia.

Johnson, P. and Wigley, M.: 1988, *Deconstructivist Architecture*, The Museum of Modern Art, New York.

Kara, H.: 2010, On Design Engineering, *AD Architectural Design* **80**(4), 46–51.

Konstantatou, M., D'Acunto, P. and McRobie, A.: 2018, Polarities in Structural Analysis and Design: n-dimensional Graphic Statics and Structural Transformations, *International Journal of Solids and Structures* **152–153**, 272–293.

Konstantatou, M. and McRobie, A.: 2016, Reciprocal Constructions Using Conic Sections and Poncelet Duality, *Proceedings of the IASS Symposium 2016 - Spatial Structures in the 21st Century*, Tokyo.

Kotnik, T. and D'Acunto, P.: 2013, Operative Diagramatology: Structural Folding for Architectural Design, *in* C. Gengnagel, A. Kilian, J. Nembrini and F. Scheurer (eds), *Rethinking Prototyping: Proceedings of Design Modelling Symposium 2013*, Universität der Künste Berlin, pp. 193–203.

Kupfer, H.: 1964, Erweiterung der Mörschschen Fachwerkanalogie mit Hilfe des Prinzips vom Minimum der Formänderungsarbeit, *CIB-Bulletin* **40**.

Kurrer, K. E.: 2008, *The History of the Theory of Structures, from Arch Analysis to Computational Mechanics*, Ernst & Sohn, Berlin.

Lachauer, L.: 2014, *Interactive Equilibrium Modelling*, PhD thesis, ETH Zürich.

Laerke, M.: 2010, Four Things Deleuze Learned from Leibniz, *in* S. Van Tuinen and N. McDonnell (eds), *Deleuze and The Fold: A Critical Reader*, Palgrave Macmillan, Basingstoke - New York.

Laman, G.: 1970, On Graphs and Rigidity of Plane Skeletal Structures, *J. Eng. Math* **4**, 331–340.

Lebée, A.: 2015, From Folds to Structures, a Review, *International Journal of Space Structures* **30**(2), 55–74.

Lee, J., Van Mele, T. and Block, P.: 2016, Form-finding Explorations through Geometric Manipulations of Force Polyhedrons, *Proceedings of the IASS Symposium 2016 - Spatial Structures in the 21st Century*, Tokyo.

Lee, J., Van Mele, T. and Block, P.: 2018, Disjointed Force Polyhedra, *Computer-Aided Design* **99**, 11–28.

Leibniz, G. W.: 2001, *The Labyrinth of the Continuum: Writings on the Continuum Problem (1672-1686)*, Yale University Press, New Haven - London. Arthur, T. W. (ed.).

Leonhardt, F.: 1965, Reducing the Shear Reinforcement in Reinforced Concrete Beams and Slabs, *Magazine of Concrete Research* **17**(53), 187–198.

Lynn, G.: 1993a, Architectural Curvilinearity: the Folded, the Pliant and the Supple, *in* G. Lynn (ed.), *Folding in Architecture*, Architectural Design Profile, Academy Group, London, pp. 8–15.

Lynn, G.: 2004, Introduction, *in* G. Lynn (ed.), *Folding in Architecture (Revised Edition)*, Architectural Design, Wiley-Academy, Chichester, pp. 9–13.

Lynn, G. (ed.): 1993b, *Folding in Architecture*, Architectural Design Profile, Academy Group, London.

Macdonald, A. J.: 2001, *Structure and architecture*, Routledge, Architectural Press, New York.

Madridejos, S. and Sancho, J. C.: 1996, Breve Conversación con Eduardo Chillida, *El Croquis* **81–82**, 14–23.

Marti, P.: 2013, *Theory of Structures: Fundamentals, Framed Structures, Plates and Shells*, Wiley-VCH Verlag GmbH & Co. KGaA, Berlin.

Maxwell, J. C.: 1864, On Reciprocal Figures, Frames and Diagrams of Forces, *Philosophical Magazine* **27**, 250–261.

Maxwell, J. C.: 1876, On Bow's Method of Drawing Diagrams in Graphical Statics with Illustrations from Peaucellier's Linkage, *Proceedings of the Cambridge Philosophical Society*, pp. 407–414.

Maxwell, J. C.: 1890, *Collected Papers*, Vol. XXVI, Cambridge University Press, Cambridge.

Mayor, B.: 1910, *Statique Graphique des Systèmes de l'Espace*, F. Rouge & Cie Librairie, Lausanne - Paris.

McRobie, A., Baker, W., Mitchell, T. and Konstantatou, M.: 2016, Mechanisms and States of Self-stress of Planar Trusses using Graphic Statics, Part II, *International Journal of Space Structures* **31**(2–4), 102–111.

Meyer, J.: 2017, *Proposition d'un Modèle Numérique pour la Conception Architecturale d'Enveloppes Structurales Plissées: Application à l'Architecture en Panneaux de Bois*, PhD thesis, Université de Lorraine.

Micheletti, A.: 2008, On Generalized Reciprocal Diagrams for Self-stressed Frameworks, *International Journal of Space Structures* **23**(3), 153–166.

Mitchell, T., Baker, W., McRobie, A. and Mazurek, A.: 2016, Mechanisms and States of Self-stress of Planar Trusses using Graphic Statics, Part I, *International Journal of Space Structures* **31**(2–4), 85–101.

Miura, K.: 1989, Folding a Plane - Scenes from Nature, Technology and Art, *Proceedings of the Interdiciplinary Symposium on Symmetry of Structure*, Budapest.

Möbius, A. F.: 1833, Über eine besondere Art dualer verhältnisse zwischen Figuren im Raume, *Journal für die reine und angewandte Mathematik* **10**, 317–341.

Morgan, G.: 1961, Cinematografo a Montecchio Maggiore presso Vicenza, *L'Architettura: Cronache e Storia* **69**, 162–167.

Mörsch, E.: 1908, *Der Eisenbetonbau, Seine Theorie Und Anwendung (Third Edition)*, Verlag Konrad Wittwer, Stuttgart.

Motro, R., Bouderbala, M., Lesaux, C. and Cévaer, F.: 2001, Foldable Tensegrities, *in* S. Pellegrino (ed.), *Deployable Structures*, Springer Verlag, Wien - New York, pp. 1–35.

Musmeci, S.: 1956, Volte ad Archi Poligonali, *L'Architettura: Cronache e Storia* **6**, 880–882.

Musmeci, S.: 1960, Copertura Pieghettata per un'Industria a Pietrasanta, *L'Architettura: Cronache e Storia* **52**, 710–713.

Musmeci, S.: 1967, Un Particolare Invariante Statico delle Strutture, *L'Ingegnere* **41**(1), 17–22.

Musmeci, S.: 1968, Il Minimo Strutturale, *L'Ingegnere* **42**(5), 407–414.

Musmeci, S.: 1971, *La Statica e le Strutture*, Poliedro, Edizioni Cremonese, Roma.

Musmeci, S.: 1979a, La Genesi della Forma nelle Strutture Spaziali, *Parametro* **10**(80), 13–33.

Musmeci, S.: 1979b, Le Tensioni non Sono Incognite, *Parametro* **10**(80), 36–47.

Muttoni, A.: 2011, *The Art of Structures*, EPFL Press, Lausanne.

Muttoni, A., Schwartz, J. and Thürlimann, B.: 1997, *Design of Concrete Structures with Stress Fields*, Birkhäuser, Basel - Boston - Berlin.

Nejur, A. and Steinfeld, K.: 2017, Ivy: Bringing a Weighted-Mesh Representation to Bear on Generative Architectural Design Applications, *ACADIA 2016 Posthuman Frontiers: Proceedings of the 36th Annual Conference of the Association for Computer Aided Design in Architecture, University of Michigan*, pp. 140–151.

Nervi, P. L.: 1956, *Structures*, F. W. Dodge Corp, New York.

Nervi, P. L.: 1965, *Costruire Correttamente*, Hoepli, Milano.

Nielsen, M. P.: 1984, *Limit Analysis and Concrete Plasticity. Prentice-Hall Series in Civil Engineering and Engineering Mechanics*, Prentice-Hall, Englewood-Cliffs.

Nordenson, G.: 2010, Collaboration, *Patterns and Structures, Selected Writings 1972-2008*, Lars Müller Publishers, Zürich, pp. 310–317.

Ohlbrock, P. O., D'Acunto, P., Jasienski, J. P. and Fivet, C.: 2017, Constraint-driven Design with Combinatorial Equilibrium Modelling, *Proceedings of the IASS Symposium 2017 - Interfaces: Architecture Engineering Science*, Hamburg.

Ohlbrock, P. O. and Schwartz, J.: 2016, Combinatorial Equilibrium Modeling, *International Journal of Space Structures* **31**(2–4), 177–189.

Oxman, R. and Oxman, R.: 2010, The New Structuralism: Design, Engineering and Architectural Technologies, *AD Architectural Design* **80**(4), 14–23.

Pedio, R.: 1959, Chiesa di San Luca in via Gattamelata, Roma, *L'Architettura: Cronache e Storia* **39**, 594–599.

Pedoe, D.: 1988, *Geometry: a Comprehensive Course*, Dover Publications, Mineola NY.

Pedreschi, R.: 2000, *The Engineer's Contribution to Contemporary Architecture: Eladio Dieste*, Thomas Telford, London.

Pellegrino, S.: 1993, Structural Computations with the Singular Value Decomposition of the Equilibrium Matrix, *International Journal of Solids and Structures* **30**(21), 3025–3035.

Pellegrino, S.: 2001, Deployable Structures in Engineering, *in* S. Pellegrino (ed.), *Deployable Structures*, Springer Verlag, Wien - New York, pp. 199–238.

Pellegrino, S. and Calladine, C.: 1986, Matrix Analysis of Statically and Kinematically Indeterminate Frameworks, *International Journal of Solids Structures* **22**(4), 409–428.

Piker, D.: 2017, Kangaroo2, ver. 2.42, http://www.food4rhino.com/app/kangaroo-physics (accessed 15.06.2018).

Pirard, A.: 1950, *La Statique Graphique*, Imprimerie H. Vaillant-Carmanne, Liège.

Plücker, J.: 1865, On a New Geometry of Space, *Philosophical Transactions of the Royal Society of London* **155**, 725–791.

Poretti, S.: 2008, *Modernismi italiani. Architettura e Costruzione nel Novecento*, Gangemi, Roma.

Poretti, S.: 2010, Pier Luigi Nervi: an Italian Builder, *in* C. Olmo and C. Chiorino (eds), *Pier Luigi Nervi: Architecture as Challenge*, Silvana Editoriale, Milano, pp. 119–137.

Pottman, H., Asperl, A., Hofer, M. and Kilian, A.: 2007, *Architectural Geometry*, Bentley Institute Press, Exton PA.

Pottmann, H. and Wallner, J.: 2001, *Computational Line Geometry*, Springer, Berlin - Heidelberg.

Prager, W. and Hodge, P. G.: 1951, *Theory of Perfectly Plastic Solids*, John Wiley & Sons, Inc., New York.

Rankine, W. J. M.: 1856, On the Mathematical Theory of the Stability of Earthwork and Masonry (Section II, Principle of the Transformation of Structures), *Proc. R. Soc. London* **8**, 60–61.

Rankine, W. J. M.: 1858, *A Manual of Applied Mechanics*, Richard Griffin and Company, Glasgow.

Rankine, W. J. M.: 1864, Principle of the Equilibrium of Polyhedral Frames, *The London, Edinburgh, and Dublin Philosophical Magazine and Journal of Science* **27**(180), 92.

Rausch, E.: 1938, *Berechnung des Eisenbetons gegen Verdrehung (Torsion) und Abscheren (Second Edition)*, Springer, Berlin.

Rinke, M. and Kotnik, T.: 2013, From Construct to Type – the Transformation of Constituents in the Development of Trusses, *Proceedings of the Second International Conference on Structures and Architecture*, Guimaraes, pp. 1947–1954.

Rippmann, M.: 2016, *Funicular Shell Design: Geometric Approaches to Form Finding and Fabrication of Discrete Funicular Structures*, PhD thesis, ETH Zürich.

Ritter, W.: 1899, Die Bauweise Hennebique (The Hennebique System), *Schweizerische Bauzeitung* **23**(7).

Robeller, C., Stitic, A., Mayencourt, P. and Weinand, Y.: 2014, Interlocking Folded Plate - Integrated Mechanical Attachment for Structural Timber Panels, *Advances in Architectural Geometry 2014* **4**, 281–294.

Roche, S., Mattoni, G. and Weinand, Y.: 2015, Rotational Stiffness at Ridges of Timber Folded-Plate Structures, *International Journal of Space Structures* **30**(2), 153–167.

Rondeaux, J. F., D'Acunto, P., Schwartz, J. and Zastavni, D.: 2017, Limit State Analysis of 2D Statically Indeterminate Networks Using Graphic Statics, *Proceedings of the IASS Symposium 2017 - Interfaces: Architecture Engineering Science*, Hamburg.

Rondeaux, J. F. and Zastavni, D.: 2018, A Fully Graphical Approach for Limit State Analysis of Existing Structures: Application to Plane ElasticPlastic Bended Structures and to Plane Masonry Arches, *International Journal of Architectural Heritage* **12**(3), 409–431.

Rosenfeld, B. A.: 1988, *A History of non-Euclidean Geometry. Evolution of the Concept of a Geometric Space*, Springer-Verlag, Berlin.

Rüsch, H.: 1964, Über die Grenzen der Anwendbarkeit der Fachewerkanalogie bei der Berechnung der Schubfestigkeit von Stahlbetonbalken (On the Limitations of Applicability of the Truss Analogy for the Shear Design of Reinforced Concrete Beams, *Festschrift F. Campus Amici et Alumni*, Université de Liége.

Saint, A.: 2007, *Architect and Engineer, a Study in Sibling Rivalry*, Yale University Press, New Haven - London.

Samuelsson, C. and Vestlund, B.: 2015, *Structural Folding: A Parametric Design Method for Origami Architecture*, Master's thesis, Chalmers University of Technology, Gothenburg.

Sancho, J. C.: 2001, The Folds, *in* J. C. Sancho and S. Madridejos (eds), *Suite en 3 movimientos*, Editorial Rueda S. L., Madrid, pp. 118–121.

Sancho, J. C.: 2014a, Folds as Laboratory Process, *in* J. C. Sancho and S. Madridejos (eds), *Collection*, S-M.A.O., Madrid, pp. 34–35.

Sancho, J. C.: 2014b, Laboratory Projects, *in* J. C. Sancho and S. Madridejos (eds), *Collection*, S-M.A.O., Madrid, pp. 64–67.

Sancho, J. C. and Madridejos, S.: 2003, Residence in Valleacerón, *DA documentos de arquitectura: Sancho-Madridejos - Pliegues* pp. 9–40.

Sancho, J. C. and Madridejos, S.: 2014, *Collection*, S-M.A.O., Madrid.

Sauer, R.: 1970, *Differenzengeometrie*, Springer, Berlin - Heidelberg - New York.

Saviotti, C.: 1888, *La Statica Grafica (Seconda Parte)*, Hoepli, Milano.

Schek, H. J.: 1974, The Force Density Method for Form Finding and Computation of General Networks, *Computer Methods in Applied Mechanics and Engineering* **3**(1), 115–134.

Schenk, M. and Guest, S. D.: 2011, Origami Folding: a Structural Engineering Approach, *in* P. Wang-Iverson, R. J. Lang and M. Yim (eds), *Origami 5: The Fifth International Meeting of Origami Science Mathematics and Education*, A K Peters/CRC Press, Boca Raton, pp. 1–16.

Schlaich, J., Schäfer, K. and Jennewein, M.: 1987, Toward a Consistent Design of Structural Concrete, *PCI Journal* **32**(3), 74–150.

Schnetzer, H., Muttoni, A., Schwartz, J. and Flury, A.: 2012, Strong Structures, *in* A. Flury (ed.), *Cooperation: The Engineer and the Architect*, Birkhäuser, Basel.

Schrems, M.: 2016, *Zur Erweiterung der grafischen Statik in die dritte Dimension*, PhD thesis, ETH Zürich.

Schrems, M. and Kotnik, T.: 2013, On the Extension of Grahic Statics into the Third Dimension, *Proceedings of the Second International Conference on Structures and Architecture 2013*, Guimaraes, pp. 1736–1742.

Schwartz, J.: 2016a, The Art of Structure, *Proceedings of the 3rd ICSA Conference - Structures and Architecture: Beyond their limits*, Guimaraes, pp. 299–305.

Schwartz, J. (ed.): 2016b, *Kleine Tragwerksobjekte (Small Structural Objects)*, Park Books, Zürich.

Schwartz, J. and Kotnik, T.: 2010, Transparenz, Stringenz, Leichtigkeit: Eleganz im Brückenbau, *Werk, Bauen + Wohnen* **97**(5).

Sedlak, V.: 1978, Folded Surface Structures, *Architectural Science Review* **21**(3), 58–59.

Smith, C.: 1886, *An Elementary Treatise on Solid Geometry*, Macmillan and Co, London.

Stitic, A., Robeller, C. and Weinand, Y.: 2015, Timber Folded Plate Structures – Folded Form Analysis, *IABSE Symposium Report* **104**(31), 1–8.

Stitic, A., Robeller, C. and Weinand, Y.: 2018, Experimental Investigation of the Influence of Integral Mechanical Attachments on Structural Behaviour of Timber Folded Surface Structures, *Thin-Walled Structures* **122**, 314–328.

Tachi, T.: 2009a, Generalization of Rigid Foldable Quadrilateral Mesh Origami, *Proceedings of the IASS Symposium 2009*, Valencia.

Tachi, T.: 2009b, Simulation of Rigid Origami, *in* R. J. Lang (ed.), *Origami 4: The Fourth International Meeting of Origami Science, Mathematics and Education*, A K Peters/CRC Press, Boca Raton, pp. 175–216.

Tachi, T.: 2010a, Architectural Origami - Architectural Form Design Systems Based on Computational Origami, *Lecture notes for MIT 6849*.

Tachi, T.: 2010b, Freeform Variations of Origami, *Journal for Geometry and Graphics* **14**(2), 203–215.

Tachi, T.: 2011, Rigid-Foldable Thick Origami, *in* P. Wang-Iverson, R. Lang and M. Yim (eds), *Origami 5: Fifth International Meeting of Origami Science, Mathematics, and Education*, A K Peters/CRC Press, Boca Raton, pp. 253–264.

Tachi, T.: 2012a, Design of Infinitesimally and Finitely Flexible Origami Based on Reciprocal Figures, *Journal Geom Graph* **16**, 223–234.

Tachi, T.: 2012b, Interactive Freeform Design of Tensegrity, *in* L. Hesselgren, S. Sharma, J. Wallner, N. Baldassini, P. Bompas and J. Raynaud (eds), *Advances in Architectural Geometry 2012*, pp. 259–268.

Tarnai, T.: 2001, Infinitesimal and Finite Mechanisms, *in* S. Pellegrino (ed.), *Deployable Structures*, Springer Verlag, Wien - New York, pp. 113–142.

Thürlimann, B., Marti, P., Pralong, J., Ritz, P. and Zimmerli, B.: 1983, *Vorlesung zum Fortbildungskurs für Bauingenieure (Advanced Lecture for Civil Engineers)*, Institut für Baustatik und Konstruktion, ETH Zürich.

Trautz, M. and Herkrath, R.: 2009, The Application of Folded Plate Principles on Spatial Structures with Regular, Irregular and Free-form Geometries, *Proceedings of the IASS Symposium 2009*, Valencia, pp. 1019–1031.

Trautz, M., Heyden, H. W., Herkrath, R., Pofahl, T., Hirt, G., Taleb-Araghi, B. and Bailly, D.: 2012, Herstellung frei geformter, selbst tragender Faltstrukturen aus Stahlblech mit der inkrementellen Blechumformung (IBU), *Stahlbau* **81**(12), 959–967.

Trautz, M., Pofahl, T. and Della Puppa, G.: 2014, Features of Foldings, *in* H. Filz. G., R. Maleczek and C. Scheiber (eds), *Form-Rule, Rule-Form 2013*, Koge Institut für Konstruktion und Gestaltung, Innsbruck University Press, pp. 118–129.

Vaccaro, G.: 1956, Scuola Nazionale di Atletica Leggera a Formia, *L'Architettura: Cronache e Storia* **8**, 86–91.

Van Mele, T. and Block, P.: 2014, Algebraic Graph Statics, *CAD Computer-Aided Design* **53**, 104–116.

Van Mele, T. Liew, A., Echenagucia, T. M. and Rippmann, M.: 2017, COMPAS: A Framework for Computational Research in Architecture and Structures, http://compas-dev.github.io/compas/ (accessed 15.06.2018).

Varignon, P.: 1725, *Nouvelle Méchanique ou Statique*, Jombert, Paris.

Vrontissi, M., Castellón González, J. J., D'Acunto, P., Enrique Monzó, L. and Schwartz, J.: 2018, Constructing Equilibrium: A Methodological Approach to Teach Structural Design in Architecture, *Proceedings of the IV International Conference on Structural Engineering Education: Structural Engineering Education Without Borders*, Madrid.

Vyzoviti, S.: 2003, *Folding Architecture: Spatial, Structural and Organizational Diagrams*, Bis Publishers, Amsterdam.

Wallner, J. and Pottmann, H.: 2008, Infinitesimally Flexible Meshes and Discrete Minimal Surfaces, *Monat Math* **153**, 347–365.

Wester, T.: 1984, *Structural Order in Space: the Plate-Lattice Dualism*, Royal Academy of Fine Arts, School of Architecture, Copenhagen.

Wester, T.: 1987, The Plate-Lattice Dualism, *in* T. T. Lan and Y. Zhilian (eds), *Proceedings of the International Colloquium on Space Structures for Sports Buildings*, Science Press, Beijing & Elsevier, pp. 321–329.

Wester, T.: 1993, Efficient Faceted Surface Structures, *in* G. A. R. Parke and C. M. Howard (eds), *Space Structures 4: Proceedings of the 4th International Conference on Space Structures*, Thomas Telford Services, pp. 1231–1239.

Wester, T.: 1996, The Fabulous Paraboloid Dual Transformation as a Design Method, *in* T. Ogawa, K. Miura, T. Masunari and D. Nagy (eds), *Katachi U Symmetry*, Springer Japan, pp. 223–230.

Wester, T.: 2011, 3D Form and Force Language: Proposal for a Structural Basis, *International Journal of Space Structures* **26**(3), 229–239.

Whiteley, W.: 1984, Infinitesimally Rigid Polyhedra, I: Statics of Frameworks, *Transactions of the American Mathematical Society* **285**(2), 431–465.

Whiteley, W.: 1987, Rigidity and Polarity I: Statics of Sheet Structures, *Geometriae Dedicata* **22**(3), 329–362.

Whitney, H.: 1933, Planar Graphs, *Fundamenta Mathematicae* **21**, 73–84.

Zwillinger, D. (ed.): 2002, *CRC Standard Mathematical Tables and Formulae (31st edition)*, Chapman and Hall/CRC Press, Boca Raton.